BIS(DITERTIARYPHOSPHINE) COMPLEXES OF RHODIUM, AND CATALYTIC ASYMMETRIC HYDROGENATION

91

by

DEVINDER MAHAJAN

M.Sc., University of British Columbia, 1976

A THESIS SUBMITTED IN PARTIAL FULFILMENT OF
THE REQUIREMENTS FOR THE DEGREE OF
DOCTOR OF PHILOSOPHY

in

THE FACULTY OF GRADUATE STUDIES
Department of Chemistry

We accept this thesis as conforming
to the required standard

The University of British Columbia

May, 1979

© Devinder Mahajan, 1979

In presenting this thesis in partial fulfilment of the requirements for an advanced degree at the University of British Columbia, I agree that the Library shall make it freely available for reference and study. I further agree that permission for extensive copying of this thesis for scholarly purposes may be granted by the Head of my Department or by his representatives. It is understood that copying or publication of this thesis for financial gain shall not be allowed without my written permission.

Department of CHEMISTRY

The University of British Columbia
2075 Wesbrook Place
Vancouver, Canada
V6T 1W5

Date May 25, 1979

DE-6 BP 75-511E

ABSTRACT

Rhodium(I)-bis(ditertiaryphosphine) complexes of the general formula $Rh(P\frown P)_2Cl$[$P\frown P = Ph_2P(CH_2)_n PPh_2$, n = 1-4, and (+)-diop (diop = 2,3-O-isopropylidene 2,3-dihydroxy-1,4 bis(diphenylphosphino)butane] have been prepared by treating $[Rh(cyclooctene)_2Cl]_2$ with the appropriate ditertiaryphosphine. The n=1, and n=4 and diop species are five-coordinate in the solid state and in non-polar solvents, while the n=2 and 3 species contain ionic chloride. The cationic complexes $Rh(P\frown P)_2^+X^-$ were prepared from the $Rh(P\frown P)_2Cl$ species by adding AgX[X=SbF_6,PF_6,BF_4]. Reaction of the chloro complexes with borohydride has yielded the hydrides, $HRh(P\frown P)_2$, for the n=2 and 3 diphosphines, and for (+)-diop. ^1H and ^{31}P nmr, as well as visible spectral data, are presented: a solvent-dependent deshielding of ortho protons of the phenyl groups is observed in some of the complexes, and the ligand CH_2 protons are coupled to the rhodium in the $Rh(Ph_2PCH_2PPh_2)_2^+$ cation; the P atom in this bis(diphenylphosphino) ligand shows an unusual highfield shift on coordination to rhodium. Preliminary kinetic data for catalytic hydrogenation of methylenesuccinic acid or itaconic acid (IA) show that the cationic and hydrido complexes are more active than the corresponding chloro complexes, and that activity generally increases with increasing chain length of the diphosphine.

The rhodium-bis(diop) complexes efficiently catalyze the asymmetric hydrogenation of a number of prochiral substrates, optical purities of >90% being obtained in the hydrogenation of N-acylaminoacrylic acids. Steric factors at the olefinic bond, and coordination of the -NHCOR group through the $\rangle C{=}O$ moiety, seem important in determining the hydrogenation rates. The rates are slower in the more strongly coordinating DMA compared to n-butanol-toluene mixtures. The solvent medium has little effect on the

degree of asymmetric induction, when using the $Rh[(+)\text{-diop}]_2^+$ or $HRh[(+)\text{-diop}]_2$ complexes, but reversal of product configuration is observed when using the $Rh[(+)\text{-diop}]_2C\ell$ complex in DMA or in n-butanol-toluene mixtures. An unusual increase in optical purity of the product with increasing temperature has been observed in the hydrogenation of IA.

Detailed kinetic and spectroscopic studies on the hydrogenation of IA catalyzed by $HRh[(+)\text{-diop}]_2$ are explained in terms of a mechanism involving the formation of a metal alkyl via coordination of the olefinic substrate, followed by reaction with H_2 to yield the saturated product (S.P.) and regenerated catalyst (equations [1]-[3]). A monodentate diop(diop*) is invoked:

$$HRh(diop)_2 \rightleftharpoons HRh(diop)(diop^*) \quad [1]$$

$$HRh(diop)(diop^*) + \text{olefin} \rightleftharpoons Rh(diop)(diop^*)(\text{alkyl}) \quad [2]$$

$$Rh(diop)(diop^*)(\text{alkyl}) + H_2 \longrightarrow HRh(diop)(diop^*) + \text{S.P.} \quad [3]$$

The initial hydride catalyst is slowly decomposed by protons of the acidic substrate to give $Rh(diop)_2^+$. To avoid this complication, a mechanistic study was carried out on the $HRh(diop)_2$-Styrene-H_2 system, which was found to proceed via the same mechanism as outlined in equations [1]-[3].

A mechanistic study on the $Rh(diop)_2^+BF_4^-$-catalyzed hydrogenation of IA shows that the reaction proceeds mainly via the 'hydride' route:

$$Rh(diop)_2^+ + H_2 \rightleftharpoons Rh(diop)_2H_2^+ \quad [4]$$

$$Rh(diop)_2H_2^+ + IA \rightleftharpoons Rh(diop)(diop^*)(H)_2(IA)^+ \quad [5]$$

$$Rh(diop)(diop^*)(H)_2(IA)^+ \longrightarrow Rh(diop)_2^+ + \text{S.P.} \quad [6]$$

A complete inhibition of the hydrogenation by small amounts of added diop(diop:Rh>0.2) is tentatively attributed to formation of an inactive polymeric species:

$$n\mathrm{Rh(diop)_2H_2^+} + \mathrm{diop} \longrightarrow [\mathrm{Rh(diop)(diop^*)H_2^+}]_n \qquad [7]$$

The forward step of Reaction [4] was studied in detail in the absence of olefinic substrate. Spectroscopic and kinetic data are best explained in terms of dihydride formation via the consecutive reactions outlined in equation [8]:

$$\mathrm{Rh(diop)_2^+} \underset{}{\overset{S}{\rightleftharpoons}} \mathrm{Rh(diop)(diop^*)S^+} \xrightarrow[H_2]{} \mathrm{Rh(diop)(diop^*)(H)_2S^+}$$

$$\mathrm{Rh(diop)_2H_2^+} \xleftarrow{-S} \qquad (S=\text{solvent}) \qquad [8]$$

The dehydrogenation reaction was also studied.

The reactions of $[\mathrm{Rh}(\overset{\frown}{\mathrm{P}}\,\overset{\frown}{\mathrm{P}})_2]\,\mathrm{A}$ complexes (A=Cℓ,BF_4) with CO,O_2,H_2 and HCℓ(g) yield several new complexes. Thus the $[\mathrm{Rh}(\overset{\frown}{\mathrm{P}}\,\overset{\frown}{\mathrm{P}})_2\mathrm{XY}]^+\mathrm{BF_4^-}$ complexes ($\overset{\frown}{\mathrm{P}}\,\overset{\frown}{\mathrm{P}}$ = dpm,dpp;XY=CO, $\overset{\frown}{\mathrm{P}}\,\overset{\frown}{\mathrm{P}}$=dpm,dpe,dpp;XY=$O_2$, $\overset{\frown}{\mathrm{P}}\,\overset{\frown}{\mathrm{P}}$=dpp, (+)-diop: XY=$H_2$, and $\overset{\frown}{\mathrm{P}}\,\overset{\frown}{\mathrm{P}}$=dpm,dpe,dpp;XY=HCℓ) were isolated and characterized. The solution structures were determined using especially variable temperature ^{31}P nmr spectroscopy. The formally six-coordinate rhodium(III) dioxygen and the dihydrido complexes were assigned cis geometries, whereas the HCℓ complexes were more fluxional and cis geometries could only be assigned with certainty to the dpp complex; for dpm and dpe complexes, the limiting spectra could not be achieved even at -60°C. For the five-coordinate rhodium(I) CO complexes, the dpp complex has been assigned a TBP structure but the dpm complex is fluxional even at -60°C.

Some stopped-flow kinetic data are presented for the addition of CO,

O_2, and H_2 to the $Rh(\overset{\frown}{P\ P})_2^+$ complexes. For the dpp system, the rate increased in the order $CO > H_2 > O_2$, although the reactions are not simple 1:1 single step additions, solvated species probably playing an important role (cf. equation [8]).

TABLE OF CONTENTS

		Page
ABSTRACT		ii
TABLE OF CONTENTS		vi
LIST OF TABLES		ix
LIST OF FIGURES		xi
ABBREVIATIONS		xv
ACKNOWLEDGEMENTS		xviii
CHAPTER I.	INTRODUCTION	1
	I.1 General	1
	I.2 Scope of this thesis	3
	I.3 Modes of hydrogen activation	5
	I.4 Rhodium catalysts in homogeneous hydrogenation	9
	I.5 Homogeneous hydroformylation	12
	I.6 Solvent transfer hydrogenation of unsaturated compounds	13
	I.7 Asymmetric homogeneous hydrogenation	14
CHAPTER II.	GENERAL EXPERIMENTAL	23
	II.1 Materials	23
	II.1.1 Solvents	23
	II.1.2 Gases	23
	II.1.3 Diphosphines	23
	II.1.4 Olefins	24
	II.1.5 Inorganic silver salts	24
	II.2 Instrumentation	25
	II.3 Gas-uptake apparatus	25
	II.4 Gas-uptake experimental procedure	27
	II.5 Solubility determination	28
	II.6 Stoichiometric gas-uptake measurements	29
	II.7 Spectrophotometric kinetic measurements	30
	II.8 Fast reaction measurements	32
	II.9 Work-up of the hydrogenated products	32
	II.9.1 Itaconic, citraconic, maleic, and atropic acids	32
	II.9.2 N-α-acetamido-acrylic and -cinnamic acids	32
	II.9.3 Liquid olefins	32
	II.9.4 Acrylamide	33
	II.10 Optical rotation measurements	33
CHAPTER III.	HOMOGENEOUS HYDROGENATION OF ACIDIC AND NON-ACIDIC SUBSTRATES USING THE HYDRIDOBIS(DIOP)-RHODIUM(I) COMPLEX	34
	III.1 Introduction	34
	III.2 Experimental	35
	III.3 The summary of studies done on the Itaconic acid - $HRh[(+)\text{-diop}]_2$ system	37
	III.4 The $HRh[(+)\text{-diop}]_2$-Styrene system	44
	III.4.1 Results	44
	III.4.2 Discussion	51

		Page
	III.5 Conclusions	56
CHAPTER IV.	BIS(DITERTIARYPHOSPHINE) COMPLEXES OF RHODIUM(I). SYNTHESIS, SPECTROSCOPY, AND ACTIVITY FOR CATALYTIC HYDROGENATION	57
	IV.1 Introduction	57
	IV.2 Experimental	58
	IV.2.1 $Rh(dpm)_2C\ell$	58
	IV.2.2 $Rh(dpe)_2C\ell$ and $Rh(dpp)_2C\ell$	58
	IV.2.3 $Rh(dpb)_2C\ell$	59
	IV.2.4 $Rh[(+)\text{-diop}]_2C\ell$	59
	IV.2.5 $Rh(\overset{\frown}{P}\overset{\frown}{P})_2^+BF_4^-$ ($\overset{\frown}{P}\overset{\frown}{P}$ = dpm, dpe, dpp, dpb, and (+)-diop)	59
	IV.2.6 $HRh(\overset{\frown}{P}\overset{\frown}{P})_2$ ($\overset{\frown}{P}\overset{\frown}{P}$ = dpe, dpp, and (+)-diop)	59
	IV.3 Results and Discussion	60
	IV.4 Catalytic hydrogenation	82
CHAPTER V.	ASYMMETRIC HOMOGENEOUS HYDROGENATION OF PROCHIRAL OLEFINIC SUBSTRATES USING RHODIUM-DIOP COMPLEXES AS CATALYSTS	89
	V.1 Introduction	89
	V.2 Experimental	89
	V.2.1 Preparation of complexes	89
	V.2.2 Determination of optical purities	90
	V.3 Results	91
	V.4 Discussion	98
CHAPTER VI.	ASYMMETRIC HOMOGENEOUS HYDROGENATION OF ITACONIC ACID USING BIS(DIOP)RHODIUM(I)TETRAFLUORO-BORATE AS CATALYST	109
	VI.1 Introduction	109
	VI.2 Experimental	110
	VI.3 Results	110
	VI.3.1 Reaction of hydrogen with $Rh(diop)_2^+BF_4^-$	110
	VI.3.1.1 Gas-uptake studies	110
	VI.3.1.2 Spectrophotometric studies	110
	VI.3.1.3 ^{31}P nmr data	115
	VI.3.2 Catalytic hydrogenation studies	121
	VI.3.2.1 Kinetic data	121
	VI.3.2.2 Spectroscopic data	121
	VI.4 Discussion	128
	VI.4.1 The hydrogen reaction	128
	VI.4.2 The catalytic hydrogenation mechanism	134
CHAPTER VII.	REACTIONS OF BIS(DITERTIARY)PHOSPHINE-RHODIUM(I) COMPLEXES WITH THE GAS MOLECULES CO, O_2, H_2, and $HC\ell$	142
	VII.1 Introduction	142
	VII.2 Experimental	143

Page

VII.2.1 CO complexes 143
VII.2.1.1 $Rh(P\frown P)_2CO^+BF_4^-$ ($P\frown P$ = dpm,dpp) 143
VII.2.1.2 Reaction of CO with $Rh(dpe)_2^+BF_4^-$ 150
VII.2.1.3 Reaction of CO with $Rh(dpb)_2^+BF_4^-$ 150
VII.2.1.4 Reaction of CO with $Rh(diop)_2^+BF_4^-$ and $Rh(diop)_2C\ell$ 150
VII.2.2 Dioxygen complexes 151
VII.2.2.1 $Rh(dpm)_2O_2^+BF_4^-$ 151
VII.2.2.2 $Rh(P\frown P)_2O_2^+BF_4^-$ ($P\frown P$ = dpe, dpp) 151
VII.2.2.3 Reaction of O_2 with $Rh(dpb)_2^+BF_4^-$ 151
VII.2.2.4 Reaction of O_2 with $Rh(diop)_2^+BF_4^-$ 151
VII.2.3 Dihydride complexes 151
VII.2.3.1 Reaction of H_2 with $Rh(P\frown P)_2^+BF_4^-$ ($P\frown P$ = dpm, dpe) 151
VII.2.3.2 $Rh(dpp)_2H_2^+BF_4^-$ 152
VII.2.3.3 $Rh(diop)_2H_2^+BF_4^-$ 152
VII.2.3.4 Reaction of H_2 with $Rh(dpb)_2^+BF_4^-$ 152
VII.2.4 $HRh(P\frown P)_2C\ell^+A^-$ complexes 152
VII.2.4.1 $HRh(dpm)_2C\ell^+C\ell^-$ 152
VII.2.4.2 $HRh(P\frown P)_2C\ell^+C\ell^-$ ($P\frown P$ = dpe and dpp) 152
VII.2.4.3 Reaction of $HC\ell$(g) with $[Rh(P\frown P)_2]A$ ($P\frown P$ = dpb and diop; A=$C\ell$, BF_4) 153
VII.2.4.4 $HRh(P\frown P)_2C\ell^+A^-$ ($P\frown P$ = dpm, dpe, and dpp; A=BF_4, PF_6, SbF_6) 154
VII.3 Results and Discussion 155
VII.3.1 The five-coordinate carbonyl complexes of rhodium(I) 155
VII.3.2 Six-coordinate complexes of rhodium(III) 161
VII.4 Attempted use of $HRh(P\frown P)_2C\ell^+A^-$ complexes in catalytic hydrogenation 172
VII.5 Preliminary kinetic studies 172

CHAPTER VIII GENERAL CONCLUSIONS, AND RECOMMENDATIONS FOR FUTURE WORK 179

REFERENCES FOR CHAPTER I 184
CHAPTER II 194
CHAPTER III 194
CHAPTER IV 195
CHAPTER V 198
CHAPTER VI 200
CHAPTER VII 201

LIST OF TABLES

Table number		Page
III.1	Maximum hydrogenation rates for the hydrogenation of styrene in n-butanol-toluene (2:1) at 45°C using $HRh[(+)\text{-diop}]_2$	46
III.2	Variation of maximum rate with temperature	50
III.3	Variation of maximum rate with added (+)-diop	50
IV.1	Analytical and molar conductivity (Λ) data for the rhodium(I) complexes	61
IV.2	Visible spectral data for the rhodium(I) complexes	63
IV.3	Infrared and high-field ^1H nmr data for various rhodium(I) complexes	64
IV.4	^{31}P nmr data for the rhodium(I) complexes at 25°C	65
IV.5	^1H nmr data for the rhodium(I) complexes at 25°C	66
IV.6	Catalytic hydrogenation of methylenesuccinic acid using the rhodium(I) complexes	83
V.1	Asymmetric homogeneous hydrogenation of unsaturated substrates using the $HRh[(+)\text{-diop}]_2$ catalyst	93
V.2	Optical purities of products from hydrogenation of olefinic substrates using the $Rh[(+)\text{-diop}]_2^+BF_4^-$ complex	94
V.3	Asymmetric homogeneous hydrogenation of prochiral olefins using the $Rh[(+)\text{-diop}]_2C\ell$ catalyst	95
V.4	The $Rh[(+)\text{-diop}]_2H_2^+BF_4^-$ - catalyzed hydrogenation of some prochiral substrates	96
V.5	Asymmetric hydrogenation of prochiral unsaturated substrates using the $[RhC\ell(CO)(+)\text{-diop}]_2$ complex	97
V.6	Asymmetric hydrogenation of unsaturated substrates using various rhodium(I)-mono(diop) complexes at 25°C and 760 mm total pressure	99
VI.1	Hydrogen - uptake data for $Rh(diop)_2^+BF_4^-$ using ampoule technique	112
VI.2	Spectrophotometric determination of first-order rate constants for the dehydrogenation of $Rh(diop)_2H_2^+BF_4^-$ in different solvents at 30°C	119
VI.3	Linear rate data for the hydrogenation of itaconic acid in n-butanol-toluene (2:1) catalyzed by $Rh(diop)_2^+BF_4^-$ at 15°C.	123
VI.4	Analysis of various stopped-flow data at 30°C in terms of two first-order reactions	133

Table number		Page
VII.1	Analytical and molar conductivity data (Λ) for the Rh(I) and Rh(III) complexes	144
VII.2	Gas-uptake data for various rhodium(I)-bis(ditertiaryphosphine) complexes at 25°C	145
VII.3	High-field ^{1}H nmr and infrared data for the rhodium(I) and rhodium(III) complexes	146
VII.4	^{1}H nmr data for various rhodium-bis(ditertiaryphosphine) complexes	147
VII.5	$^{31}P\{^{1}H\}$ nmr data for various rhodium-bis(ditertiaryphosphine) complexes	148
VII.6	Pseudo first-order rate constant k at 30°C for the reaction $Rh(P\frown P)_2^+BF_4^- + XY \longrightarrow Rh(P\frown P)_2XY^+BF_4^-$	173
VII.7	Data at 30°C for the determination of equilibrium constant K_1 for the reaction $Rh(dpe)_2^+ + O_2 \rightleftharpoons Rh(dpe)_2O_2^+$	177

LIST OF FIGURES

Figure number		Page
I.1	Structure of (-)-(2R,3R)-DIOP	3
I.2	Mechanism for ruthenium(II) chloride-catalyzed hydrogenation of olefins	7
I.3	Scheme for neutral and cationic rhodium(I) complexes	10
I.4	Pathways for olefin hydrogenation and isomerization	11
I.5	Some effective ligands used in catalytic asymmetric hydrogenation	17
I.6	Stereochemical model proposed for olefin hydrogenation catalyzed by neutral mono(diop)-rhodium complexes	18
I.7	Possible conformations of saturated five-membered chelate rings	19
I.8	Crystal structure of the $[Rh(COD)(S,S\text{-chiraphos})]^+$ complex	19
II.1	Constant pressure gas-uptake apparatus	26
II.2	Ampoule technique	30
II.3	Anaerobic spectral cell	31
III.1	Solubility of hydrogen in n-butanol-toluene (2:1) mixture at various pressures at 30°C	36
III.2	Solubility of hydrogen in n-butanol-toluene (2:1) mixture at various temperatures	36
III.3	Rate plots for the hydrogenation of itaconic acid using $HRh(diop)_2$ as catalyst	38
III.4	Maximum rate dependence on itaconic acid in n-butanol-toluene(2:1) at 30°C using 1.5×10^{-3}M Rh; curve a, 740 mm H_2; curve b, 132 mm H_2	40
III.5	$^{31}P\{^1H\}$ nmr spectra in n-butanol-toluene-acetone-d_6 mixture at 25°C of: (a) $HRh(diop)_2$(130 mg in 2 ml solvent) under Ar; (b) (a) + 130 mg IA; (c) (b) under H_2	42
III.6	High-field ^1H nmr spectra in n-butanol-toluene-acetone-d_6 mixture at 25°C of: (a) $HRh(diop)_2$ (130 mg in 2 ml solvent) under Ar; (b)(a) + 130 mg IA under H_2	43
III.7	Rate plot for the hydrogenation of styrene using $HRh(diop)_2$ catalyst	45
III.8	Maximum rate dependence on $HRh(diop)_2$ concentration	47
III.9	Plot of maximum rate against styrene concentration	48
III.10	Dependence of maximum rate on H_2 pressure	49

Figure number		Page
III.11	Absorption spectra of $HRh(diop)_2$ (1.4×10^{-3}M) under argon in n-butanol-toluene (2:1) in the presence of styrene (0.1M) at 45±2°C	52
III.12	Arrhenius plot for the hydrogenation of styrene using $HRh(diop)_2$ catalyst	53
III.13	Absorption spectra of $HRh(diop)_2$ (1.4×10^{-4}M) in n-butanol-toluene (2:1) in the presence of diethyl maleate (1.0×10^{-2}M) at 30±1°C: (a) solution under argon; (b) solution under hydrogen	55
IV.1(A)	Visible absorption spectra of the $Rh(P\frown P)_2C\ell$ complexes in methanol under argon at 25°C ($P\frown P$ = a.dpm, b.dpe, c.dpp, and d.dpb)	68
IV.1(B)	Visible spectra of the $Rh(P\frown P)_2C\ell$ complexes in toluene under argon at 25°C ($P\frown P$ = e.dpm, f. dpb, and g. diop).	69
IV.2	Visible spectra of various $Rh(P\frown P)_2{}^+BF_4{}^-$ complexes in methanol under argon at 25°C ($P\frown P$ = a. dpm, b. dpe, c. dpp, d. dpb, and e. diop)	70
IV.3	Absorption spectra of the $HRh(P\frown P)_2$ complexes in toluene under argon at 25°C ($P\frown P$ = a. dpe and b. dpp).	71
IV.4	High-field ^1H nmr spectra of (1) $HRh(dpe)_2$ (2) $HRh(dpp)_2$ (3) $HRh(diop)_2$ in C_6D_6 at 25°C	73
IV.5	X-ray crystal structure of the $HIr(dpe)_2$ complex	74
IV.6	Crystal structure of the $HRh[(+)\text{-diop}]_2$ complex	75
IV.7	$^{31}P\{^1H\}$ nmr spectrum of $HRh[(+)\text{-diop}]_2$ under argon in n-butanol-toluene-acetone-d_6 (a) at 25°C and (b) at -50°C.	76
IV.8	^{31}P nmr spectrum of $Rh(dpm)_2C\ell$ in (a) C_6D_6 and (b) $CH_2C\ell_2$-acetone-d_6 at 25°C.	77
IV.9	^1H nmr spectrum of $Rh(dpm)_2{}^+BF_4{}^-$ in acetone-d_6 at 25°C	80
IV.10	^1H nmr (phenyl region) spectra of (1) $HRh(dpe)_2$ (2) $HRh(dpp)_2$ (3) diop (4) $HRh(diop)_2$ in C_6D_6 at 25°C	81
IV.11	Rate plot for the hydrogenation (100%) of methylenesuccinic acid using $HRh(dpp)_2$ as catalyst	84
IV.12	Rate plots for the hydrogenation (50%) at one atmosphere pressure of methylenesuccinic acid using: a. $HRh(dpe)_2$, b. $Rh(dpe)_2{}^+BF_4{}^-$, c. $Rh(dpp)_2{}^+BF_4{}^-$, d. $Rh(dpb)_2C\ell$	85
IV.13	Rate plots for the hydrogenation (50%) at one atmosphere pressure of methylenesuccinic acid using: a. $HRh(diop)_2$, b. $Rh(diop)_2{}^+BF_4{}^-$, c. $Rh(dpb)_2{}^+BF_4{}^-$	86
V.1	Some substrates used in catalytic asymmetric hydrogenation	92

Figure number		Page
V.2	Proposed intermediates for hydrogenations catalyzed by rhodium-mono(diop) complexes	102
V.3	Crystal structure of the $[Rh(dpe)(PhC(H)=C(COOCH_3)(NHCOCH_3))]^+$ cation	102
V.4	Plot of variation of optical yield with temperature of: 1. (+)-2-methylsuccinic acid using a. $HRh[(+)\text{-diop}]_2$; b. $Rh[(+)\text{-diop}]_2^+BF_4^-$ as catalysts in n-butanol-toluene (2:1); 2. N-acetyl-S(+)-phenylalanine using the $Rh[(+)\text{-diop}]_2C\ell$ complex in n-butanol-toluene (2:1)	106
V.5	Variation of optical yield of (+)-2-vinyl-norbornane with temperature using a nickel catalyst in chlorobenzene	106
VI.1	Solubility of hydrogen in n-butanol-toluene (2:1) mixtures at various pressures at 15°C. Inset gives data at different temperatures	111
VI.2	Visible spectrum of $Rh(diop)_2^+BF_4^-$ in n-butanol-toluene (2:1) at 25°C	113
VI.3	Visible spectrum of $Rh(diop)_2^+BF_4^-$ at 25°C in n-butanol-toluene (2:1)(in absence, or presence of diop(diop:Rh=3:1)). (a) under H_2 and (b) under Ar	114
VI.4	Plot of log (A_t-A_∞) vs time of the stopped-flow data for H_2-uptake by $Rh(diop)_2^+BF_4^-$ in DMA at 30°C	116
VI.5	Spectral changes obtained for H_2 loss from $Rh(diop)_2H_2^+BF_4^-$ in methanol (under argon) at 30°C	117
VI.6	Plot of $\log(A_t-A_\infty)$ vs time for spectral changes in Fig.VI.5	118
VI.7	$^{31}P\{^1H\}$ nmr spectra of $Rh(diop)_2^+BF_4^-$ in $CH_2C\ell_2$-acetone-d_6 a. under argon: 1. at 25°C and 2. at -50°C; b. under hydrogen at 25°C	120
VI.8	H_2-uptake plot for the $Rh(diop)_2^+BF_4^-$-catalyzed hydrogenation of itaconic acid	122
VI.9	Plot of linear rate against $Rh(diop)_2^+BF_4^-$ concentration	124
VI.10	Dependence of linear rate on IA concentration	125
VI.11	Plot of linear rate against hydrogen pressure	126
VI.12	Spectral changes observed on adding IA to solutions of $Rh(diop)_2^+BF_4^-$ in n-butanol-toluene(2:1)(under argon) at 30°C (in the absence, or presence of added diop)	127
VI.13	Analysis of data from Fig. VI.4 in terms of two first-order reactions (A and B)	132
VI.14	Arrhenius plot for the $Rh(diop)_2^+BF_4^-$ - catalyzed hydrogenation of IA	135
VI.15	Plot of $[IA]^{-1}$ vs linear rate^{-1}	140

Figure number		Page
VII.1	^{31}P nmr spectra of $Rh(dpm)_2CO^+BF_4^-$ in $CH_2C\ell_2$-acetone-d_6(2:1=V/V). a. Under Ar at 25°C. b. Under Ar at -50°C. c. Under CO at -50°C	158
VII.2	^{31}P nmr spectra of $Rh(dpp)_2CO^+BF_4^-$ in $CH_2C\ell_2$-acetone-d_6(2:1=V/V). a. Under Ar at 25°C. b. Under CO at 25°C. c. Under CO at -50°C.	159
VII.3	^{31}P nmr spectra in $CH_2C\ell_2$-acetone-d_6(2:1=V/V) at 25°C of: a. $Rh(dpm)_2O_2^+BF_4^-$. b. $Rh(dpp)_2O_2^+BF_4^-$	164
VII.4	High-field ^1H nmr spectra at 25°C (under H_2) of: a. $Rh(dpp)_2H_2^+BF_4^-$ in acetone-d_6. b. $Rh(diop)_2H_2^+BF_4^-$ in $CDC\ell_3$	166
VII.5	$^{31}P\{^1H\}$ nmr spectra in $CH_2C\ell_2$-acetone-d_6 (2:1=V/V) of: (a) $Rh(dpp)_2H_2^+BF_4^-$ at -50°C and (b) $Rh(diop)_2H_2^+BF_4^-$ at (1) 25°C, (2) -50°C, and (3) -85°C.	167
VII.6	High-field ^1H nmr spectra of: (a) $HRh(dpm)_2C\ell^+C\ell^-$, (b) $HRh(dpe)_2C\ell^+C\ell^-$, and (c) $HRh(dpp)_2C\ell^+C\ell^-$ in $CDC\ell_3$ at 25°C.	169
VII.7	$^{31}P\{^1H\}$ nmr spectra of $HRh(dpe)_2C\ell^+C\ell^-$ in $CH_2C\ell_2$-acetone-d_6 (2:1=V/V) at a. 25°C and b. -60°C.	170
VII.8	$^{31}P\{^1H\}$nmr spectra of $HRh(dpp)_2C\ell^+C\ell^-$ in $CH_2C\ell_2$-acetone-d_6 (2:1=V/V) at: a. 25°C, b. -50°C, and c. -85°C.	171
VII.9(A)	Spectral changes obtained for O_2 loss from $Rh(dpe)_2O_2^+BF_4^-$ in methanol at 30°C (solution under argon)	175
VII.10(A)	Spectral changes obtained at 30°C on adding O_2 (1 atm) to solutions of $Rh(dpe)_2^+BF_4^-$ in methanol	175
VII.9(B)	Plot of $\log(A_t-A_\infty)$ vs time for spectral changes in Figure VII.9(A)	176
VII.10(B)	Plot of $\log(A_t-A_\infty)$ vs time for spectral changes in Figure VII.10(A)	176

ABBREVIATIONS

A	anion, SbF_6^-, PF_6^-, BF_4^-, $C\ell^-$
acetone-d_6	deuterated acetone ($CD_3-\overset{\overset{O}{\|}}{C}-CD_3$)
Ar	argon
atm	atmosphere
benzene-d_6	deuterated benzene (C_6D_6)
c	concentration in g/100 ml
Calc.	calculated
Cat*	chiral catalyst
C_8H_{14}	cis-cyclooctene
COD	1,5-cyclooctadiene
config.	configuration
cps	cycles per second, Hz
d	day(s)
(+)-diop	[(+)-(2S,3S)-O-isopropylidene-2,3-dihydroxy-1, 4-bis(diphenylphosphino) butane]
diop*	'monodentate' or 'dangling' diop
DMA	N,N-dimethylacetamide ($H_3CCON(CH_3)_2$)
DMA.HCℓ	N,N-dimethylacetamidehydrochloride ($H_3CCON(CH_3)_2.HC\ell$)
DMSO	dimethylsulfoxide $(CH_3)_2SO$
dpm	bis(diphenylphosphino) methane ($\phi_2P-CH_2-P\phi_2$)
dpe	1,2-bis(diphenylphosphino) ethane ($\phi_2P\{CH_2\}_2P\phi_2$)
dpp	1,3-bis(diphenylphosphino) propane ($\phi_2P\{CH_2\}_3P\phi_2$)
dpb	1,4-bis(diphenylphosphino) butane ($\phi_2P\{CH_2\}_4P\phi_2$)
dppp	1,2-bis(diphenylphosphino) propane
e.e.	enantiomeric excess
Et	ethyl
Fig.	Figure(s)
g	gram(s)
h	hour(s)
Hz	cps
IA	itaconic acid
ir	infrared
J	coupling constant, cps or Hz

L	ligand
ln	natural logarithm
log	common logarithm
M	molarity, metal atom
Max.	maximum
Me	methyl
MeOH-d_4	deuterated methanol (CD_3OD)
min	minute(s)
NBD	norbornadiene
nm	nanometer (10^{-9} meter) = 1 millimicron (mμ)
nmr	nuclear magnetic resonance
O.D.	optical density, absorbance
ol	olefin
Ph or φ	phenyl
$^{31}P\{^{1}H\}$	proton-decoupled ^{31}P
ppm	parts per million
$\overset{\frown}{P\ P}$	a chelating diphosphine
P.S.	"proton sponge" (1,8-bis(dimethylamino) naphthalene)
py	pyridine
R	aryl; alkyl
Ref.	reference
R.T.	room temperature
s	second(s)
S	substrate; solvent
SA	succinic acid
t	time
T	Temperature
THF	tetrahydrofuran
TMS	tetramethylsilane
UV	ultraviolet
V/V	volume by volume
Vis	visible
vpc	vapor phase chromatography
X	halogen
τ	chemical shift, ppm
δ	chemical shift, ppm; $\tau = 10-\delta$

Λ	molar conductivity
λ_{max}	wavelength of maximum absorption
ν	frequency, cm^{-1}
ε	molar extinction coefficient

For olefinic substrates abbreviations, see p.92.

ACKNOWLEDGEMENTS

I wish to thank Professor B. R. James for his expert advice and valuable suggestions during the course of this work.

I would like to express my gratitude to Dr. K. J. Reimer for introducing me to some useful synthetic techniques, to Dr. M. Preece for proof-reading this manuscript, and to Drs. R. Ball and J. Trotter for the crystal structure determination of a rhodium-diop complex.

Thanks are also due to Ms. Anna Wong for doing a superb job in typing this thesis.

CHAPTER I

INTRODUCTION

I.1 General

The separation of two enantiomeric forms of sodium ammonium tartrate by Louis Pasteur in 1848[1] has proved to be the dawn of a new era in chemistry. With an ever increasing understanding of processes going on in the human body and together with isolation of some chemical compounds involved in these processes, the importance of the role that enantiomeric forms play in our existence has been realized. Although enantiomeric (or mirror image) forms differ only in the direction that they rotate the plane of polarized light, clockwise or counterclockwise, usually for a specific process only one form is effective while the other may be useless or may even inhibit the particular process. Nature has provided enzymes to carry out the stereoselective chemistry necessary for life processes. However, most compounds in nature exist as racemic 'DL' mixtures and a ready separation of these biologically inactive compounds remains a challenging problem. Numerous compounds e.g. single isomers of monosodium glutamate[2,3], lysine[2,3], and menthol[4] have been produced efficiently using biochemical processes. Generally, production of optically active compounds involves use of large quantities of optically active reagents and optical yields of the stereoisomers are often quite low.

An alternative approach for resolution is available using catalytic asymmetric synthesis. There are many natural products where a hydrogen atom is on the chiral centre, usually carbon (C*). Such compounds can thus be generated in principle by hydrogenation of some unsaturated precursors.

Since most industrial processes involve heterogeneous catalysis, asymmetric hydrogenation studies were first started in the heterogeneous phase. In 1956 Akabori and coworkers[5,6] succeeded in affecting asymmetric hydrogenation of various oxime and oxazolone derivatives to optical yields of upto 35% using a catalyst consisting of metallic palladium adsorbed on silk. The same group subsequently achieved 50% e.e. in the hydrogenation of methylacetoacetate using Raney nickel modified with asymmetric molecules.[7] Today heterogeneous asymmetric catalysis appears less promising than the use of transition metal complexes (see below), although methylacetoacetate and amino-acid precursors have been hydrogenated with 90% optical yields in some cases.[8,9] The mechanism of these heterogeneous hydrogenation reactions is poorly understood, however, because of difficulties in defining the active sites at the metal surfaces.

Since Wilkinson's discovery[10,11] in 1965 that solutions of rhodium-phosphine complexes catalyzed hydrogenation of olefins under mild conditions, studies for asymmetric synthesis have been focused on the use of soluble transition metal complexes containing chiral ligands. The overall process involves activation of both substrate and hydrogen by the complex (cat*). During the hydrogenation process the chiral ligand on the metal may interact with the substrate in such a way that hydrogen subsequently adds preferentially to one face of the olefin and produces one enantiomer in excess over the other. Thus prochiral substrates can yield optically active products when the reaction is catalyzed by catalysts containing chiral ligands (equation [I.1]):

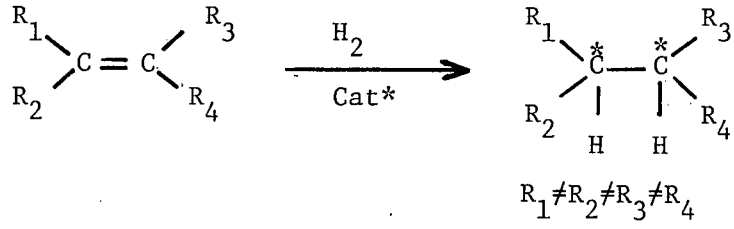

$R_1 \neq R_2 \neq R_3 \neq R_4$ [I.1]

Since 1968 many soluble metal complexes have been used for the asymmetric hydrogenation of various prochiral substrates, and the most efficient catalysts have been found to be rhodium-chiral phosphine complexes[12-17] (see section I.7). Recently α-N-acylaminoacrylic acids have been hydrogenated to corresponding products with almost complete stereospecificity.[18-20]

I.2 Scope of this thesis

Synthesis of a new chiral bis(ditertiaryphosphine) ligand '(-)-diop' [diop=2,3-O-isopropylidine-2,3-dihydroxy-1,4-bis(diphenylphosphino)butane] (Figure I.1) by Dang and Kagan[21] from cheap, naturally occurring (+)-tartaric acid, and subsequent use of the ligand with rhodium has proved very effective for asymmetric hydrogenation of olefins[21-23] and asymmetric hydrosilylation of ketones.[23] Since the earlier work, numerous reports have appeared involving the use of rhodium-mono(diop) complexes for asymmetric hydrogenation of olefins.[24-28]

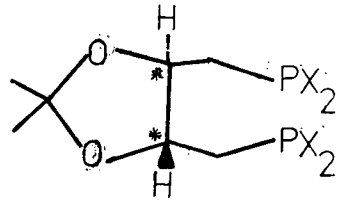

(*) = chiral centre

X = Ph

(-)-(2R,3R)-Diop

Figure I.1

The present work is based on the isolation of the first bis(diop)-rhodium complex, $HRh[(+)\text{-diop}]_2$, prepared in this laboratory by Cullen and coworkers.[29] The complex proved to be an efficient and effective catalyst for asymmetric hydrogenation of itaconic acid and α-N-acetamidoacrylic acid.[29] This finding contradicted a previous report[30] that rhodium-bis(diphosphine) complexes were inactive as hydrogenation catalysts. Detailed studies involving syntheses of various rhodium-bis(ditertiaryphosphine) complexes and their potential as homogeneous hydrogenation catalysts were thus undertaken in the present work (chapter IV). The first kinetic studies on the use of a bis(ditertiaryphosphine)-rhodium complex were presented recently and these described the hydridobis(diop)rhodium(I)-itaconic acid system[31]; this work showed that in the hydrogenation of such acid substrates, the catalyst slowly decomposed to $Rh(diop)_2^+$ species via reaction [I.2]:

$$HRh[(+)\text{-diop}]_2 + H^+ \longrightarrow Rh[(+)\text{-diop}]_2^+ + H_2 \qquad [I.2]$$

To avoid such a complication it was decided to carry out kinetic and mechanistic studies on styrene, a non-acidic substrate (chapter III).

Various complexes containing diop, which are described in chapter IV, were then used for the asymmetric hydrogenation of several prochiral substrates (chapter V). The effect of temperature, solvent, and other parameters on optical purities was also studied in detail and a general comparison made of the various mono(diop)- and bis(diop)-systems (chapter V).

The decomposition reaction [I.2] inadvertently produces a new catalytically active cationic species and since many of the reported

rhodium catalysts used in asymmetric hydrogenation are cationic, a kinetic study was also done on the $Rh[(+)\text{-diop}]_2^+$-itaconic acid system (chapter VI). Kinetic and mechanistic studies on a neutral[32] and a cationic[33] mono(diop)-rhodium system appeared during the course of the present studies, and these proved useful for comparison purposes (chapter VI).

Following reports by Pruchnik[34,35] that $[HRh(dpe)_2Cl]Cl$ is one of the most active homogeneous hydrogenation catalysts for olefin hydrogenation, various compounds of the type $[HRh(\overset{\frown}{PP})_2Cl]A$ ($\overset{\frown}{P\ P}$=dpm,dpe, and dpp;A=BF_4 or Cl) were prepared and tested for such hydrogenation to establish the effect of increasing chain length of the diphosphines (chapter VII).

Several other complexes were also isolated by adding CO, O_2, or H_2 to complexes of the type $Rh(\overset{\frown}{P\ P})_2^+$ described in chapter IV. The dihydride complexes so isolated proved useful in helping establish hydrogenation mechanisms discussed in chapters III, IV, and VI.

Variable temperature ^{31}P nmr was primarily used to establish the structure of the various phosphine complexes in solution (chapters IV and VII), while the solid state structure of $HRh[(+)\text{-diop}]_2$ has also been established using X-ray crystallography (chapter IV).

I.3 Modes of hydrogen activation

In general, mechanism of homogeneous hydrogenation of olefins at a metal centre involves three basic processes: (a) hydrogen activation, (b) substrate activation, and (c) a subsequent hydrogen transfer to give saturated products. It appears that irrespective of the detailed

hydrogenation mechanism, molecular hydrogen is at some stage split by the catalyst. This splitting results in the formation of a metal-hydride complex that is an active intermediate in hydrogenation reactions. Thus catalytic activity depends to a considerable extent on the stability and lability of these hydrido complexes. Effective hydrogenation catalysts were initially recognized as those containing group VIII metals in their lower oxidation (d^6-d^8) states. More recently several complexes of Ti, Hf, Zr and Nb with d^2 or d^3 configurations have been reported to be effective catalysts.[36]

Three recognizable pathways have been observed in the hydrogen activation process -

(a) Heterolytic splitting

This process has been observed in cases[37-39] where the complex usually has a substitutional lability. The overall hydrogen addition to the complex results in formation of a stable hydride complex with concomitant release of a proton. The released proton can be stabilized by some base that is present.[40] The process is thus a net substitution of a hydride ligand for another ligand with no change in the oxidation state of the metal (for example, equations [I.3] and [I.4]):

$$ML_n + H_2 \longrightarrow M\begin{matrix}L_n\\ H^-\\ H^+\end{matrix} \xrightarrow{\text{base}} ML_{n-1}H^- + H^+.\text{base} + L \qquad [I.3]$$

$$RuCl_6^{III\,3-} + H_2 \rightleftharpoons HRuCl_5^{III\,3-} + H^+ + Cl^- \qquad [I.4]^{37}$$

For example, in hydrogenations catalyzed by a ruthenium(II)

chloride system[41], the olefin molecule first coordinates to the metal; subsequent heterolytic splitting of H_2 followed by insertion into the Ru-H bond yields a σ-alkyl complex. Electrophilic attack by a proton at the carbon attached to the metal then results in release of the saturated product and regeneration of the Ru(II) catalyst[42] (Figure I.]):

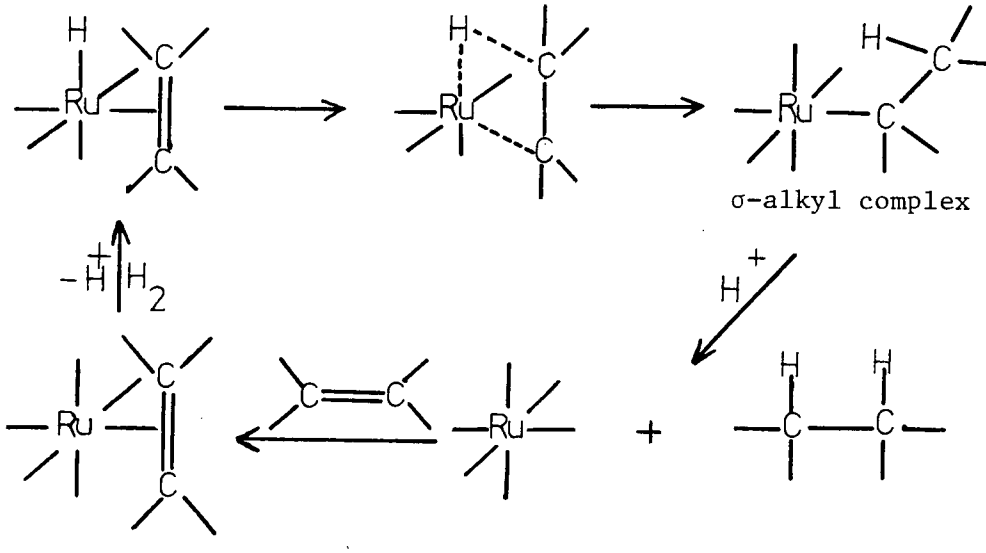

Mechanism for ruthenium(II) chloride-catalyzed hydrogenation of olefins.

Figure I.2

(b) Homolytic splitting

In this case hydrogen addition to the complex results in an increase of the oxidation state and, generally, the coordination number of the metal by one.[43-45] The driving force for the reaction is the susceptibility of the metal to oxidation and the ability to expand its coordination shell (equations [I.5] and [I.6]):

$$2ML_n + H_2 \rightleftharpoons 2ML_{n-1}H + 2L \qquad [I.5]$$

$$2[Co^{II}(CN)_5]^{3-} + H_2 \rightleftharpoons 2[HCo^{III}(CN)_5]^{3-} \qquad [I.6]$$

In this particular cobalt example, subsequent olefin insertion into the hydrido-cobalt complex gives an alkyl complex which in turn can react with another mole of hydride complex to produce saturated product and release the catalyst via equation [I.7].[46,47]

$$[(NC)_5Co\text{-alkyl}]^{3-} + [HCo(CN)_5]^{3-} \longrightarrow 2[Co(CN)_5]^{3-} + \text{alkane} \qquad [I.7]$$

The hydrogenation of arenes and alkenes, catalyzed by metal carbonyl hydrides, may also proceed through mechanisms in which intermediate free radicals are formed by H-atom transfer from the metal hydride to the olefin[48,49] (for example, equations [I.8]-[I.10])[49]:

$$HMn(CO)_5 + A \rightleftharpoons {}^{\cdot}Mn(CO)_5 + {}^{\cdot}AH \qquad [I.8]$$

$$HMn(CO)_5 + {}^{\cdot}AH \longrightarrow {}^{\cdot}Mn(CO)_5 + AH_2 \qquad [I.9]$$

$$2{}^{\cdot}Mn(CO)_5 \longrightarrow Mn_2(CO)_{10} \xrightarrow{H_2} 2HMn(CO)_5 \qquad [I.10]$$

(A=α-methylstyrene)

(c) Dihydride formation

Hydrogen activation can also be achieved if the metal atom has the ability to increase its oxidation state and coordination number by two[50,51], i.e. via oxidative addition (equations [I.11] and [I.12]):

$$ML_n + H_2 \rightleftharpoons ML_nH_2 \qquad [I.11]$$

$$Ir^{I}Cl(CO)(PPh_3)_2 + H_2 \rightleftharpoons Ir^{III}(H_2)Cl(CO)(PPh_3)_2 \qquad [I.12]$$

The formation of products and release of the catalyst can proceed via a subsequent coordination of olefin at the metal followed by consecutive transfer of two hydrogen atoms via a σ-alkyl hydride intermediate.[45,52]

It should be noted that an overall heterolytic splitting of H_2 can also result via initial oxidation adduct followed by reductive elimination of H-base, e.g. equation [I.13][53]:

$$Ru^{II}Cl_2(PPh_3)_2 + H_2 \rightleftharpoons [Ru^{IV}H_2Cl_2(PPh_3)_2] \rightleftharpoons HRu^{II}Cl(PPh_3)_2 + H^+ + Cl^- \qquad [I.13]$$

I.4 Rhodium catalysts in homogeneous hydrogenation

Although hydrogenation of inorganic and organic substrates catalyzed by rhodium(III)-amine complexes was known even back in 1935[54,55] it was not until about 1956, when Halpern's group[56-59] started investigating hydrogen activation by various metal ions in aqueous solution that such systems were shown to be homogeneous. The discovery of $RhCl(PPh_3)_3$ in 1965, as a versatile catalyst for homogeneous hydrogenation of olefins[10,11], established the catalytic activity of rhodium-phosphine complexes. Two basic mechanistic pathways have been established for the hydrogenation of olefinic compounds using either the neutral or the later discovered[60-66] cationic rhodium complexes (Figure I.3).

The K_1k_1 'unsaturate' route involves initial formation of a rhodium-olefin complex, followed by hydrogen addition and subsequent transfer of

hydrogen via a hydridoalkyl intermediate to give saturated product (H_2A) and Rh(I) catalyst. The K_2k_2 'hydride' route proceeds via an initial dihydride complex which after coordination to the olefin passes through the same hydridoalkyl intermediate before regenerating Rh(I) complex and giving the saturated product.

Extensive studies[67-75] on the $RhCl(PPh_3)_3$ complex have shown that this complex generally hydrogenates via the 'hydride' route with initial formation of a cis-dihydride intermediate complex $RhCl(H)_2(PPh_3)_3$ that has an extremely labile phosphine. The 'unsaturate' route has been found to operate in the hydrogenation of organic substrates with

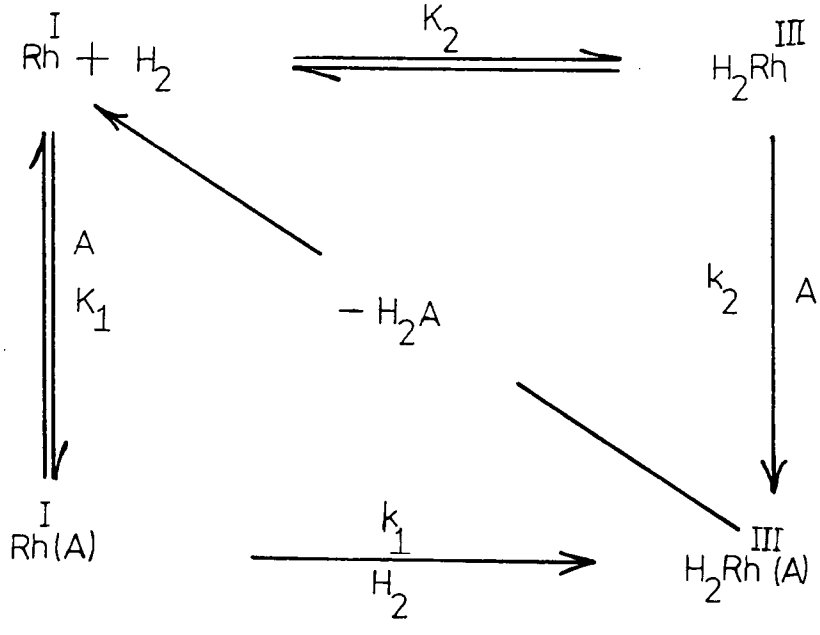

(A=olefin; H_2A=alkane)

Scheme for neutral and cationic rhodium(I) complexes.

Figure I.3

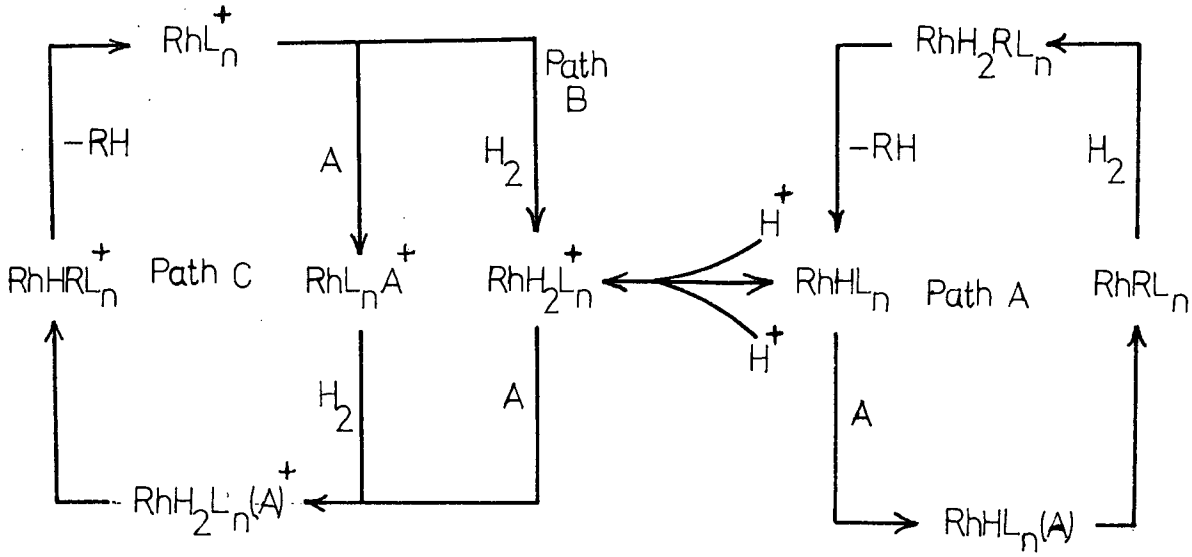

(A=olefin, n=2 or 3, R=alkyl, RH=alkane, L=ligand, S_x and S_y are omitted)

Pathways for olefin hydrogenation and isomerization.

Figure I.4

chlororhodate(III) species, and other phosphine free systems in DMA.[76] Hydrogenations of hex-1-ene using $HRh(PPh_3)_4$[77] or other related monohydride complexes (e.g. $HRh(CO)(PPh_3)_3$)[78] also proceed via 'unsaturate' routes.

One of the most active series of homogeneous catalysts is that provided by cationic complexes of the type $Rh(diene)L_2^+$ (L=tertiary phosphine, phosphite, or arsine), first used by Osborn's group[60-63] for hydrogenation of olefins, acetylenes, and ketones. These systems were subsequently studied extensively[64-66] and appear to operate via a 'hydride' route (equation [I.15]). The important equilibria governing formation of the active catalysts are given in equations [I.14]-[I.16]:

$$Rh(diene)L_n^+ + 2H_2 \longrightarrow \text{alkane} + RhL_nS_x^+ \qquad [I.14]$$

$$RhL_nS_x^+ + H_2 \longrightarrow RhL_nH_2S_y^+ \qquad [I.15]$$

$$RhL_nH_2S_y^+ \rightleftharpoons H^+ + RhHL_nS_z \qquad [I.16]$$

(n=2 or 3; x, y and z unknown; S=solvent)

An interesting feature of the cationic system is the reversibility of the two active catalysts illustrated in equation [I.16]. This equilibrium is sensitive to the nature of L and S, and can be shifted by adding acid or base to give solutions containing the dihydride or monohydride, respectively. The monohydride species is a powerful hydrogenation catalyst for simple olefins as well as an isomerization catalyst, whereas the dihydride is a moderately active olefin hydrogenation catalyst and does not give rise to concomitant isomerization. The catalytic cycles involved in both cases are summarized in Figure I.4.

Many other group VIII metal complexes especially those of Fe(0), Co(I), Ni(II), Pd(II), Ir(I), Pt(II), Pt(0), and Ru(II), have also been used for the catalytic reduction of olefins. The literature upto 1972 has been covered in a book by James[12] and other more recent reviews[17,79,80] have appeared.

The ability to fix transition metal complexes (particularly of rhodium) to various polymers, first described in patents[81], led Grubbs's group[82,83] to use such polymer-supported catalysts for hydrogenation of olefins. The resin used was commonly a copolymer of styrene and divinylbenzene incorporated with diphenylphosphino groups as potential coordinating sites for the metal. An advantage of using these systems is the easy separation of catalyst from the reaction mixture after the hydrogenation process. Many reviews have appeared on the subject of polymer-supported catalysts or the so called heterogenized homogeneous catalysts.[80,84-99]

I.5 Homogeneous hydroformylation

Cobalt and rhodium complexes have been found most effective for

hydroformylation of olefins to give aldehydes, and both metals have been used industrially.[100,101] Several papers and reviews[102-109] indicate that rhodium complexes are especially promising for the production of optically active aldehydes via asymmetric hydroformylation (for example, equation [I.17])[107]:

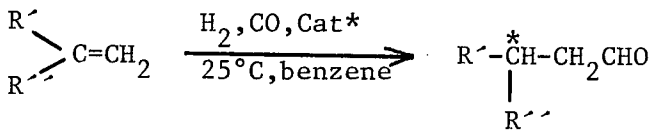

[I.17]

Cat*=in situ[$HRh(CO)(PPh_3)_3$+(-)-diop] (R)-22.7% e.e. for R´=H; R´´=C_6H_5

I.6 Solvent transfer hydrogenation of unsaturated compounds

This method involves hydrogenation of unsaturated bonds using solvent as a hydrogen source instead of molecular hydrogen. An example is the hydrogenation of ketones using alcoholic solvents, usually isopropyl alcohol, with various catalysts (equation[I.18]):

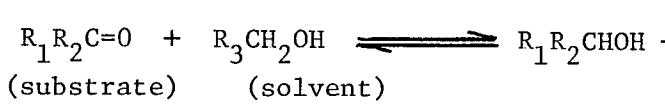

[I.18]

Widely studied compounds used in such hydrogenation of olefins, saturated and unsaturated ketones, and aldehydes, are phosphine complexes of rhodium(I) and ruthenium(II), e.g. $RhCl(PPh_3)_3$[110-112], $HRh(PPh_3)_4$[113], $RuCl_2(PPh_3)_3$[114-116], and $H_2Ru(PPh_3)_4$[117-119]. $HIrCl_2(DMSO)_3$[120,121] and $RhCl(DMSO)(PPh_3)_2$[122] are also effective. A not very well understood mechanism has been proposed for these hydrogen transfer reactions[110,111, 113,115,118,119] that have been reviewed.[123,124]

The fact that solvent is involved in the hydrogen transfer process led Descotes and Sinou[116] to use $RuCl_2(PPh_3)_2$ with a chiral glucofuranose derivative as a donor solvent. Asymmetric hydrogenation of prochiral α,β-unsaturated ketones to the saturated ketones was achieved with upto 34% e.e. in the case of cyclohexene-3-one. $Ru_2Cl_4(diop)_3$ and $RuCl_2L_3$[L= P*MePhR(R=o- or p-anisyl, benzyl, propyl) or neomenthyldiphenylphosphine] have been used for the hydrogenation of activated olefins using racemic alcohols such as 1-phenylethanol[125-128]; these systems are of interest in that they lead to slight resolution of the donor alcohol. An in situ rhodium(I) catalyst with neomenthyl phosphine has also been used similarly.[129] Optical purities upto 22% have been achieved in the transfer hydrogenation of α-methylcrotonic acid by a chiral ruthenium-phosphine complex in alcoholic solvents.[130]

I.7 Asymmetric homogeneous hydrogenation

In 1968, Horner and coworkers[131-133] reported the hydrogenation of α-ethylstyrene and α-methoxystyrene to S-(+)-2-phenylbutane (7-8% e.e.) and R-(+)-1-methoxy-1-phenylethane (3-4% e.e.), respectively, using an in situ rhodium catalyst containing the chiral phosphine S-(+)-$P^*MePhPr^n$. Knowles and Sabacky[134] at about the same time hydrogenated atropic acid and itaconic acid to hydratropic acid (15% e.e.) and 2-methylsuccinic acid (30% e.e.), respectively, using $RhCl_3L_3$(L=$P^*PhMePr^i$). The optical yield with atropic acid was reduced drastically from 15% to 1% e.e. with L=$PPh(CH_2\overset{*}{C}HMeEt)_2$ where the chirality was on the carbon atom of an alkyl group rather than on the phosphorus atom.

Optical yields of >50% were then obtained in the hydrogenation of

methyl-3-phenyl-but-2-enoate to methyl-3-phenylbutanoate using McQuillin's catalyst formed from $[py_2SRhCl_2BH_4]$ where S is a chiral amide solvent such as $PhCH^{*}MeNHCHO$, $PhMe^{*}NHCHO$ etc..[135,136] Morrison et al.[137] achieved the reduction of (E)-α- and (E)-β-methylcinnamic acids and atropic acid to products with 61% e.e., 52% e.e., and 28% e.e. respectively using $RhClL^{*}_3$ (L^{*}=I in Figure I.5) complex as catalyst.

It was in 1972 when Kagan and Dang[21,22] first reported the preparation of diop (Figure I.1), and used it effectively to hydrogenate α-acylaminoacrylic acids in >70% e.e. with in situ rhodium catalyst. Optical yields of upto 90% were later achieved by Knowles et al.[138,139] in some cases.

Various other rhodium complexes have been used for the asymmetric hydrogenation of prochiral olefinic substrates. Figure I.5 lists some representative ligands (I to XV) which form effective catalysts when bound to a rhodium centre. Other metals, e.g. Ru(II), Pt(II), Ni(II), Ir(I), Co(II), etc., have also been used but generally these have been found to be less effective or less efficient at least for the asymmetric hydrogenation of α,β unsaturated acids and ketones.[17]

Since mono(diop)-rhodium systems have been found to be efficient and effective catalysts[21-28], studies have been directed using these complexes to establish the mechanism by which hydrogenation takes place. This work was published during the course of the present studies. A mechanism involving a 'hydride' route, proposed by Gelbard and Kagan[27] for a neutral mono(diop)-rhodium system is almost certainly incorrect judging by a more recent ^{31}P nmr study on an analogous cationic mono(diop)-rhodium complex[33] where it was shown that hydrogenation proceeded via an 'unsaturate' route. This later study parallels other work done on

I. (+)-Neomenthyldiphenylphosphine (NMDPP).

II. (-)-(2R,3R)-O-Isopropylidene-2,3-dihydroxy-1,4-bis(diphenylphosphino)butane (Diop), X=Ph.

III. (+)-O-Anisylcyclohexylmethylphosphine (ACMP).

IV. (R,R)-1,2-Ethanediylbis[O-anisylphenylphosphine] (BAPPE).

V. (2S,3S)-Bis(diphenylphosphino)butane (CHIRAPHOS).

VI. (S)-α-[(R)-2-Diphenylphosphinoferrocenyl]ethyl dimethylamine ([S,R]-PPFA), X_1=H; X_2=NMe_2.

VII. (+)-1,2,2-Trimethyl-1,3-bis(diphenylphosphinomethyl)cyclopentane (CAMPHOS).

VIII. cis-Myrtanyldiphenylphosphine (MYRTPHOS).

IX. (1S,2S)-trans-1,2-Bis(diphenylphosphinomethyl)Cyclobutane.

X. Menthylmethylphenylphosphine (MMPP).

XI. (2S,4S)-4-Diphenylphosphine-2-diphenylphosphinomethylpyrrolidine (PPM), R=H.

XII. 2,2-Bis(diphenylphosphinitemethyl)-1,1-binaphthyl, X=O.

XIII. trans-1,2-Bis(diphenylphosphinoxy)cyclohexane (BDPCH), n=4.

XIV. 1,2-Bis(N-diphenylphosphino,N-methylphenylmethyl amino)ethane.

XV. Methyl 2,3-bis-O-diphenylphosphino-4,6-O-benzylidene-α-D-glucopyranoside.

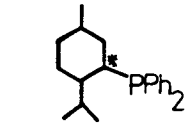

I[137]

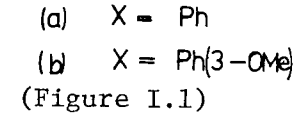

(Figure I.1)

II

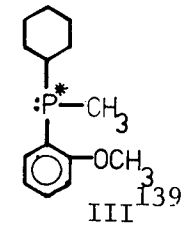

III[139]

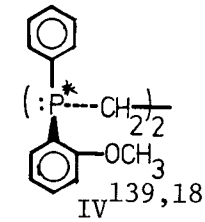

IV[139,18]

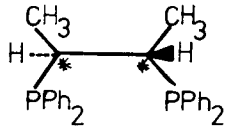

V[19]

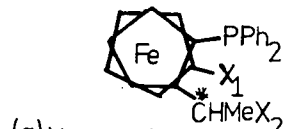

VI

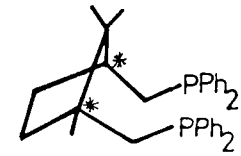

VII[16,141]

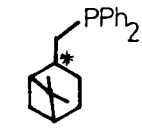

VIII[16,141]

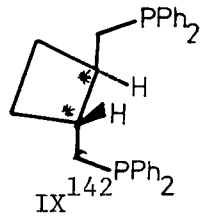

IX[142]

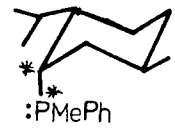

X[143]

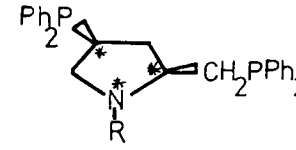

XI[144]

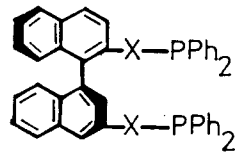

(a) X = CH_2
(b) X = O

XII[145]

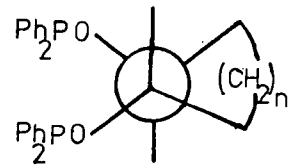

(a) n = 3
(b) n = 4

XIII

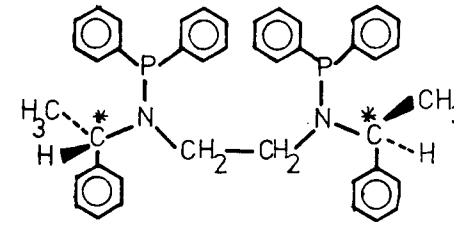

XIV[148]

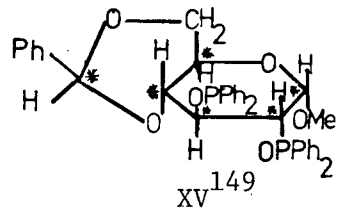

XV[149]

Chiral centre (*)

Some effective ligands used in catalytic asymmetric hydrogenation (chirality is at carbon, or phosphorus, or both).

Figure I.5

$[Rh(NBD)dpe]^+$ by Halpern et al.[150], but the findings are in contrast to rhodium-bis(monodentate phosphine) systems where hydrogenation proceeds via a 'hydride' route.[64-66,75] A detailed kinetic study using an in situ [RhCℓ(diop)S] (S=solvent) catalyst has also appeared[32], and suggests that the hydrogenation proceeds via both the 'hydride' and 'unsaturate ' routes.

Glaser et al.[142,151-155], in order to rationalize the cause of asymmetric induction, have presented a stereochemical model for neutral mono(diop)-rhodium catalyzed hydrogenations using space-filling CPK-type molecular models, considering only steric effects. Thus using the model shown in Figure I.6, they were able to predict correctly the configuration of the major products from hydrogenation of various amino acids e.g. $CH_2=C(S)(L)$ except in two cases ($S=CO_2Me$,L=Ph and S=Et, L=Ph).

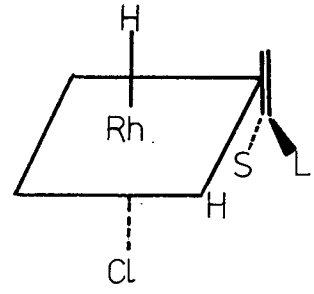

S=small
L=large

Stereochemical model proposed for olefin hydrogenation catalyzed by neutral mono(diop)-rhodium complexes.

Figure I.6

Glaser's group has also done studies[142,151-155] in terms of determining the effect on optical purity of various substituents at the double bond of the substrate. These studies have been augmented by the determination of the crystal structure of a related iridium complex [Ir(COD)(diop)Cℓ], which is a distorted trigonal bipyramid in which diop

is an apical-equatorial bidentate ligand.[156]

Bosnich's group have reported[19] the preparation of $[Rh(COD)(S,S\text{-chiraphos})]^+C\ell O_4^-$ (chiraphos=V in Figure I.5), and with this catalyst α-N-acylaminoacrylic acids were hydrogenated with 91-100% optical yields. These excellent optical yields were explained on the basis that of the two normally interconvertible conformations for saturated five-membered chelate rings[157] (Figures I.7 (a) and (b)), chiraphos (a five-membered ring substituted at the aliphatic link) adopts only one static conformation (a).

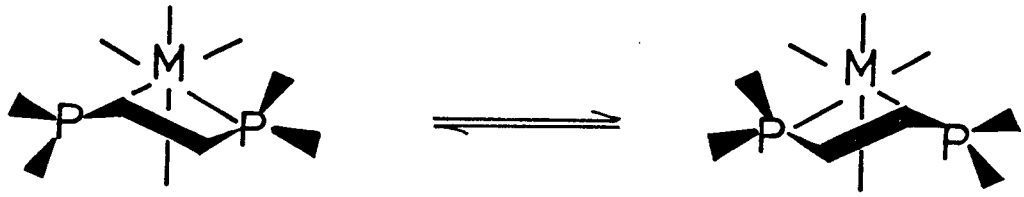

(a) (b)

Possible conformations of saturated five-membered chelate rings

Figure I.7

This has been confirmed by determination of the crystal structure of the $[Rh(COD)(S,S\text{-chiraphos})]^+$ complex (Figure I.8).[158]

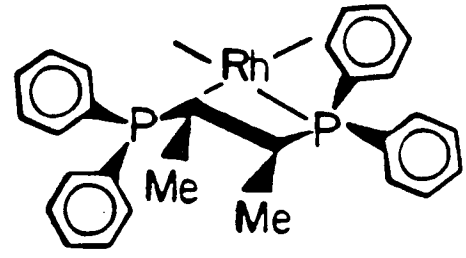

Crystal structure of the $[Rh(COD)(S,S\text{-chiraphos})]^+$ complex

Figure I.8

From the structure it appeared that the orientation of phenyl groups held by the puckered chelate ring was responsible for the diastereotopic interaction that discriminates the prochiral faces of the substrate. A similar explanation has also been presented by Knowles's group[18,159] to explain the greater than 90% e.e. obtained in the hydrogenation of α-N-acylaminoacrylic acids using $[Rh(1,5\text{-}COD)L_2]^+ C\ell O_4^-$ where L_2 is the ligand shown in Figure I.5(IV).

Good optical yields in other cases, e.g. hydrogenation of α-benzamidocinnamic acids with a $[Rh(COD)(diop)]^+$ catalyst, have been attributed to (1) conformational rigidity of the diphosphine, and (2) the participation of the acetamido group which coordinates to rhodium metal via the O atom; a recent variable temperature ^{31}P nmr study[33] confirms bonding by the amide group.

Asymmetric hydrogenation of saturated ketones to alcohols has also been achieved using various chiral phosphine ligand systems.[160-163] Optical purities upto 83% have been achieved for the hydrogenation of pyruvic to lactic acid using a Rh-BPPFOH catalyst[160] (Figure I.5(VI), $X_1=PPh_2, X_2=OH$). Pyruvates are also converted to lactates in 65-75% e.e.

$$CH_3COCO_2R + H_2 \longrightarrow CH_3\overset{*}{C}H(OH)CO_2R \qquad [I.19]$$

using BPPM and CPPM ligand systems[161-163] (Figure I.5(XI), BPPM ($R=CO_2\text{-}Bu^t$) and CPPM ($R=CO_2C_{27}H_{45}$)). The C=N bond of the Schiff base $PhMeC{=}NCH_2Ph$ has also been reduced with 22% e.e. using the $[Rh(NBD)(diop)]^+C\ell O_4^-$ complex in alcoholic solvents.[164]

Ketones and imine groups can also be reduced readily via a hydrosilylation procedure followed by acid hydrolysis to give the optically

active alcohols or amines (equation [I.20]):

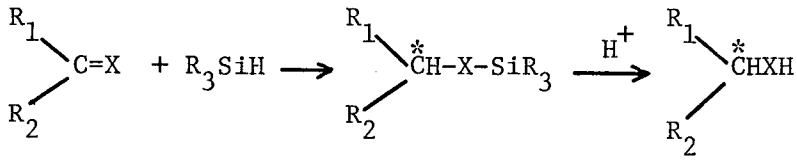

[I.20]

$R_1 \neq R_2$; X=O (ketones); X=N-R (imines)

This procedure gives optical purities upto 60-85% for the hydrogenation of pyruvates and glyoxalate substrates $R_1COCO_2R_2$ (R_1=Me,Ph; R_2=alkyl or menthyl).[165] Secondary imines have been isolated in upto 65% e.e. while aromatic amines give products upto 39% e.e.[24,166] These and other references have been catalogued in a recent review by James.[17]

A clearer insight generally into the cause of asymmetric induction has been provided by Bosnich's group[19,167] who discuss two types of interaction that occur between chiral molecules: (a) a total interaction which may be quite large, and (b) part of interaction (a) which is discriminatory and leads to asymmetric induction. This asymmetric induction is further attributed to three types of interactions: (a) ligand-olefin (b) metal-olefin, and (c) ligand-metal. To understand the importance of these interactions, a study was conducted on [cis-$PtCl_2$(S-MPTSO)(olefin)] complexes(MPTSO=methylp-tolyl sulfoxide; olefin=ethylene, propene, butenes, styrene, etc). The following conclusions were drawn on the basis of nmr data:-

(1) The olefin moiety in the two diastereomers is rotating as seen from fluxional behaviour on the nmr time scale. This fluxional exchange can

occur either by complete rotation about the olefin-platinum axis (e.g. as with ethylene), or by an oscillatory motion, where one end of the olefin always passes through the same cis group but is unable to pass the other under the same conditions (e.g. as with but-1-ene, propene etc.). These conclusions were based on an earlier study by Lewis[168] on [cis-$PtCl_2$(L)(olefin)] complexes, where it was shown that a cis halogen offered more hindrance to rotation than other cis ligands.

(2) The total interaction between the olefin and the sulfoxide undoubtedly increased as the bulk of the olefinic side-chains was increased, but contrary to expectation only marginal increase in diastereotopic interaction was observed. Furthermore, the chiral sulfoxide generated diastereomers of opposite configuration with the two closely related olefins, propene and 1-butene, suggesting that the chiral sulfoxide ligand itself was rotating. With rotation of the chiral sulfoxide ligand, the distinction between the prochiral faces of coordinated olefins is essentially 'washed out', and even increasing the bulk of substituent groups on the olefin gave very small asymmetric induction.

CHAPTER II

GENERAL EXPERIMENTAL

All solutions were handled under an argon atmosphere using Schlenk techniques.[1]

II.1 Materials

II.1.1 Solvents - A.R. grade solvents were used without purification, but were stored over molecular sieves (BDH,type 5A) for synthetic purposes and were vacuum-degassed before use.

For hydrogenation experiments all the solvents were distilled before use. Toluene was refluxed with calcium hydride, alcohols with magnesium metal and iodine mixture, while DMA was stirred overnight with calcium hydride and then vacuum distilled. After distillation, all solvents were stored in flasks under an argon atmosphere over molecular sieves (BDH, type 5A), except alcohols which were stored without molecular sieves. DMA was stored in the dark.

II.1.2 Gases - Research grade hydrogen and C.P. grade carbon monoxide were obtained from the Matheson Gas Co.. Purified argon and oxygen were supplied by Canadian Liquid Air Limited. Hydrogen was passed through a "deoxo" catalytic purifier before use. Argon was purified by passing it through a calcium chloride drying tower containing fresh P_2O_5 and molecular sieves (BDH,type 5A). Lecture bottles of anhydrous hydrogen chloride were obtained from the Matheson Gas Co. and were used without further purification.

II.1.3 Diphosphines - Dpm, dpe, dpp, and (+)-diop diphosphines were obtained from Strem Chemicals Inc.. A literature method[2] with a slight modification was used to prepare dpb as follows -

26.5 g (0.12 mole) of $P(C_6H_5)_2C\ell$ in 150 ml of dioxane (dried over

molecular sieve) was refluxed with 12.5 g (0.5 mole) of sodium under nitrogen for 7h with strong mechanical stirring to generate $P(C_6H_5)_2Na$. The yellow reaction mixture was cooled to room temperature, and 100 ml of anhydrous THF then added. 9.72 g (0.045 mole) of 1,4-dibromobutane in 50 ml THF was then added dropwise and the mixture stirred for 2h. The solid NaBr was filtered off, washed with benzene, and the filtrate then evaporated to dryness on the rotary evaporator. The remaining residue was dissolved in 60 ml ethanol which was then cooled to 0°C. After few hours, a yellowish white solid precipitated and this was filtered and washed with cold ethanol. The crude diphosphine was recrystallized twice from ethanol to give pure white crystals of dpb (yield ∿60%).

All diphosphines were recrystallized from hot ethanol before use.

II.1.4 Olefins - Olefinic substrates were obtained as C.P. grade.

Itaconic acid, mesaconic acid, maleic acid, and α-methylstyrene were supplied by Eastman Kodak Co., acrylamide by K & K Laboratories Inc., α- and β-methylcinnamic acids by Aldrich Chemical Co. Inc., α-N-acetamidocinnamic and -acetamidoacrylic acids, and citraconic acid by Fluka Chemical Co. Hex-1-ene was obtained from ICN Pharmaceuticals Inc., and styrene and cyclohexene from MCB Co.. Atropic acid was prepared by a known procedure.[3]

Liquid olefins were distilled and passed through an alumina column before use. Solid olefins were recrystallized from hot ethanol.

II.1.5 Inorganic silver salts - $AgSbF_6$, $AgPF_6$, and $AgBF_4$ were supplied by Alpha Inorganics and Cationics Inc., and were stored in a vacuum desiccator for protection from moisture.

$RhCl_3.3H_2O$ was a loan from Johnson Matthey Limited (39%Rh).

II.2 Instrumentation

All infrared (ir) spectra were recorded on a Perkin Elmer 457 grating spectrophotometer. Solid state spectra were obtained as Nujol mulls between NaCℓ, KBr, or CsI plates and solution spectra were recorded using 0.1 mm NaCℓ cells.

Visible spectra were recorded on Perkin Elmer 202 or Cary 14 spectrometers, both instruments being fitted with thermostated cell compartments. Quartz cells of path lengths 1 mm, 2 mm, and 10 mm were used.

All ^{1}H nmr spectra were measured using a T-60 or XL100 spectrometer. Tetramethylsilane (TMS) was used as an external or internal standard.

^{31}P Nmr spectra were obtained at 40.5 MHz using a XL100 spectrometer operating in the Fourier Transform mode and equipped with a variable temperature attachment. A P_4O_6 capillary was used as an external standard for room temperature spectra, while solutions of triphenylphosphine were used as a standard for low temperature spectra. All chemical shifts were then converted to values relative to 85% H_3PO_4, with upfield shift taken as positive.

Conductivity measurements were made at 25°C under argon using a Thomas Serfass conductivity bridge and cell.

Melting points were recorded using a Fisher Johns Melting Point apparatus and are uncorrected.

Elemental analyses were performed by Mr. P. Borda of this department.

II.3 Gas-uptake apparatus

The constant pressure apparatus shown in Fig. II.1 was used for

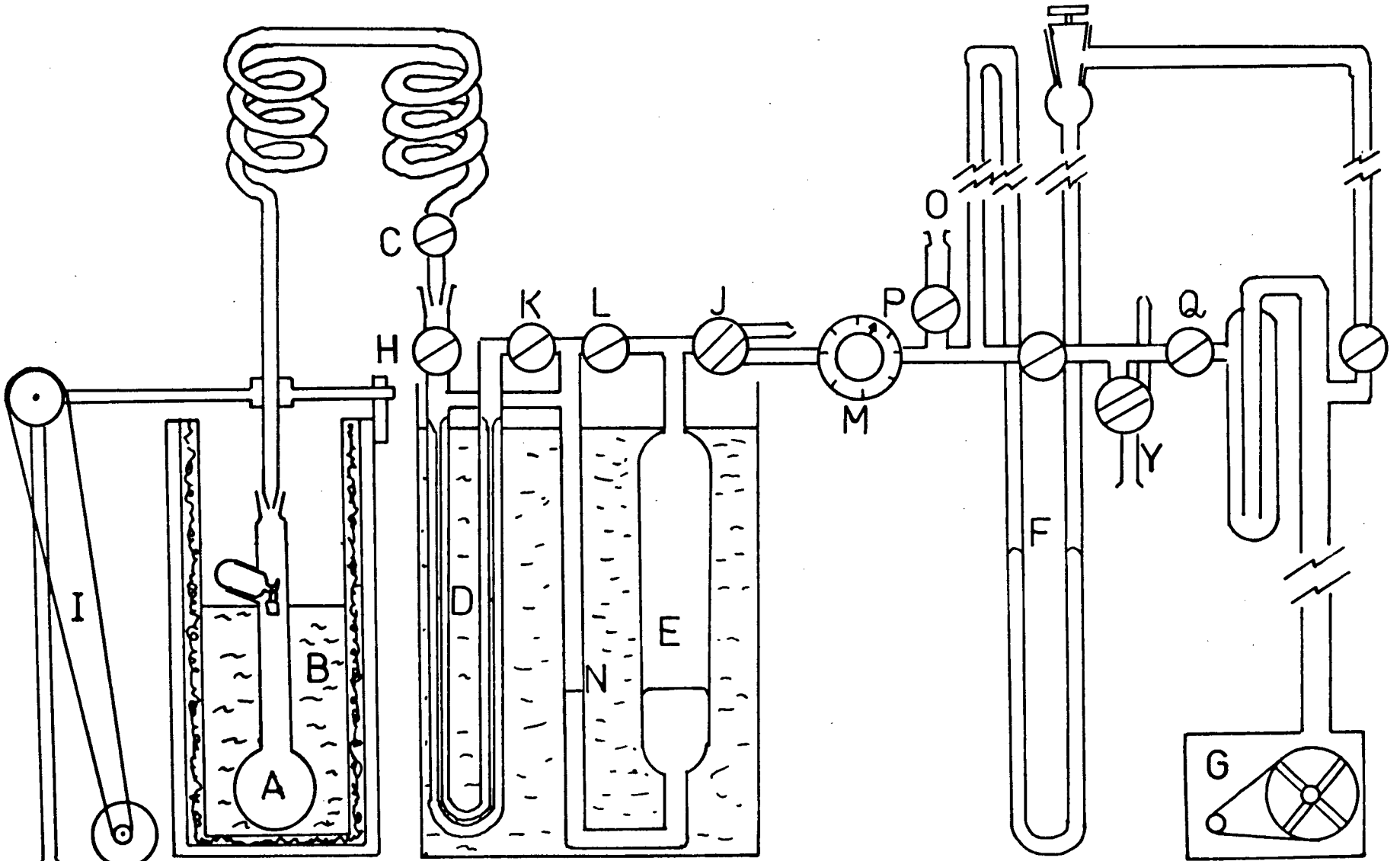

Figure II.1. Constant pressure gas-uptake apparatus.

kinetic and for stoichiometric gas uptake experiments. A flexible glass spiral tube connected a capillary manometer D at tap C to a pyrex two-necked reaction flask A equipped with a dropping side arm bucket. The reaction flask was thermostated in an oil bath B and shaken by means of a piston-rod and driven by an offset wheel connected to a Welch variable speed electric motor. The manometer D contained n-butyl phthalate and was connected to a gas-measuring burette consisting of a mercury reservoir E and a 10 ml pipette N of known diameter. The gas burette was connected via an Edwards high-vacuum metering valve M to the gas-handling part of the apparatus. This part consisted of a mercury manometer F, gas inlet Y, and vacuum pump G. The capillary manometer and gas burette were thermostated at 25°C in a perspex water-bath. Thermostating of the oil bath and water bath was controlled by Jumo thermo-regulators and Merc to Merc rely control circuits, with heating accomplished by a 40 watt elongated light bulb. The baths were well stirred, and the oil bath insulated, the temperature being held to ±0.05°C. A vertical mounted cathetometer followed the gas uptake in the burette, and time was recorded with a Labchron 1400 timer.

II.4 Gas-uptake experimental procedure

In a typical gas-uptake experiment, 5 ml of solvent was placed in the 25 ml reaction flask A. Weighed substrates were added to the solvent directly and weighed catalyst via the bucket after the solvent was degassed and the flask filled with reactant gas. Degassing for DMA solvent was effected by pumping on the solvent while shaking. For higher vapour pressure solvents the freeze thaw under static vacuum technique was employed. For both methods a degas-refill cycle was repeated three times.

Initially the reaction flask was filled with reactant gas via 0 at a pressure somewhat less than that required for the experiment (Fig.II.1). The taps C and P were then closed and the reaction flask complete with spiral disconnected from 0 and attached to H and the shaker rod. The whole system up to tap C was then pumped down with taps H, K, L J and M open. Reactant gas was admitted to this part of the system at a pressure greater than that in the reaction flask but less than that desired for the reaction. After thermal equilibration of the reaction flask was attained (≈15 min), tap C was opened and the pressure of the whole system adjusted to the desired reaction pressure by introduction of gas through Y.

Shaking of the reaction vessel was then done to saturate the solvent with gas at the reaction pressure (≈5 min). An experimental run was then started by dropping the catalyst bucket, starting the shaker, closing taps K and L and starting the timer. Gas-uptake was indicated by a difference in oil levels in manometer D. The manometer was balanced by admitting gas into the burette through the metering valve M. Corresponding changes in mercury levels in the pipette N were translated to moles of gas reacted.

Diffusion control of the reaction was eliminated by using fast shaking rates and a large indented reaction flask.

II.5 Solubility determination

5 ml of the solvent was put into the reaction flask A which was then connected by the spiral and tap C to the gas-handling part of the apparatus at 0. The solution was then degassed by alternate cooling with pumping and warming, and then taps C and P were closed. The flask and spiral arrangement were disconnected from 0 and transferred into the

thermostated oil bath with the spiral connected to the oil-manometer D through tap H. Needle valve M and tap H were opened and after the air between taps H and C was pumped out, tap Q was closed Tap C was opened and the initial reading of the mercury level in N was taken. The desired gas was admitted to the gas uptake apparatus at a desired pressure. Taps K and L were closed after closing tap J and needle valve M. The timer and the shakes were started simultaneously and the uptake of the gas was measured.

II.6 Stoichiometric gas-uptake measurements

Several of the complexes in this work were sensitive in the solid state to gases, and so ampoules instead of buckets were used in the uptake procedure. A bulb was blown on a glass tube, a constriction was placed in the stem and a glass rod was melted onto the bottom of the bulb to weaken it. The latter trick was essential to guarantee breakage of the ampoule. After being tested for leaks, the bulb was filled with sample and then sand, and then sealed off under argon using the hydrogenation balloon to regulate the pressure as in Figure II.2. These precautions minimize gas uptake when the ampoule breaks. The glass was sealed off in the shape of a hook (Figure II.2) so that the ampoule can be hooked to the bucket dropper of the uptake flask.

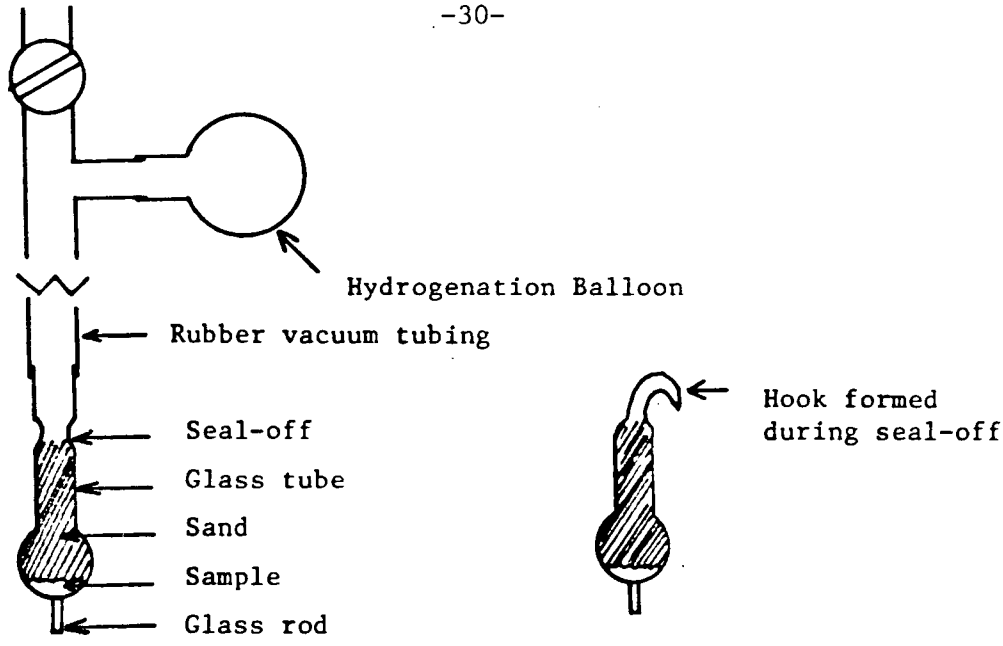

Figure II.2

II.7 Spectrophotometric kinetic measurements

All optical density measurements in the ultraviolet visible region were carried out with the cell shown in Figure II.3. In a typical reaction involving gas-uptake, use of a relatively large volume of gas ($\sim$25 ml), with low rhodium concentrations ($\sim 10^{-3} - 10^{-4}$ M) in small volumes of solution ($\sim$5 ml), ensured that the partial pressure of the gas over the solution remained essentially constant throughout the reaction. In a typical experiment, a known amount of a compound was added into the quartz part of the cell through A (Figure II.3) and the solvent and the substrate (if any) were added through B using a pipet. The solvent was degassed three times and the required gas was then admitted. Upto this point, the cell was handled carefully so as not to wet the solid. The cell was then placed in the thermostated cell compartment to allow the solution temperature to equilibrate. The solvent and the solid were then quickly mixed and the spectrum was recorded at regular intervals. During spectral measurements, the cell was agitated to ensure thermal and physical equilibration of the solution.

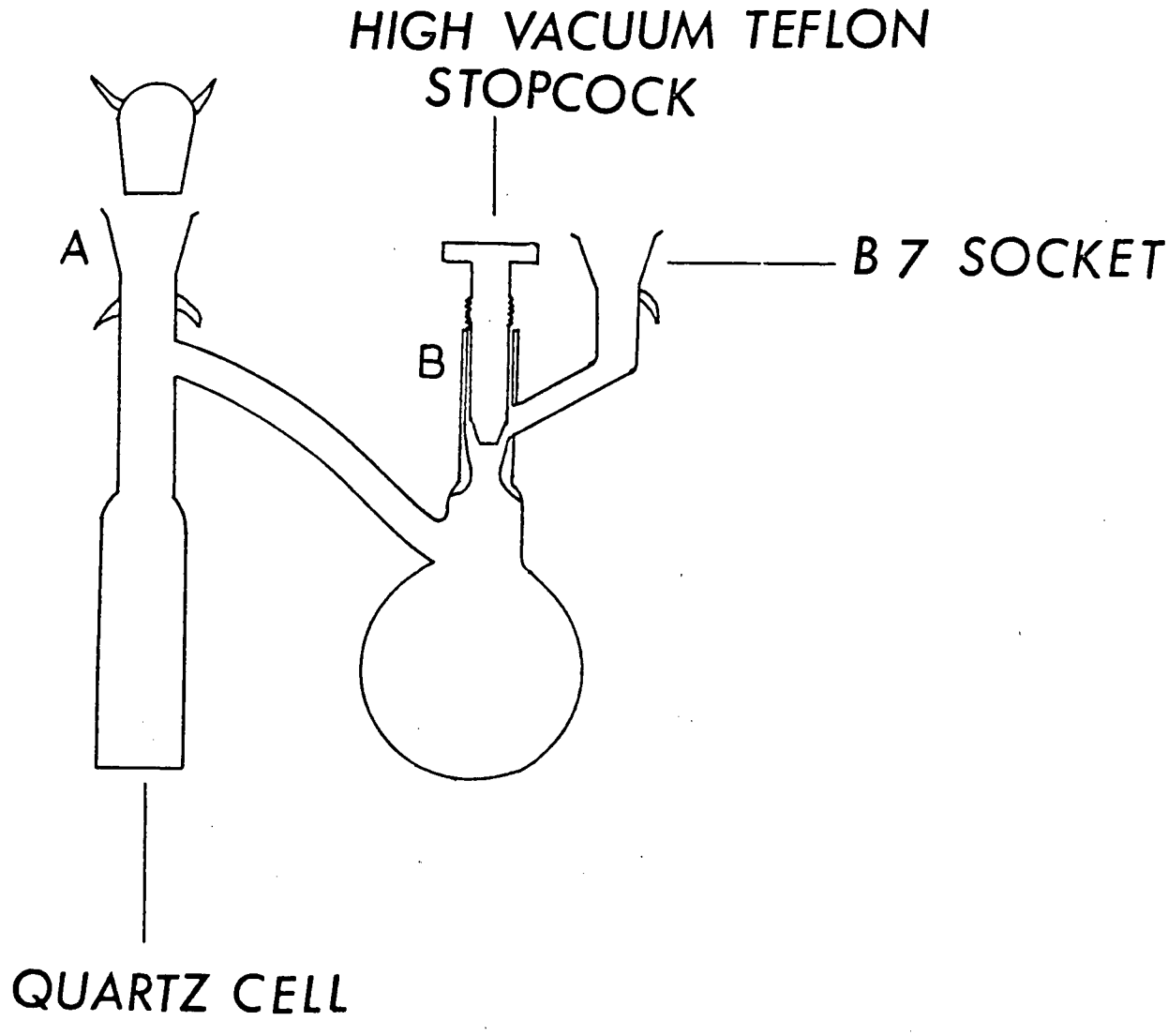

Figure II.3 Anaerobic spectral cell

II.8 Fast reaction measurements

All fast reactions were studied by means of a Durrum 110 stopped-flow spectrophotometer equipped with a 2 cm path length cuvette and a thermostated cell compartment. During a typical experiment, a solution of the complex ($\sim 10^{-4}$ M) in a solvent, under argon, was mixed with the same solvent saturated with the desired gas at a known pressure.

II.9 Work-up of the hydrogenated products

The solution mixture resulting from hydrogenation experiments was evaporated to give a gummy residue. The hydrogenated products of the following olefins were separated as follows -

II.9.1 Itaconic, citraconic, maleic, and atropic acids - The residue was dissolved in 25 ml of 5% NaOH solution, stirred for a few minutes and filtered through Celite to give a colorless filtrate. After acidifying with 10% HCℓ the solution was extracted twice with diethyl ether (25 ml). Anhydrous $MgSO_4$ was added to the ether extract. After $\sim$½h the solution was filtered and the final product obtained after evaporation of the ether.

II.9.2 N-α-acetamido-acrylic and-cinnamic acids - The residue was dissolved in $CH_2C\ell_2$ ($\sim$10 ml) and the mixture stirred for few minutes when a yellowish white compound separated; this was washed with $CH_2C\ell_2$ to give a pure white product that was recrystallized by dissolution in water ($\sim$5 ml) and extraction with chloroform ($\sim$15 ml). The aqueous layer was then freeze-dried to recover the pure product.

II.9.3 Liquid olefins - The hydrogenated solutions from styrene and α-methylstyrene were vacuum-distilled, and that from hex-1-ene was distilled at one atmosphere, a microscale distillation apparatus being used.

II.9.4 Acrylamide - The residue was heated to 100°C under vacuum when white crystals of propionamide sublimed.

The products so obtained were identified from their ^1H nmr spectra.

II.10 Optical rotation measurements

All optical rotation values were recorded on a Perkin Elmer 141 spectrometer at room temperature using a one decimeter path-length cell which could hold 1 ml of solution. The rotations were measured at the sodium-D line (589 nm).

The specific rotation of any chiral compound can be calculated using equation [II.1]:

$$[\alpha]_D^T = \frac{\alpha}{\ell x c} \qquad [II.1]$$

where $[\alpha]_D^T$ = specific rotation at temperature T measured at the sodium-D line.

α = observed rotation (+) or (-).

ℓ = path length of the cell in decimeters.

c = concentration of solution in g/ml.

The enantiomeric excess (e.e.) of the hydrogenated product was then determined using equation [II.2]:

$$\text{e.e.} = \frac{[\alpha]_D^T \text{ (from equation [II.1])}}{[\alpha]_D^T \text{ of either pure form of the product}} \times 100 \qquad [II.2]$$

CHAPTER III

HOMOGENEOUS HYDROGENATION OF ACIDIC AND NON-ACIDIC SUBSTRATES USING THE HYDRIDOBIS(DIOP)RHODIUM(I) COMPLEX

III.1 Introduction

In the last decade, the area of asymmetric homogeneous hydrogenation has been studied extensively. General reviews[1-3] have appeared from time to time to keep pace with the important developments in this field. One general conclusion, drawn from the data obtained so far using various transition metal complexes, is that rhodium-chiral phosphine complexes have proved to be the most effective asymmetric hydrogenation catalysts (see section I.7, chapter I). Indeed quite recently, Bosnich and Fryzuk[4] have used rhodium-bis(diphosphine) catalysts for the reduction of N-acylaminoacrylic acids to amino-acid derivatives in almost 100% e.e.; some other rhodium complexes are almost as effective (section I.7, chapter I).

A widely used and commercially available chiral phosphine is the so-called "diop" (Figure I.1), initially synthesized by Kagan's group[5,6], and the catalysts have usually been generated *in situ* by adding diop to rhodium(I) precursors such as $[RhCl(diene)]_2$ or $[RhCl(olefin)_2]_2$. The active species have been written as RhCl(diop)(solvent)[2,6] although in the polar medium usually employed, cationic species seem likely, and $[Rh(diene)(diop)]^+$ complexes are equally effective.[2,3,7,8] Recently, some mono(diop)-rhodium complexes have been isolated and formulated, for example, as $[RhCl(diop)(C_6H_6)]_2$.[9] These isolated complexes, along with other *in situ* mono(diop)-rhodium complexes, have been used effectively for the hydrogenation of olefins and ketones (for details see section I.7,

chapter I).

Synthesis of a bis(diop)-rhodium(I) complex, $HRh[(+)\text{-diop}]_2$, and its effective use in asymmetric hydrogenation[10] was of interest because the related chelated complex $Rh(dpe)_2^+$ is relatively inactive for hydrogenation under mild conditions.[11] A kinetic and mechanistic study was thus undertaken on the $HRh[(+)\text{-diop}]_2$-itaconic acid system[12,13], and since this work formed the basis of many of the studies described in this thesis, a summary of this mechanistic study is given in section III.3 together with some new ^{31}P and ^{1}H nmr data. Studies involving a non-acidic substrate, styrene, will then be described.

III.2 Experimental

$HRh[(+)\text{-diop}]_2$ was prepared using the literature method.[10] In a typical preparation, 0.13 g (0.5 mmol) of $RhCl_3.3H_2O$ in ethanol (5 ml) and 0.20 g (3.6 mmol) of KOH in ethanol (10 ml) were successively added to a vigorously stirred and boiling solution of 0.55 g (1.1 mmol) of (+)-diop in 15 ml ethanol. A yellow solid separated instantaneously and this was filtered, washed with ethanol, water, ethanol, and finally with n-hexane. The yellow solid was recrystallized from warm n-hexane to give yellow flaky needles (yield ~70% based on Rh), and was characterized by high-field ^{1}H nmr (21.0τ in benzene-d_6 at 20°C) and ir (ν(Rh-H)=2040 cm^{-1} in Nujol), as well as by elemental analysis.

The solubility of hydrogen in n-butanol-toluene mixtures at different pressures and temperatures was calculated from the data in Figures III.1 and III.2 respectively, assuming Henry's law is applicable at each temperature. It is surprising that the solubility increases with temperature (Fig.III.2) but the data were reproducible and are

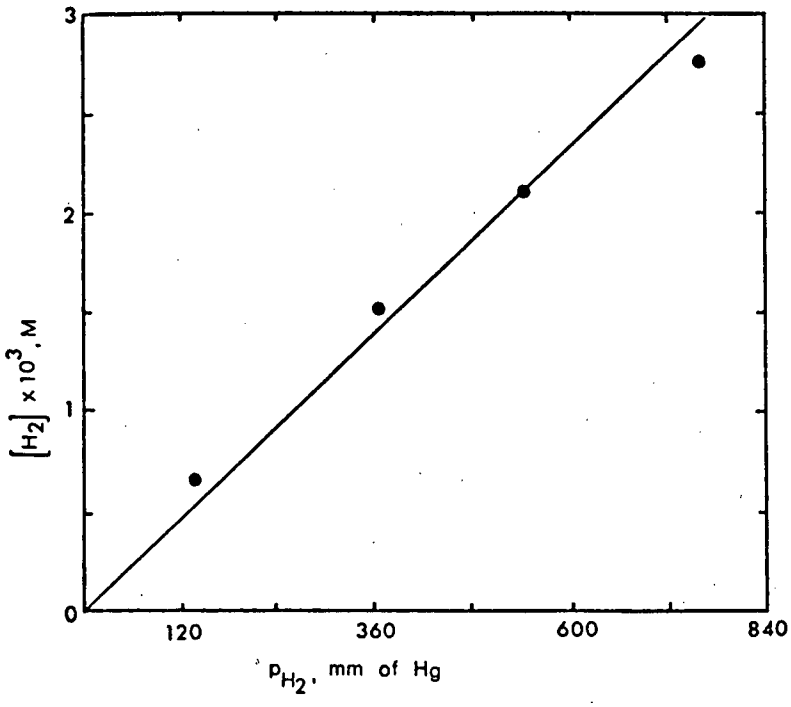

p_{H_2}, mm	$[H_2] \times 10^3$, M
132	0.67
360	1.53
550	2.11
740	2.76

Figure III.1 Solubility of hydrogen in n-butanol-toluene (2:1) mixture at various pressures at 30°C.

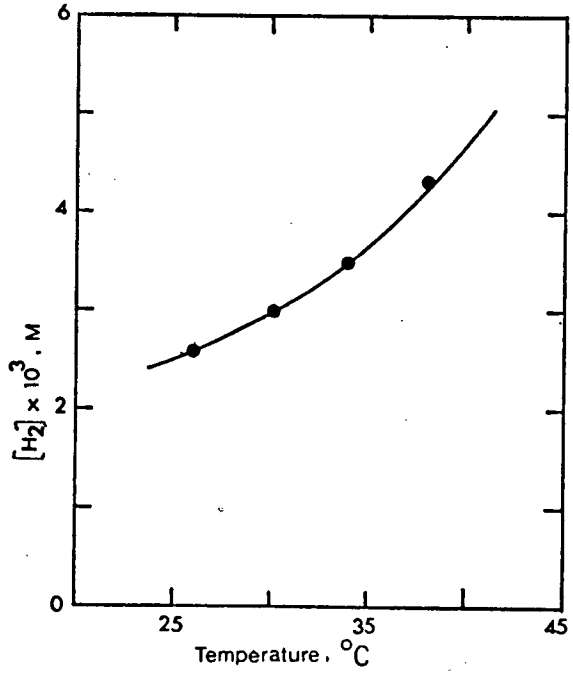

t, °C	$[H_2] \times 10^3$, M atm^{-1}
26	2.60
30	3.01
34	3.45
38	4.33

Figure III.2 Solubility of hydrogen in n-butanol-toluene (2:1) mixture at various temperatures.

considered valid.

Other experimental procedure follows that given in chapter II.

III.3 The summary of studies done on the Itaconic acid - $HRh[(+)\text{-diop}]_2$ system

The itaconic acid system proved convenient for a kinetic study since this substrate could be completely hydrogenated in a reasonable period of time; Figure III.3 shows the typical S-shaped H_2-uptake plots obtained for the IA system in n-butanol-toluene. Measurement of the maximum rates over concentration ranges of $(0.4\text{-}3.0)\times10^{-3}$M $HRh[(+)\text{-diop}]_2$, $(0.5\text{-}12.0)\times10^{-2}$M IA, and 56-740 mm H_2, demonstrated a first-order dependence on Rh, and between zero-and first-order on both IA and H_2. Addition of small amounts of (+)-diop had a remarkable inhibiting effect on the rate of catalytic hydrogenation (for example, a 100-fold decrease using added diop: rhodium = 1:3).

Solutions of the $HRh[(+)\text{-diop}]_2$ complex under argon showed an absorption maximum at 350 nm (ε=12,300M^{-1} cm^{-1}) in a spectrum that was invariant with time and was unaffected by addition of diop, or H_2.

On the basis of kinetic and visible data, the following hydrogenation mechanism was proposed (equations [III.1]-[III.3]):

$$HRh(diop)_2 \overset{K^*}{\rightleftharpoons} HRh(diop)(diop^*) \qquad [III.1]$$

$$HRh(diop)(diop^*) + A \underset{k_{-1}}{\overset{k_1}{\rightleftharpoons}} Rh(diop)(diop^*)(alkyl) \qquad [III.2]$$

$$Rh(diop)(diop^*)(alkyl) + H_2 \xrightarrow{k_2} HRh(diop)(diop^*) + \text{saturated product} \qquad [III.3]$$

(A=IA)

where $diop^*$ refers to a monodentate diop.

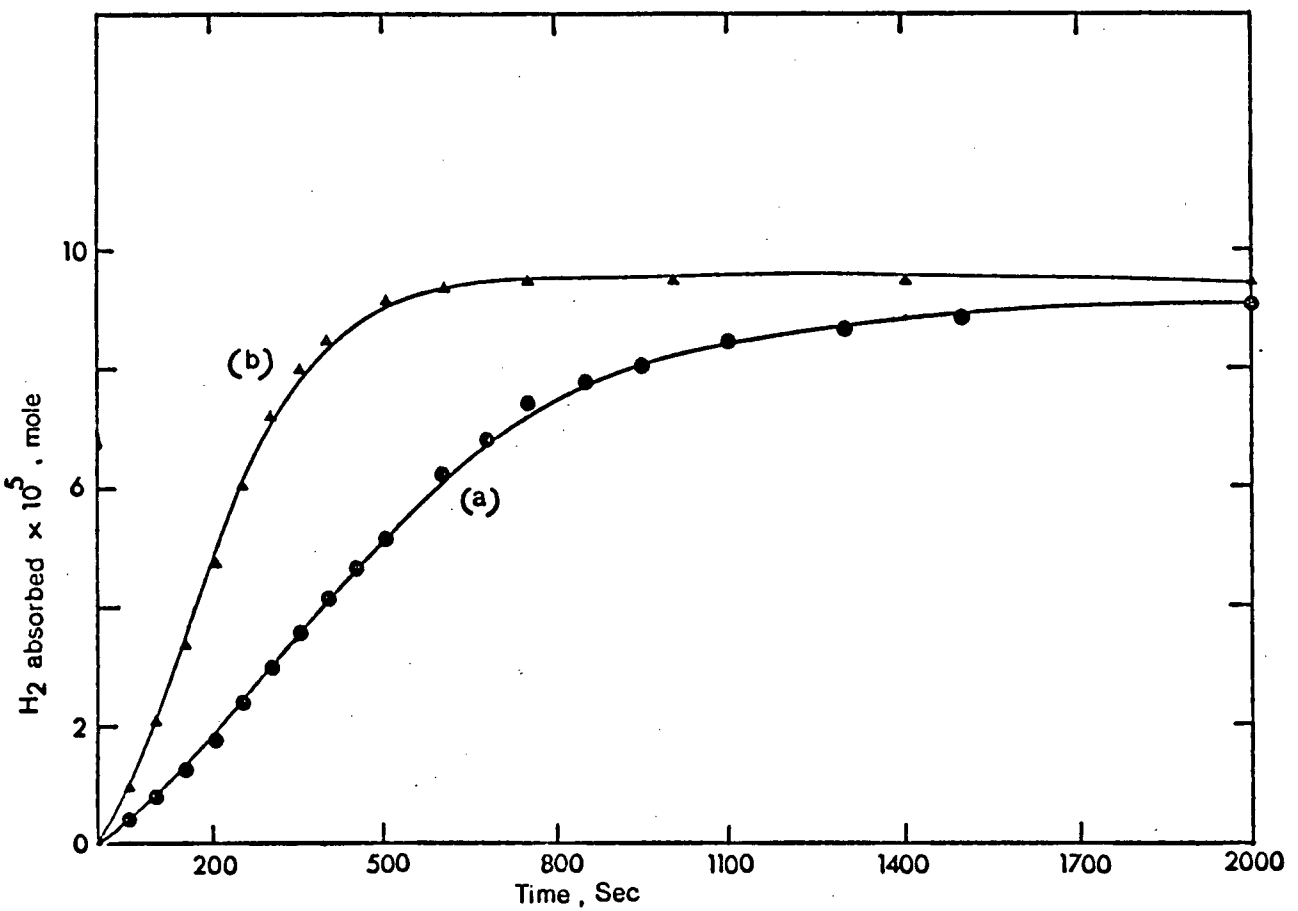

Figure III.3 Rate plots for the hydrogenation of itaconic acid using $HRh(diop)_2$ as catalyst. (30°C, 740 mm P_{H_2}, 2.0 x 10^{-2}M itaconic acid, n-butanol-toluene (2:1)=5 ml, (a) [Rh]=1.0 x 10^{-3}M; (b) [Rh]=2.0 x 10^{-3}M). Taken from ref.12.

The maximum rate in terms of total rhodium, and assuming $K^*<<1$ (i.e. $[HRh(diop)_2]>>[HRh(diop)(diop^*)]$), was given by

$$\text{Rate} = \frac{K^* k_1 k_2 [Rh]_T [IA][H_2]}{k_{-1}+k_2[H_2]+k_1 K^*[IA]} \qquad [III.4]$$

which accounted for the kinetic dependences on Rh, H_2, and IA; a slow build-up of the $HRh(diop)(diop^*)$ species to a steady state concentration explained the S-shaped curves shown in Fig. III.3. Rate law [III.4] was readily analyzed using standard inverse plots (e.g. $rate^{-1}$ vs $[IA]^{-1}$). The unusual marked diop dependence was attributed to a further equilibrium [III.5], giving rise to an inactive species containing two monodentate diop ligands:

$$HRh(diop)(diop^*) + diop \overset{K_2^*}{\rightleftharpoons} HRh(diop)(diop^*)_2 \qquad [III.5]$$

Rate law [III.4] suggests that the fall-off from first to zero order in IA with increasing [IA] should be more readily attained at lower $[H_2]$. Some data obtained since completion of my Master's thesis[12] verify this prediction (Fig.III.4), and further substantiate rate law [III.4].

Decomposition of the hydride catalyst

Visible spectral studies under argon at 30°C on yellow solutions of $HRh(diop)_2$ and itaconic acid (and also maleic and succinic acids) indicated some alkyl formation (equation [III.2]) followed by a very slow formation of the orange $Rh(diop)_2^+$ species (λ_{max} 442 nm), which has been synthesized by another route (chapter IV). The final solution absorbed H_2 reversibly, and these findings were attributed[12] to reactions [III.6] and [III.7]:

$$HRh(diop)_2 + H^+ \rightleftharpoons Rh(diop)_2H_2^+ \qquad [III.6]$$

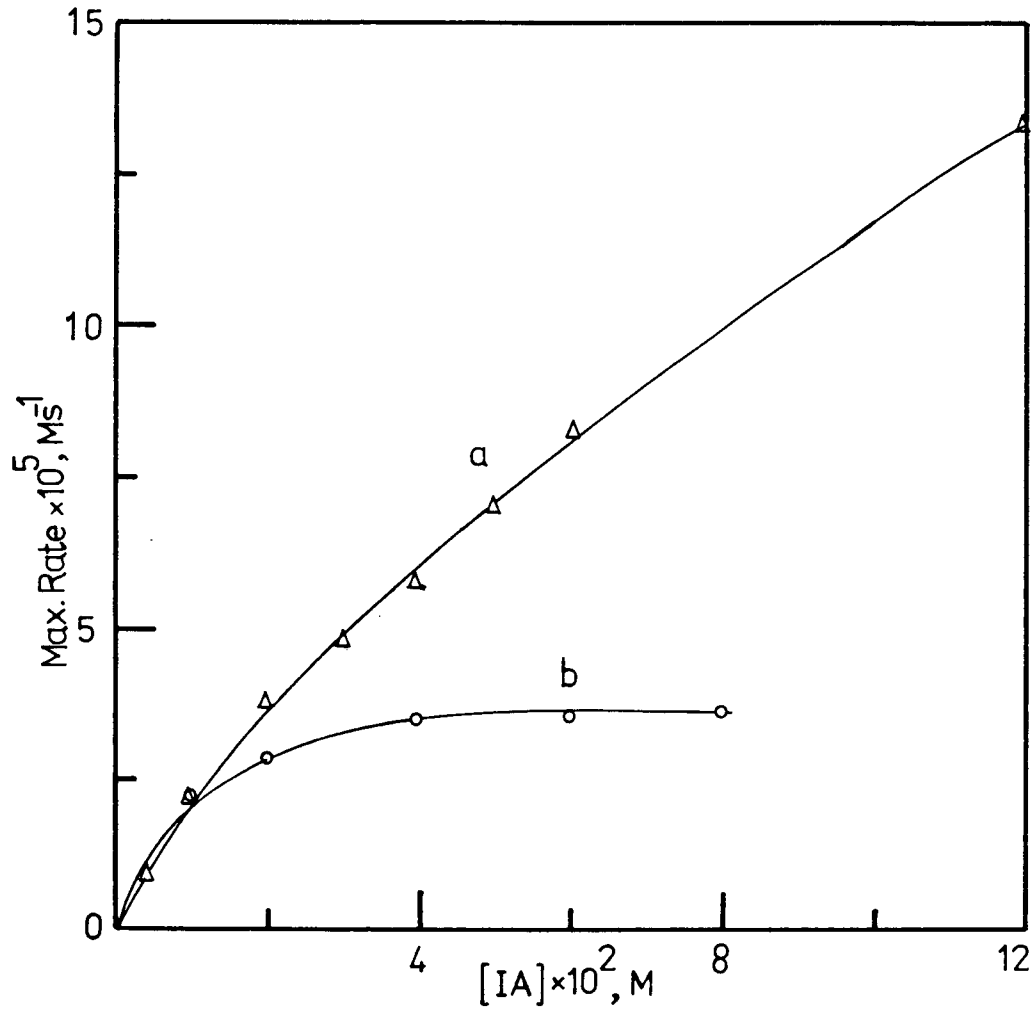

Figure III.4 Maximum rate dependence on itaconic acid in n-butanol-toluene (2:1) at 30°C using 1.5 x 10^{-3}M Rh; curve a, 740 mm H_2; curve b, 132 mm H_2 (Curve a taken from ref. 12).

$$Rh(diop)_2H_2^+ \rightleftharpoons Rh(diop)_2^+ + H_2 \qquad [III.7]$$

Solutions of the dihydride were pale yellow with a low intensity continuum in the 400-450 nm region.

Equilibria [III.6] and [III.7] have now been confirmed using high-field ^1H nmr and ^{31}P nmr spectroscopy. The $^{31}P\{^1H\}$ nmr spectrum of the $HRh(diop)_2$ complex in an n-butanol-toluene-acetone-d_6 mixture at 25°C under argon showed a doublet at -21.0 ppm with J_{Rh-P}=149 Hz (Fig. III.5(a)) . The high-field ^1H nmr of the same solution gave a doublet of quintets (Fig. III.6(a)). Both spectra were invariant over two days and the yellow colour of the solution remained unchanged.

The same solutions of $HRh(diop)_2$ in the presence of itaconic acid under argon changed from yellow to deep orange in $\sim$½h. The $^{31}P\{^1H\}$ nmr spectrum of this solution was a broadened doublet at 25°C (Fig. III.5(b)), but was a complicated pattern at -50°C; no hydride signal was detected in the high-field ^1H nmr spectrum. When the experiment was repeated in the presence of H_2 instead of Ar, the color of the solution changed from yellow to light yellow after $\sim$2h. The $^{31}P\{^1H\}$ nmr spectrum of this final solution was a doublet of doublet of triplets (Figure III.5(c)) while the ^1H nmr spectrum was a pair of multiplets centered around 20τ (Fig. III.6(b)).

The nmr data are consistent with reaction [III.6] and [III.7]. The broadened ^{31}P nmr doublet (Fig.III.5(b)) and absence of the high-field hydride signal are attributed to the formation of some alkyl intermediate but there could also be some $Rh(diop)_2^+$ present formed according to equilibria [III.6] and [III.7]. The complicated nature of the $^{31}P\{^1H\}$ nmr spectrum at -50°C will be discussed in chapter IV. In

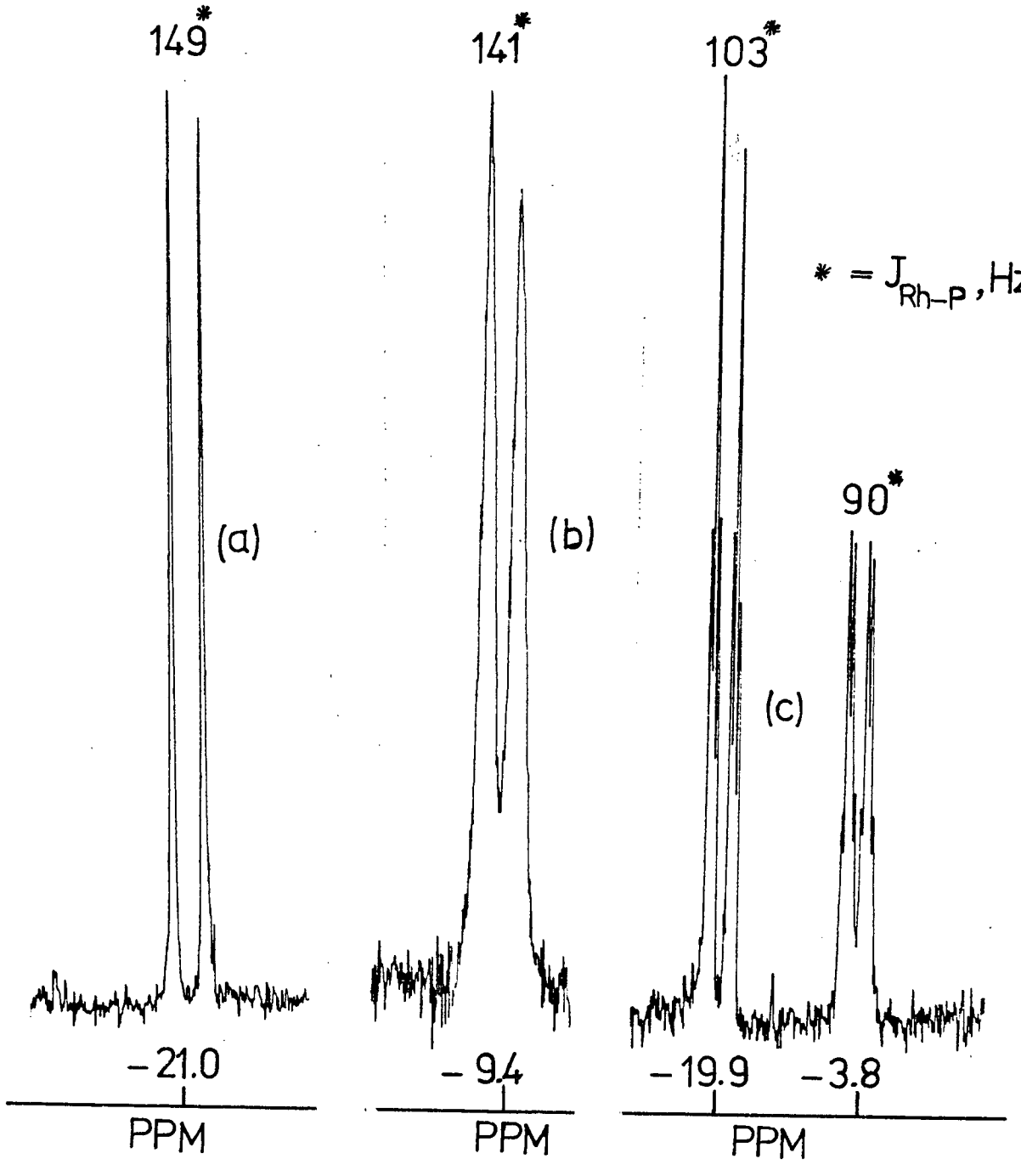

Figure III.5 $^{31}P\{^{1}H\}$ nmr spectra in n-butanol-toluene-acetone-d_6 mixture at 25°C of:

(a) $HRh(diop)_2$ (130 mg in 2 ml solvent) under Ar.
(b) (a) + 130 mg IA.
(c) (b) under H_2.

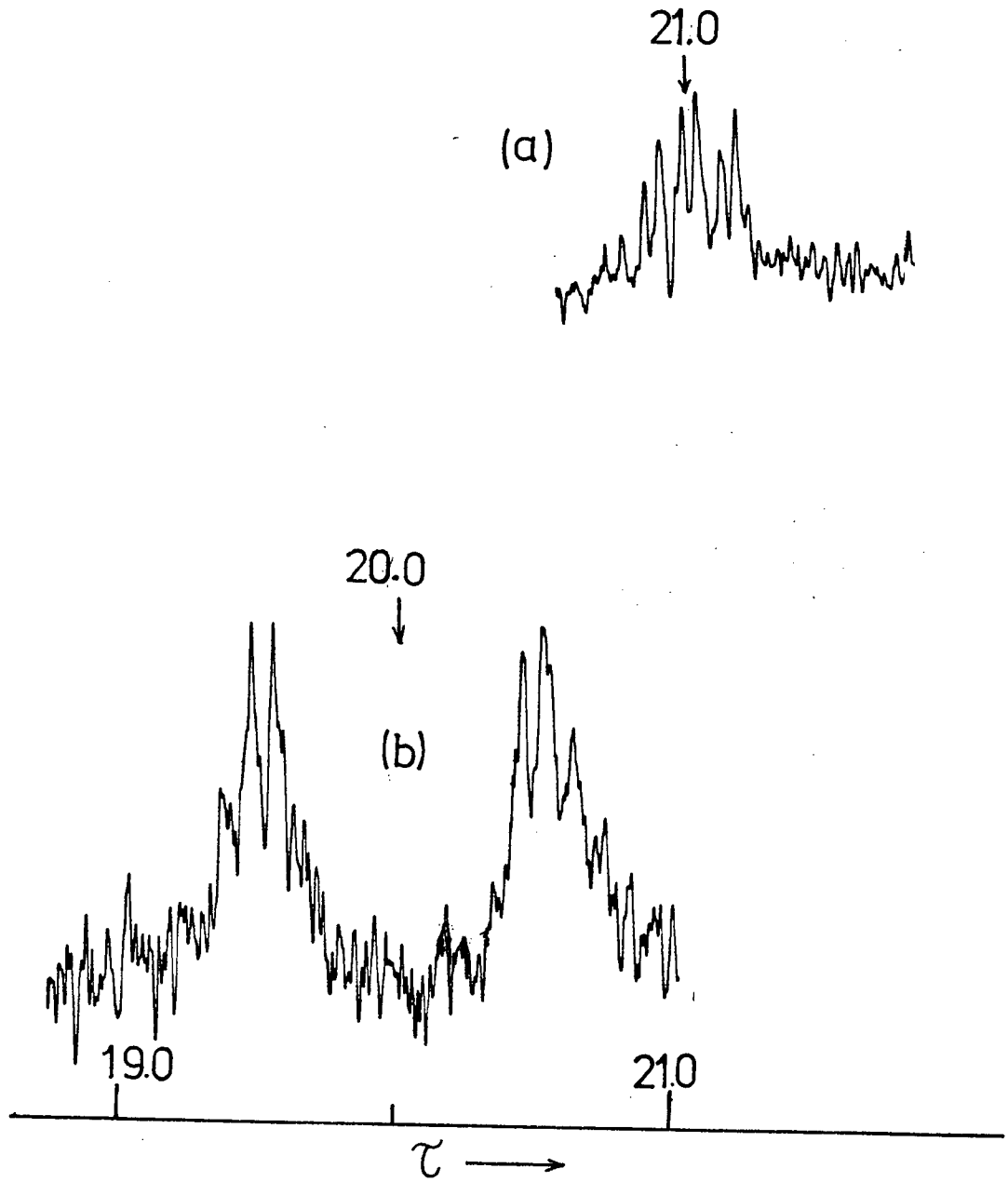

Figure III.6 High-field ^{1}H nmr spectra in n-butanol-toluene-acetone-d_6 mixture at 25°C of:

(a) $HRh(diop)_2$ (130 mg in 2 ml solvent) under Ar.
(b) (a) + 130 mg IA under H_2.

the presence of H_2, the spectra obtained (Figs.III.5(c) and III.6(b)) are due to the cis-$Rh(diop)_2H_2^+$ species (see chapter VII). The reversible dihydride formation is well documented in various other rhodium-tertiary-phosphine systems where similar $^{31}P\{^1H\}$ and high-field nmr patterns have been observed.[14]

III.4 The $HRh[(+)\text{-diop}]_2$-Styrene system

III.4.1 Results

The hydrogenation of styrene was achieved at 45°C in n-butanol-toluene (2:1) solutions at a conveniently measurable rate using the $HRh(diop)_2$ catalyst. S-shaped H_2-uptake curves were obtained (Figure III.7), and the hydrogenation rates were readily determined from the maximum slope. The reproducibility of the rates (±5%) was established by repeating several experiments. The kinetic data obtained are listed in Table III.1.

The uptake rates at constant hydrogen and olefin concentrations varied linearly with increasing catalyst concentration over the range studied $(2.0\text{-}6.0)\times10^{-3}$M (Fig. III.8), and the reaction was first-order both in styrene (0.05-0.25M, Fig. III.9) and H_2 (110-718 mm, Fig.III.10).

The rates increased with temperature (Table III.2), and decreased drastically on addition of even small amounts of excess (+)-diop (Table III.3).

The solution remained yellow during and after the hydrogenation reactions (see below).

On adding 0.1M styrene to catalytic concentrations of $HRh(diop)_2$ under argon at 45°C, there were practically no visible spectral changes

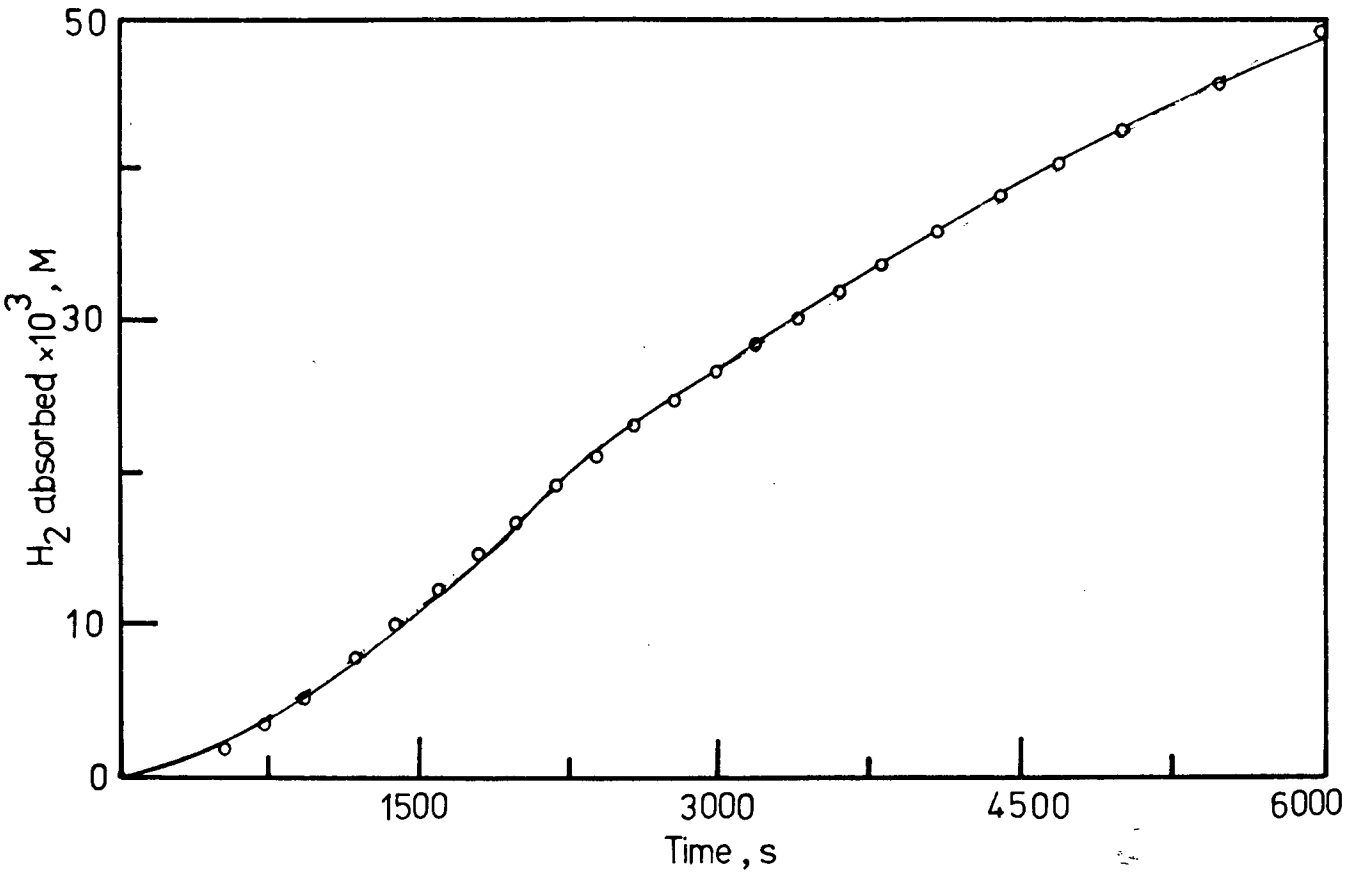

Figure III.7 Rate plot for the hydrogenation of styrene using $HRh(diop)_2$ catalyst (45°C, [Rh]=3.0 x 10^{-3}M, [styrene]=0.1M, P_{H_2}=718 mm, n-butanol-toluene (2:1)).

Table III.1 Maximum hydrogenation rates for the hydrogenation of styrene in n-butanol-toluene (2:1) at 45°C using $HRh[(+)\text{-diop}]_2$.

$[Rh]\times10^3$,M	$[Styrene]\times10^1$,M	P_{H_2},mm[a]	$[H_2]\times10^3$,M[b]	Max.rate x 10^6 Ms^{-1}	$k,M^{-2}s^{-1}$
2.0	1.0	718	5.37	8.74	8.14
3.0	"	"	"	11.12	6.90
4.0	"	"	"	17.04	7.93
5.0	"	"	"	19.40	7.23
6.0	"	"	"	25.60	7.95
3.0	0.5	"	"	5.80	7.20
"	1.5	"	"	17.78	7.36
"	2.0	"	"	22.22	6.90
"	2.5	"	"	27.60	6.85
"	1.0	110	0.83	1.74	7.00
"	"	262	1.95	4.82	8.10
"	"	414	3.09	6.76	7.30
"	"	566	4.24	9.08	7.14

Average k = 7.38 $M^{-2}s^{-1}$

a A solvent pressure of 42 mm Hg at 45°C was calculated for the 2:1 n-butanol-toluene mixture assuming it obeyed Raoult's Law.

b Calculated from Figures III.1 and III.2.

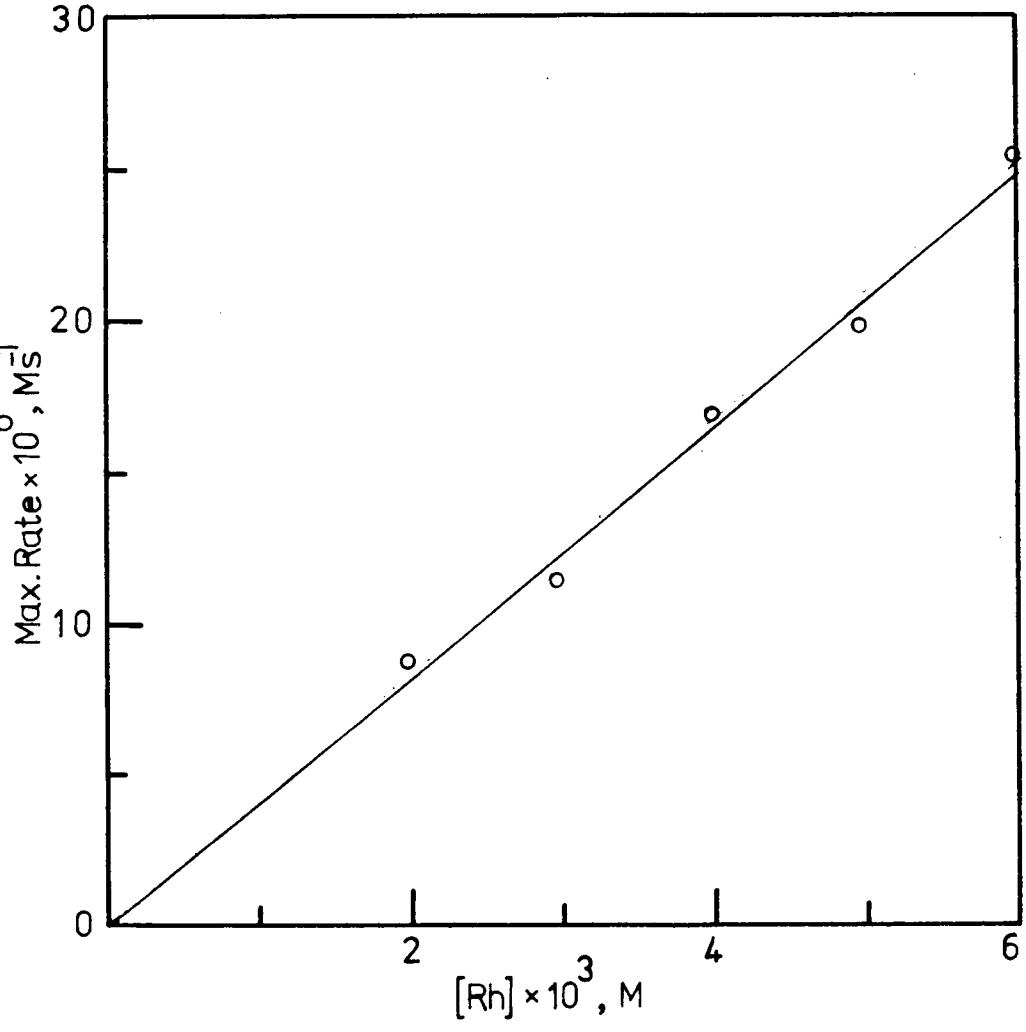

Figure III.8 Maximum rate dependence on $HRh(diop)_2$ concentration ([styrene]=0.1M, P_{H_2}=718 mm, n-butanol-toluene (2:1), 45°C).

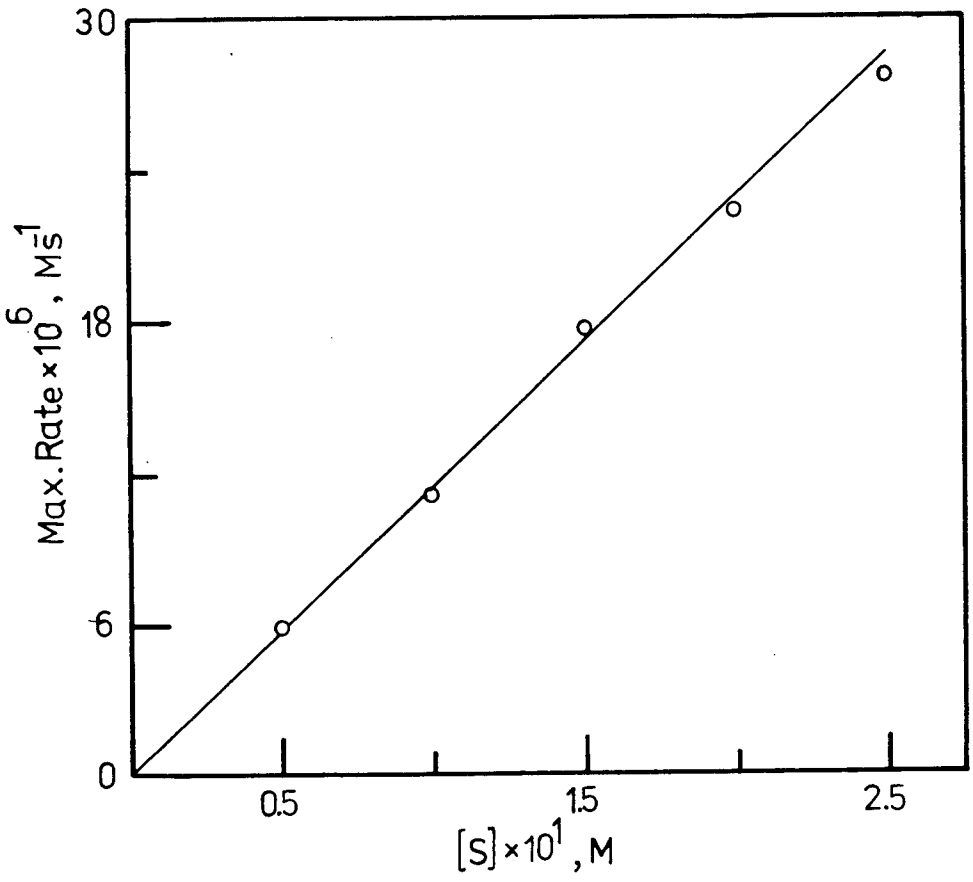

Figure III.9 Plot of maximum rate against styrene concentration (45°C, P_{H_2}=718 mm, [Rh]=3.0 x 10^{-3}M, n-butanol-toluene (2:1)).

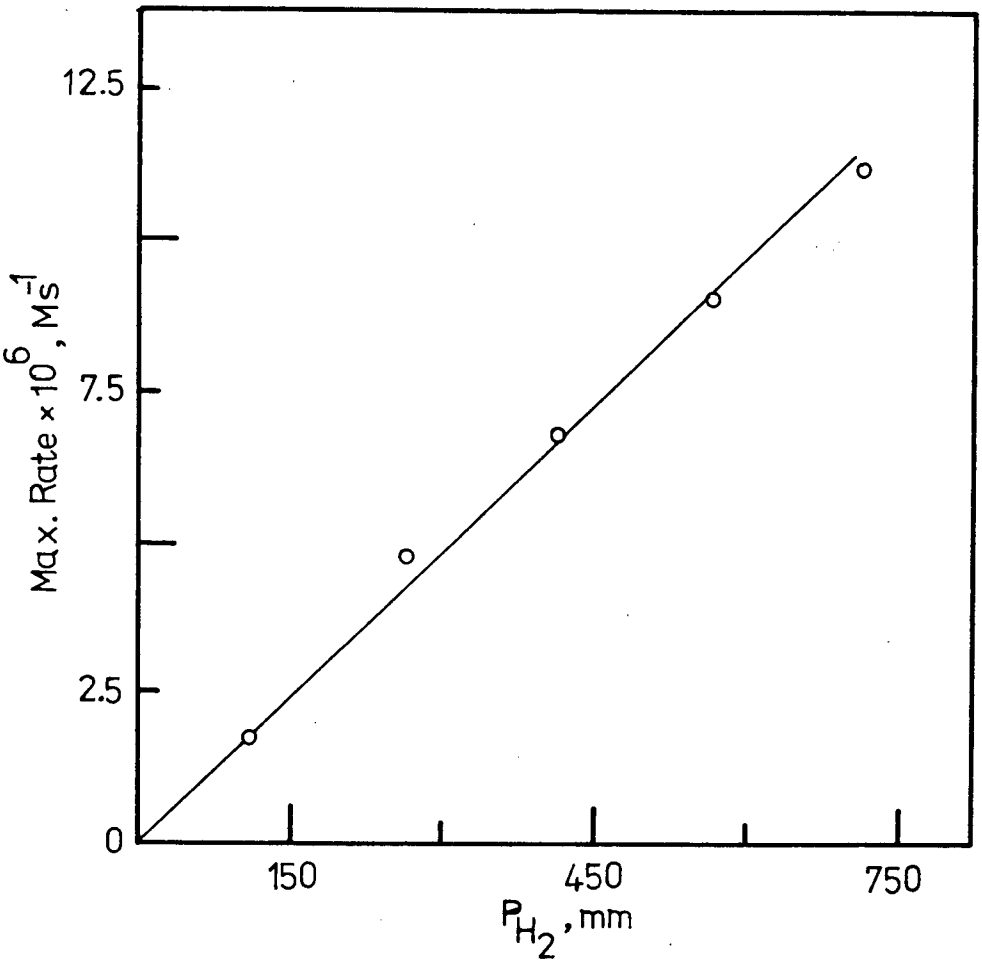

Figure III.10 Dependence of maximum rate on H_2 pressure (45°C, [Rh]=3.0 x 10^{-3}M, [styrene]=0.1M, n-butanol-toluene (2:1)).

Table III.2 Variation of maximum rate with temperature

([styrene]=0.1M, [$HRh(diop)_2$]=3.0×10^{-3}M, P_{H_2}=674 mm, n-butanol-toluene(2:1)).

T,°C	Vapour pressure of the solvent,mm	$[H_2] \times 10^3$,M	Max.Rate x 10^6,Ms^{-1}	k,$M^{-2}s^{-1}$
45	42	5.05	11.00	7.26
50	54	"	17.46	11.52
55	68.5	"	28.36	18.72
60	86	"	38.40	25.35

Table III.3 Variation of maximum rate with added (+)-diop

(45°C, [styrene]=0.1M, [$HRh(diop)_2$]=3.0×10^{-3}M, P_{H_2}=718 mm, n-butanol-toluene (2:1)).

[(+)-diop] x 10^4,M	Max.Rate x 10^6, Ms^{-1}
0.0	11.12
1.0	10.28
2.0	5.44
3.0	2.64
10.0	— [a]

a Immeasurably slow.

(Fig. III.11). Similarly on sampling the solution during a catalytic hydrogenation, the visible spectrum indicated the presence of only $HRh(diop)_2$; more concentrated solutions used for hydrogenation showed the same high-field ^1H nmr spectrum as that of starting hydride. Thus only $HRh(diop)_2$ is detected during the catalytic hydrogenation.

III.4.2 Discussion

The kinetics for the hydrogenation can be written as:

$$\frac{-d[H_2]}{dt} = k[Rh][styrene][H_2] \qquad [III.8]$$

where k is an overall third-order rate constant of average value 7.38 $M^{-2}s^{-1}$ (Table III.1). The kinetics are consistent with the mechanism postulated previously[12] (equations [III.1]-[III.3]; A=styrene), but in which 'all' the rhodium is present as $HRh(diop)_2$ (as observed spectroscopically). The S-shaped uptake curve (Fig. III.7) is thought to result from a build-up of a kinetically significant amount of Rh(diop)(diop*)(alkyl); the rate would then become:

$$\frac{K^* k_1 k_2 [Rh]_T [styrene][H_2]}{k_{-1} + k_2[H_2]} \qquad [III.9]$$

With $k_2[H_2] \ll k_{-1}$, rate [III.9] reduces to the observed rate law [III.8] with $k = K^* k_1 k_2 / k_{-1}$ or $K^* K_1 k_2$ where $K_1 = k_1/k_{-1}$. Variation of k with temperature yields a reasonable Arrhenius plot (Fig. III.12) and the activation parameters $\Delta H^{\ddagger}$=17.7±1 Kcal.mole^{-1}, E_a=18.3±1 Kcal.mole^{-1}, and $\Delta S^{\ddagger}$=1±4 eu.; these presumably refer to the composite constant $K^* K_1 k_2$. These values are close to those measured for the itaconic acid system

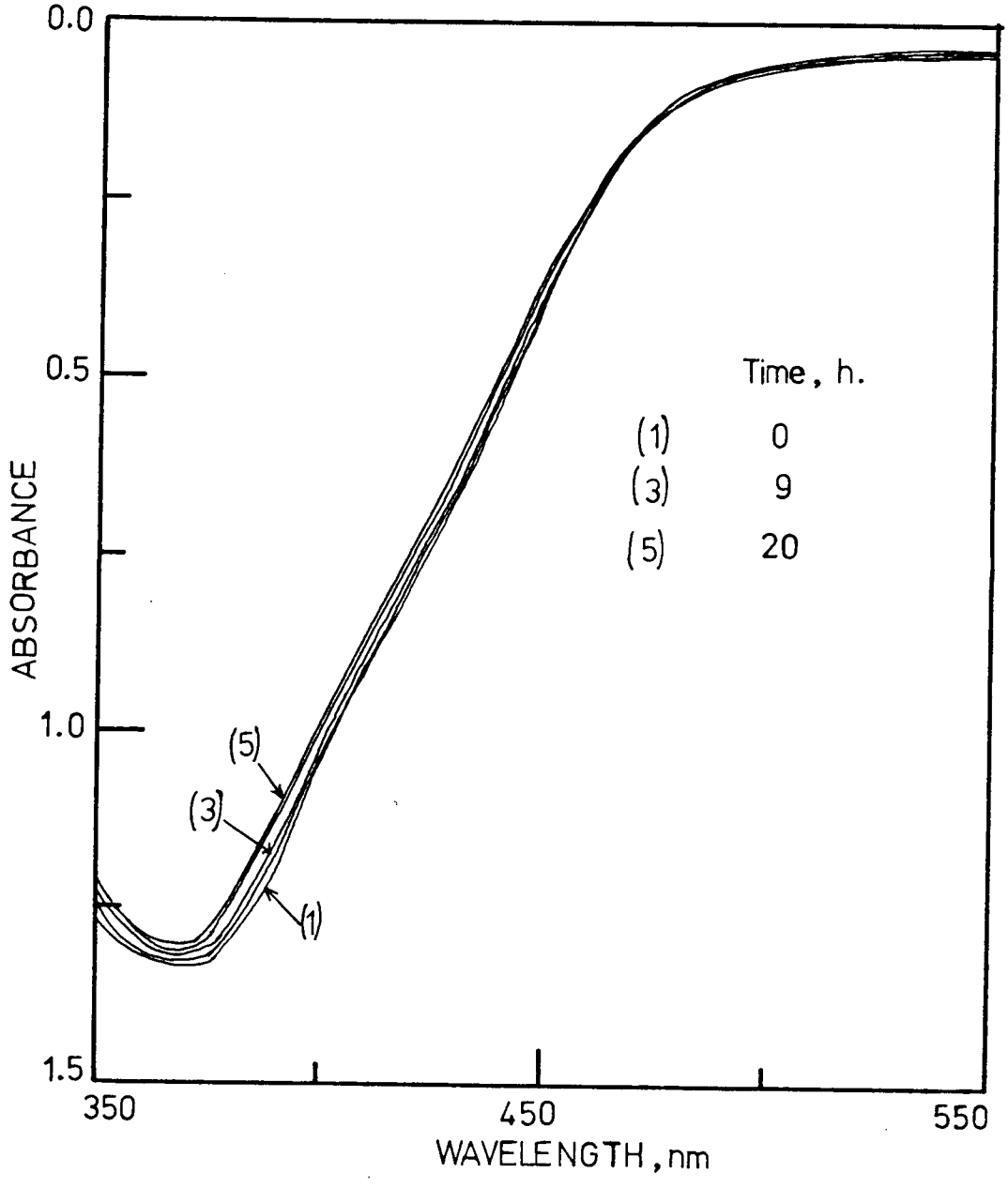

Figure III.11 Absorption spectra of $HRh(diop)_2$ (1.4×10^{-3}M) under argon in n-butanol-toluene (2:1) in the presence of styrene (0.1M) at 45±2°C.

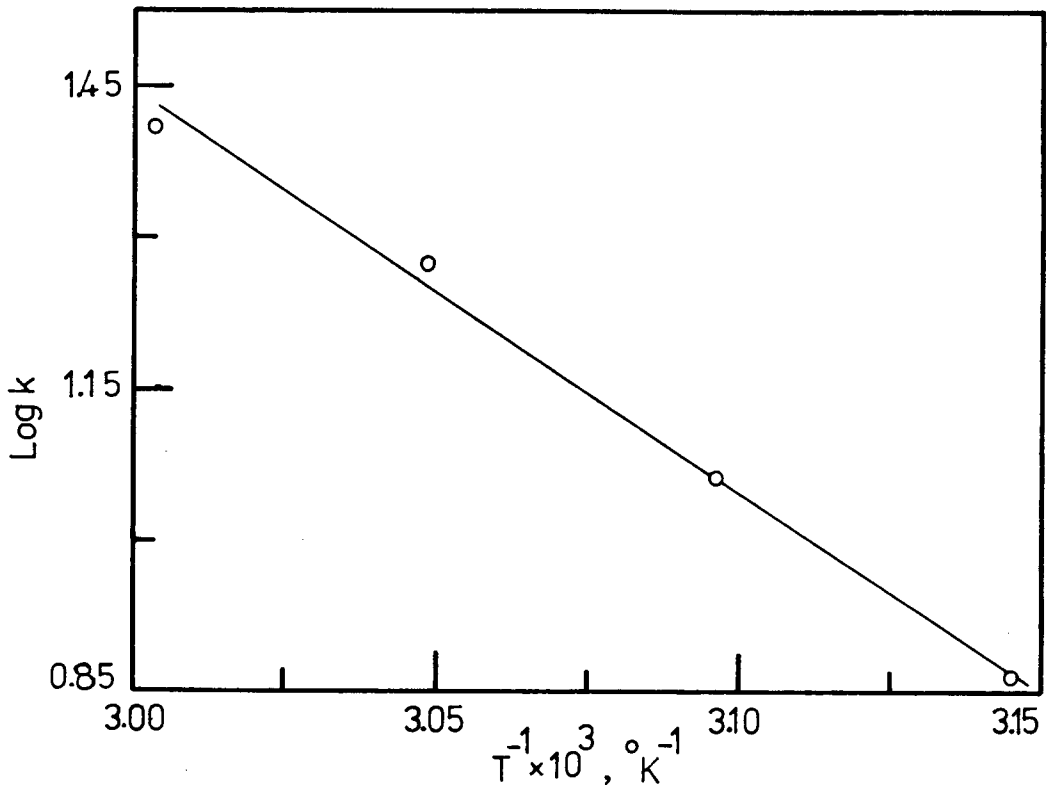

Figure III.12 Arrhenius plot for the hydrogenation of styrene using $HRh(diop)_2$ catalyst ([Rh]=3.0 x 10^{-3}M, [styrene]=0.1M, P_{H_2}=674 mm, n-butanol-toluene (2:1)=5 ml).

(E_a=16.4±1 Kcal.mole^{-1}, $\Delta H^{\ddagger}$=15.8±1 Kcal.mole^{-1}, and $\Delta S^{\ddagger}$=-6 e.u.).[12] However, these parameters were measured under conditions that were zero-order in H_2 and first-order in itaconic acid and so refer to $K^{*}k_1$.

The marked inhibition on added diop in the styrene system is of the same order of magnitude as that measured for the itaconic acid system, and is attributed to equilibrium [III.5]. Species containing monodentate diop ligands are now well established, $RuCl_2(diop)(diop^{*})$[15] and $[Rh(CO)_2(diop)(diop^{*})]Cl$[16] complexes having been isolated and characterized.

In the diethyl maleate system discussed previously[12], the visible spectral data in the absence of H_2 (under argon) at 30°C was surprising since it essentially showed "full" formation of $Rh(diop)_2^{+}$ with an excellent isosbestic point at 450 nm (Fig. III.13(a)). High-field ^1H nmr of this dark orange solution did not show any hydride signal. The data show that the cation must be formed in some way from the alkyl complex. A reasonable explanation involves protonolysis via butanol:

$$Rh(diop)(diop^{*})(alkyl) + BuOH \longrightarrow Rh(diop)_2^{+}OBu^{-} + \text{saturated product} \qquad [III.10]$$

Addition of H_2 to the dark orange solution resulted in a slow change of colour to yellow; high-field ^1H nmr spectra of this yellow solution showed the characteristic hydride peak (Fig. III.6(a)) and the visible spectrum resembled that of $HRh(diop)_2$ (Fig. III.13(b)). A distinct possibility is establishment of equilibrium [III.6]. Such an equilibrium has been suggested by Schrock and Osborn[14] for some related tertiary phosphine and arsine systems, although they were unable to isolate the monohydride species. In the case of acidic substrates

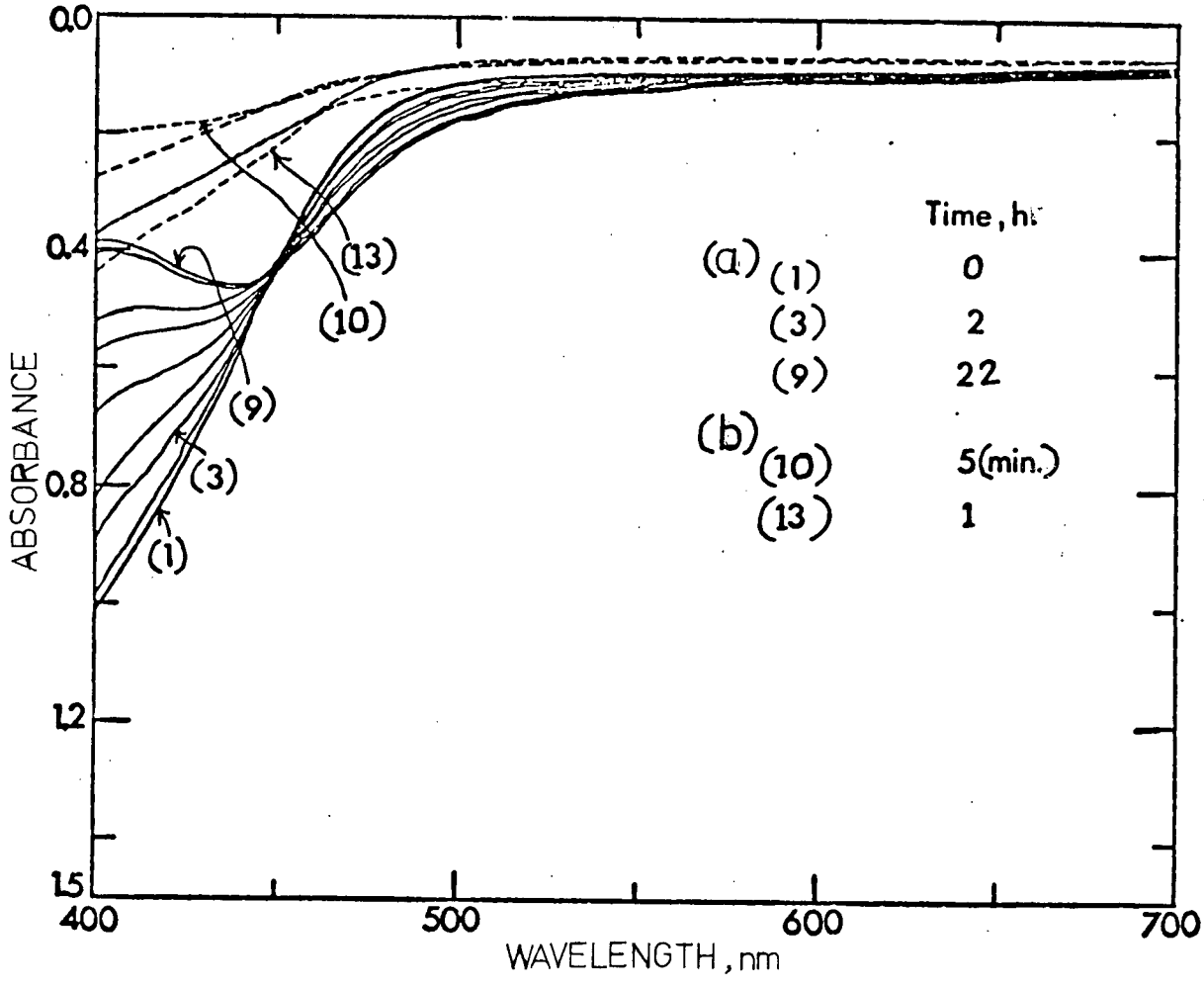

Figure III.13 Absorption spectra of $HRh(diop)_2$ (1.4×10^{-4}M) in n-butanol-toluene (2:1) in the presence of diethyl maleate (1.0×10^{-2}M) at 30±1°C.

(a) —— Solution under argon.
(b) --- Solution under hydrogen.

(Data taken from ref. 12).

(e.g. IA) equilibrium [III.6] is not observed, the H^+ concentration presumably maintaining dihydride formation.

Strong evidence for the involvement of butanol in cation production using non-acidic substrates (reaction [III.10]) is that in toluene alone no 440 nm peak is generated, and the slight decrease in absorbance in the visible spectrum and absence of the high-field hydride signal are attributed to the formation of the alkyl complex.

In the styrene system, the presence of a high-field hydride signal due to the initial $HRh(diop)_2$ complex, and insignificant spectral changes in Fig. III.11 are due to equilibrium [III.2] lying far to the left consistent with rate law [III.9]. Reaction [III.10] is not observed in this case due to insignificant amounts of alkyl present.

III.5 Conclusions

From sections III.3 and III.4 it is clear that the nature of substrates has a pronounced effect on the course of hydrogenation reactions. Although the basic mechanism involved in both IA and styrene systems is the well established 'unsaturate' route (Fig. I.4), dependences of reaction rates on various parameters differ in both cases and yield different rate laws [III.4] and [III.9] respectively. Spectrophotometric studies indicate that non-acidic substrates definitely involve $HRh(diop)(diop^*)$ as the active catalytic species whereas the acidic substrates may involve the $Rh(diop)_2^+$ complex as well (depending on the rate of hydrogenation) produced by slow decomposition of the hydride catalyst by protons of acidic substrates. Detailed kinetic studies using the $Rh(diop)_2^+$ complex will be presented in chapter VI.

CHAPTER IV

BIS(DITERTIARYPHOSPHINE) COMPLEXES OF RHODIUM(I). SYNTHESIS, SPECTROSCOPY, AND ACTIVITY FOR CATALYTIC HYDROGENATION

IV.1 Introduction

Although the bis(ditertiaryphosphine) $Ph_2P(CH_2)_nPPh_2$ complexes of iridium(I) and iridium(III) have been studied fairly extensively[1-4], few details have been reported for the rhodium analogues. The $Rh(dpe)_2X$ complexes, X=H, Cℓ, ClO_4, are well-known[5], and in terms of activation of small gas molecules and catalytic activity, the crystal structure of the cationic dioxygen complex $Rh(dpe)_2O_2^+PF_6^-$ has been reported.[6] The $Rh(dpe)_2Cℓ$ complex is a 1:1 electrolyte in polar solvents[2,5], and is ineffective as a catalyst for hydrogenation of olefinic substrates under mild conditions.[2,7] The $Rh(dpe)_2^+$ cation is unreactive toward H_2.[8,9a] Recently, the $[Rh(dpe)_2]Cℓ$ and $[Rh(dppp)_2]Cℓ$ complexes have been used for the catalytic decarbonylation of aldehydes.[9b]

Our interest in these bis(diphenylphosphino) systems increased after our finding that an isolated $HRh[(+)\text{-diop}]_2$ complex was an efficient catalyst for asymmetric hydrogenation of certain prochiral olefinic carboxylic acids under mild conditions.[10,11] The diop ligand (Fig.I.1) can be considered, for example, as a derivative of the dpb ligand, and this led us to look at the bis$[PPh_2(CH_2)_nPPh_2]$ systems, including the hydrido, chloro and cationic complexes, with a view to learning more of reactivity patterns generally as a function of n. Such data have appeared on the use of 1:1 rhodium(I)/$Ph_2P(CH_2)_nPPh_2$ hydrogenation catalysts formed *in situ* from rhodium(I) precursors[12],

and depending on the media, the catalysts may be neutral or cationic.[13]

The synthesis and characterization of various bis(diphenylphosphino) complexes are reported in this chapter along with some preliminary data concerning their catalytic activity for hydrogenation of the prochiral substrate, methylenesuccinic acid. We[11] and Kagan's group[14] have reported earlier on the characterization of the cationic complexes $Rh(diop)_2^+$ and $Rh(diop)_2H_2^+$, and Slack and Baird[15] reported on some *in situ* dpp and diop systems while this work was in progress. The luminescence of the $Rh[PPh_2(CH_2)_nPPh_2]_2^+$ cations (n=1-3) has been discussed but no other details on the complexes were given.[16,17]

IV.2 Experimental

All solutions were handled under an argon atmosphere using Schlenk techniques.

Preparation of Complexes - The cyclooctene dimer $[RhCl(C_8H_{14})_2]_2$ was prepared by a literature procedure[18]; yields of 90% were obtained on leaving the reaction mixture for 10d.

IV.2.1 $Rh(dpm)_2Cl$

To a benzene solution (5 ml) of $[RhCl(C_8H_{14})_2]_2$ (0.30 mmol, 0.215 g) was added dpm (1.32 mmol, 0.50 g) in benzene (5 ml), and the resulting solution was freeze-dried. The residue obtained was recrystallized from CH_2Cl_2 - ether to give orange needles.

IV.2.2 $Rh(dpe)_2Cl$ and $Rh(dpp)_2Cl$

A benzene solution (10 ml) of the phosphine (1.1 mmol, 0.44 g dpe or 0.45 g dpp) was added to a red, benzene solution (10 ml) of $[RhCl(C_8H_{14})_2]_2$ (0.25 mmol, 0.18 g). The precipitated yellow dpe complex or light yellow dpp complex was washed with warm benzene and

dried in vacuo. The complexes have been prepared previously by other methods.[5,16]

IV.2.3 $\underline{Rh(dpb)_2Cl}$

A benzene solution (15 ml) of $[RhCl(C_8H_{14})_2]_2$ (0.30 mmol, 0.215 g) and dpb (1.32 mmol, 0.56 g) was refluxed under Ar for 3h. Concentration to a 5 ml volume, followed by addition of n-hexane gave a yellow solid that was filtered, recrystallized from CH_2Cl_2- ether and dried in vacuo.

IV.2.4 $\underline{Rh[(+)\text{-diop}]_2Cl}$

A benzene solution (15 ml) of $[RhCl(C_8H_{14})_2]_2$ (0.30 mmol, 0.215 g) and (+)-diop (1.32 mmol, 0.66 g) was refluxed under Ar for 3h. The solution was evaporated to dryness under vacuum. The resulting residue was recrystallized from n-hexane to give an orange powder.

IV.2.5 $\underline{Rh(\overset{\frown}{P}\ \overset{\frown}{P})_2{}^+BF_4{}^-\ (\overset{\frown}{P}\ \overset{\frown}{P}}$ = dpm,dpe,dpp,dpb, and (+)-diop)

The complexes were prepared in each case from the corresponding chloro complex. For example, a mixture of a CH_2Cl_2 solution (5 ml) of $Rh(dpm)_2Cl$ (0.30 mmol, 0.27 g) and a methanol solution (5 ml) of $AgBF_4$ (0.30 mmol, 0.58 g) was stirred for 30 m. Removal of the AgCl and evaporation to dryness left a residue that was recrystallized from CH_2Cl_2 - ether to give red crystals of $Rh(dpm)_2{}^+BF_4{}^-$. The dpb analogue was dark red, while the dpe, dpp, and diop complexes were light orange.

IV.2.6 $\underline{HRh(\overset{\frown}{P}\ \overset{\frown}{P})_2}$ ($\overset{\frown}{P}\ \overset{\frown}{P}$=dpe,dpp, and (+)-diop)

The literature method[5], involving treatment of the chloro complexes (0.50 mmol) with a 3 mole excess of sodium borohydride in ethanol (10 ml), was used in attempts to prepare the corresponding hydrides. The red dpe[5], orange dpp, and yellow diop complexes were recrystallized

from benzene-ethanol. The diop complex has been prepared earlier by a different route[19] (section III.2,chapter III). Use of the dpm ligand yielded a deep red precipitate but this decomposed even under Ar, so the compound could not be characterized. Borohydride reduction of $Rh(dpb)_2C\ell$ yielded a mixture of complexes that have not been separated; borohydride species are almost certainly present as judged by ir bands in the 2340-2390 cm^{-1} region.[20] Attempts to synthesize the $HRh(dpb)_2$ complex via the routes used to synthesize the diop analogue from $RhC\ell_3 \cdot 3H_2O$[10,11,19] were similarly unsuccessful.

The yields of all the isolated complexes described in this section were in the 75-90% range.

IV.3 Results and Discussion

Cleavage of the chloride bridge in $[RhC\ell(diene)]_2$ complexes by a Lewis base L, including monodentate phosphines, can yield both $RhC\ell(diene)L$ and $Rh(diene)L_2^+C\ell^-$ species, depending on the amount of L used and the polarity of the solvent used.[21] Reaction of the diene dimer with 2 moles of a chelating diphosphine is assumed to yield $RhC\ell(diphosphine)(solvent)$ or $Rh(diene)(diphosphine)^+$, depending on the solvent, and the cationic complexes are readily synthesized.[12-15,22-24] We have used the cyclooctene precursor $[RhC\ell(C_8H_{14})_2]_2$ to prepare the $Rh(\overset{\frown}{P}\ \overset{\frown}{P})_2C\ell$ complexes (Table IV.1) via reaction [IV.1]. While these studies were in progress, a report appeared[25] describing the synthesis

$$[RhC\ell(C_8H_{14})_2]_2 + 4\overset{\frown}{P}\ \overset{\frown}{P} \xrightarrow{C_6H_6} 2Rh(\overset{\frown}{P}\ \overset{\frown}{P})_2C\ell + 4C_8H_{14} \qquad [IV.1]$$

of a $[RhC\ell(diop)(C_6H_6)]_2$ complex via a similar reaction, but using the

Table IV.1. Analytical and molar conductivity (Λ) data for the rhodium(I) complexes

Complex	Decomposition point(°C)[a]	Analysis				Λ[b] ($ohm^{-1}cm^2mol^{-1}$)
		%C		%H		
		Found	Calculated	Found	Calculated	
$Rh(dpm)_2Cl$	97	62.03[c]	66.20	4.46	4.85	71
$Rh(dpe)_2Cl$	205-209	66.64	66.80	5.27	5.20	61
$Rh(dpp)_2Cl$	162-165	67.43	67.33	5.30	5.40	74 (49)[d]
$Rh(dpb)_2Cl$	108	65.66[e]	67.85	5.85	5.65	49
$Rh(diop)_2Cl$	79	64.97[e]	65.58	5.96	5.64	35
$Rh(dpm)_2^+BF_4^-$	124	61.50[f]	62.65	4.55	4.59	79
$Rh(dpe)_2^+BF_4^-$	273-276	61.40[f]	63.31	4.86	4.87	78
$Rh(dpp)_2^+BF_4^-$	180	63.14[f]	63.92	5.05	5.13	81
$Rh(dpb)_2^+BF_4^-$	169-173	63.22[f]	64.51	5.40	5.38	75
$Rh(diop)_2^+BF_4^-$	174-177	60.91[f]	62.74	5.09	5.40	78
$HRh(dpe)_2$	167	69.70	69.33	5.50	5.44	71 (2)[d]
$HRh(dpp)_2$	143-146	69.35	69.84	5.65	5.71	51 (12)[d]
$HRh(diop)_2$	128	66.70	67.64	6.28	6.00	4 (2)[d]

a Uncorrected, in air.

b 10^{-3}M in CH_3NO_2 at 25°C under Ar.

c Complex hygroscopic.

d Value in DMA.

e Solids O_2-sensitive.

f Low carbon due to presence of CH_2Cl_2, detected in nmr; the calculated values are uncorrected.

bis(ethylene) dimer precursor with 2 moles of the diphosphine.

Reaction [IV.1] at room temperature precipitates in analytically pure forms the dpe and dpp complexes, and probably the dpm complex but this is very hygroscopic and does not give satisfactory analytical data. The preparations are simpler than ones reported earlier using rhodium(I) carbonyl precursors.[5,15,26] Synthesis of the dpb and diop complexes via reaction [IV.1] requires a refluxing procedure; the complexes are air-sensitive and this could explain the slightly low carbon analyses.

The $Rh(\overset{\frown}{P\ P})_2^+A^-$ complexes ($A^-=BF_4^-$, PF_6^-, SbF_6^-), readily prepared from the chloro complexes by treatment with Ag^+A^-, can be recrystallized from $CH_2C\ell_2$ - ether; the carbon analyses are somewhat low due to the presence of dichloromethane in the crystals (Table IV.1). Details are given only for the tetrafluoroborate complexes since these proved to have more convenient solubility properties for the catalytic studies (see section IV.4).

The borohydride method of Sacco and Ugo[5] was used to synthesize the $HRh(\overset{\frown}{P\ P})_2$ complexes from the chloro analogues. A presumedly dpm species decomposed spontaneously, at least at room temperature, and it was not possible to isolate the dpb by this route or one developed by Robinson's group starting from rhodium trichloride.[27] This latter method, in fact, proved to be unsatisfactory for all the hydrides, except $HRh(diop)_2$.[19]

Tables IV.1-IV.5 report conductivity and spectroscopic data for the various complexes.

The molar conductivity data (Table IV.1) show that dpm, dpe, and dpp chloro complexes are 1:1 electrolytes in nitromethane, and the

Table IV.2. Visible spectral data for the rhodium(I) complexes[a]

Complex	Medium	λ_{max} nm ($\varepsilon \times 10^{-3}$ $\underline{M}^{-1} \cdot cm^{-1}$)
$Rh(dpm)_2Cl$	methanol	385 (3.8), 446 (3.5)
	toluene	406[b] (3.3)
$Rh(dpe)_2Cl$	methanol	406[b] (4.5)
$Rh(dpp)_2Cl$	methanol	410[b] (2.6)
$Rh(dpb)_2Cl$	methanol	435[c]
	toluene	420 sh (1.6)
$Rh(diop)_2Cl$	methanol	440[c]
	toluene	continuum
$Rh(dpm)_2^+BF_4^-$	methanol	385 (3.7), 446 (3.5)
$Rh(dpe)_2^+BF_4^-$	methanol	407[d] (5.0)
$Rh(dpp)_2^+BF_4^-$	methanol	412[d] (2.8)
$Rh(dpb)_2^+BF_4^-$	methanol	435 (3.3)
$Rh(diop)_2^+BF_4^-$	methanol	442 (3.6)
$HRh(dpe)_2$	toluene	406 (8.1)
$HRh(dpp)_2$	toluene	continuum
$HRh(diop)_2$	toluene	355 (13.4)

a Under Ar at room temperature.

b In solid state, ~410 nm.

c Intensity increases with time.

d In solid state, ~412 nm.

Table IV.3. Infrared and high-field ^1H nmr data for various rhodium(I) complexes.

Complex	Nmr data[a]			ir data[b]	
	Rh-H, τ	J_{P-H}, Hz	J_{Rh-H}, Hz	ν(Rh-H), cm^{-1}	ν(Rh-Cℓ), cm^{-1}
$Rh(dpb)_2C\ell$					281 (w)
$Rh(diop)_2C\ell$					284 (w)
$HRh(dpe)_2$	20.1	18.0	10.0	1900 (s)	
$HRh(dpp)_2$	19.8	20.8	8.0	2100 (s)	
$HRh(diop)_2$	21.0	17.0	6.0	2040 (w)	

Free ligand[c]	ir data[b]
	ν(280-400 cm^{-1} bands)
dpm	350(s), 387(s)
dpe	345(s), 393(s)
dpp	303(s), 335(s), 393(s)

a In C_6D_6 at 25°C under argon.

b In Nujol; s=sharp, w=weak.

c Dpb and diop ligands have no absorption bands in the 280-400 cm^{-1} region.

Table IV.4. ^{31}P nmr data for the rhodium(I) complexes at 25°C.

Complex	Medium	$\delta(P)$[a]	J_{Rh-P}, Hz	Coordination Shift (Δ)[b], ppm
$Rh(dpm)_2Cl$	CH_2Cl_2-acetone-d_6 (2:1 V/V)	+22.80	115.3	+0.55
	C_6D_6	+17.38	105.3	-4.87
$Rh(dpe)_2Cl$	CH_2Cl_2-C_6D_6 (2:1 V/V)	-57.18	134.2	-69.69
$Rh(dpp)_2Cl$	CH_2Cl_2-acetone-d_6 (2:1 V/V)	-7.79	132.3	-25.04
$Rh(dpb)_2Cl$	"	See text		
$Rh(diop)_2Cl$	"	See text		
$Rh(dpm)_2^+BF_4^-$	CH_2Cl_2-C_6D_6 (2:1 V/V)	+23.50	117.0	+1.25
$Rh(dpe)_2^+BF_4^-$	"	-57.22	132.7	-69.73
$Rh(dpp)_2^+BF_4^-$	"	-7.38	130.5	-24.63
$Rh(dpb)_2^+BF_4^-$	"	-21.09	132.0	-37.04
$Rh(diop)_2BF_4^-$	"	-9.22	140.0	-31.72
$HRh(dpe)_2$	C_6D_6	-56.43	142.5	-68.94
$HRh(dpp)_2$	"	-18.26	141.8	-35.51
$HRh(diop)_2$	"	-22.46	146.0	-44.96

a Measured in ppm (upfield positive) from 85% H_3PO_4. Shifts (CH_2Cl_2 or $CDCl_3$) for the free ligands occur at +22.25 (dpm), +12.51 (dpe), +17.25 (dpp), +15.95 (dpb), and +22.50 (diop).

b $\Delta = \delta_{complex} - \delta_{ligand}$.

Table IV.5. ^{1}H nmr data for the rhodium(I) complexes at 25°C.

Complex	δ(H)[a]	
	Aliphatic	Phenyl[b]
$Rh(dpm)_2Cl$	3.4m[a']	6.5m,7.2m[a']
$Rh(dpe)_2Cl$	2.15m	7.2m
$Rh(dpp)_2Cl$	1.8m,2.2m	7.1m
$Rh(dpb)_2Cl$	1.6m,2.0m	7.3m
$Rh(diop)_2Cl$	1.10s,2.3m,3.6m	6.7m,7.2m
$Rh(dpm)_2^+BF_4^-$	5.1m (4.85m)[c]	7.3m(7.4m,7.6m)[c]
$Rh(dpe)_2^+BF_4^-$	2.15m	7.25m
$Rh(dpp)_2^+BF_4^-$	1.85m,2.3m	7.2m
$Rh(dpb)_2^+BF_4^-$	1.7m,2.15m	7.15m,7.4m
$Rh(diop)_2^+BF_4^-$	1.10s,2.3m,3.8m	7.2m,7.4m
$HRh(dpe)_2$	2.2m[a']	7.0m,7.6m[a']
$HRh(dpp)_2$	1.6m,2.1m[a']	7.1m,7.7m[a']
$HRh(diop)_2$	1.26s,2.2m,3.4m,	7.0m,7.1m,7.5m,
	3.6m[a']	7.9m[a']
Free diphosphine		
dpm	2.85t(2.75t)[a']	7.3m(7.0m,7.4m)[a']
dpe	2.1t(2.2m)[a']	7.2m(7.0m,7.3m)[a']
dpp	1.7m,2.2m(1.55m,2.0m)[a']	7.2m(7.1m,7.3m)[a']
dpb	1.5m,1.9m(1.45m,1.8m)[a']	7.1m(7.1m,7.4m)[a']
diop	1.28s,2.3m,3.8m	7.2m
	1.28s,2.4m,4.0m[a']	7.0m,7.3m[a']

a Measured in ppm (downfield positive) from TMS in $CDCl_3$ unless otherwise indicated; s=singlet, t=triplet, m=multiplet.

a' In C_6D_6.

b For phenyl region, lower shift when discernible is due to m- and p-protons and the higher shift due to o-protons; for $HRh(diop)_2$, the 2 lower shifts are due to m-,p-protons, and the higher shifts due to o-protons.

c In acetone-d_6.

visible spectral data in methanol (Fig.IV.1(A)) correspond also to those of the BF_4^- salts (Fig.IV.2;Table IV.2). The solid state spectra of the dpe and dpp chloro complexes also show absorption maxima at wavelengths similar to the solution values, indicating the same ionic structure in the solid state. These complexes have always been considered as ionic in the solid state with square planar cations (or approximately so[17]), and this appears to be based on electronic absorption and emission spectral data.[16,17,28] The dpm complex, unlike the other two, is soluble in toluene and the visible absorption spectrum in this solvent (Fig.IV.1(B)) and the solid state differs from that in methanol (Fig. IV.1(A)). We thus consider $Rh(dpm)_2C\ell$ to be five-coordinate in the solid state and toluene. Detection of possible Rh-Cℓ stretching frequencies in the ir is prevented, due to absorption by the dpm (and dpe, dpp) ligands in the 400-280 cm^{-1} region (Table IV.3). The dpb and diop chloro complexes also appear to be five-coordinate in the solid state and in non-polar solvents; the conductivity data in nitromethane suggest incomplete dissociation of chloride, and their solubility in toluene (the corresponding fluoroborates being insoluble) is also consistent with coordinated chloride. Further, weak ir bands at 281 and 284 cm^{-1} for the dpb and diop complexes, respectively, (not present in the BF_4^- analogues) are attributed to ν(Rh-Cℓ). The visible spectral data are solvent dependent and, in methanol, correspond to those of the cations, thus showing loss of ionic chloride in this medium. The absorption maximum in the cationic systems moves to higher wavelengths as n increases from 2 to 4 (Fig.IV.2). The dpm system is different in showing two maxima in the 380-450 nm region; "anomalous" ^{31}P nmr shifts are also noted with

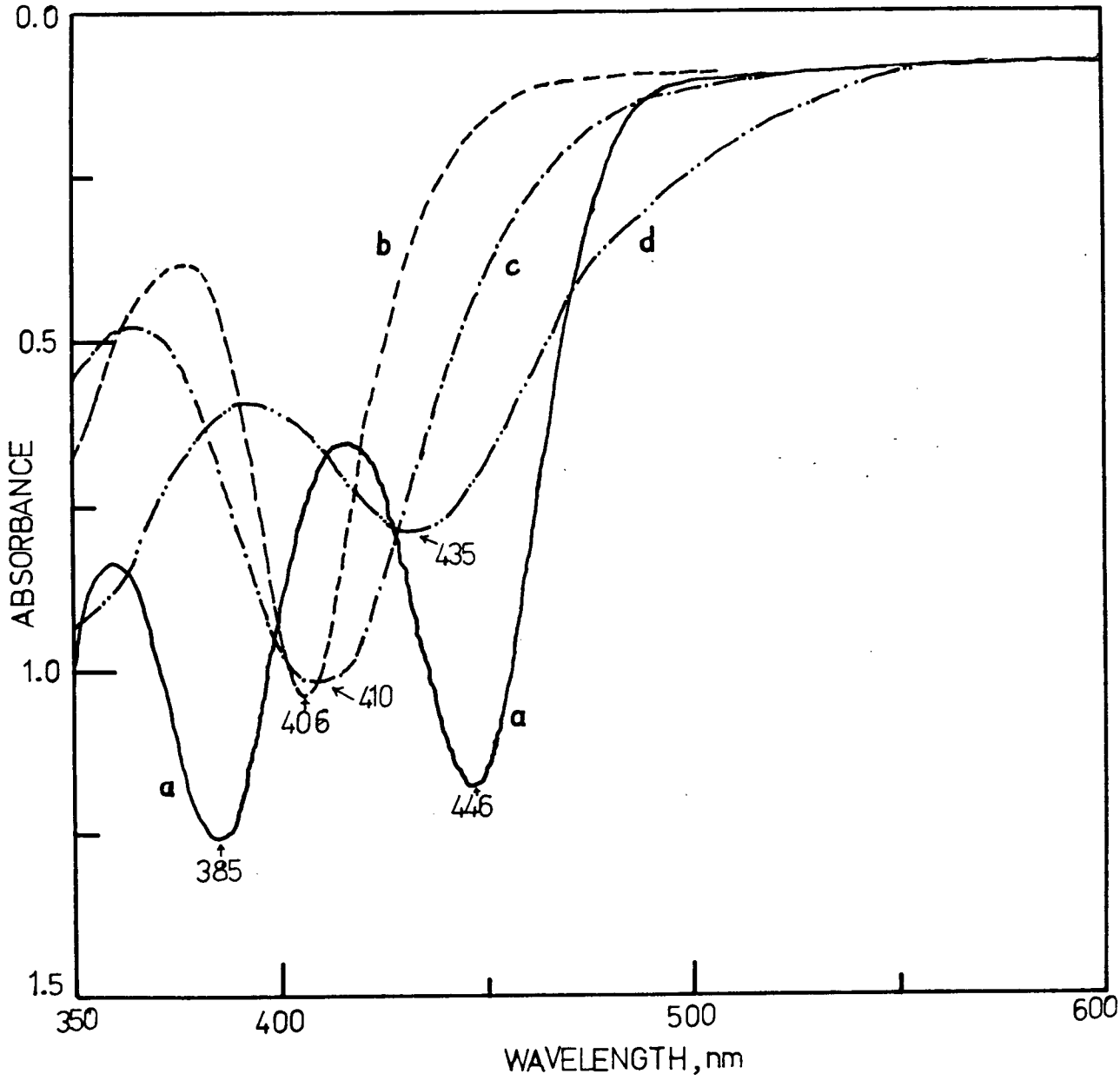

Figure IV.1(A) Visible absorption spectra of the $Rh(\overset{\frown}{P\ P})_2C\ell$ complexes in methanol under argon at 25°C ($\overset{\frown}{P\ P}$ = a.dpm, b.dpe, c.dpp, and d.dpb).

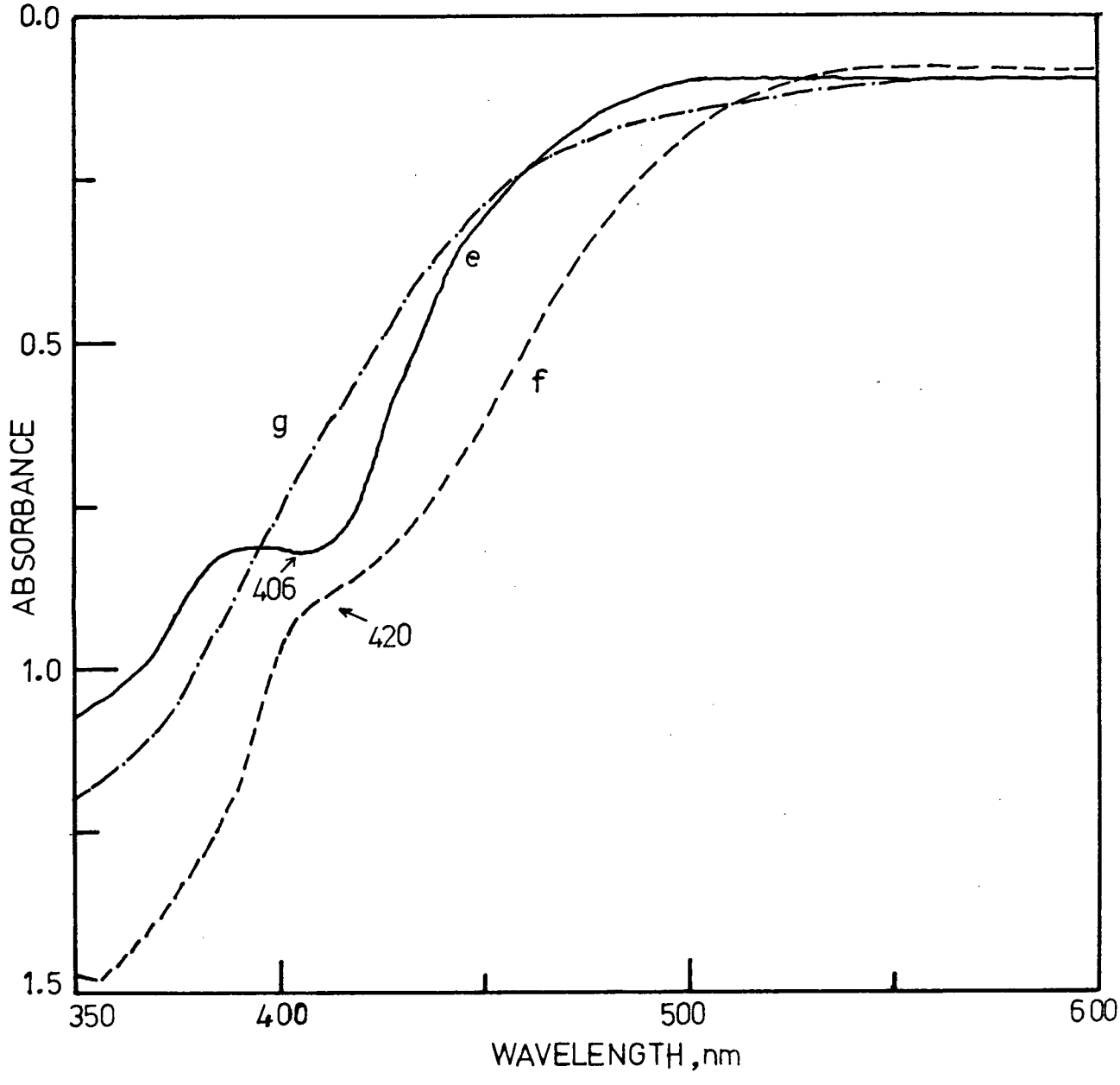

Figure IV.1(B) Visible spectra of the $Rh(\overset{\frown}{P\ P})_2Cl$ complexes in toluene under argon at 25°C ($\overset{\frown}{P\ P}$ = e.dpm, f.dpb, and g.diop).

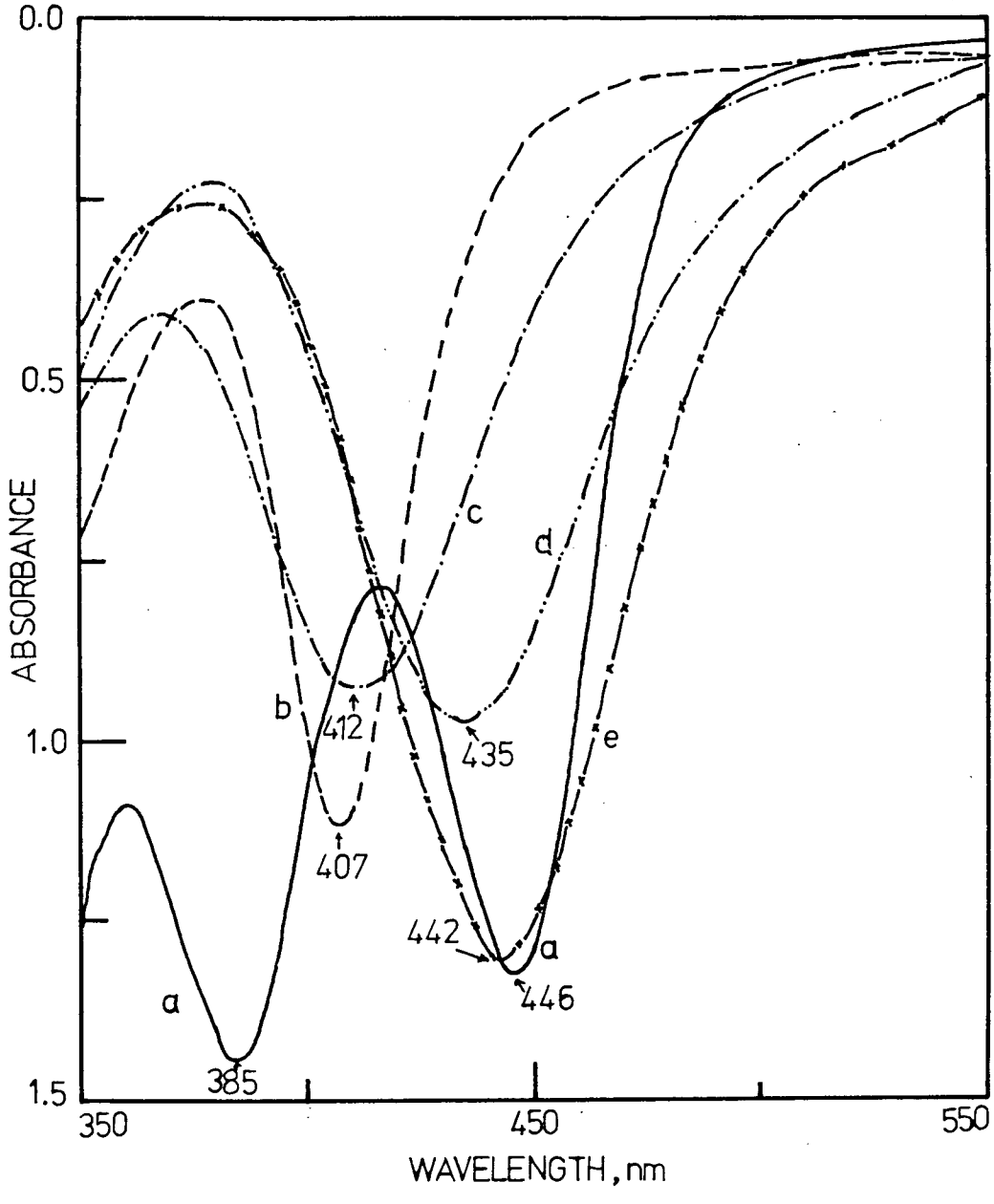

Figure IV.2 Visible spectra of various $Rh(\overset{\frown}{P\ P})_2^+BF_4^-$ complexes in methanol under argon at 25°C ($\overset{\frown}{P\ P}$ = a.dpm, b.dpe, c.dpp, d.dpb, and e.diop).

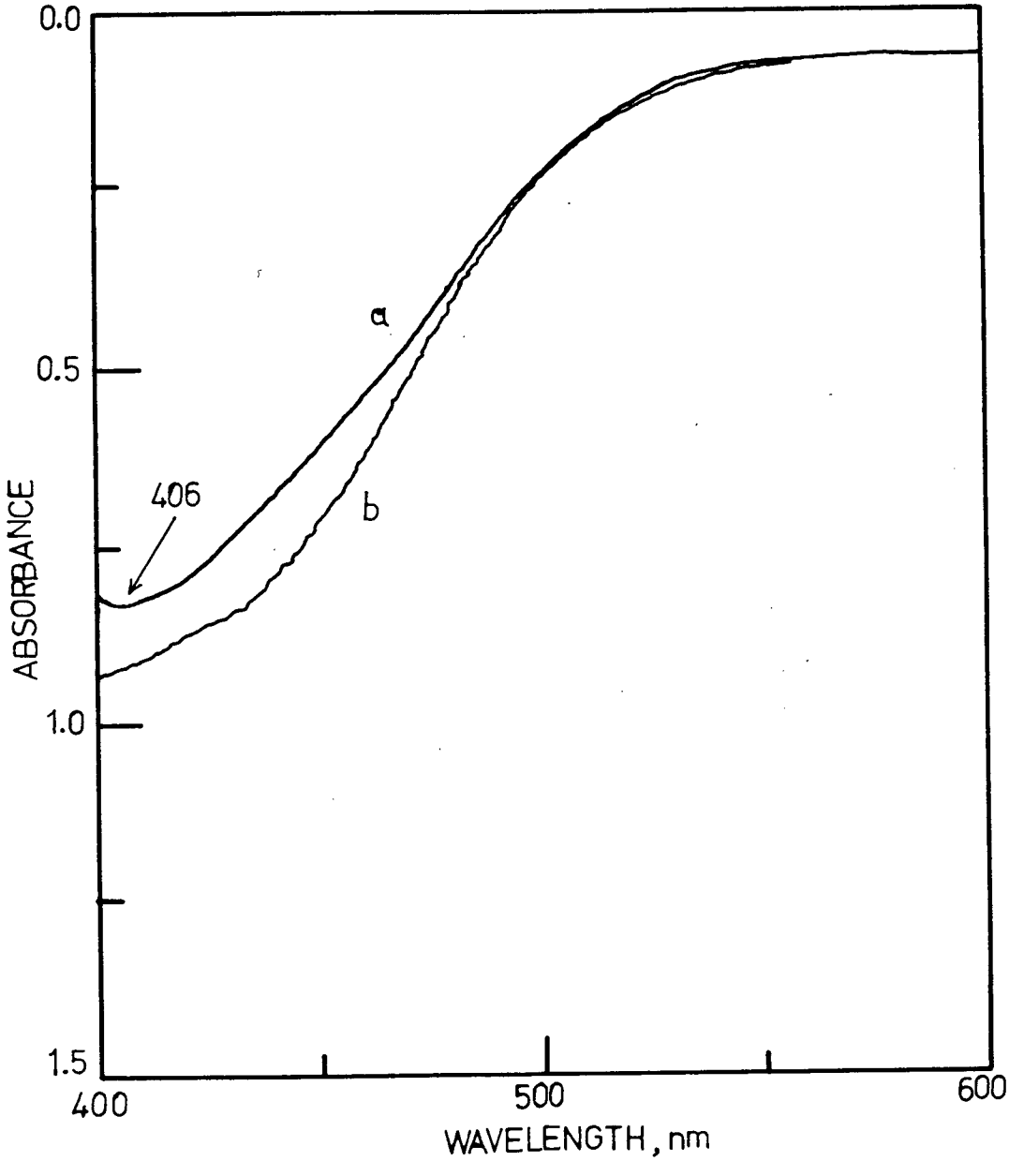

Figure IV.3 Absorption spectra of the $HRh(\overset{\frown}{P\ P})_2$ complexes in toluene under argon at 25°C ($\overset{\frown}{P\ P}$ = a.dpe and b.dpp).

this system (see below).

Measurement of the conductivity of the five-coordinate hydrides in nitromethane gave unexpectedly high values for the dpe and dpp complexes, while the diop species exhibited normal behaviour (Table IV.1). All the hydrides were essentially non-conducting in polar DMA.[29] Reaction of the hydrides with the nitromethane is indicated, although the limited solubility of the complex and the extreme sensitivity of the solutions to oxygen presented difficulties for further investigations. Reaction of platinum metal hydride complexes with nitroalkanes is not unprecedented; several aromatic and aliphatic compounds have been reduced to corresponding amines catalyzed, for example, by $HRuCl(PPh_3)_3$ in benzene-ethanol(1:1 V/V)[30] (equation [IV.2]):

$$\begin{matrix} R \\ R' \end{matrix}\!\!>\!CH\text{-}NO_2 + 3H_2 \xrightarrow{HRuCl(PPh_3)_3} \begin{matrix} R \\ R' \end{matrix}\!\!>\!CH\text{-}NH_2 + 2H_2O \qquad [IV.2]$$

The hydride ligand of the $HRh(\overset{\frown}{P\ P})_2$ complexes is readily detected by ir, and the high field ^1H nmr, a well resolved doublet of quintets at room temperature (Table IV.3, Fig.IV.4), is consistent with four equivalent phosphorus atoms. The same nmr pattern with similar coupling constants (J_{Rh-H} = 7 Hz, J_{P-H} = 18 Hz) has been reported for $HRh[Ph_2P(CH_3)]_4$ at -60°C, and this was attributed to a tetragonal pyramid structure[31], although others have considered that a fluxional C_{3v} structure is more likely.[32] The solid state structure of $HRh(PPh_3)_4$ with the hydrogen atom omitted is tetrahedral, and a threefold axis of symmetry implies that the hydrogen lies on this axis or must be randomly disordered in the crystal.[33,34] A recent structure determination of $HIr(dpe)_2$ shows it to be approximately

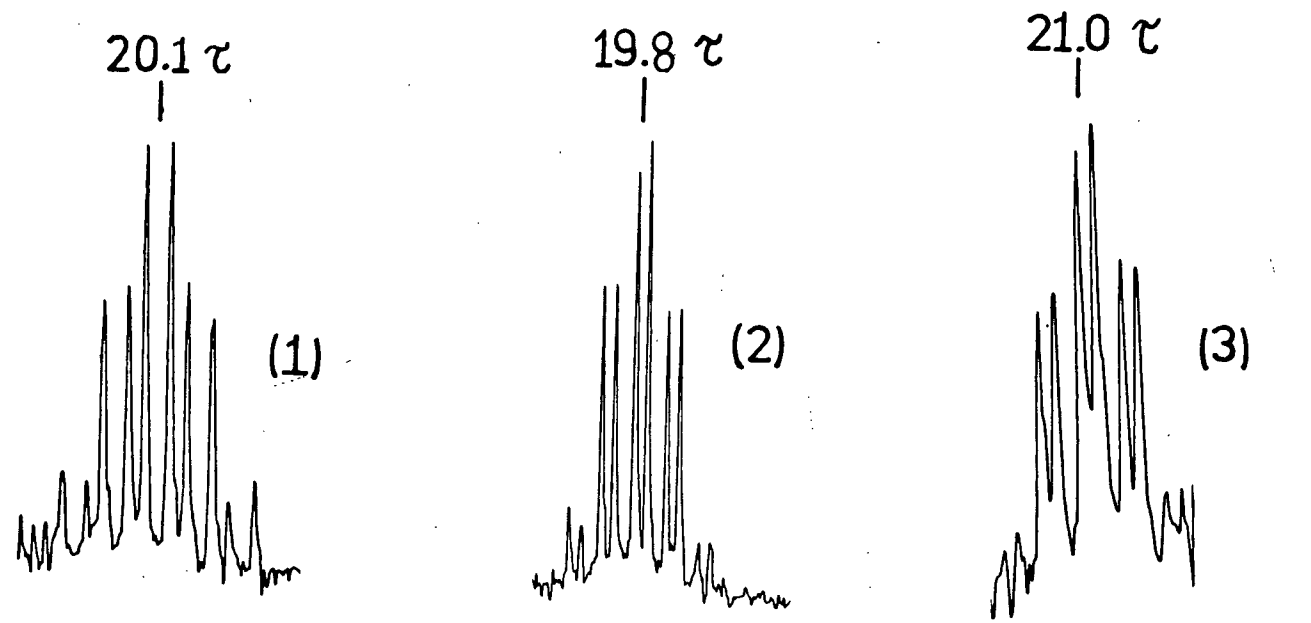

Figure IV.4 High-field ^{1}H nmr spectra of (1) $HRh(dpe)_2$ (2) $HRh(dpp)_2$ (3) $HRh(diop)_2$ in C_6D_6 at 25°C.

trigonal bipyramidal with the hydride presumed to be at an axial site[35] (Figure IV.5); the high field ^{1}H nmr is the quintet expected of a fluxional solution structure, and by analogy the $HRh(\widehat{P\ P})_2$ structures are likely to be similar.

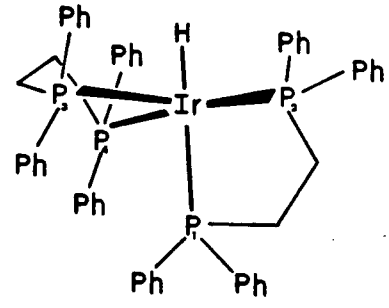

X-ray crystal structure of the $HIr(dpe)_2$ complex.
Figure IV.5

A single crystal x-ray structure determination of $HRh[(+)\text{-diop}]_2$, now in progress, has revealed a distorted trigonal bipyramid structure (Figure IV.6), very similar to that shown in Figure IV.5 for $HIr(dpe)_2$. Various bond lengths and bond angles are listed with Figure IV.6. As expected, due to the high trans influence of the hydride ligand[36,37], the Rh-P_1 bond length (2.340Å) is found to be longer than those for the other three Rh-P bonds. The $^{31}P\{^{1}H\}$ nmr signal of this complex is a doublet at 25°C but gives rise to a complicated spectrum at -50°C (Figure IV.7). The correlation between the solid state structure and the low temperature solution spectrum of this complex needs further elucidation.

The ^{31}P nmr signals (proton-decoupled for the hydrides) for all the complexes at 25°C appear as sharp doublets due to equivalent phosphorus atoms coupling to the rhodium (Table IV.4; e.g. Figure IV.8). No general trends in δ values are apparent, although the dpm ligand is different in undergoing upfield shifts (Δ positive) on coordination to the metal. Such

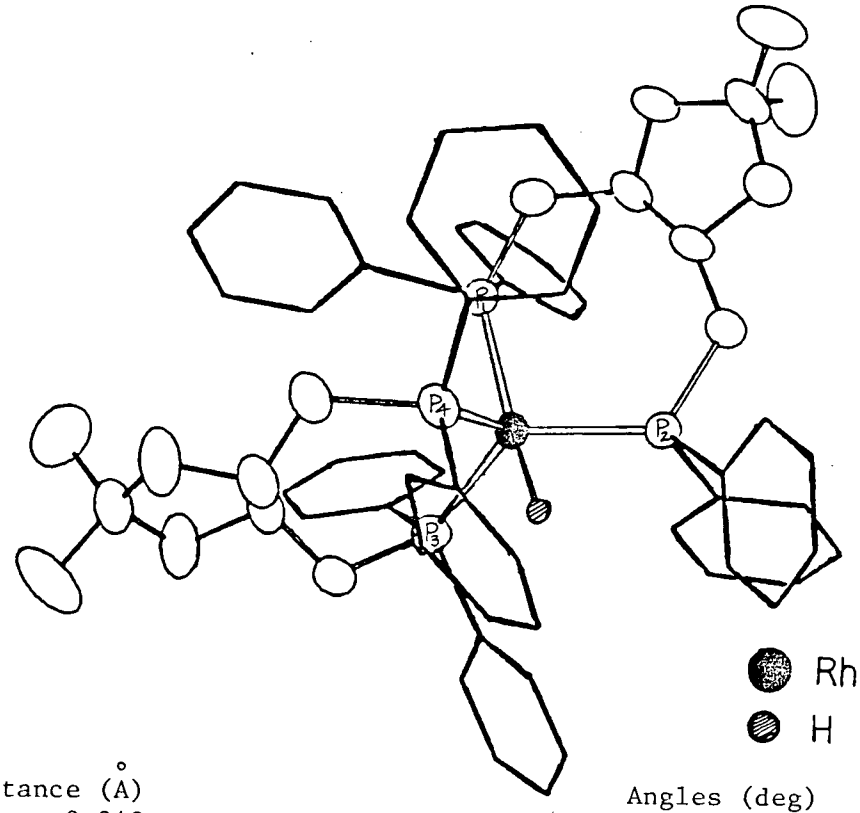

Distance (Å)	
Rh-P1	2.340
Rh-P2	2.291
Rh-P3	2.310
Rh-P4	2.315
Rh-H	~1.6

P-C(aryl) mean = 1.85(2)
P-C(alkyl) mean = 1.854(3)

Angles (deg)	
P2-Rh-P3	122.94
P4-Rh-P1	97.03
P1-Rh-P2	102.23
P3-Rh-P4	106.09
P2-Rh-P4	117.34
P3-Rh-P1	107.42
P1-Rh-H	164.70
P2-Rh-H	76.21
P3-Rh-H	85.47
P4-Rh-H	71.07

Figure IV.6 Crystal Structure of the $HRh[(+)\text{-diop}]_2$ complex.

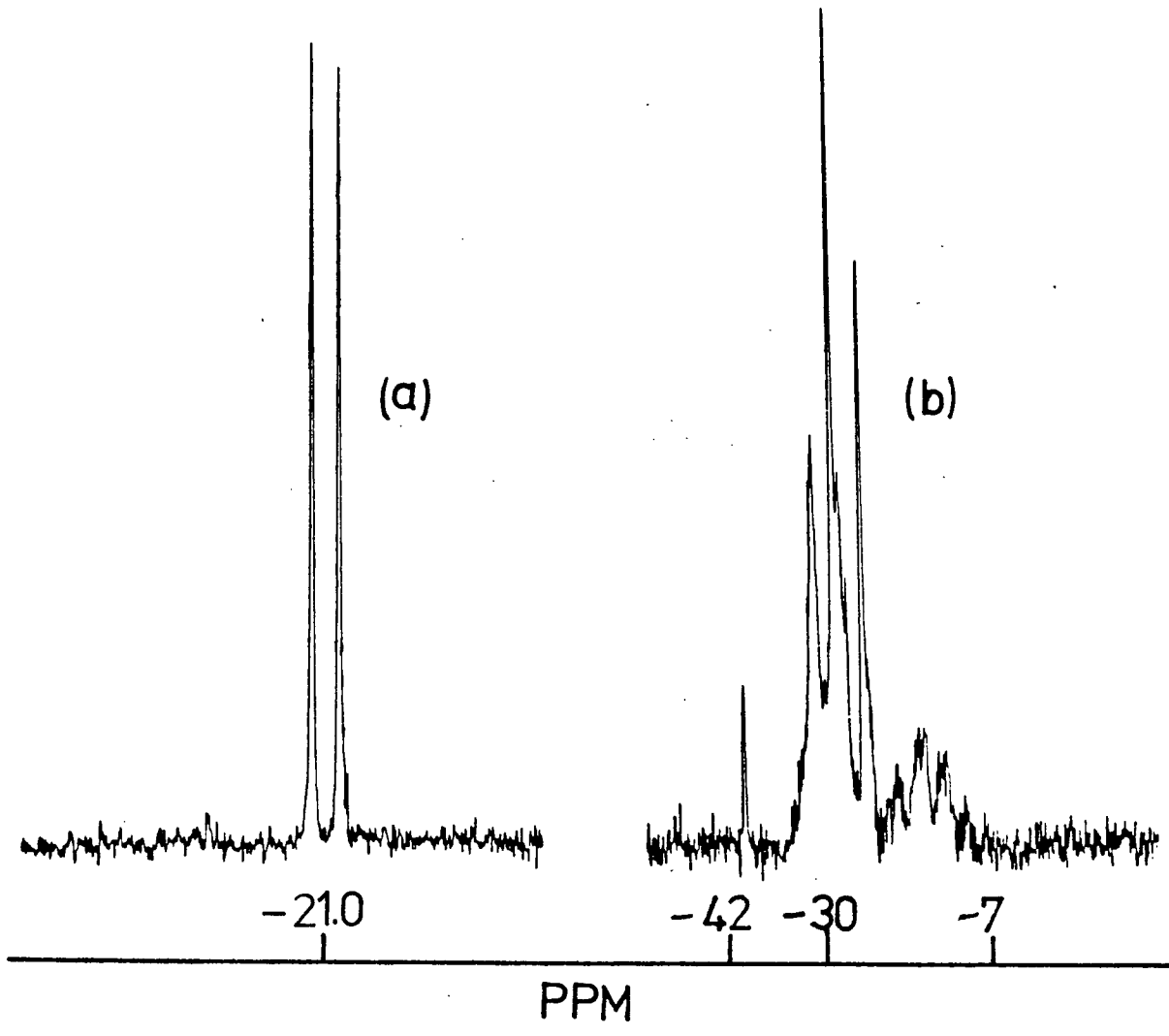

Figure IV.7 $^{31}P\{^{1}H\}$nmr spectrum of $HRh[(+)\text{-diop}]_2$ under argon in n-butanol-toluene-acetone-d_6(a) at 25°C and (b) at -50°C.

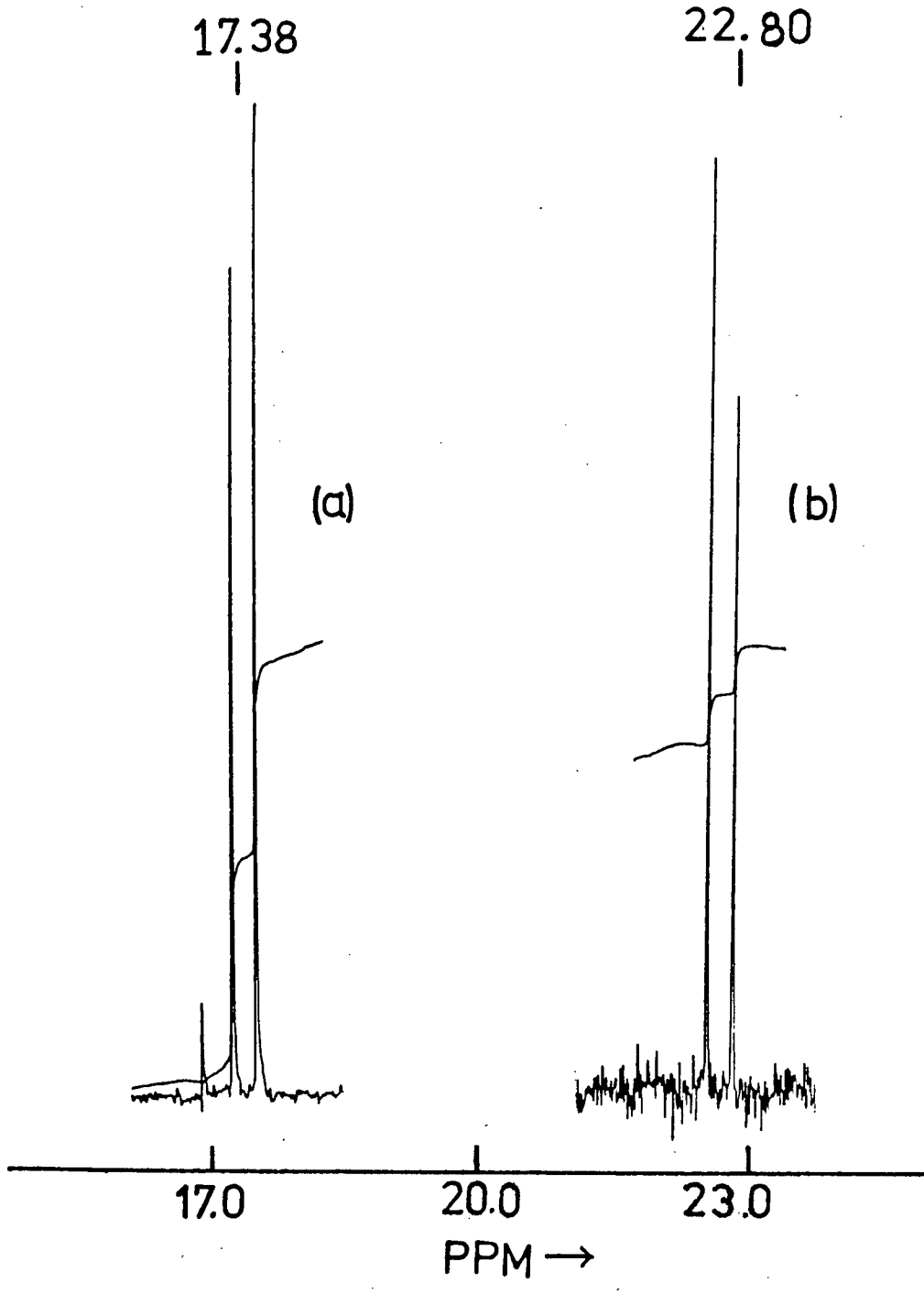

Figure IV.8 ^{31}P nmr spectrum of $Rh(dpm)_2C\ell$ in (a) C_6D_6 and (b) $CH_2C\ell_2$-acetone-d_6 at 25°C.

upfield shifts have been reported for both dpm and dpp ligands in some iridium complexes[3] (e.g. in $[Ir(CO)(dpm)_2]C\ell$ and $[Ir(CO)(dpp)_2]C\ell$), and the factors determining such shifts have been enunciated[38,39] in terms of metal-ligand interactions and rehybridization effects on coordination of ligand to the metal. The substantially large downfield shifts noted for the dpe complexes provide further examples of the large degree of deshielding apparent in five-membered ring systems.[39] The data for the chloro and tetrafluoroborate complexes are consistent with the dpe and dpp complexes being ionic, and the variation of the ^{31}P chemical shift for $Rh(dpm)_2C\ell$ with solvent is also consistent with ionic character in polar solvents and covalent character in benzene (Table IV.4; Fig.IV.8). Complex ^{31}P spectra were obtained at 25°C for the $Rh(dpb)_2C\ell$ and $Rh(diop)_2C\ell$ complexes in both C_6D_6 and $CH_2C\ell_2$ - acetone-d_6. Complications could arise by (a) partial ionization in the polar medium, (b) a more rigid five-coordinate structure [cf. the distorted trigonal bipyramidal structure of $HRh[(+)\text{-diop}]_2$ (Fig.IV.6)], since increasing chelate ring size leads to decreased fluxional behaviour[2,3], (c) the occurrence of multinuclear species, which are becoming increasingly evident in rhodium-diphosphine chemistry.[40,41] The simple doublet pattern of $Rh(diop)_2^+BF_4^-$ in CD_3OD also gives way to a complex spectrum at -60°C; formation of associated species seems the most likely explanation. More detailed variable temperature nmr studies have been done to help clarify the complications and will be discussed in chapter VI.

Data for the ^1H nmr in the phosphine region are given in Table IV.5. The shift of ligand protons on coordination is generally small except for the CH_2 protons of dpm which move downfield by ~0.6 and ~2.3

ppm in the $Rh(dpm)_2C\ell$ and $Rh(dpm)_2^+ BF_4^-$ complexes, respectively, the different shifts further confirming the non-ionic character of the chloro complex. These CH_2 resonances are somewhat solvent dependent (Table IV.5), and appear as a sextet due to "virtual coupling" with the rhodium (Figure IV.9) Such a phenomenon is not unprecedented and has been observed by Schrock and Osborn[42] for CH_3 resonances in $[Rh(COD)\{P(C_6H_5)_2CH_3\}]^+$ which appeared as a complex multiplet due to rhodium to methyl coupling ($J_{Rh-CH_3} \simeq 3$ Hz). The ortho protons of the phenyl groups in the dpe and dpp complexes experience an anisotropic deshielding compared to the meta and para protons. The phenomenon is more apparent from data in benzene-d_6 (Figure IV.10) since in $CDC\ell_3$ the phenyl absorption region is broad; for example, free dpe gives multiplets (3:2) at $\delta\sim7.0$ (meta,para) and 7.3 (ortho), while in the $HRh(dpe)_2$ complex these absorptions appear at 7.0 and 7.6 ppm, respectively (Table IV.5). Similar deshielding of ortho protons has been noted, for example[43], in some iridium alkyl complexes, $IrC\ell_2(CO)(PPh_3)_2(alkyl)$, (alkyl=$C_nH_{2n+1}$ (n=2-5, and 7); $CH_2CH_2C_6H_5$), although a shielding of the ortho protons occurs in the cis-octahedral complexes $Ir(dpe)_2X_2^+$ (X=O,S,Se)[44], in various cis-dpe complexes of Ir(III), Ru(III), Cr(0), Mo(0), and W(0) and in the $Rh(dpm)_2C\ell$ complex reported here (Table IV.5).

The low field ^1H nmr of the $HRh(diop)_2$ complex is of interest (Fig.IV.10) in that the aromatic protons appear as four distinct multiplets of relative intensity 3:3:2:2 at δ7.0, 7.1 (meta, para) and δ7.5, 7.9 (ortho); the deshielding through coordination is again well demonstrated, and there are now two sets of phenyl groups. These very likely approximate an edge-face conformation, a geometry that has been demonstrated recently in several $Ph_2P\frown PPh_2$ complexes, including

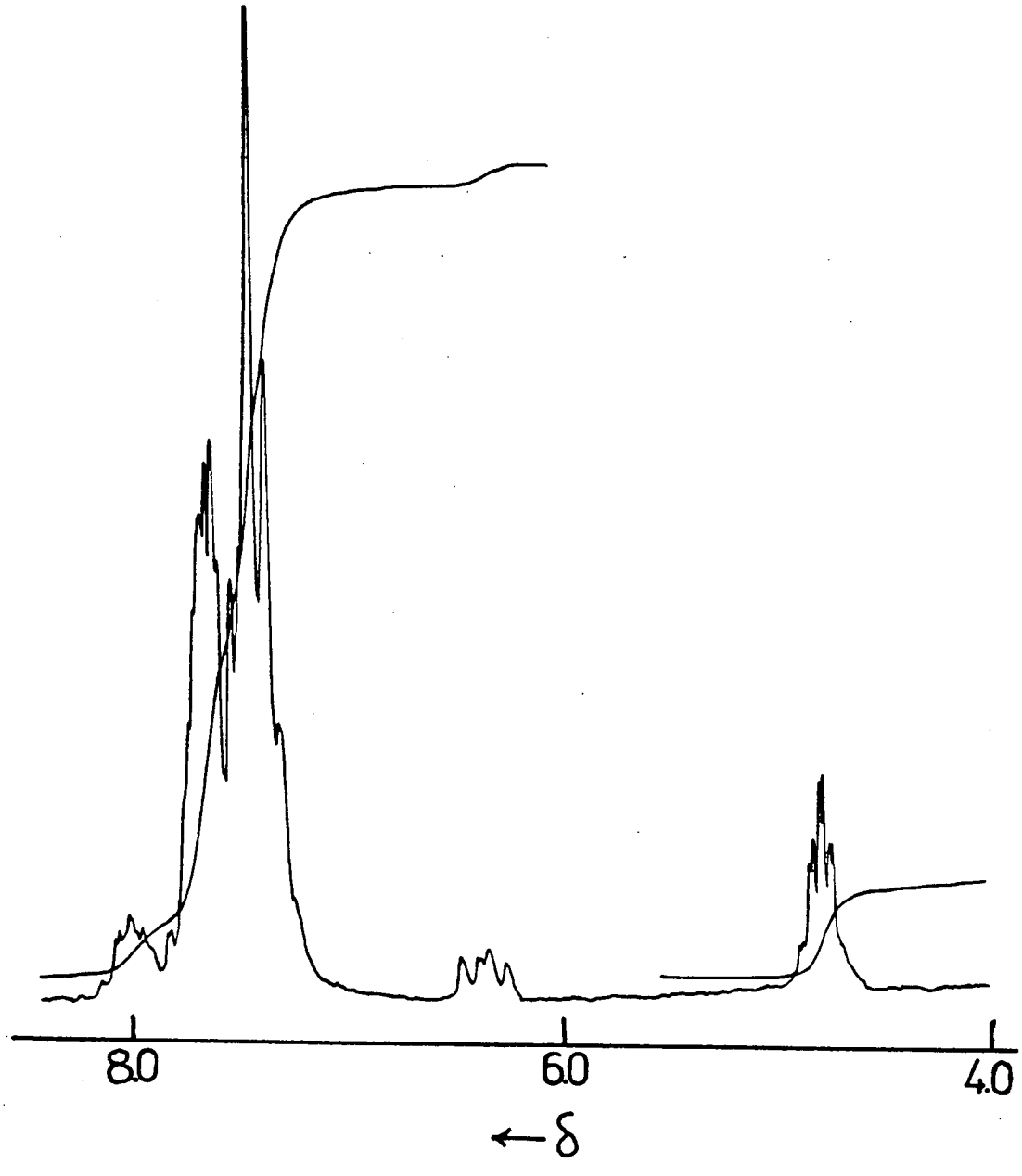

Figure IV.9 ^{1}H nmr spectrum of $Rh(dpm)_2^+BF_4^-$ in acetone-d_6 at 25°C.

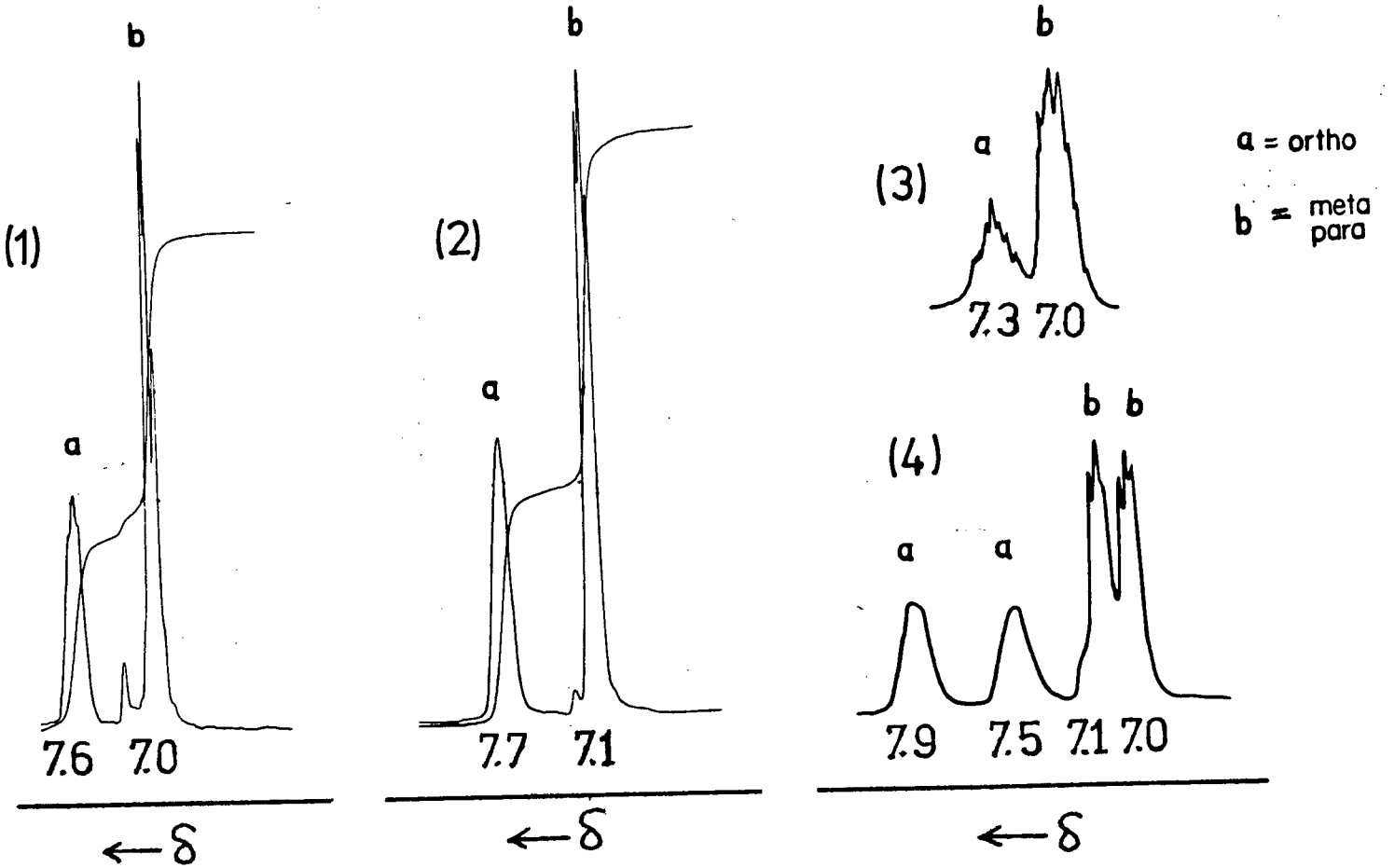

Figure IV.10 ^{1}H nmr (phenyl region) spectra of (1) $HRh(dpe)_2$ (2) $HRh(dpp)_2$ (3) diop (4) $HRh(diop)_2$ in C_6D_6 at 25°C.

$IrCl(COD)(diop)$[45] and $Rh(COD)(diphosphine)^+$ species[46-48], where COD= 1,5-cyclooctadiene and diphosphine=1,2-bis[(anisole)(phenylphosphino)] ethane and 2,3-bis(diphenylphosphino)butane. The orientation of the phenyl groups appears critical for the high efficiency of such complexes as catalysts for asymmetric hydrogenation of prochiral olefinic substrates.[13,46,48] All the complexes reported here are oxygen-sensitive in solution; in the solid state, only the chloride and fluoroborate complexes containing dpe and dpp are reasonably air-stable.

IV.4 Catalytic hydrogenation

Some preliminary kinetic data for hydrogenation of methylenesuccinic acid to 2-methylsuccinic acid are summarized in Table IV.6.

Figures IV.11-IV.13 show typical gas-uptake plots for the hydrogenation of methylenesuccinic acid at convenient conditions using some of the complexes listed in Table IV.6. The shape of the curves vary with the catalyst used, and only maximum rates were measured.

In agreement with others[2,7], it has been found that $Rh(dpe)_2^+Cl^-$ shows very low activity, and until our discovery of the activity of $HRh(diop)_2$[10,11], we and probably other workers, because of the early report[2], had not considered rhodium(I)-bis(diphosphine) chelate complexes as likely catalysts; a reason was considered to be the difficulty in providing a vacant coordination site.[49] Such complexes can clearly lead to quite high activity (Table IV.6), and in the case of $HRh(diop)_2$, the vacant site is thought to arise by one of the diphosphine ligands becoming monodentate[11,50] (chapter III).

Initially surprising is that $Rh(dpe)_2^+BF_4^-$ shows about ten times the activity of $Rh(dpe)_2^+Cl^-$ under corresponding conditions, and a similar difference in behaviour is noted for the dpb complexes. Presumably chloride must coordinate and deactivate some intermediate (e.g.

Table IV.6. Catalytic hydrogenation of methylenesuccinic acid using the rhodium(I) complexes[a]

Complex	[Rh] x 10^3 M	[Substrate] M	Max. rate x 10^6, M s^{-1}	$t_{1/2}$[b] x 10^{-3} s
$Rh(dpm)_2^+BF_4^-$	4.0	0.2	4.3	27
$Rh(dpe)_2Cl$	4.0	0.2	v.slow	72[c]
$Rh(dpe)_2^+BF_4^-$	4.0	0.2	9.6	10(6)[c]
	4.0	0.2	v.slow[d]	72[e]
	4.0	0.1	9.3	5
	2.0	0.1	8.0	6
	2.0	0.05	6.8	4
	1.0	0.05	4.6	7
$HRh(dpe)_2$	4.0	0.1	7.9[f]	7
$Rh(dpp)_2^+BF_4^-$	2.0	0.05	31.6	2
	1.0	0.05	17.8	3
	1.0	0.1	25.4	4
$HRh(dpp)_2$	4.0	0.1	41[f]	3
$Rh(dpb)_2Cl$	2.0	0.1	18.2[g,h]	3
$Rh(dpb)_2^+BF_4^-$	2.0	0.1	130[g,h]	0.4
	2.0	0.1	13[d,g]	7
$Rh(diop)_2Cl$	1.0	0.1	-	0.6[f,g]
$Rh(diop)_2^+BF_4^-$	1.0	0.1	135	0.4[f,g]
$HRh(diop)_2$	1.0	0.1	150	0.4[f,g]

a Typical experiment involved 5 ml n-butanol, at 1 atm total pressure and 60°C.

b Approx. reaction time for 50% hydrogenation of the substrate.

c 30% hydrogenation.

d In DMA.

e 20% hydrogenation.

f In n-butanol-toluene (2:1 V/V).

g At 30°C.

h In ethanol.

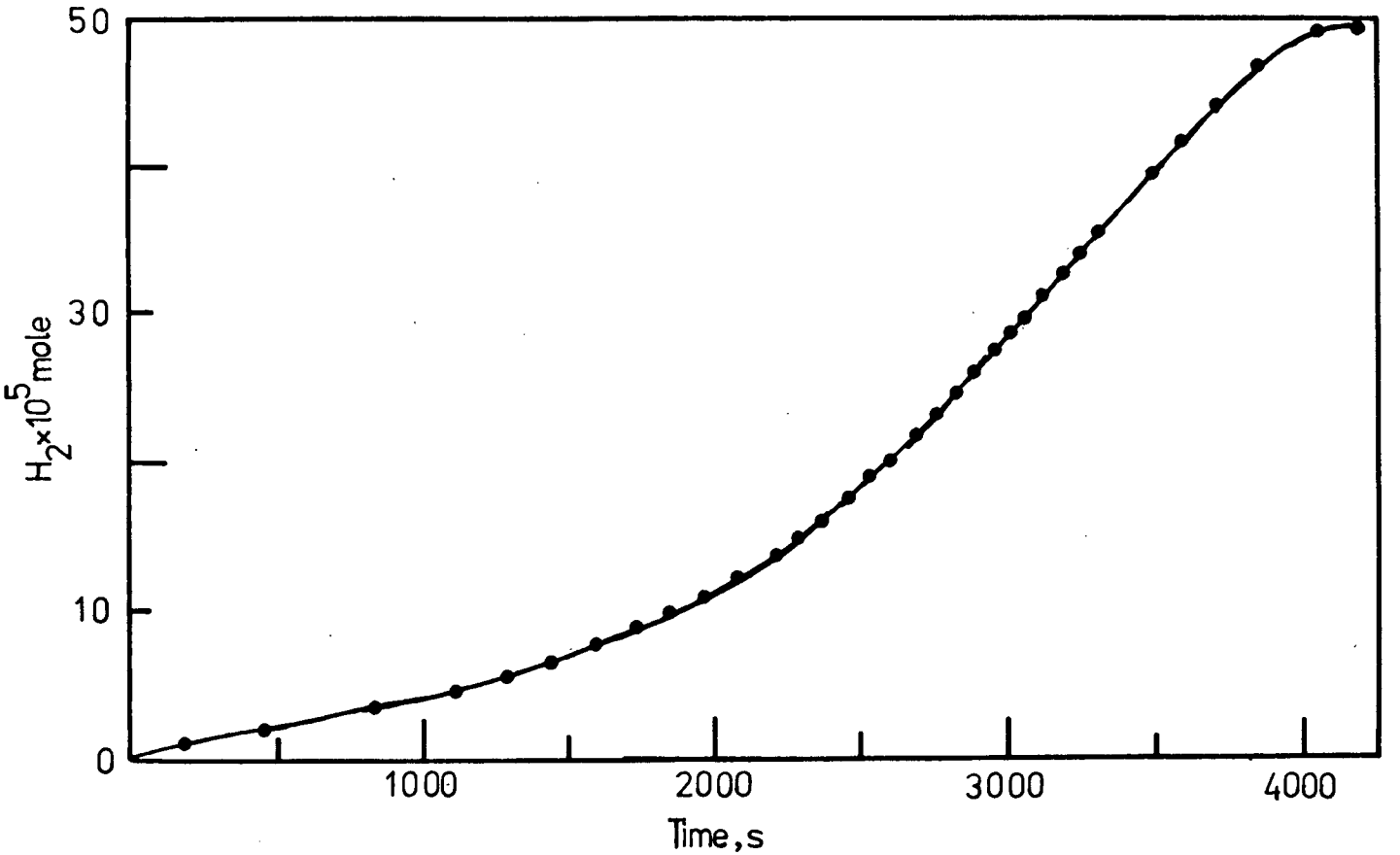

Figure IV.11 Rate plot for the hydrogenation (100%) of methylenesuccinic acid using $HRh(dpp)_2$ as catalyst ([Rh]=4×10^{-3}M, [S]=0.1M, 60°, n-butanol-toluene (2:1)=5 ml, P_t=1 atm).

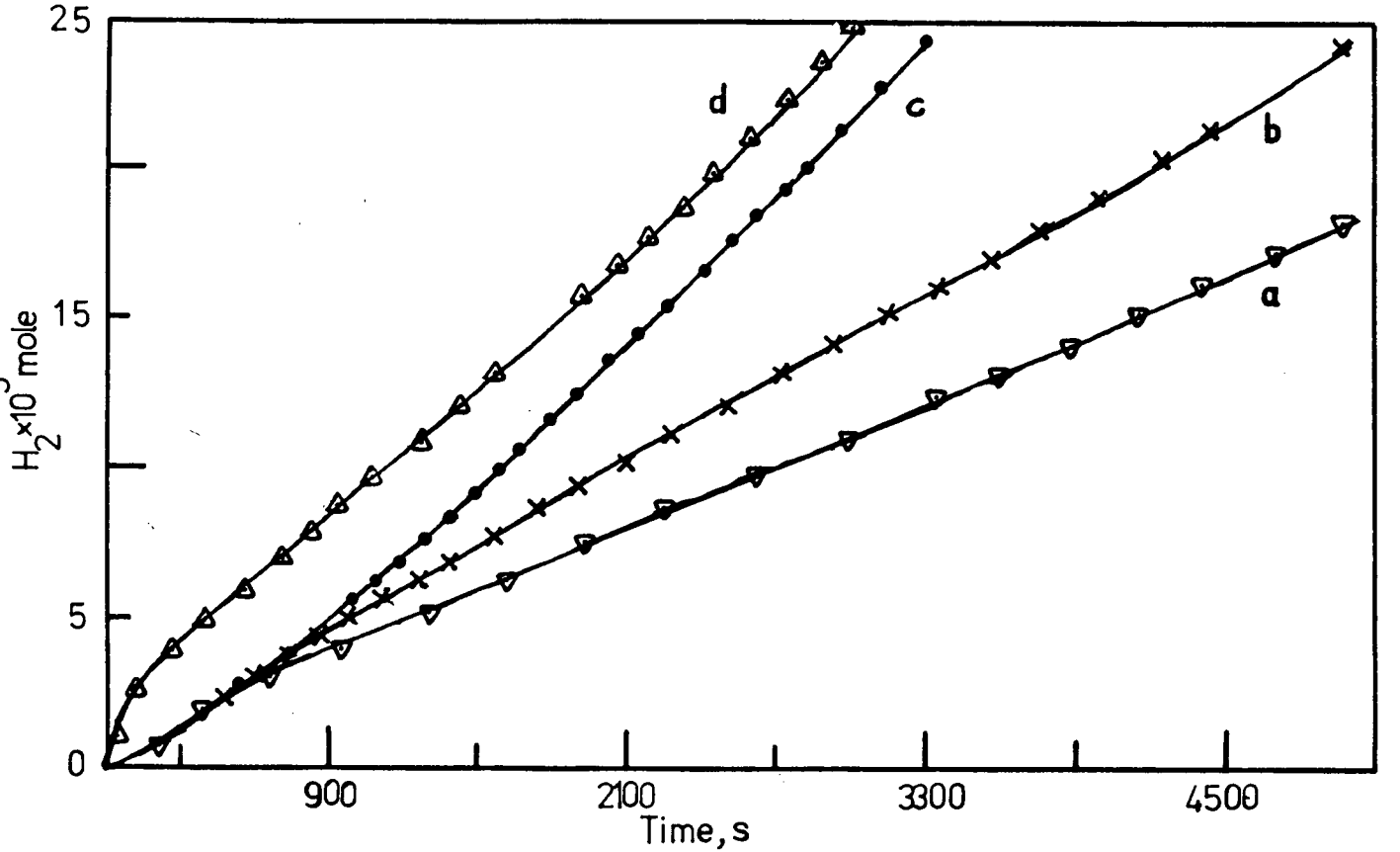

Figure IV.12 Rate plots for the hydrogenation (50%) at 1 atmosphere pressure of methylenesuccinic acid using

a. $HRh(dpe)_2$ ([Rh]=$4x10^{-3}$M, [S]=0.1M, 60°, n-butanol-toluene(2:1)=5ml).

b. $Rh(dpe)_2^+BF_4^-$ ([Rh]=$4x10^{-3}$M, [S]=0.1M, 60°, n-butanol=5ml).

c. $Rh(dpp)_2^+BF_4^-$ ([Rh]=$4x10^{-3}$M, [S]=0.1M, 60°, n-butanol=5ml)

d. $Rh(dpb)_2C\ell$ ([Rh]=$2x10^{-3}$M, [S]=0.1M, 30°, 2-methoxyethanol=5ml).

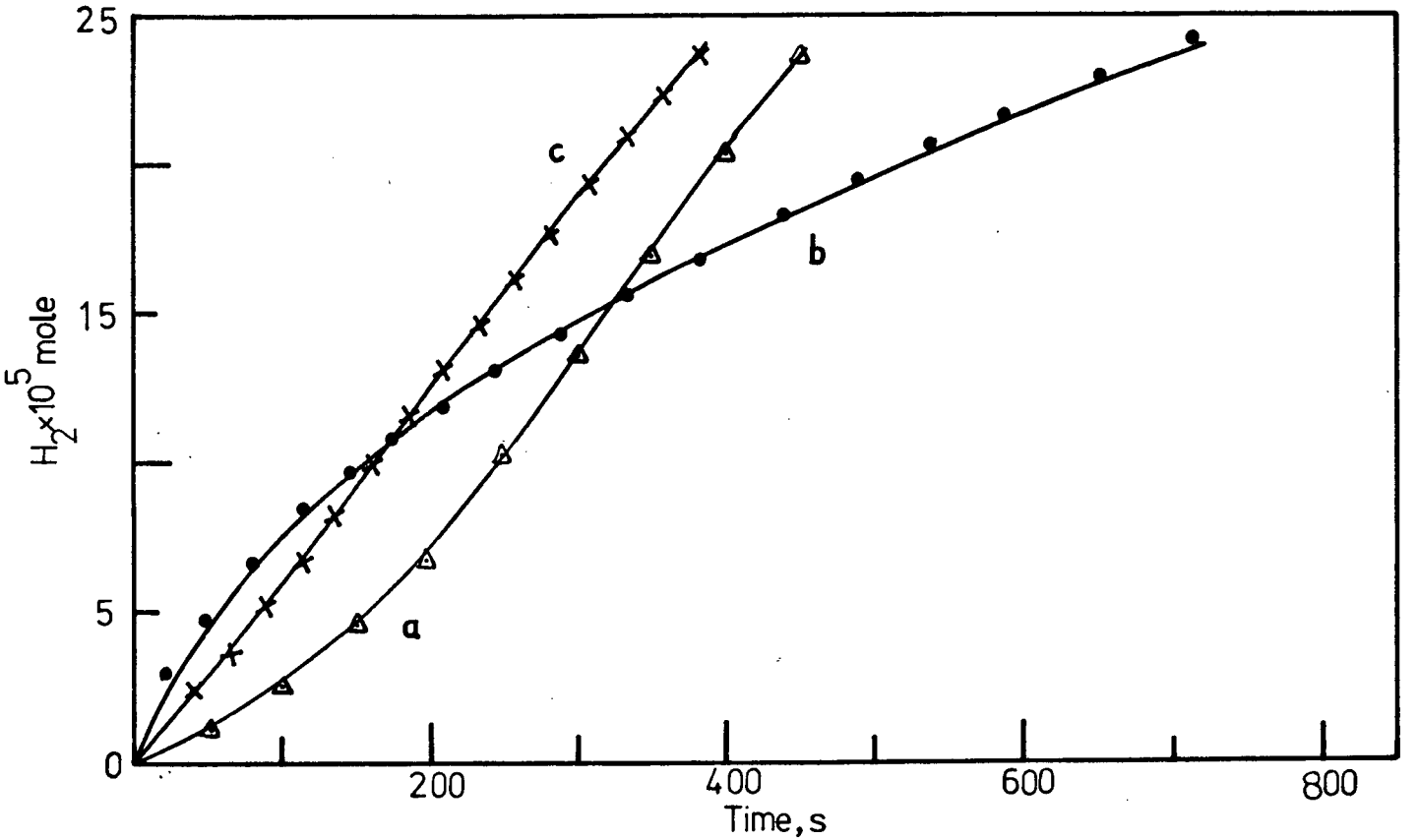

Figure IV.13 Rate plots for the hydrogenation (50%) at 1 atmosphere pressure of methylenesuccinic acid using

a. $HRh(diop)_2$ ([Rh]=1.5×10^{-3}M, [S]=0.10M, 30°, n-butanol-toluene(2:1)=5ml).

b. $Rh(diop)_2^+BF_4^-$ ([Rh]=2×10^{-3}M, [S]=0.10M, 15°, n-butanol-toluene(2:1)=5ml).

c. $Rh(dpb)_2^+BF_4^-$ ([Rh]=2×10^{-3}M, [S]=0.10M, 30°, 2-methoxyethanol=5ml).

an alkyl) in the catalytic cycle. The activity of the $Rh(diop)_2^+$ cation, however, is essentially the same whether the associated anion be chloride or tetrafluoroborate. The cations generally are much less active in the polar and more strongly coordinating DMA. For example, under similar conditions, $Rh(dpb)_2^+\overline{B}F_4^-$ hydrogenates the substrate ten times faster in ethanol (max. rate = $13x10^{-5}Ms^{-1}$) than in DMA (max.rate = $13x10^{-6}Ms^{-1}$)(Table IV.6).

The hydrides show activity comparable to that of the corresponding fluoroborate salts. The two species are interconvertible by the equilibria outlined in equation [IV.3][5,11], although these are unimportant for

$$HRh(\overset{\frown}{P\ P})_2 + H^+ \rightleftharpoons Rh(\overset{\frown}{P\ P})_2H_2^+ \rightleftharpoons H_2 + Rh(\overset{\frown}{P\ P})_2^+ \qquad [IV.3]$$

the diop complex in n-butanol-toluene with the methylenesuccinic acid substrate used.[11] Equilibrium [IV.3] has been studied in more detail for the $\overset{\frown}{P\ P}$ = diop system and will be discussed in chapter VI; the corresponding dpe and dpp systems have not been studied.

Comparison of the data for the fluoroborate salts at substrate concentrations $\geq$0.1 M shows that catalytic activity increases with chain length, n=4 (and diop) > n=3 > n=2 > n=1 (Table IV.6). Kagan's group[12] reported a similar trend for rhodium(I)-mono(diphosphine) systems formed *in situ* from $[RhCl(C_2H_4)_2]_2$ for the hydrogenation of α-acetamidocinnamic acid in benzene-ethanol at 20°C, the n=1 system being inactive; however, the n=6 system had activity comparable to that for n=3. Although these types of data are of use in designing better catalysts (including chiral ones), rationalizations to explain such trends, based solely on rate data

measured at a set of convenient conditions, should not be attempted. These systems typically show saturation behaviour in their kinetics; that is, the rates level off at higher substrate and/or H_2 concentrations[11], and the rate vs concentration profiles will vary for different systems. The limited data in Table IV.6 show that the rates for the $Rh(dpe)_2^+BF_4^-$ system are close to zero order in olefinic substrate and are fractional in catalyst, while for the $Rh(dpp)_2^+BF_4^-$ system the rates are close to first order in both substrate and catalyst. Detailed kinetic studies are necessary to elucidate the mechanisms, and then comparable rate constants can possibly be extracted by suitable analysis. In this particular case, it has been found that while $Rh(dpe)_2^+$ does not form a dihydride at ambient conditions [as noted by others[8]], the dpp analogue readily gives an isolable cis-$Rh(dpp)_2H_2^+$ complex (see chapter VII), and the mechanisms for catalytic hydrogenation may well differ. A quite different reactivity pattern has also been found, for example, for the monodiphosphine systems referred to above, when used to hydrogenate styrene in benzene [n=3 > n=1,5 > n=4 > diop > n=2].[12]

The diop systems $Rh(diop)_2X$ (X=Cℓ,BF_4,H) all gave rise to similar optical enrichment in the 2-methylsuccinic acid product (chapter V). These diop complexes have also been used effectively for the asymmetric hydrogenation of other prochiral substrates (chapter V).

CHAPTER V

ASYMMETRIC HOMOGENEOUS HYDROGENATION OF PROCHIRAL OLEFINIC SUBSTRATES USING RHODIUM-DIOP COMPLEXES AS CATALYSTS

V.1 Introduction

Since the preparation of the "diop" ligand by Dang and Kagan[1], well characterized as well as many in situ mono(diop)-rhodium(I) complexes have been used for the hydrogenation of various substrates.[2,3] In some cases, for example enamides, optical yields up to 92% have been obtained[4], while N-acylaminoacrylic acids have been hydrogenated[2,4-8] in ∿80% e.e. proving the versatility of such catalysts. Diop systems have been studied extensively in terms of the effects on the optical purities of the hydrogenated product by varying, for example a) concentrations of catalyst and substrate[1], b) anions associated with the catalyst[8], c) temperature[1], d) groups attached to the substrate[1,4,5,7,9-13], e) substitution at the phenyl groups of the diop ligand[6], f) solvent medium.[4,5] On the other hand, bis(diop)-rhodium complexes which overall should be "more rigid" than corresponding mono(diop) systems have not been studied, except for work from this laboratory.[14,15]

In this chapter, the potential of several bis(diop)-rhodium complexes, as well as a carbonyl mono(diop) complex, for catalytic asymmetric hydrogenation will be described. Optical purities of the hydrogenated substrates are compared with those obtained using mono(diop)-rhodium(I) systems.

V.2 Experimental

V.2.1 Preparation of complexes - The preparations of $HRh[(+)\text{-diop}]_2$, $Rh[(+)\text{-diop}]_2C\ell$, and $Rh[(+)\text{-diop}]_2^+BF_4^-$ are already described in chapter IV. The synthesis of $Rh[(+)\text{-diop}]_2H_2^+BF_4^-$ will be described in chapter VII.

$[RhCl(CO)_2]_2$ was prepared by the literature method.[16]

$[RhCl(CO)(+)\text{-diop}]_2$

To a pale yellow solution of $[RhCl(CO)_2]_2$ (0.194 g, 0.50 mmol) in degassed benzene (5 ml) was added (+)-diop (0.50 g, 1.0 mmol) in benzene (3 ml). The solution, which turned lemon yellow and evolved CO, was concentrated (ca. 5 ml), and cooled to 0°C after adding diethyl ether (10 ml). The resulting lemon yellow powder was filtered, washed with ether, and dried in vacuo. Calculated for $[RhCl(CO)(+)\text{-diop}]_2$:C=57.80%; H=4.82%. Found: C=58.10%; H=5.09%. The infrared (Nujol) showed bands due to ν(CO) and ν(Rh-Cl) at 1970 and 307 cm^{-1}, respectively. The compound was reported[2,17] and characterized as a dimer with bridging diop ligands[17] while our studies were in progress; both syntheses reported[2,17] involved carbonylation of Rh(I)/diop solutions.

V.2.2 Determination of optical purities - All experiments were performed on the gas-uptake apparatus described previously in chapter II (Fig.II.1). In a typical experiment, 0.2 g of the olefinic substrate was dissolved in 10 ml of the solvent and the solution was degassed before adding the catalyst. The reaction was monitored till completion. The final solution was worked-up to isolate the hydrogenated product as described in section II.9. The product (0.1 g) was dissolved in the appropriate solvent and the optical rotation of the solution was measured at room temperature using a Perkin Elmer 141 polarimeter. Some experiments were repeated to check the accuracy of the rotation values obtained (±2%).

The enantiomeric excesses (e.e.) were calculated based on rotation values for pure isomers as follows: R(+)- and S(-)- 2-methylsuccinic acid $[\alpha]_D^{25}=\pm 17.09°$ (c10.5, C_2H_5OH);[18] R(+)- and S(-)- N-acetylalanine $[\alpha]_D^{25}=\pm 66.5°$ (c2, H_2O);[19] R(-)- and S(+)- 2-phenylpropionic acid $[\alpha]_D^{25}=\mp 76.1°$ (c8.06,

$CHC\ell_3$)[20]; N-acetyl-[(S) or (R)]-phenylalanine $[\alpha]_D^{25}=\pm 46.5°$ (cl, C_2H_5OH)[8].

V.3 Results

Hydrogenation of various prochiral α,β-unsaturated carboxylic acids was achieved at one atmosphere total pressure using bis(diop)-rhodium complexes (Tables V.1-V.4) and the $[RhC\ell(CO)(+)\text{-diop}]_2$ complex (Table V.5).

Itaconic acid was hydrogenated several hundred times faster than one of its isomers, citraconic acid (Tables V.1-V.5). α-Methylcinnamic acid was hydrogenated very slowly (Tables V.2 and V.3), while no hydrogenation of ethyl methyl ketone was observed (Tables V.1 and V.2).

The catalyst as isolated seems pure as either a powder or crystallized form (the $[\alpha]_D^{25}$ of both forms of the catalyst were identical [-3.4° in benzene]) and the optical yields remained unchanged for R(+)-2-methylsuccinic acid product when using either sample of $HRh[(+)\text{-diop}]_2$ (Table V.1).

Data in Tables V.1 and V.2 for the hydrogenation of itaconic acid show an increase in optical purity with increasing temperatures when either $HRh[(+)\text{-diop}]_2$ or $Rh[(+)\text{-diop}]_2^+BF_4^-$ was used as catalyst. However, a decrease in optical purity with increasing temperature was observed for the hydrogenation of N-acetamidocinnamic acid using $Rh[(+)\text{-diop}]_2C\ell$ as catalyst (Table V.3).

Solvent medium had little effect on optical purities of products except in the case of citraconic acid which gave the R(+) and the S(-) isomers of 2-methylsuccinic acid product in n-butanol-toluene (2:1) and in DMA, respectively, using the $Rh[(+)\text{-diop}]_2^+BF_4^-$ catalyst (Table V.2). Strong solvent effects were noted for the hydrogenation of N-acetamidocinnamic acid which afforded S(+)- or R(-)-N-acetylphenylalanine in n-butanol-toluene (2:1) or DMA, respectively, irrespective of temperature using

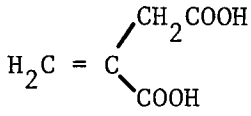

Methylenesuccinic acid
or Itaconic acid

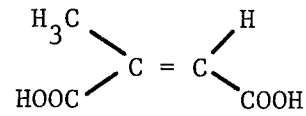

Citraconic acid

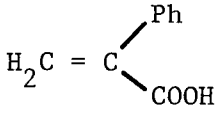

Atropic acid

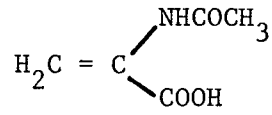

N-or α-Acetamidoacrylic acid

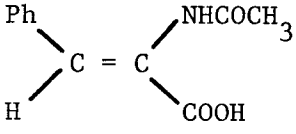

(Z)-N-Acetamidocinnamic acid

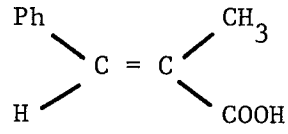

(E)-α-methylcinnamic acid

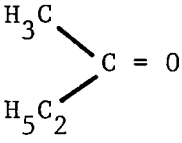

Ethyl methyl ketone

Some substrates used in catalytic asymmetric hydrogenation.

Figure V.1

Table V.1 Asymmetric homogeneous hydrogenation of unsaturated substrates using the $HRh[(+)\text{-diop}]_2$ catalyst.[a]

Substrate,S	$[Rh]x10^3$,M	$[S]x10^1$,M	Temp.,°C	Solvent	Product config.,%e.e.[b]	Approx.total reaction time,t
Itaconic acid	2.0	2.5	15	n-butanol-toluene(2:1)	R(+),26	8h
"	"	3.0	27	"	R(+),37	2.5h
"	"	2.0	30	"	R(+),40	2h
"	"	"	30	"	R(+),40[c](20)	2.5h
"	"	3.0	60	"	R(+),48	30 min
"	1.0	"	80	"	R(+),52	15 min
"	"	"	80	DMA	R(+),56	30 min
Citraconic acid	2.0	2.5	70	DMA	S(-),6	4d
N-Acetamidoacrylic acid	"	4.0	30	DMA	S(-),70[c]	5d
"	"	3.0	30	n-butanol-toluene(2:1)	S(-),96[d]	1.5d
"	"	4.0	30	DMA	S(-),71	4d
(Z)-N-Acetamidocinnamic acid	5.0	2.5	80	DMA	S(+),87	9d
Atropic acid	2.0	4.0	50	n-butanol-toluene(2:1)	R(-),37	2.5d
"	"	"	60	"	R(-),33	1.5d
Ethyl methyl ketone	"	"	30	"	——— [e]	

[a] At 760 mm total pressure using $HRh[(+)\text{-diop}]_2$ crystallized from n-hexane.

[b] % e.e. corresponds to uncrystallized product.

[c] Catalyst used without recrystallization (the value in brackets taken from Ref. 15 is in error).

[d] After the product was twice recrystallized.

[e] No hydrogenation.

Table V.2 Optical purities of products from hydrogenation of olefinic substrates using the $Rh[(+)\text{-diop}]_2^+BF_4^-$ complex.[a]

Substrate,S	$[Rh]x10^3$,M	$[S]x10^1$,M	Temp.°C	Solvent	Product config.,%e.e.	Approx.total reaction time,t
Itaconic acid	1.0	2.5	15	n-butanol-toluene(2:1)	R(+),19	8h
"	"	3.0	27	"	R(+),36	2h
"	"	"	30	"	R(+),37	2h
"	"	"	60	"	R(+),50	20 min
"	"	"	80	"	R(+),52	15 min
"	"	"	80	DMA	R(+),56	45 min
Citraconic acid	2.0	2.5	70	DMA	S(-),6	3d
"	"	"	70	n-butanol-toluene(2:1)	R(+),6	1.5d
N-Acetamidoacrylic acid	"	1.5	30	"	S(-),70	16h
"	1.5	2.5	60	"	S(-),73	2h
(Z)-N-Acetamidocinnamic acid	2.0	1.5	80	"	S(+),94	7d
"	6.0	3.0	80	DMA	S(+),86	6d
Atropic acid	2.0	2.5	50	n-butanol-toluene(2:1)	R(-),41	2d
"	1.0	"	60	"	R(-),30	2.5d
(E)-α-Methylcinnamic acid	6.0	3.0	70	n-butanol toluene(2:1)	——— [b]	
Ethyl methyl ketone	2.0	4.0	30	"	——— [c]	

[a] At 760 mm total pressure.

[b] ∿10% reaction complete in 5 days.

[c] No hydrogenation.

Table V.3 Asymmetric homogeneous hydrogenation of prochiral olefins using the $Rh[(+)\text{-diop}]_2C\ell$ catalyst[a]

Substrate,S	$[Rh]x10^3$,M	$[S]x10^1$,M	Temp.°C	Solvent	Product config.,%e.e.	Approx.total reaction time,t
Itaconic acid	2.0	2.5	15	n-butanol-toluene(2:1)	R(+),45	8h
"	"	"	30	"	R(+),49	2h
"	"	"	40	"	R(+),48	1h
Citraconic acid	"	"	70	DMA	S(-),3	3d
N-Acetamidoacrylic acid	"	"	30	n-butanol-toluene(2:1)	S(-),81	8h
(Z)-N-Acetamidocinnamic acid	"	1.2	20	"	S(+),92	20h
"	"	"	40	"	S(+),68	6h
"	"	"	40	DMA	R(-),13	2d
"	"	"	70	n-butanol-toluene(2:1)	S(+),14	4h
"	"	"	70	DMA	R(-),5	6h
"	"	2.0	80	DMA	R(-),4	4h
Atropic acid	"	2.5	50	n-butanol-toluene(2:1)	R(-),23	1d
(E)-α-Methylcinnamic acid	"	1.5	80	"	——— [b]	

[a] At 760 mm total pressure.

[b] Reaction too slow to measure

Table V.4 The $Rh[(+)\text{-diop}]_2H_2^+BF_4^-$-catalyzed hydrogenation of some prochiral substrates.[a]

Substrate,S	$[Rh]x10^3$,M	$[S]x10^1$,M	Temp.°C	Solvent	Product config.,%e.e.	Approx. total reaction time, t
Itaconic acid	1.0	3.0	30	n-butanol-toluene(2:1)	R(+),28	2h
"	"	"	60	"	R(+),42	20 min
Citraconic acid	3.0	"	70	DMA	S(-),5	2.5d
N-Acetamidoacrylic acid	2.0	"	30	n-butanol-toluene(2:1)	S(-),83	13h
(Z)-N-Acetamidocinnamic acid	5.0	"	80	DMA	S(+),88	6.5d
Atropic acid	2.0	"	60	n-butanol-toluene(2:1)	R(-),33	26h

a At 760 mm total pressure.

Table V.5 Asymmetric hydrogenation of prochiral unsaturated substrates using the $[RhCl(CO)(+)\text{-diop}]_2$ complex.[a]

Substrate,S	$[Rh]x10^3$,M	$[S]x10^1$,M	Temp.°C	Solvent	Product config.,%e.e.	Approx.total reaction time,t
Itaconic acid	2.0	3.0	40	DMA	R(+),52	8d
Citraconic acid	4.0	2.5	80	"	S(-),22	10d
N-Acetamidoacrylic acid	4.0	"	50	"	S(-),73	2.5d
(Z)-N-Acetamidocinnamic acid	6.0	2.0	80	"	S(+),52	8d
Atropic acid	4.0	2.5	80	"	R(-),10	4d

a At 760 mm total pressure.

$Rh[(+)\text{-diop}]_2C\ell$ as catalyst (Table V.3). The data for some substrates suggest that hydrogenation is faster in n-butanol-toluene (2:1) than in DMA (Tables V.1-V.3).

Table V.6 lists selected data from the literature concerning hydrogenation of prochiral substrates using mono(diop)-rhodium(I) complexes.

V.4 Discussion

$HRh[(+)\text{-diop}]_2$ effects the catalytic hydrogenation of unsaturated carboxylic acids under mild conditions (Table V.1). Itaconic and N-acetamidoacrylic acids, substrates containing a terminal $= CH_2$ group, are most readily hydrogenated using $HRh[(+)\text{-diop}]_2$. Substitution at the α-carbon also affects the hydrogenation rates as seen from the data for atropic acid which requires much longer reaction times. Hydrogenation of N-acetamidocinnamic acid, containing a trisubstituted olefinic group $\rangle C = CHC_6H_5$, is very much slower again (Table V.1). Similar rate trends are noted for the $Rh[(+)\text{-diop}]_2^+$ complex (Table V.2), the $Rh[(+)\text{-diop}]_2H_2^+$ complex (Table V.4), and the $Rh[(+)\text{-diop}]_2C\ell$ complex (Table V.3), although the last mentioned catalyst requires much milder conditions to effect hydrogenation. For example, N-acetamidocinnamic acid can be hydrogenated to products with 92% optical yield at 20°C using $Rh[(+)\text{-diop}]_2C\ell$, while the hydrido and cationic systems hydrogenate the same substrate very slowly indeed even at 80°C. The results indicate that steric factors at the olefinic group are certainly important in terms of the rates of these hydrogenation reactions. The participation of the acid function of substrates does not seem important, at least in terms of hydrogenation rates, in the $HRh[(+)\text{-diop}]_2$-catalyzed systems since under similar conditions styrene was (max. rate $\sim 14 \times 10^{-6} Ms^{-1}$ at 50°C) hydrogenated somewhat faster than atropic

Table V.6 Asymmetric hydrogenation of unsaturated substrates using various rhodium(I)-mono(diop) complexes at 25°C and 760 mm total pressure.

Complex	Substrate, S	Solvent	$[Rh]\times10^3$, M	[S], M	%e.e. (config.)	$t_{1/2}$, min	Ref.
$([(C_2H_4)_2RhCl]_2$+2(+)-diop)[a]	$H_2C=C(\emptyset)NHCOCH_3$	ethanol/benzene = 1/0	4.0	0.2	42.5(R)	5	5
"	"	" = 1/1	"	"	30(R)	20	"
"	"	" = 1/9	"	"	39(S)	66	"
"	"	" = 0/1	"	"	44(S)	76	"
$[(COD)Rh(+)\text{-diop}]^+ClO_4^-$	"	ethanol	3.0	0.3	38.5(R)	17	4
"	"	benzene	"	"	68(R)	5.5	"
$([(C_8H_{14})_2RhCl]_2$+2(-)-diop)[a]	$\emptyset(H)C=C(NHCOCH_3)COOH$	ethanol/benzene = 2/1	3.0	0.3	70(R)[b]	1.5	1
"	"	"	1.0	0.54	72(R)	-[c]	"
" +(Et_3N/Rh=3/1)	"	"	2.0	0.06	70(R)	-[c]	"
$[(COD)Rh(-)\text{-diop}]^+BF_4^-$ [d]	"	ethanol	3.0	0.3	81.3(R)	10.5	8
$[(COD)Rh(-)\text{-diop}]^+BF_4^-$ [e]	"	"	"	"	82.1(R)	10.5	"

a In situ
b At 50°C.
c Not reported.
d Freshly prepared.
e Used after 48h under argon

Table V.6 contd.

Complex	Substrate, S	Solvent	[Rh]x10^3, M	[S], M	%e.e. (config.)	$t_{1/2}$, min	Ref.
$([(COD)RhCl]_2$+2(-)-diop)[a]	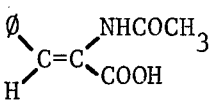	ethanol	3.0	0.3	81.9(R)	12	8
$([(C_2H_4)_2RhCl]_2$+2(+)-diop)[a]	"	ethanol / benzene = 3/1	"	"	81(S)	6.5	7
"	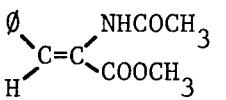	"	"	"	55(S)	1.5	"
"	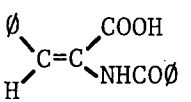	"	"	"	70(S)	6	"
"	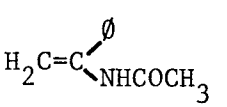	ethanol / benzene = 2/1	4.0	0.2	45(R)	- [c]	5
"	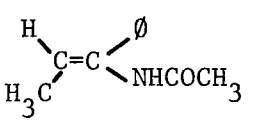	"	"	"	83(R)	- [c]	"
"	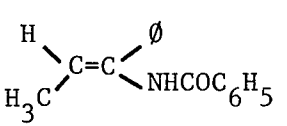	"	"	0.1	73(R)	- [c]	"

Table 6 contd.

Complex	Substrate,S	Solvent	$[Rh]x10^3$,M	[S],M	%e.e. (config.)	$t_{1/2}$,min	Ref.
$[(COD)Rh(+)\text{-diop}]^+C\ell O_4^-$	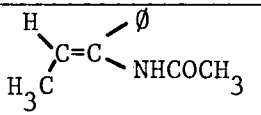	benzene	3.0	0.3	92(R)	11	4
"	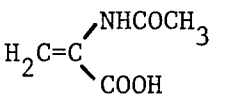	ethanol	"	0.15	42(S)	42	"
"	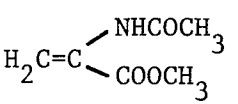	benzene	"	"	60(S)	2	"
$([(C_2H_4)_2RhC\ell]_2+2(-)\text{-diop})$[a]	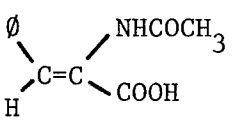	$\frac{\text{ethanol}}{\text{benzene}}$ = 2/1	3.0	0.3	81(R)	5	6
" + $-P(2\text{-}MeC_6H_4)_2$[f]	"	"	"	"	27(R)	200	"
" + $-P(3\text{-}MeC_6H_4)_2$[f]	"	"	"	"	87.5(R)	1	"

f Both Ø groups attached to $-P\emptyset_2$ moieties of the diop ligand are substituted.

acid (max rate $\sim 8 \times 10^{-6} Ms^{-1}$ at 50°C).[15] The Monsanto group[21] had initially considered H-bonding (between the carboxylate group of unsaturated acidic substrate and O and H atoms of the catalyst ligand) important in their very effective systems using o-anisolephosphine derivatives, but more recent studies[22] tend to deemphasize such interactions. Coordination of the -NHCOR group (if present) at rhodium cannot be ruled out, however, because a variable temperature ^{31}P nmr study[23] of the hydrogenation of (Z)-N-acetamidocinnamic acids and their methyl esters by $[Rh(NBD)(+)\text{-diop}]^+A^-$ ($A=BF_4, C\ell$) complexes has revealed such coordination (Figure V.2(A)). A similar intermediate (Figure V.2(B)) was proposed earlier by Kagan et.al.[5] to

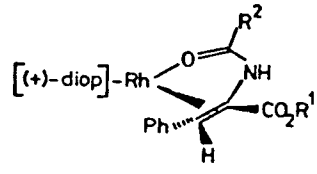

$R_1=H, R_2=Ph; R_1=Me, R_2=Ph; R_1=H, R_2=Me$

(A)

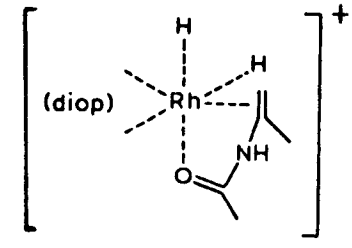

(B)

Proposed intermediates for hydrogenations catalyzed by rhodium-mono(diop) complexes.

Figure V.2

explain good optical yields for enamide substrates. Quite recently[24], such an interaction has been further substantiated by the crystal structure of a related cationic complex $[Rh(dpe)(PhC(H)=C(COOCH_3)(NHCOCH_3))]^+$ (Figure V.3).

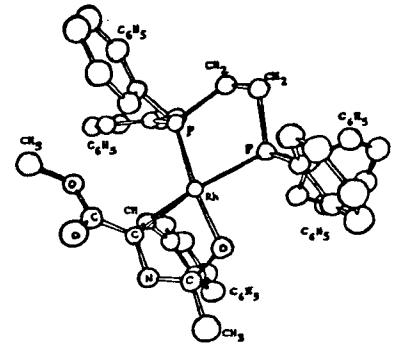

Crystal structure of the $[Rh(dpe)(PhC(H)=C(COOCH_3)(NHCOCH_3))]^+$ cation.

Figure V.3

In our bis(diop)-rhodium systems, such an interaction could at least explain why N-acetamidocinnamic acid hydrogenates faster than α-methylcinnamic acid.

The data in Tables V.1 and V.2 suggest that the $Rh[(+)\text{-diop}]_2^+$ system hydrogenates substrates slightly faster than the $HRh[(+)\text{-diop}]_2$ system although the %e.e. of hydrogenated products are almost the same in most cases. The optical purities did not vary appreciably when preformed $Rh[(+)\text{-diop}]_2H_2^+BF_4^-$ rather than $Rh[(+)\text{-diop}]_2^+$ was used as catalyst (Table V.4). These results suggest that the geometries around the hydride-metal-substrate part of the intermediates are similar in all three systems (e.g. HRh(diop)(diop*)(olefin) for the $HRh[(+)\text{-diop}]_2$-catalyzed hydrogenation (chapter III) and Rh(diop)(diop*)$(H)_2$(olefin) for the $Rh[(+)\text{-diop}]_2^+$-catalyzed hydrogenation (chapter VI)).

Glaser's group[9-13,25,26] has presented a stereochemical model (Fig.I.6) for [RhCℓ(diop)S]-catalyzed hydrogenation of various substrates based on space-filling CPK-type molecular models to explain the effect of olefin substitution on optical purities; the rationalization considered only steric effects and ignored the cis-trans geometry of the olefins. Major products in terms of R and S configuration were correctly predicted except in a few cases.[9] In the bis(diop)-rhodium systems, any model will necessitate incorporation of two diop ligands, one of which is 'monodentate'. Since the stereochemistry of this intermediate species (e.g. HRh(diop)(diop*)(olefin) for the $HRh[(+)\text{-diop}]_2$- catalyzed reactions, (chapter III)) is yet to be established, the effect of substituents of olefinic substrates on the configuration of the hydrogenated product could not be predicted.

The data in Tables V.1-V.3 show that hydrogenation rates are affected by the nature of the solvent. In general, hydrogenation proceeds more slowly

in DMA (a basic and coordinating solvent) than in n-butanol-toluene mixture. With four and five coordinate rhodium(I) complexes, $Rh[(+)\text{-diop}]_2^+$ and $HRh[(+)\text{-diop}]_2$, which do not completely dissociate a diop ligand in solution (see chapters III and VI), solvent effects appear to be unimportant generally (Tables V.1 and V.2), although there is a change in configuration with change in solvent in the case of citraconic acid with the $Rh[(+)\text{-diop}]_2^+$ catalyst (Table V.2). The reason for this is not clear but different mechanisms are clearly operating in the two solvents at the higher temperatures used for this substrate.

The more marked solvent effects observed using $Rh[(+)\text{-diop}]_2C\ell$ as catalyst (Table V.3) are in contrast to the hydride and cationic analogs. Although the hydrogenation mechanism using the chloride has not been elucidated, visible spectral studies have shown that this complex does not obey Beer's law and is in equilibrium with some other species (Table IV.2, chapter IV). Interestingly, these solvent effects are comparable to those obtained using mono(diop)-rhodium(I) species where a change of solvent medium has a dramatic effect on the configuration of the hydrogenated product.[5] For example, using an <u>in situ</u> $[RhC\ell((+)\text{-diop})S]$(S=solvent) catalyst, the substrate ($H_2C=C(\emptyset)NHCOCH_3$) was hydrogenated to product which was 42.5% e.e., (R), in ethanol and 44% e.e., (S), in benzene (Table V.6). These solvent effects can be rationalized qualitatively, since in the mono(diop) system solvent occupies coordination site(s) on the rhodium and thus can probably affect the configuration of the hydrogenated product. It is possible that the mechanism for the chloride system involves loss of one diop ligand but this has not been substantiated.

In the hydrogenation of itaconic acid using $HRh[(+)\text{-diop}]_2$ or $Rh[(+)\text{-diop}]_2^+$ catalysts (Tables V.1 and V.2), optical yields of the product

at different temperatures show an unusual trend (Figure V.4): optical purity increases generally from 20∿50% with increasing temperature but levels off at about 80°C. A decrease in optical purity with increasing temperature has usually been observed for hydrogenation[21] and other asymmetric syntheses.[27] An example of the latter is found[27] in the codimerization of norbornene(I) with ethylene in chlorobenzene at +10°C to -97°C to give optically active exo-(+)-2-vinylnorbornane(II), using a catalyst prepared from π-allylnickel chloride, triethyldialuminum trichloride, and optically active (-)-isopropyldimethylphosphane. The variation of optical yield with temperature (Figure V.5) shows a linear

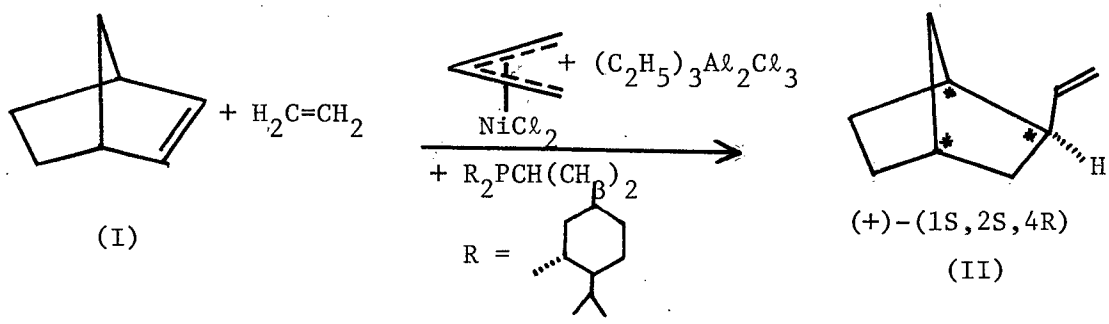

(I)

(+)-(1S,2S,4R)
(II)

[V.1]

increase in optical purity with decreasing temperature. The Rh[(+)-diop]$_2$Cℓ system behaves differently and shows roughly a linear decrease in optical purity with increasing temperature for the hydrogenation of N-acetamidocinnamic acid (Figure V.4), behaviour similar to that observed for reaction [V.1], but in contrast to a previous temperature study[1] on an <u>in situ</u> [RhCℓ(diop)S] system for hydrogenation of the same substrate that showed an independence of optical purity with temperature (70% e.e. at 50°C, and 72% e.e. at 30°C). At present, there are no satisfactory rationalizations for these variable temperature behaviours. More rigid structures at lower temperatures would be expected to lead to high optical enrichment, but

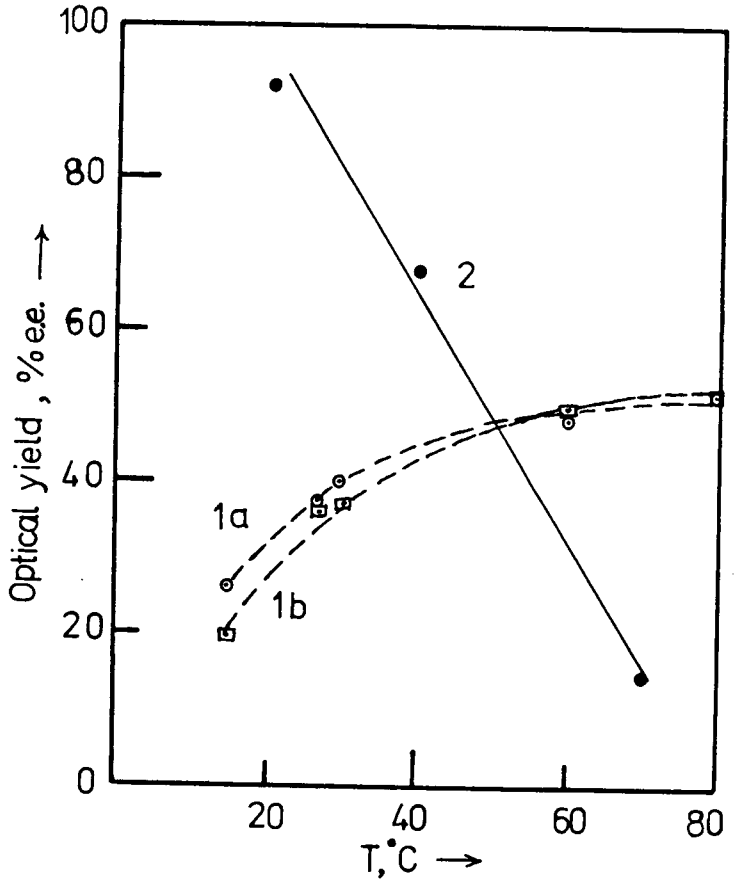

Figure V.4 Plot of variation of optical yield with temperature of:
1. (+)-2-methylsuccinic acid using a. $HRh[(+)\text{-diop}]_2$; b. $Rh[(+)\text{-diop}]_2^+BF_4^-$ as catalysts in n-butanol-toluene(2:1).
2. N-acetyl-S(+)-phenylalanine using the $Rh[(+)\text{-diop}]_2C\ell$ complex in n-butanol-toluene (2:1).

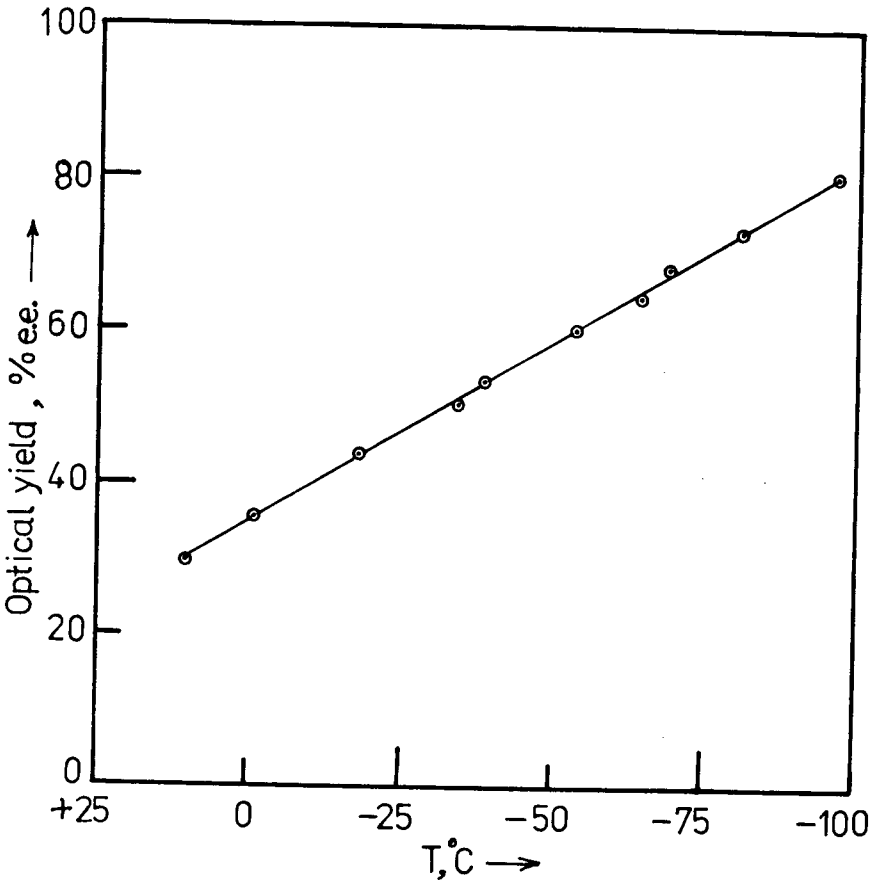

Figure V.5 Variation of optical yield of (+)-2-vinylnorbornane with temperature using a nickel catalyst in chlorobenzene (data taken from ref.27).

different mechanisms could be operative at higher temperatures. The hydrogenation of N-acetamidocinnamic acid at 20°C gives 92% e.e. S(+)-N-acetylphenylalanine using the $Rh[(+)\text{-diop}]_2C\ell$ catalyst is noteworthy in that the asymmetric induction is among the highest yet recorded for this substrate.

Asymmetric hydrogenation of substrates is also effected using the $[RhC\ell(CO)(+)\text{-diop}]_2$ dimer (Table V.5). The hydrogenation of itaconic acid at 40°C and citraconic acid at 80°C afforded 52% e.e. of R(+) and 22% e.e. of S(-) isomers of 2-methylsuccinic acid, respectively. These values are among the highest reported so far[3] for these substrates. A drawback of this catalyst is that it is far less active than the <u>in situ</u> $[RhC\ell(diop)S]$ or the bis(diop) complexes. The introduction of a π-acid carbonyl ligand into a complex generally reduces activity for catalytic hydrogenation, and this is usually traced to a less favoured oxidative addition step somewhere in the catalytic cycle, due to reduced electron density at the metal center.[28]

Comparison of data in Tables V.1-V.6 shows that mono(diop)-rhodium complexes hydrogenate several times faster than bis(diop)-rhodium species, but the latter can give better optical yields in some cases. Optical yields as high as 96% are observed with N-acetamidoacrylic acid (Table V.1). There are only a few other catalysts reported to be equally effective.[22,26,29,30]

The results obtained in the present studies (Tables V.1-V.5) together with representative literature data (Table V.6) show the effect of a number of variables on the induced asymmetry in the hydrogenated product. These include: temperature[1,21], the age of the catalyst[8], the concentrations of catalyst and olefin[1], the nature of the anion[8,31], added

bases[1], and systematic ligand effects (e.g. varying substituents on the phenyl groups of diphenylphosphino moieties[6]). However, it remains impossible to match a priori substrates and catalyst system to give optimum optical yields; this is still very much an empirical art.

CHAPTER VI

ASYMMETRIC HOMOGENEOUS HYDROGENATION OF ITACONIC ACID USING BIS(DIOP)-RHODIUM(I)TETRAFLUOROBORATE AS CATALYST

VI.1 Introduction

During an investigation of itaconic acid hydrogenation using the hydridobis(diop)rhodium(I) complex, spectroscopic studies indicated that the initial hydride complex was slowly decomposed by protons from the substrate to a corresponding cationic species and this was also thought to be an important active species during hydrogenation of other acidic substrates[1] (chapter III):

$$HRh[(+)\text{-diop}]_2 + H^+ \rightleftharpoons Rh[(+)\text{-diop}]_2^+ + H_2 \qquad [VI.1]$$

The cationic bis(diop)rhodium(I) complex was thus isolated via a more convenient route starting from the cyclooctene dimer $[RhCl(C_8H_{14})_2]_2$ (chapter IV):

$$[RhCl(C_8H_{14})_2]_2 + 4(+)\text{-diop} \longrightarrow Rh[(+)\text{-diop}]_2Cl \qquad [VI.2]$$

$$Rh[(+)\text{-diop}]_2Cl + AgA \longrightarrow Rh[(+)\text{-diop}]_2^+A^- \qquad [VI.3]$$

$$(A=BF_4, PF_6, SbF_6)$$

This cation was then found to be a very effective asymmetric hydrogenation catalyst for certain substrates, with optical yields of >90% being obtained in some cases (see chapter V). A kinetic study was therefore carried out on the $Rh[(+)\text{-diop}]_2^+BF_4^-$-IA system in an attempt to elucidate the hydrogenation mechanism involved.

VI.2 Experimental

The $Rh[(+)\text{-diop}]_2^+A^-$ and $Rh[(+)\text{-diop}]_2H_2^+A^-$ complexes were prepared by procedures given in chapters IV and VII, respectively. The hydrogen solubility data are summarized in Figure VI.1.

VI.3 Results

VI.3.1 Reaction of hydrogen with $Rh(diop)_2^+BF_4^-$

VI.3.1.1 Gas-uptake studies - The uptake of H_2 by $Rh(diop)_2^+$ was measured on the gas-uptake apparatus using the ampoule technique to establish the stoichiometry of the reaction. A rapid uptake was observed which slowed down after ∿1 min and the final stoichiometry was obtained after ∿½h; the reaction being accompanied by a colour change from red to light yellow. Using this technique the complex dissolves relatively slowly, and it is impossible to use the uptake curves for quantitative kinetics. The H_2:Rh ratio was found to be essentially independent of the associated anion, the solvent medium, hydrogen pressure, temperature, added Et_3N, added proton sponge, and the rhodium concentration (Table VI.1).

VI.3.1.2 Spectrophotometric studies - n-Butanol-toluene (2:1) or DMA solutions of $Rh(diop)_2^+BF_4^-$ under argon obeyed Beer's Law between $\sim 10^{-3}$-10^{-4}M concentration range and showed an absorption maximum at 442 nm (ε=3550±100 $M^{-1}\ cm^{-1}$) that was independent of added diop (Figure VI.2(a)). Some changes were observed on exposing the solution to air over long periods of time (Figure VI.2(b)).

Addition of H_2 to a solution of the cation resulted in a rapid disappearance of the 442 nm band (orange → yellow), followed by relatively slow and small spectral changes to give a final steady spectrum after ∿½h (Figure VI.3(a)); these changes were independent of added diop. On pumping

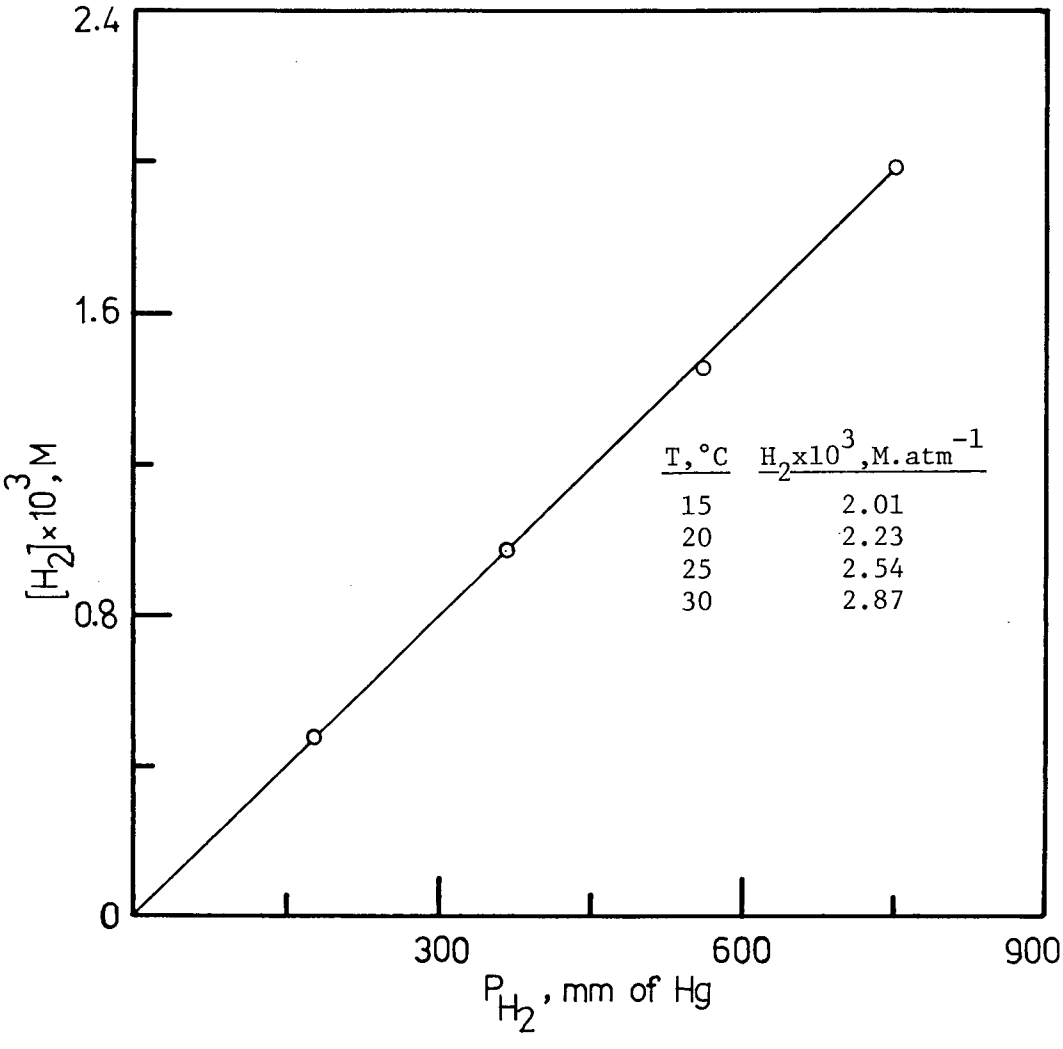

Figure VI.1 Solubility of hydrogen in n-butanol-toluene (2:1) mixtures at various pressures at 15°C. Inset gives data at different temperatures.

Table VI.1 Hydrogen-uptake data for $Rh(diop)_2^+BF_4^-$ using the ampoule technique.

[Rh]x10^3,M	T,°C	Pressure[a],atm	Solvent	H_2/Rh[b]
10	15	1.00	n-butanol-toluene (2:1)	0.86
10	15	0.50	"	0.80
10	15	0.25	"	0.83
10	25	1.00	n-BuOH	0.84[c]
5	25	1.00	"	0.70
2.5	25	1.00	"	0.75
5+(+)-diop ($5x10^{-3}$M)	25	1.00	"	0.70
6	12	1.00	DMA	0.81[c]
10	12	1.00	"	0.82[c]
5[d]	25	1.00	"	0.76
5+Et_3N(0.1M)	25	1.00	n-BuOH	0.73
5+P.S. ($5x10^{-3}$M)	25	1.00	"	0.75

a Total pressure.

b Ratio corresponds to uptake after ~½h; values (±0.1) in error due to use of the ampoule technique.

c Based on an average of two experiments.

d Using $Rh(diop)_2^+SbF_6^-$.

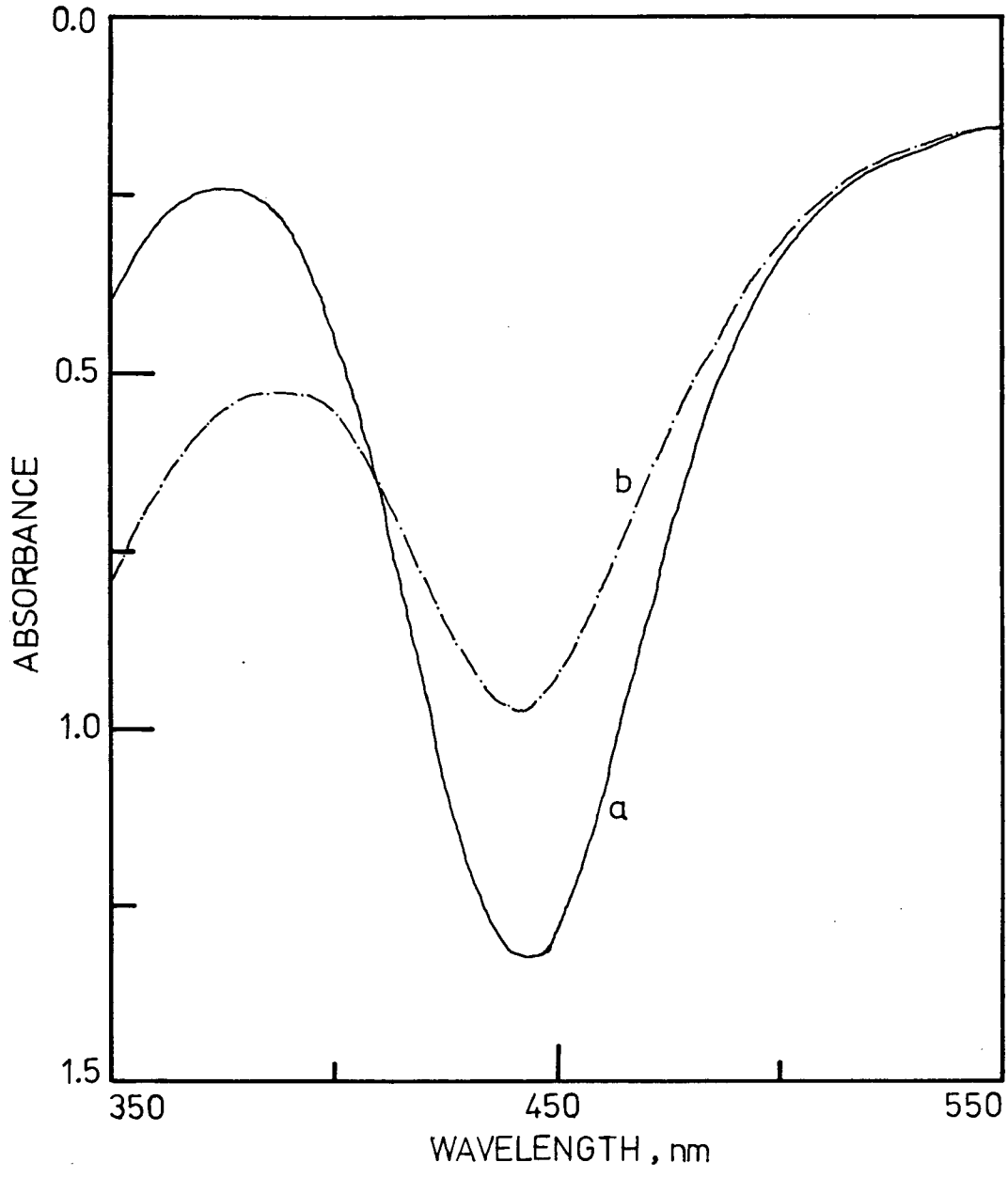

Figure VI.2 Visible spectrum of $Rh(diop)_2^+BF_4^-$ in n-butanol-toluene (2:1) at 25°C.

a. Under argon.
b. 20h after exposing solution (a) to air.

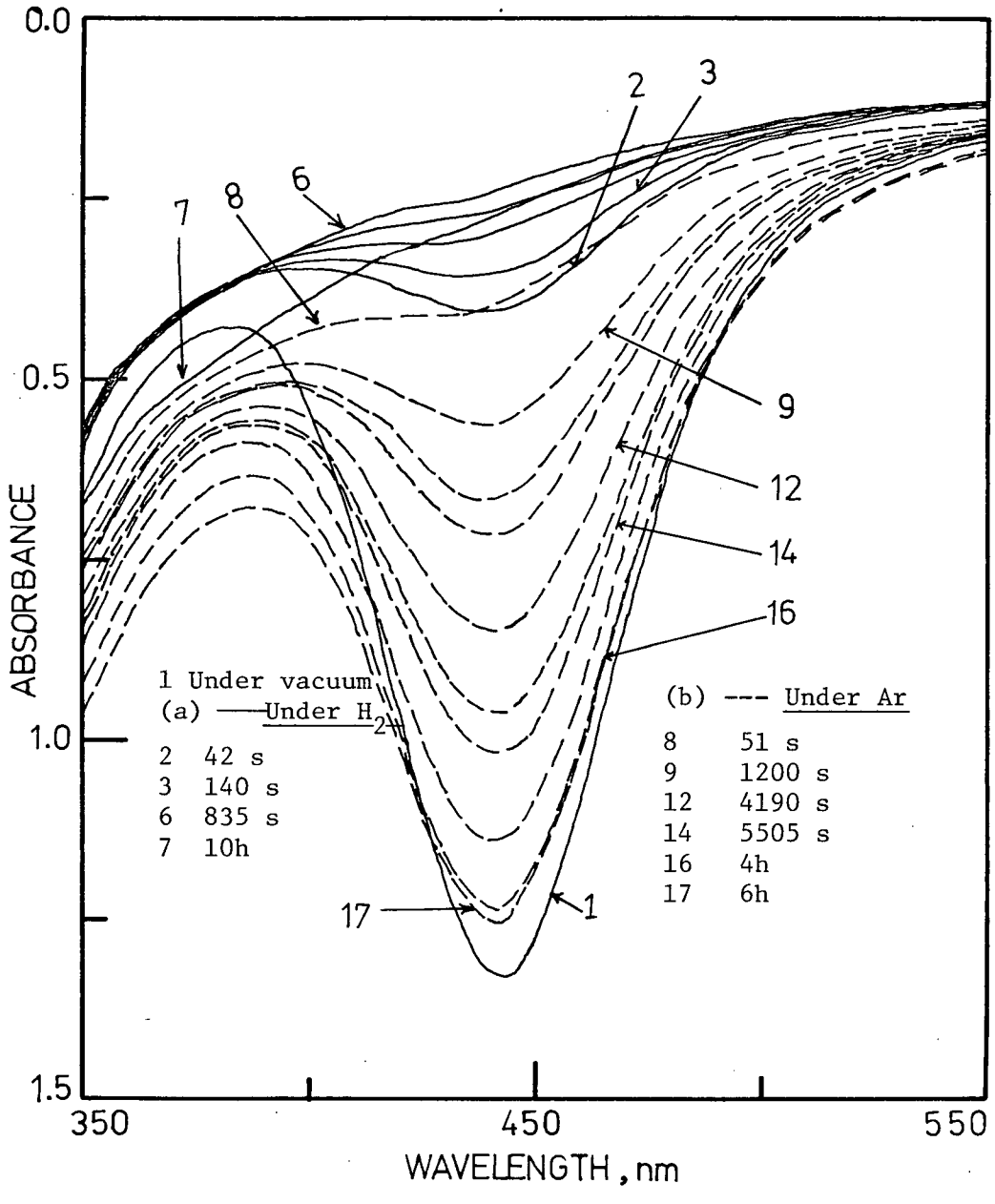

Figure VI.3 Visible spectrum of $Rh(diop)_2^+BF_4^-$ at 25°C in n-butanol-toluene (2:1) (in absence, or presence of diop (diop:Rh=3:1)).

(a) ——— Under H_2

(b) ------ Under Ar

hydrogen off from these solutions, a band at 442 nm was regenerated but the optical density in the 350-400 nm region increased and was different from that of the initial spectrum of the $Rh(diop)_2^+$ cation (Figure VI.3(b)).

The hydrogen-reaction with $Rh(diop)_2^+$ ($\sim 1 \times 10^{-4}$M) in DMA at 30°C was studied using the stopped-flow spectrometer. The data obtained do not analyze for a simple first-order reaction (Fig. VI.4), even though the H_2 concentration is in about a 10:1 excess (the solution saturated with H_2 at one atmosphere total pressure becomes diluted by a factor of two in the mixing chamber of the stopped-flow apparatus). Similar data were obtained in $CH_2C\ell_2$, DMA, and MeOH.

The loss of H_2 from solutions of the synthesized $Rh(diop)_2H_2^+BF_4^-$ complex was measured spectrophotometrically under argon in methanol at 30°C (Figure VI.5). The spectral changes analyzed for a first-order reaction with slope $\simeq 2.1 \times 10^{-4} s^{-1}$ (Figure VI.6). In $CH_2C\ell_2$ and DMA very similar changes analyzed to give slopes of $\simeq 2.1 \times 10^{-4} s^{-1}$ and $3.4 \times 10^{-4} s^{-1}$, respectively (Table VI.2).

VI.3.1.3 ^{31}P nmr data

The ^{31}P nmr spectrum of $Rh(diop)_2^+BF_4^-$ in $CH_2C\ell_2$-acetone-d_6 at 25°C under argon showed a doublet at -9.3 ppm, J_{Rh-P}=140 Hz, (Figure VI.7(a.1)), but a more complex pattern was observed at -50°C (Figure VI.7(a.2)). This spectrum remained invariant on further cooling to -85°C and essentially consisted of three main doublets at -10.6 ppm (J_{Rh-P}=140 Hz), -15.5 ppm (J_{Rh-P}=134 Hz), and -16.5 ppm (J_{Rh-P}=134 Hz). When the solution was put under H_2 at 25°C, a doublet of doublet of triplets was obtained (Figure VI.7(b)). The ^1H nmr data are described in section VI.3.2.2.

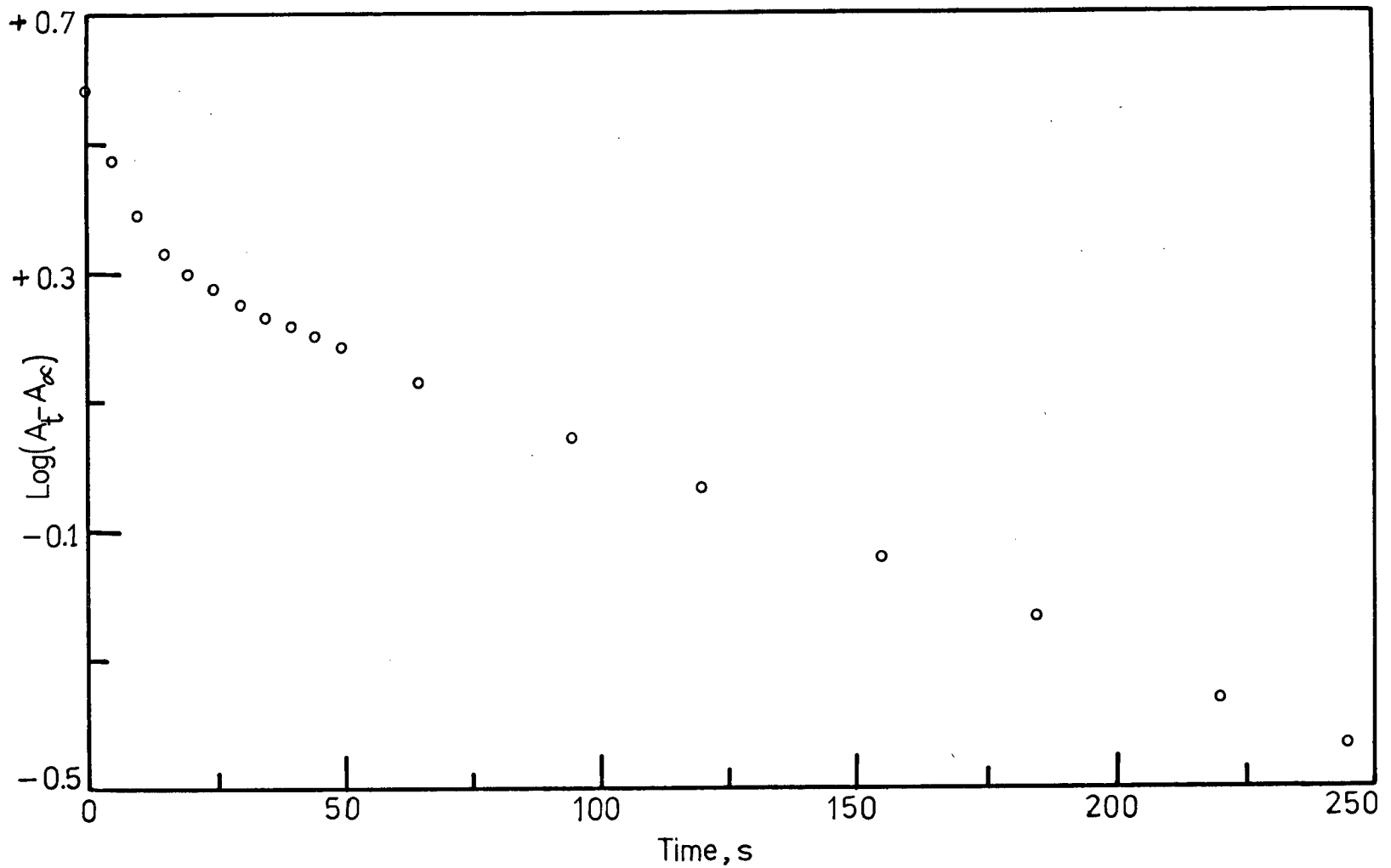

Figure VI.4 Plot of $\log_{+}(A_t - A_\infty)$ vs time of the stopped-flow data for H_2-uptake by $Rh(diop)_2^{+}BF_4^{-}$ (1.1×10^{-4}M) in DMA at 30°C.

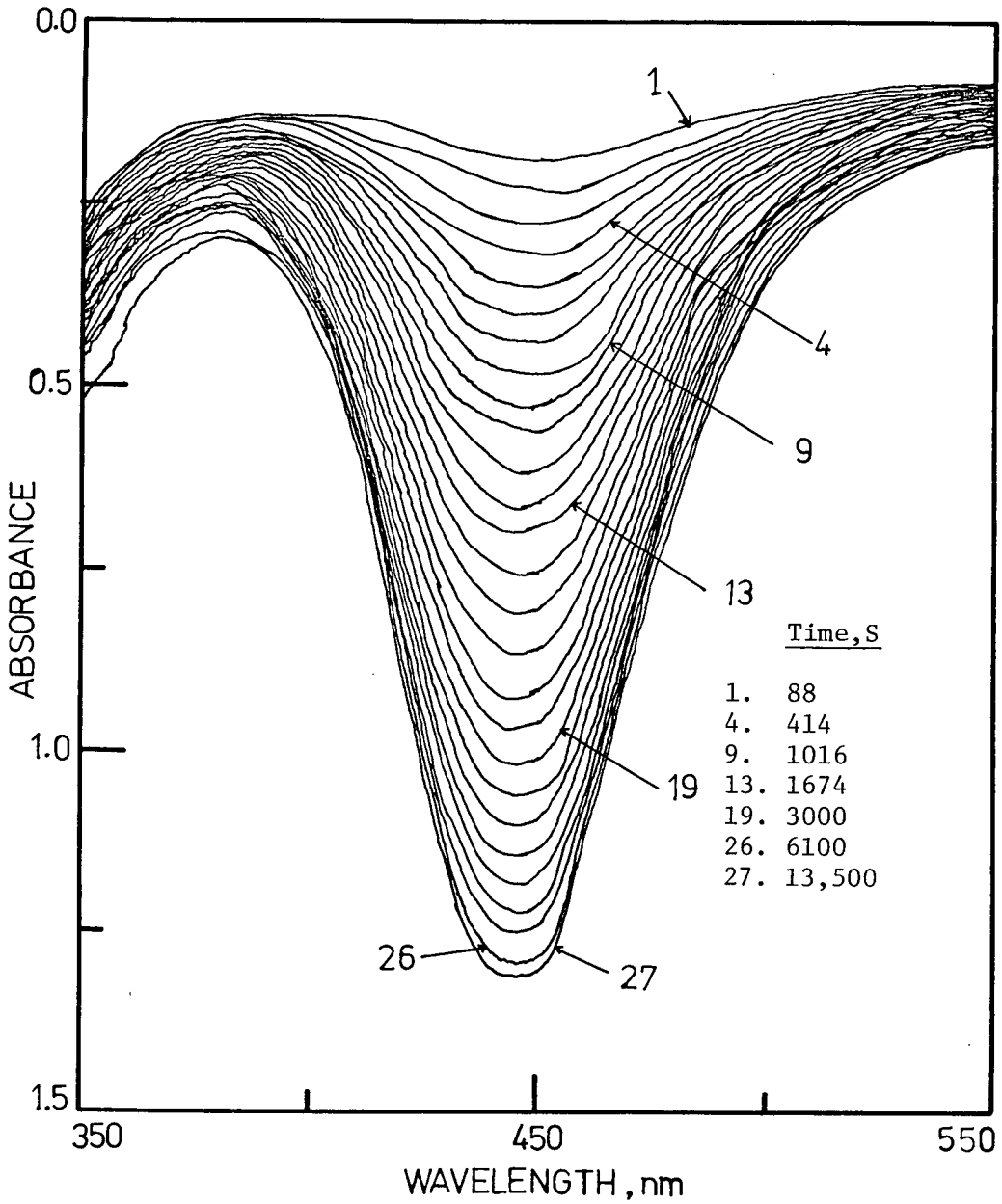

Figure VI.5 Spectral changes obtained for H_2 loss from $Rh(diop)_2H_2^+BF_4^-$ (4.2×10^{-4}M) in methanol (under argon) at 30°C.

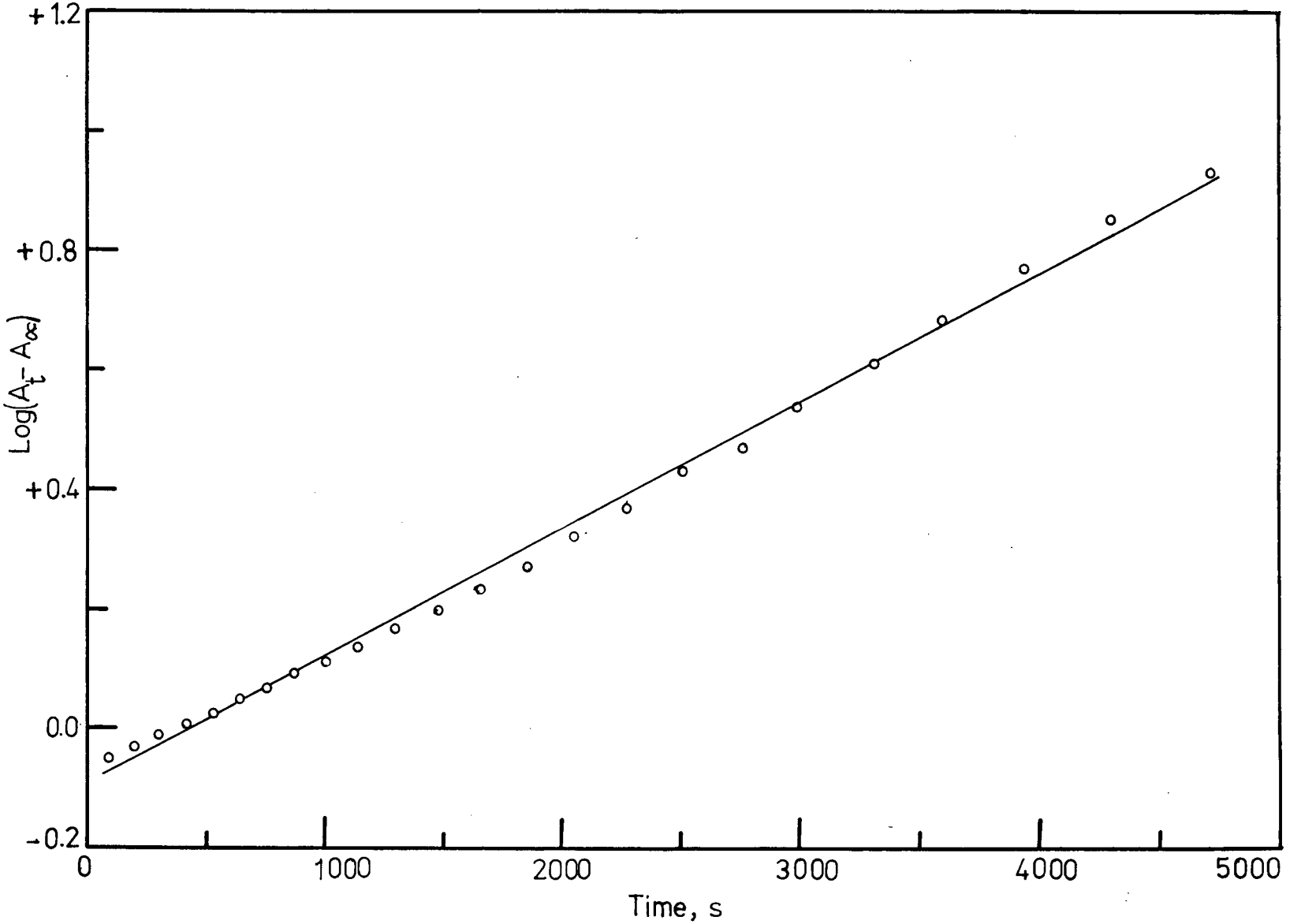

Figure VI.6 Plot of $\log(A_t - A_\infty)$ vs time for spectral changes in Fig. VI.5.

Table VI.2 Spectrophotometric determination of first-order rate constants in different solvents at 30°C for the reaction

$$Rh(diop)_2H_2^+ \xrightarrow[Ar]{k_{-1}} Rh(diop)_2^+ + H_2$$

$[Rh]x10^4$,M	Solvent[a]	$k_{-1}x10^4$,[b] s^{-1}
4.21	MeOH	4.85
4.21	CH_2Cl_2	4.85
4.12	DMA	7.74

a 10 ml.

b Determined in a 1 cm cell shown in Figure II.3 under one atm of argon.

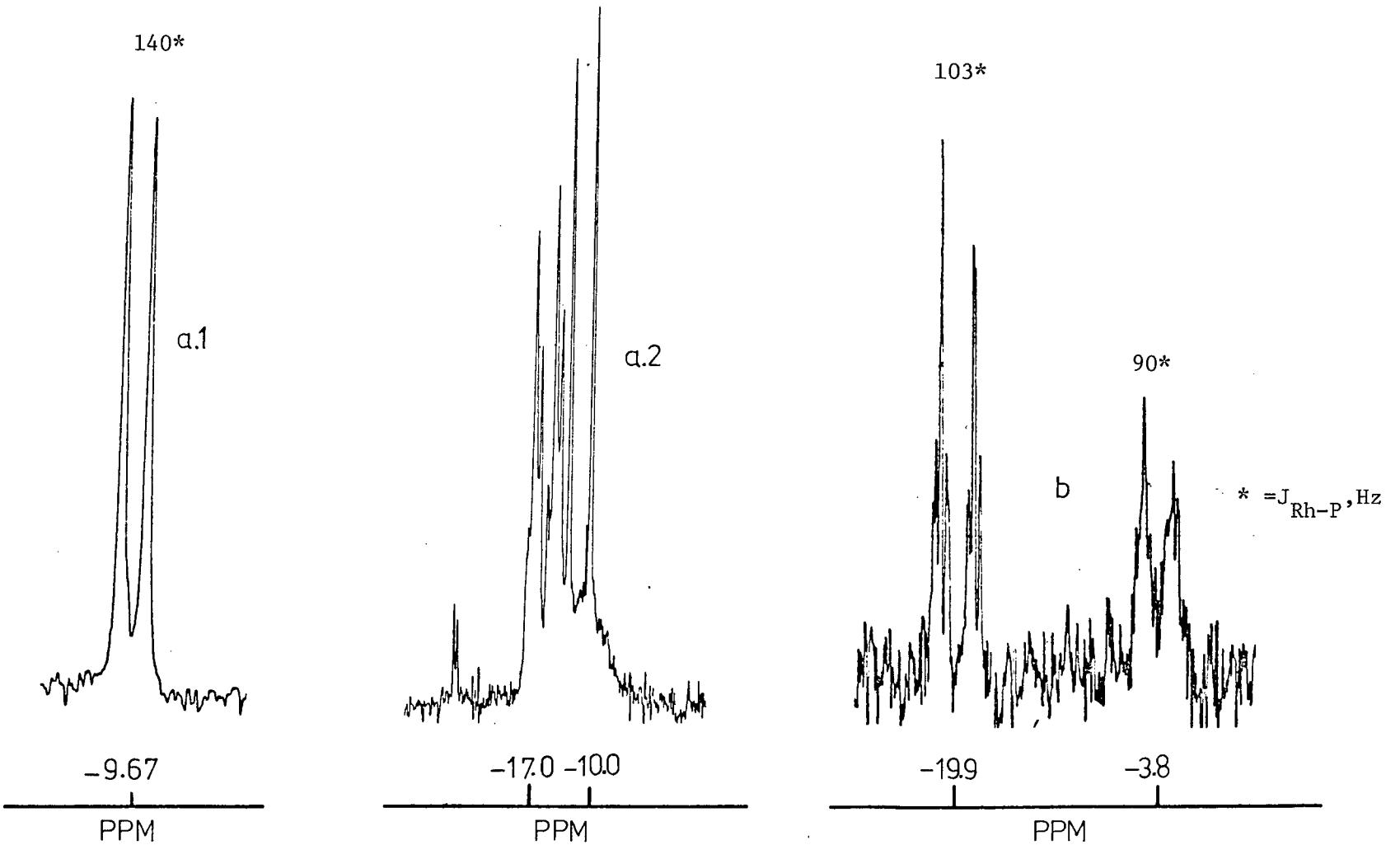

Figure VI.7 $^{31}P\{^{1}H\}$ nmr spectra of $Rh(diop)_2^+BF_4^-$ in $CH_2C\ell_2$-acetone-d_6. (Similar spectra were obtained in MeOH-d_4).

a. Under argon: 1. at 25°C.

2. at -50°C.

b. Under hydrogen at 25°C.

VI.3.2 Catalytic hydrogenation studies

VI.3.2.1 Kinetic data - The hydrogenation of itaconic acid was achieved at 15°C in n-butanol-toluene (2:1) using the $Rh(diop)_2^+BF_4^-$ complex. Figure VI.8 shows a typical H_2-uptake plot. The initial faster uptake slowed down somewhat, and the hydrogenation rates were measured in the subsequent linear region (Table VI.3).

The rates varied linearly with rhodium in the concentration range $(0.5\text{-}2.5)\times10^{-3}$M (Figure VI.9). The dependence on itaconic acid varied from first-order at lower concentrations to considerably less than first-order at ∿0.2M (Figure VI.10). A zero-order dependence on hydrogen pressure was observed in the 144-752 mm pressure range studied (Figure VI.11). Addition of even small amounts of added diop completely inhibited the hydrogenations (Table VI.3, footnote c). The rates increased with temperature (Table VI.3).

VI.3.2.2 Spectroscopic data - Very slow spectral changes were observed on adding IA to solutions of $Rh(diop)_2^+$ under argon; for the same experiment in the presence of added diop, no spectral changes were observed (Figure VI.12). Use of succinic acid instead of itaconic acid gave very similar spectral changes.

The high-field ^1H nmr spectrum of a light yellow solution of $Rh(diop)_2^+BF_4^-$ in methanol-benzene-d_6, under H_2 and at 25°C, was a pair of multiplets centered around 20τ (Fig. III.6(b)). This spectrum and the colour, immediately (5 min) after adding a saturated methanol solution (∿1M) of itaconic acid, were unchanged at 5°C, a lower temperature being used to slow down the hydrogenation reaction. After ∿15 minutes the solution turned red and the hydride signal disappeared; the visible spectrum of the red solution corresponded to that of $Rh(diop)_2^+$.

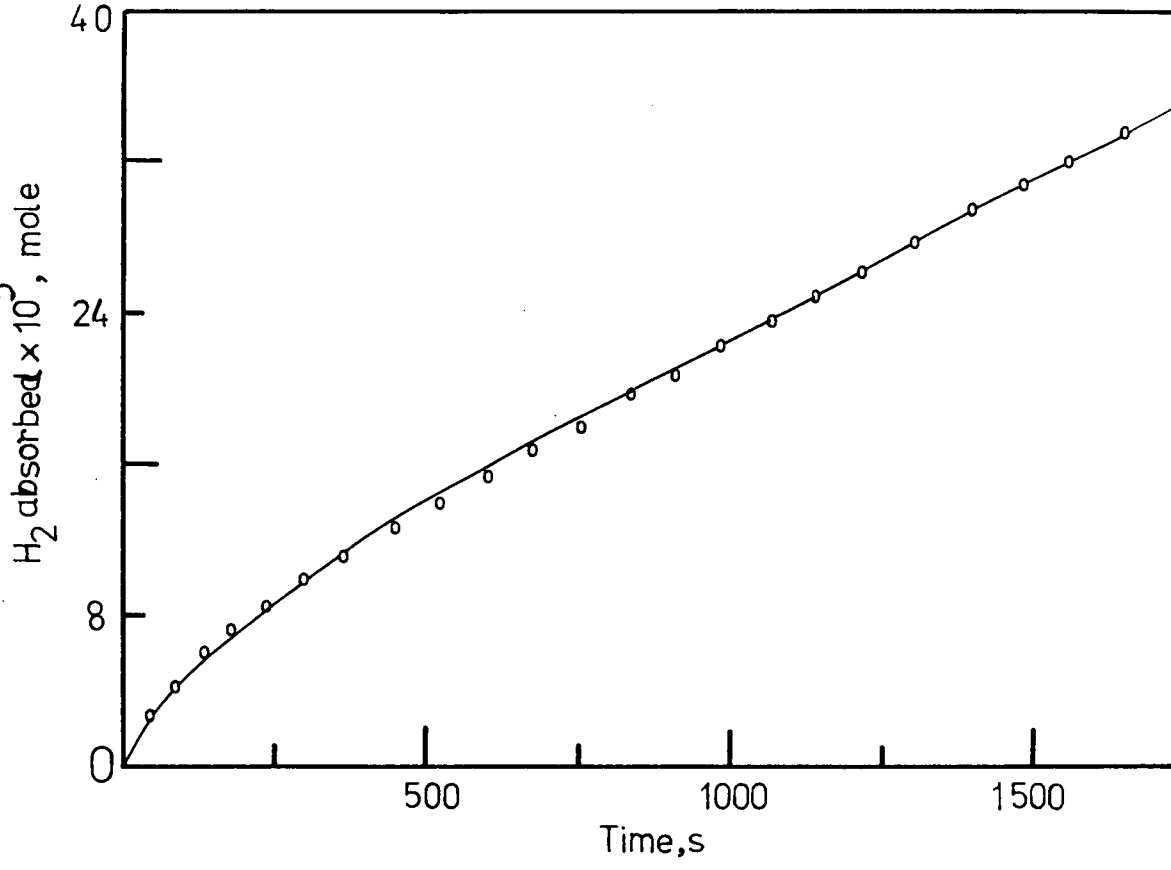

Figure VI.8 H_2-uptake plot for the $Rh(diop)_2^+BF_4^-$-catalyzed hydrogenation of itaconic acid (15°C, [Rh]=$1.0x10^{-3}$M, [IA]=0.2M, P_{H_2}=752 mm, n-butanol-toluene(2:1)=5 ml; uptake shown corresponds to 35% hydrogenation).

Table VI.3 Linear rate data for the hydrogenation of itaconic acid in n-butanol-toluene (2:1) catalyzed by $Rh(diop)_2^+BF_4^-$ at 15°C, unless stated otherwise.

$[Rh]x10^3$, M	$[IA]x10^1$, M	P_{H_2}, mm	$[H_2]x10^3$, M[a]	Linear rate x 10^5 Ms^{-1}	k, [b] $M^{-1}s^{-1}$
0.5	1.0	752	2.0	1.41	0.28
1.0[c]	"	"	"	3.12	0.31
1.5	"	"	"	5.10	0.34
2.0	"	"	"	7.24	0.36
2.5	"	"	"	8.70	0.35
1.0	0.4	"	"	1.57	0.39
"	0.7	"	"	2.42	0.35
"	1.4	"	"	3.64	-
"	1.8	"	"	4.30	-
"[c]	2.0	"	"	4.16	-
1.0	1.0	144	0.36	3.00	0.30
"	"	296	0.77	2.92	0.29
"	"	448	1.18	3.22	0.32
"	"	600	1.58	3.30	0.33
"[d]	"	752	2.0	5.52	0.552
"[e]	"	"	"	7.54	0.754
"[f]	"	"	"	13.56	1.356

a Calculated from Figure VI.1.
b See text
c Addition of $\geq 2x10^{-4}$M diop completely inhibited the hydrogenations
d At 20°C
e At 25°C
f At 30°C

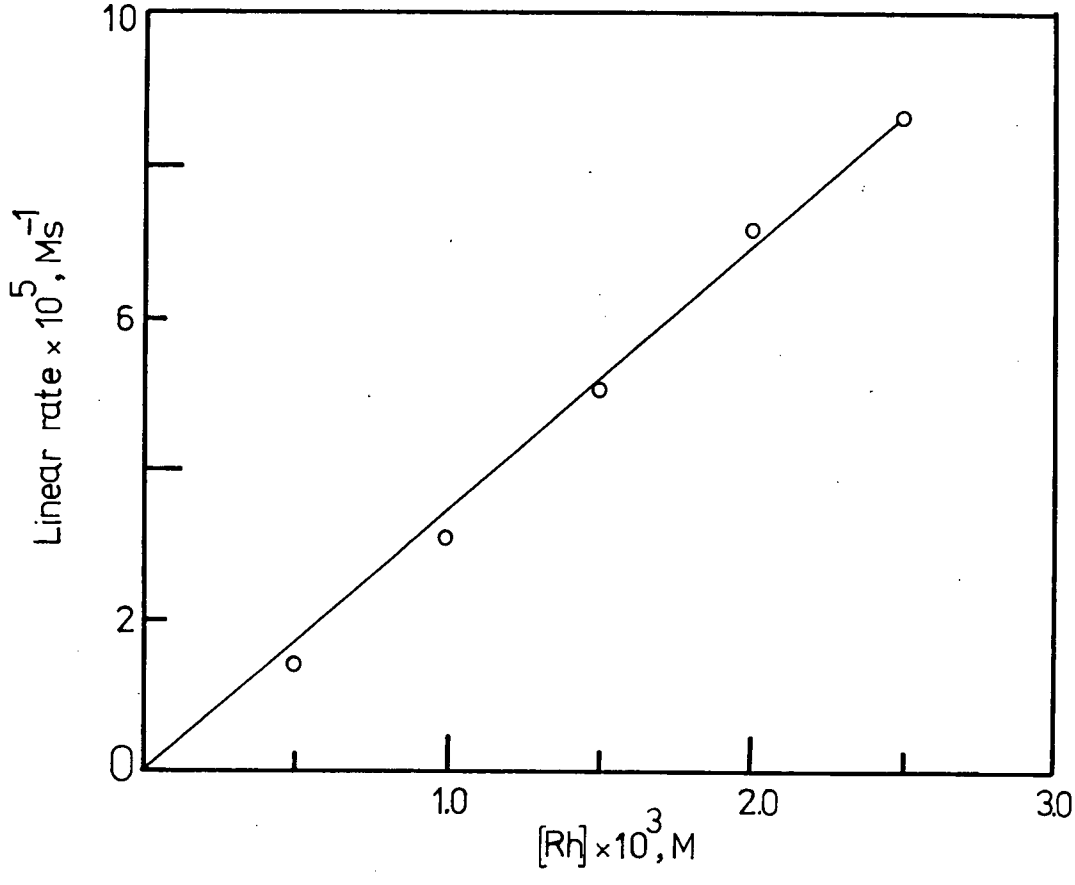

Figure VI.9 Plot of linear rate against $Rh(diop)_2^+BF_4^-$ concentration (15°C, 0.1M IA, 752 mm P_{H_2}, n-butanol-toluene(2:1)).

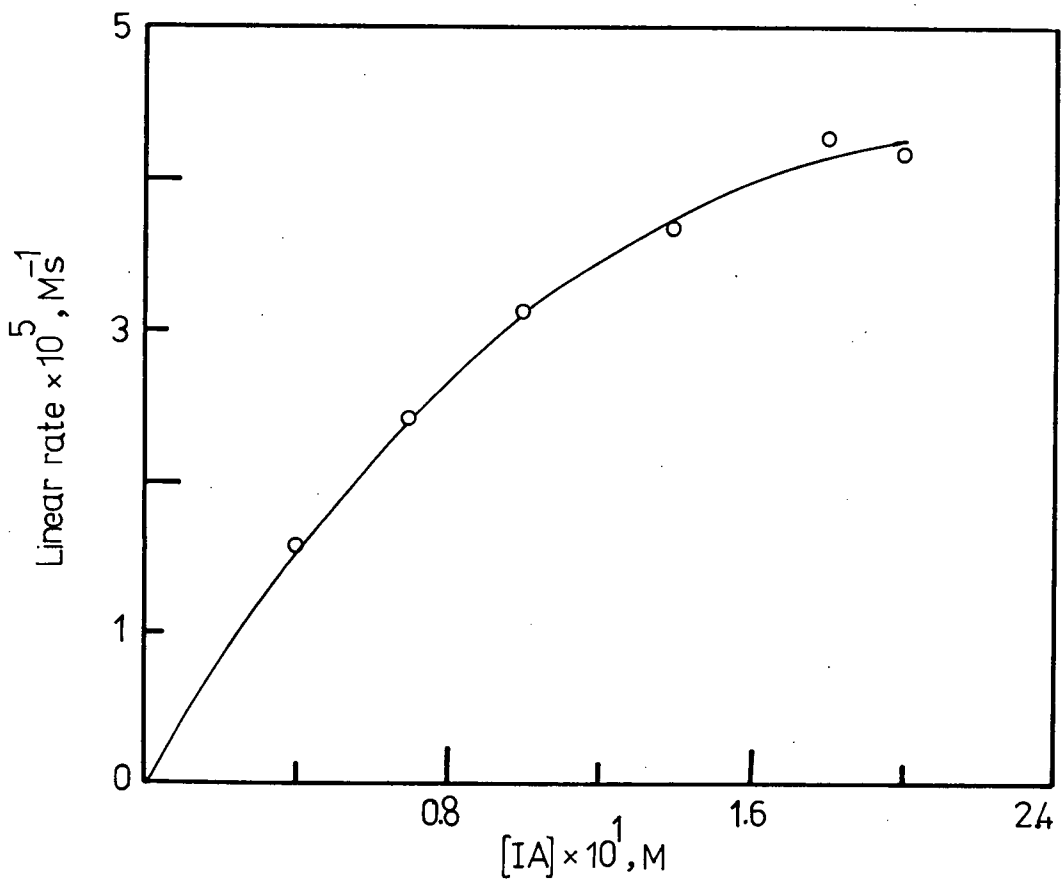

Figure VI.10 Dependence of linear rate on IA concentration (15°C, [Rh]=1.0×10^{-3}M, 752 mm P_{H_2}, n-butanol-toluene (2:1)).

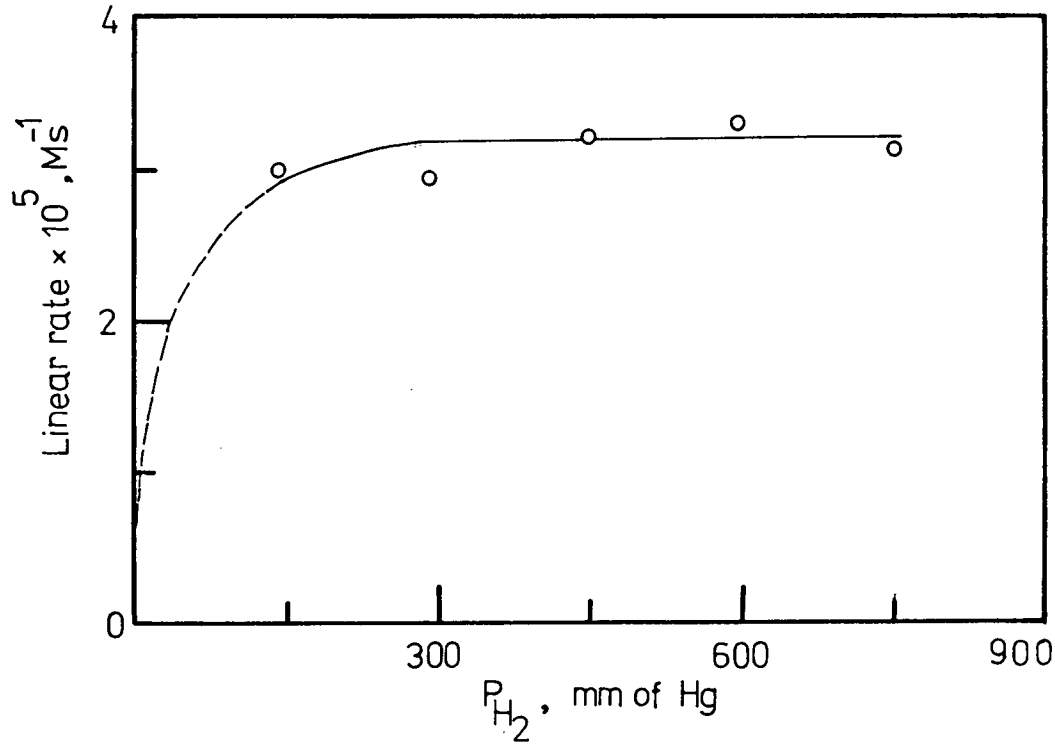

Figure VI.11 Plot of linear rate against hydrogen pressure (15°C, 0.1M IA, [Rh]=1.0x10^{-3}M, n-butanol-toluene (2:1)).

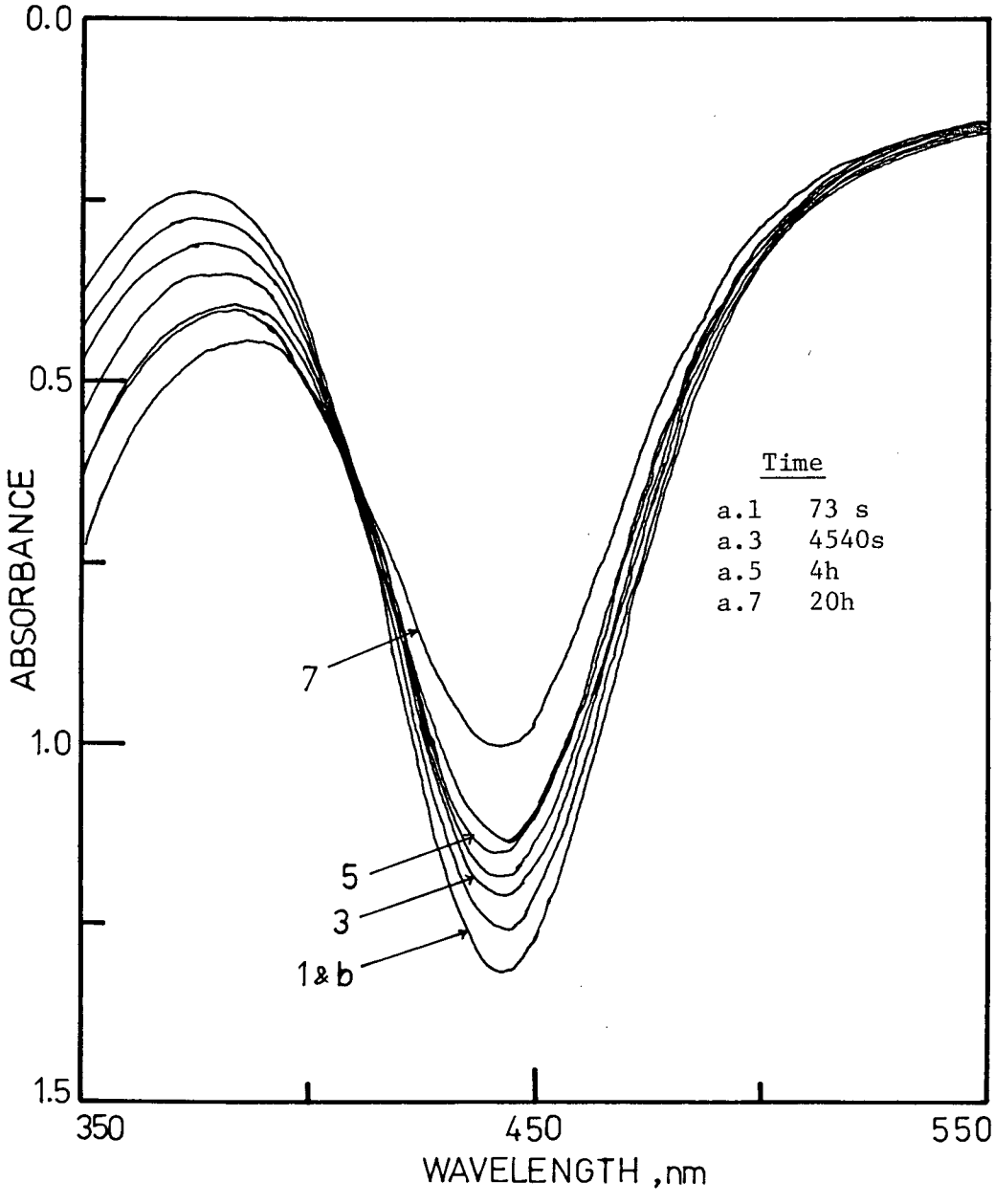

Figure VI.12 Spectral changes observed on adding itaconic acid to solutions of $Rh(diop)_2^+BF_4^-$ ($3.4x10^{-4}$M) in n-butanol-toluene (2:1)(under argon) at 30°C.

a. No added diop

b. In the presence of diop ($1x10^{-3}$M).

On adding IA (0.02 or 0.2M) to solutions of $Rh(diop)_2^+$ ($\sim 5 \times 10^{-4}$M) at 25°C under 1 atm H_2, very small spectral changes were observed in the 350-400 nm region; no peak due to $Rh(diop)_2^+$ was detected. The resulting final spectrum corresponds to the final one of Fig. VI.3(a).

VI.4 Discussion

VI.4.1 The hydrogen reaction

Treatment of solutions of $Rh(diop)_2^+$ with molecular hydrogen readily leads to the formation of dihydride species as shown synthetically (chapter VII and ref. 2) and spectroscopically (section VI.3.1)(equation [VI.4]):

$$Rh(diop)_2^+ + H_2 \overset{K}{\rightleftharpoons} Rh(diop)_2H_2^+ \qquad [VI.4]$$

Such reactions are well known; several rhodium(I)-phosphine (or arsine) complexes oxidatively add molecular hydrogen to give the corresponding rhodium(III) dihydrides.[3,4] The H_2:Rh stoichiometry (Table VI.1) was always somewhat less than the expected value of unity, and was independent of hydrogen pressure and so the stoichiometry problem is not simply due to establishment of the equilibrium shown in equation [VI.4]. A further complicating equilibrium [VI.5], that has been established in some rhodium-phosphine complexes[5], was ruled out since addition of P.S. or Et_3N again did not affect the H_2:Rh ratio.

$$Rh(diop)_2H_2^+ \rightleftharpoons H^+ + HRh(diop)_2 \qquad [VI.5]$$

The spectrophotometric and gas-uptake studies indicate that the hydrogen reaction with $Rh(diop)_2^+$ is not a simple pseudo first-order

process. Visible and stopped-flow studies show a rapid uptake followed by a slow uptake. Similar visible spectral changes obtained in the presence of excess diop indicate that the complex does not dissociate a diop ligand in solution during the hydrogen-reaction and this is consistent with the absence of any free diop or monodentate diop signal in the ^{31}P nmr spectrum of the complex under argon or under H_2 (Figure VI.7; also see below).

The ^{31}P nmr spectrum of $Rh(diop)_2^+$ showed a doublet at 25°C characteristic of four equivalent phosphorus atoms around rhodium (Figure VI.7 (a.1)). Surprisingly, this doublet changed to a complicated pattern that remained unchanged from -50°C to -85°C (Figure VI.7(a.2)). The doublet at -10.6 ppm (J_{Rh-P}=140 Hz) is presumably due to the $Rh(diop)_2^+$ species; since there is no signal due to dissociated diop, the presence of mono(diop)-rhodium species can be ruled out. Moreover, recent studies[4] have shown that mono(diop)-rhodium(I) complexes do not form detectable amounts of dihydrides under H_2, and in our system, the ^{31}P nmr spectrum of $Rh(diop)_2^+$ under H_2 gave a doublet of doublet of triplets at 25°C (Fig.VI.7(b)) characteristic of formation of a pure cis-dihydride complex.[3] Thus the other two multiplets at -15.5 ppm and -16.5 ppm observed in Fig. VI.7(a.2) are possibly associated with a solvated $Rh(diop)_2^+$ species although the ^{31}P nmr peaks have not been assigned. A distorted trigonal bipyramid structure, comparable to that of $HRh(diop)_2$ (section IV.3) seems plausible, but associated species with bridging diop ligands[6], or in which one rhodium is bonded to a phenyl ring of a diop ligand of another rhodium[7], cannot be ruled out.

Quite recently, evidence for solvated (MeOH) species has been obtained by Brown et al.[8] in a closely related ^{31}P nmr study done on various bicyclo-[2.2.1]heptadienebis(phosphine)rhodium(I) complexes. Thus, for example,

hydrogenation of complex I(a) in methanol produced exclusively species II(a).

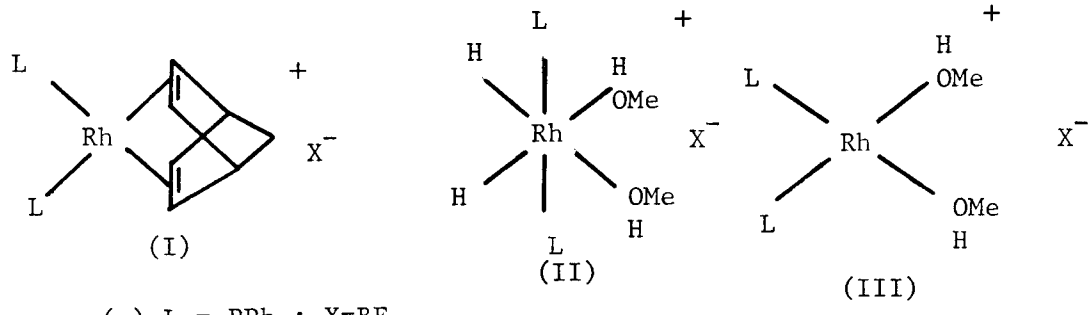

(I) (II) (III)

(a) L = PPh_3; X=BF_4

(b) L = O-MeC_6H_4PPhMe; X=BF_4

On removing H_2 from solutions of complex II(a), very small amounts of species III(a) was observed. On the other hand,when H_2 was added to complex I(b), the initial product under H_2 was exclusively III(b) which on further hydrogenation was slowly converted to complex II(b). Thus attainment of equilibrium between species II and III was extremely sensitive to the nature of the phosphine ligand attached to rhodium.

The kinetic scheme shown in equation [VI.6] accounts reasonably well for the $Rh(diop)_2^+/H_2$ reaction, and is compatible with the findings of Brown et al.[8] The stopped-flow data for the DMA system (Figure VI.4) can be analyzed in terms of two consecutive pseudo first-order reactions with rate constants k_2 and k_2' (Figure VI.13). The values are 10.2×10^{-2} and $7.4 \times 10^{-3} s^{-1}$, respectively, and data in other solvents were obtained similarly (Table VI.4).

$$Rh(diop)_2^+ + S \underset{k_{-3}}{\overset{k_3}{\rightleftharpoons}} Rh(diop)(diop^*)S^+ \xrightarrow[H_2]{k_3'} Rh(diop)(diop^*)(H)_2S^+ \quad \text{(Reaction A)}$$

$$\xrightarrow[k_3'']{-S} Rh(diop)_2H_2^+ \quad \text{(Reaction B)} \qquad [VI.6]$$

The faster k_2 step is identified with Reaction A, formation of $Rh(diop)(diop^*)(H)_2S^+$ via $Rh(diop)(diop^*)S^+$, while the slower k_2' step is identified with loss of solvent to give the six-coordinate $Rh(diop)_2H_2^+$.

For Reaction A, assuming a steady-state treatment for the intermediate species, the rate law is,

$$\text{Rate} = \frac{k_3 k_3'[Rh(diop)_2^+][H_2]}{k_{-3} + k_3'[H_2]} \qquad [VI.7]$$

and the measured k_2 equals $k_3 k_3'[H_2]/(k_{-3}+k_3'[H_2])$. The k_2 is essentially independent of $[H_2]$ from 130-320 mm suggesting that $k_3'[H_2] >> k_{-3}$ and hence $k_2 \sim k_3$, referring to dissociation of one P atom of the chelating diop. The independence of k_2 with solvent (Table VI.4) suggests a minor role for the solvent in the transition state for the k_3 step. Reaction B($k_3'' = k_2'$) should be zero-order in H_2, while the data (Table VI.4) indicate about a 1/3rd order. The greater solvent dependence noted for k_2', the step involving dissociation of solvent, adds some support to the tentative explanation outlined in equation [VI.6], although the rate surprisingly seems to increase with coordinating ability of the solvent.

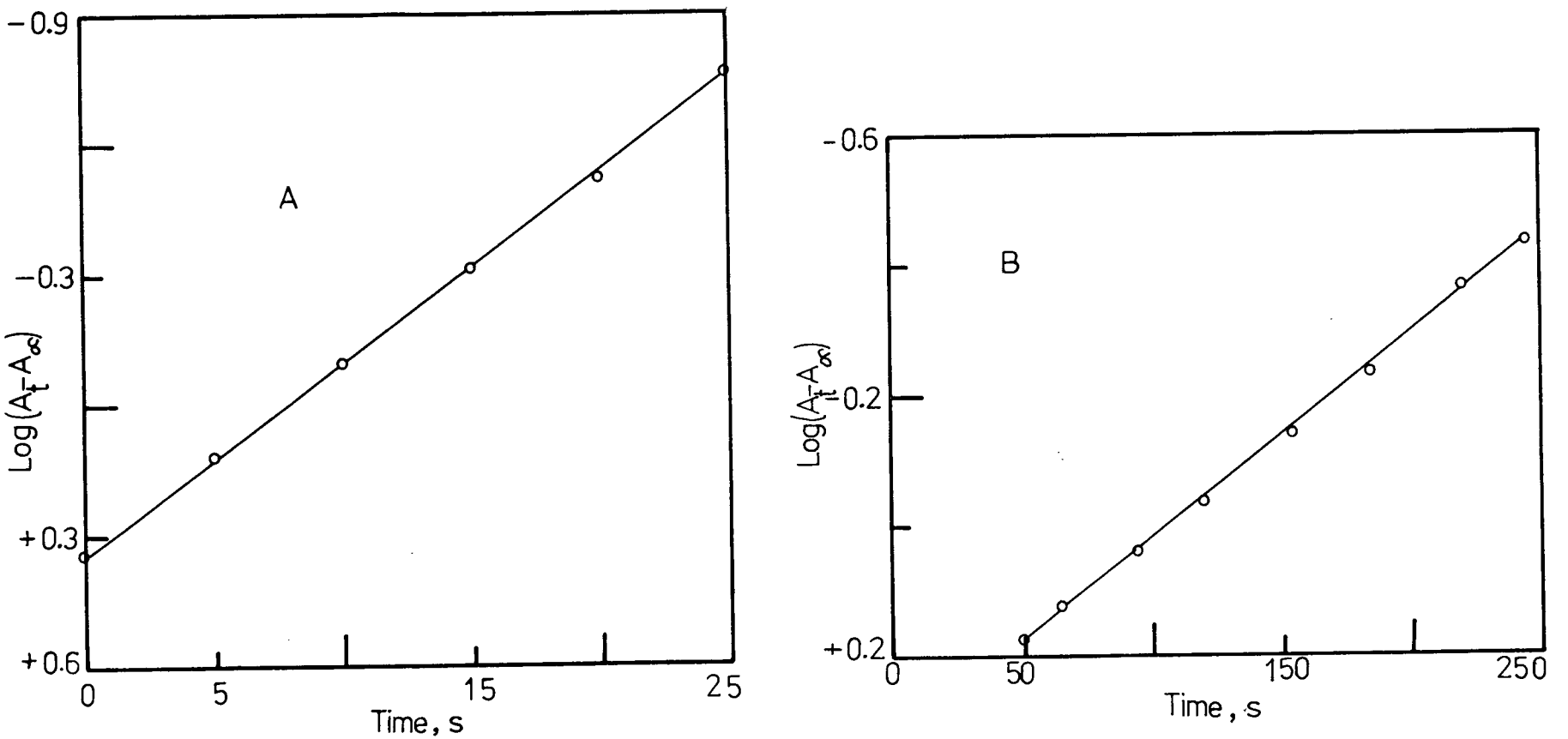

Figure VI.13 Analysis of data from Figure VI.4 in terms of two first-order reactions (A and B).

Table VI.4 Analysis of various stopped-flow data at 30°C in terms of two first-order reactions([Rh] ~1 x 10^{-4}M).

Solvent	P_{H_2},mm	k_2[a] x 10^2,s^{-1}	k_2'[a] x 10^3,s^{-1}
DMA	380	10.2	7.4
n-BuOH	375	9.2	5.1
$CH_2C\ell_2$	280	9.9	3.8
MeOH	320	8.2	4.3
MeOH	225	8.1	4.1
MeOH	130	7.4	3.3
MeOH	~35	~6.6	~2.2

a pseudo first-order rate constants.

The data on the loss of H_2 from $Rh(diop)_2H_2^+$ in different solvents under argon (Table VI.2) suggest that the reaction is first-order in rhodium and is solvent dependent. More strongly coordinating solvents (e.g. DMA) promote dehydrogenation presumably via the reverse of the process outlined in equation [VI.6] (Law of Microscopic Reversibility): the reverse of the k_3' step seems likely to be rate-determining, and thus may depend more on solvent polarity than coordinating ability.

VI.4.2 The catalytic hydrogenation mechanism

A general rate law for the hydrogenation of itaconic acid can be written as:

$$-\frac{d[H_2]}{dt} = k'[Rh]^{n_1}[IA]^{n_2}[H_2]^{n_3} \qquad [VI.8]$$

where k' is an overall rate constant. The kinetics at the conditions used showed that $n_1=1$ and $n_3=0$, and thus equation [VI.8] modifies to:

$$-\frac{d[H_2]}{dt} = k[Rh][IA]^{n_2} \qquad [VI.9]$$

Approximate values of k were computed for particular values of [IA] (upto $\sim$0.1M) where the rate is approximately first-order in IA i.e. $n_2=1$ (Fig. VI.10). The average value of k was calculated to be $\sim$0.33 $M^{-1}s^{-1}$ (Tables VI.3), while the slope of Fig. VI. 9 gave k = 0.34 $M^{-1}s^{-1}$, in good agreement.

Thermodynamic parameters were also calculated for the IA hydrogenation reaction, by plotting the data from Table VI.3 (Figure VI.14). The slope

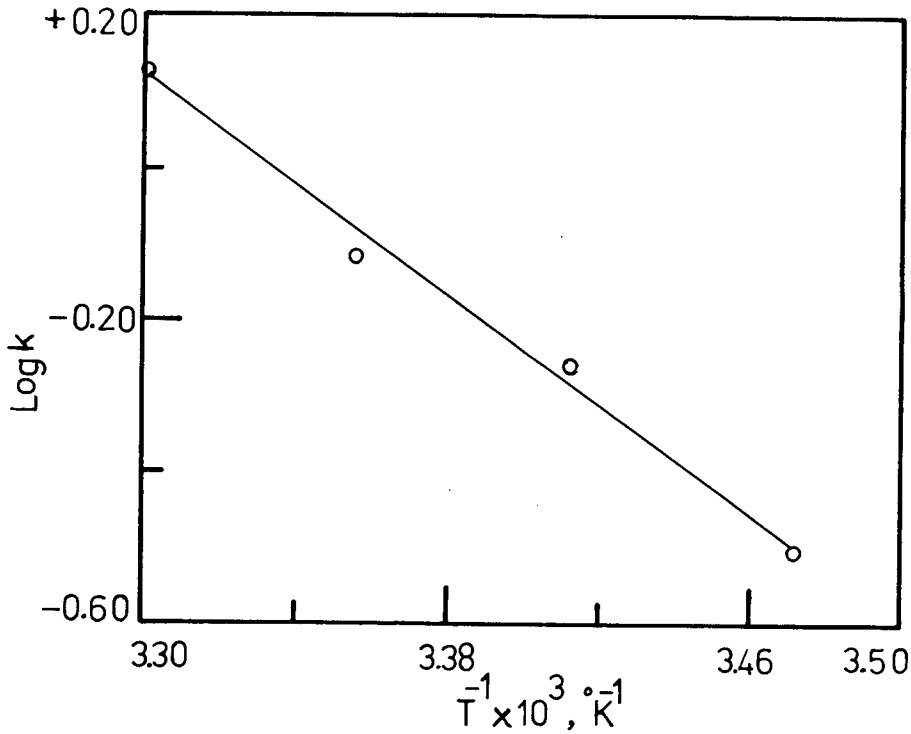

Figure VI.14 Arrhenius plot for the $Rh(diop)_2^+BF_4^-$-catalyzed hydrogenation of IA ([IA]=0.1M, [Rh]=1.0×10^{-3}M, 752 mm P_{H_2}, n-butanol-toluene (2:1)).

of the Arrhenius plot gave the activation energy, E_a = 17.0±1 Kcal mole^{-1}. $\Delta H^{\ddagger}$ and $\Delta S^{\ddagger}$ were calculated to be 16.4±1 Kcal mole^{-1} and -3.8±3 e.u. respectively.

The mechanism by which hydrogenation takes place can be postulated on the basis of the kinetic and spectroscopic studies. Since solutions of $Rh(diop)_2^+BF_4^-$ obey Beer's Law, and the visible spectrum is invariant with added diop, and further, since no free (or monodentate) diop signal was detected in the ^{31}P nmr spectrum of the complex, there is no evidence for any involvement of the equilibria outlined in equation [VI.10] (this equilibrium was proposed in section VI.4.1 to account for the kinetics of the rapid dihydride formation (stopped-flow) but it is not significant here during the relatively slow catalytic hydrogenation):

$$Rh(diop)_2^+ \rightleftharpoons \begin{matrix} Rh(diop)(diop^*)^+ \text{ or} \\ Rh(diop)^+ + diop \end{matrix} \qquad [VI.10]$$

The behavior of the system is in marked contrast to that shown by the $HRh(PPh_3)_4$ system which becomes active after a readily detectable dissociation of one of the PPh_3 ligands in solution.[9] Visible spectral studies show that $Rh(diop)_2^+$ reacts with H_2 extremely rapidly and completely to give a dihydride; any reaction with IA alone (or SA) (Figure VI.12) is partial and very slow compared to the catalytic hydrogenation. Spectral studies under all hydrogenation conditions show instantaneous loss of the cation. These results suggest that the hydrogenation reaction involves mainly the well established 'hydride route' (see Figure I.4), for example:

$$\underset{IV}{Rh(diop)_2^+} + H_2 \overset{K}{\rightleftharpoons} \underset{V}{Rh(diop)_2H_2^+} \qquad [VI.11]$$

$$Rh(diop)_2H_2^+ + IA \underset{k_{-4}}{\overset{k_4}{\rightleftharpoons}} \underset{VI}{Rh(diop)(H)_2(IA)^+} + diop \qquad [VI.12]$$

or

$$\underset{k_{-5}}{\overset{k_5}{\rightleftharpoons}} \underset{VII}{Rh(diop)(diop^*)(H)_2(IA)^+} \qquad [VI.13]$$

$$Rh(diop)(H)_2(IA)^+ \xrightarrow{k_6} \underset{VIII}{Rh(diop)^+} + alkane \qquad [VI.14]$$

or

$$Rh(diop)(diop^*)(H)_2(IA)^+ \xrightarrow{k_7} \text{or } Rh(diop)_2^+ + alkane \qquad [VI.15]$$

$$Rh(diop)^+ + diop \xrightarrow{Fast} Rh(diop)_2^+ \qquad [VI.16]$$

(diop* = a 'monodentate' or 'dangling' moiety)

Thus once $Rh(diop)_2H_2^+$ (a six-coordinate rhodium(III) species is formed, a diop ligand could dissociate completely or partially to become monodentate during the process of olefin coordination to provide the necessary vacant coordination site. The intermediate species thus formed (VI or VII) could release the saturated product by consecutive hydride transfers; a fast reassociation of the diop ligand could then regenerate the cationic $Rh(diop)_2^+$ complex.

The rate law for the mechanism outlined by equations [VI.11], [VI.12], [VI.14], and [VI.16], assuming a steady state for the $Rh(diop)(H)_2(IA)^+$ intermediate, is given by:

$$Rate = \frac{Kk_4k_6[IV][IA][H_2]}{k_{-4}[diop] + k_6} \qquad [VI.17]$$

In terms of total rhodium concentration $[Rh]_T$, this becomes

$$Rate = \frac{Kk_4k_6[Rh]_T[IA][H_2]}{(k_{-4}[diop]+k_6)(1+K[H_2])+Kk_4[H_2][IA]} \qquad [VI.18]$$

where $[Rh]_T = [IV] + [V] + [VI]$

In the H_2 pressure range studied, the rate was found to be independent of $[H_2]$ and this is consistent with the finding that K is large, equilibrium [VI.11] lies far to the right and the concentration of IV is negligible; i.e. $1+K[H_2] \sim K[H_2]$, and rate law [VI.18] reduces to:

$$\text{Rate} = \frac{k_4 k_6 [Rh]_T [IA]}{k_{-4}[diop] + k_6 + k_4[IA]} \qquad [VI.19]$$

where $[Rh]_T = [V] + [VI]$

Rate law [VI.19] is at first sight in accordance with the observed first-order dependence on rhodium and the zero- to first- order dependence on itaconic acid. A marked inverse diop dependence observed can be explained qualitatively by equilibrium [VI.12] where added diop successfully competes with the olefin coordination, but the rhodium dependence at conditions first-order in IA should then become fractional (approaching half-order), since the [diop] term in equation [VI.19] increases with increasing $[Rh]_T$: this is not the case.

The rate law for the closely related mechanism (equations [VI.11], [VI.13], and [VI.15]), assuming a steady state for the Rh(diop)(diop*)-$(H)_2(IA)^+$ species, is given by:

$$\text{Rate} = \frac{k_5 k_7 [Rh]_T [IA]}{k_{-5} + k_7 + k_5[IA]} \qquad [VI.20]$$

This rate expression [VI.20] now accounts for all the observed kinetic and spectroscopic data except again for the inverse diop dependence. Both mechanisms outlined above indicate that at high [IA], the dihydrido itaconic

species should be fully formed (zero-order in IA), the rate becoming simply k_7[VII] (or k_6[VI]). Even under these conditions, however, a small amount of added diop (diop: Rh=1:3) completely inhibits the catalytic hydrogenation. Even if one-third of the rhodium were completely deactivated by some diop coordination, then two-thirds of the activity should still remain. Since an equilibrium such as [VI.12] is ruled out, we can only speculate the reason for the very marked inverse diop dependence. One possibility is the formation of an inactive polymeric species, initiated by a small amount of added diop ligand; polymerization via diop bridges could tie up available coordination sites and successfully compete with the IA coordination step [VI.13]:

$$n\ Rh(diop)_2H_2^+ + diop \xrightarrow{K^*} [Rh(diop)(diop^*)H_2^+]_n \qquad [VI.21]$$

The validity of rate law [VI.20] can be tested by an inverse plot. Rearranging gives

$$\frac{1}{Rate} = \frac{k_{-5}+k_7}{k_5k_7[Rh]_T} \cdot \frac{1}{[IA]} + \frac{1}{k_7[Rh]_T} \qquad [VI.22]$$

The plot of $Rate^{-1}$ vs $[IA]^{-1}$ is a straight line with slope and intercept equal to 2×10^3s and $1.3\times10^4 M^{-1}s$ respectively (Figure VI.15). The intercept gives a k_7 value of $\sim$0.08 s^{-1}. The ratio of slope/intercept gives $\frac{k_{-5}+k_7}{k_5} \simeq 0.15M$. The value of k in equation [VI.9] now corresponds to $k_5k_7/k_{-5}+k_7$ and equals $\sim$0.5 $M^{-1}s^{-1}$. This value of k compares with that of 0.34 $M^{-1}s^{-1}$ estimated from the slope of Fig. VI.9. Since a reasonable Arrhenius plot is obtained (Fig. VI.14), it suggests

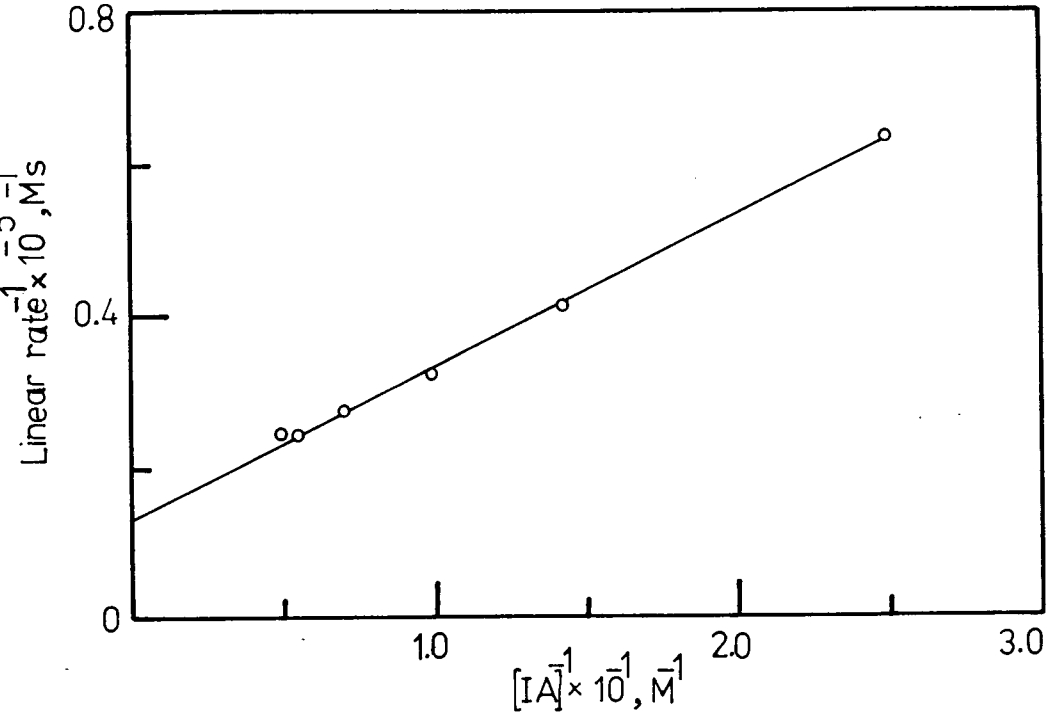

Figure VI.15 Plot of $[IA]^{-1}$ versus linear $rate^{-1}$ (data taken from Fig. VI.10).

that k_7 is small, and rate determining. Thus $k=K_5k_7$ which gives $K_5 \sim 4M^{-1}$.

Under the conditions zero-order in IA, the only species present in solution should be $Rh(diop)(diop^*)(H)_2(IA)^+$, reaction [VI.15] being the rate determining step. Unfortunately, the high-field ^1H nmr data of $Rh(diop)_2H_2^+BF_4^-$ in methanol-benzene-d_6 under H_2 saturated in IA were not conclusive since the conditions necessary to produce detectable amounts of the $Rh(diop)(diop^*)(H)_2(IA)^+$ species were probably not met at the concentration scales used for the experiment. Moreover, the limited concentration of H_2 in the nmr tube also presented difficulties in studying the reaction.

The initial faster part of the uptake plots (Fig. VI.8) has not been considered; the mechanism discussed concerns only the region of linear rates. The initial rapid dihydride formation (equation [VI.11]) based on the amount of catalyst used is too small to account for the initial curvature; a possibility is a contribution from an 'unsaturate' route (mechanism [VI.23]):

$$\begin{array}{ccc} Rh(diop)_2^+ + IA & \rightleftharpoons & Rh(diop)_2(IA)^+ \\ & & \Big\downarrow H_2 \\ & & Rh(diop)_2^+ + \text{saturated product} \end{array} \qquad [VI.23]$$

CHAPTER VII

REACTIONS OF BIS(DITERTIARYPHOSPHINE)-RHODIUM(I) COMPLEXES WITH THE GAS MOLECULES CO, O_2, H_2, AND HCℓ

VII.1 Introduction

There has been recent interest in determining the stereochemistry of various five-and six-coordinate iridium(I) and iridium(III) bis(diphosphine) complexes in solution using nmr spectroscopy.[1-4] These complexes exhibit fluxional behaviour and in some cases static structures could not be achieved even at low temperatures.[3] X-Ray crystal structures of $Ir(dpe)_2CO^+$[5] and $M(dpe)_2O_2^+$[6] (M = Ir,Rh) have been reported, and all three complexes have approximately trigonal bipyramidal configurations (considering O_2 as a monodentate ligand). In contrast to iridium, no systematic solution studies have been reported on analogous rhodium complexes. The few rhodium complexes reported include $Rh(dpe)_2O_2^+PF_6^-$ which is a reversible O_2 binder[6], $HRh(dpe)_2C\ell^+C\ell^-$ which is reported to be one of the most active catalysts for hydrogenation of terminal olefins[7,8], and $[Rh(\widehat{P\ P})_2]C\ell$ species ($\widehat{P\ P}$ = dpe and dppp) which have been used for catalytic decarbonylation of aldehydes[9]; the decarbonylation report appeared after completion of the CO studies described in this chapter.

The synthesis and characterization of neutral and cationic rhodium(I)-bis(ditertiaryphosphine) (ditertiaryphosphine = $\phi_2P(CH_2)_nP\phi_2$ (n=1-4) and (+)-diop) complexes were discussed in chapter IV. In this chapter, the synthesis of several rhodium(I) and rhodium(III) complexes obtained by addition of CO, O_2, H_2, and HCℓ to the $[Rh(\widehat{P\ P})_2]A$ (A=Cℓ, BF_4) complexes will be described. Such methods have been used earlier[10-14] to

synthesize some rhodium and related iridium complexes. Spectroscopic studies done on the isolated rhodium complexes to establish their solution structure are presented along with kinetic data on the ease of addition of O_2, CO, and H_2 to the $Rh(P\frown P)_2^+BF_4^-$ complexes.

VII.2 Experimental

Solutions of the starting rhodium(I) complexes were handled using inert atmosphere techniques. Stopped-flow data were obtained on a Durrum 110 spectrophotometer equipped with a 2-cm light path cuvette. Stoichiometric gas-uptake experiments were performed using the ampoule technique described in section II.6. PPh_3 in an appropriate solvent was used as a reference standard for all the low temperature ^{31}P nmr spectra.

Tables VII.1 - VII.5 report analytical, conductivity, reaction stoichiometry, infrared, and ^1H and ^{31}P nmr data for the well characterized complexes (see section VII.3). Gas-uptake data are also given for systems for which pure complexes were not isolated (Table VII.2).

Preparation of complexes

The $[Rh(P\frown P)_2]A$ ($P\frown P = \phi_2P(CH_2)_nP\phi_2$ (n=1-4) and (+)-diop; A=Cℓ, BF_4) complexes were synthesized from the $[RhCℓ(C_8H_{14})_2]_2$ dimer as described in Chapter IV.

VII.2.1 CO complexes

VII.2.1.1 $Rh(P\frown P)_2CO^+BF_4^-$ ($P\frown P$ = dpm, dpp) - Through a red solution of $Rh(dpm)_2^+BF_4^-$ (0.28 g, 0.29 mmol) or $Rh(dpp)_2^+BF_4^-$ (0.30 g, 0.30 mmol) in $CH_2Cℓ_2$ (5 ml) was bubbled CO gas. Addition of diethyl ether precipitated a yellow complex that was filtered after cooling to 0°C, washed with ether a few times, and then dried over an atmosphere of CO. The solids were stored

Table VII.1 Analytical and molar conductivity (Λ) data for the Rh(I) and Rh(III) complexes.

Complex	Decomposition point[a], °C	Analysis(%) Found C	Found H	Calculated C	Calculated H	Λ[b] ($mho.cm^2mol^{-1}$)
$Rh(dpm)_2CO^+BF_4^-$	168	61.74	4.44	62.09	4.46	85[c]
$Rh(dpp)_2CO^+BF_4^-$	179-182	63.43	5.13	63.34	4.99	81[c]
$Rh(dpm)_2O_2^+BF_4^-$	209-211	61.00	4.50	60.62	4.44	83
$Rh(dpe)_2O_2^+BF_4^-$	164-167	61.26	4.69	61.31	4.72	84
$Rh(dpp)_2O_2^+BF_4^-$	197-201	61.54	5.19	61.97	4.97	81
$Rh(dpp)_2H_2^+BF_4^-$	86	63.74	5.22	63.80	5.32	81[d]
$Rh(diop)_2H_2^+BF_4^-$	153	61.22[e]	5.65	62.64	5.56	79[d]
$HRh(dpm)_2Cl^+Cl^-$	144	58.96[f]	4.73	63.64	4.77	67
$HRh(dpe)_2Cl^+Cl^-$	136	60.77[f]	5.00	64.28	5.05	68
$HRh(dpp)_2Cl^+Cl^-$	152	62.34[f]	5.43	64.88	5.31	68
$HRh(dpm)_2Cl^+BF_4^-$	204	59.95	4.56	60.35	4.53	95
$HRh(dpe)_2Cl^+BF_4^-$	184	60.89	4.87	61.06	4.79	96
$HRh(dpp)_2Cl^+BF_4^-$	164-167	59.36[e]	5.01	61.71	5.05	95

a In air (uncorrected).

b In nitromethane (under argon) at 25°C.

c Under CO atmosphere.

d Under hydrogen atmosphere.

e Analysis low due to the presence of solvent in the complex (see discussion).

f See text.

Table VII.2 Gas-uptake data for various rhodium(I)-bis(ditertiaryphosphine) complexes at 25°C.[a]

Complex	H_2/Rh	O_2/Rh	CO/Rh
$Rh(dpm)_2^+BF_4^-$	——[b,c]	0.9[c]	0.9[d]
$Rh(dpe)_2^+BF_4^-$	——[b]	——[c,e]	——[b]
$Rh(dpp)_2^+BF_4^-$	0.9[c] 0.9[d]	1.0[c]	1.0[d]
$Rh(dpb)_2^+BF_4^-$	0.6[d]	2.8[c]	1.7[d]
$Rh(diop)_2^+BF_4^-$	0.8[f] 0.8[g]	——[b´]	1.3

a In methanol using the ampoule technique; values ±0.1 in error ([Rh]=5×10^{-5} mole).

b No uptake observed.

b´ Immeasurably slow.

c In 1,2 $C_2H_4Cl_2$

d In DMA

e Small uptake observed; see section VII.5.

f In n-butanol.

g In DMA at 12°C.

Table VII.3 High-field ^{1}H nmr and infrared data for the rhodium(I) and rhodium(III) complexes

Complex	Nmr data[a] H-Rh, τ	ir data[b] (cm^{-1})
$Rh(dpm)_2CO^+BF_4^-$		ν(CO) = 1948
$Rh(dpp)_2CO^+BF_4^-$		" = 1961
$Rh(dpm)_2O_2^+BF_4^-$		$\nu(O_2)$ = 881
$Rh(dpe)_2O_2^+BF_4^-$		" = 888
$Rh(dpp)_2O_2^+BF_4^-$		" = 896
$Rh(dpp)_2H_2^+BF_4^-$	18.5	ν(H-Rh) = 2052
$Rh(diop)_2H_2^+BF_4^-$	20.0	" = 2020,2080
$HRh(dpm)_2C\ell^+C\ell^-$	22.0	ν(H-Rh) = 2064
$HRh(dpe)_2C\ell^+C\ell^-$	25.9	" = 2086
$HRh(dpp)_2C\ell^+C\ell^-$	25.0	" = 2100(br)
$HRh(dpm)_2C\ell^+BF_4^-$	22.0	" = 2065
$HRh(dpe)_2C\ell^+BF_4^-$	26.0	" = 2084
$HRh(dpp)_2C\ell^+BF_4^-$	25.0	" = 2100(br)

a In $CDC\ell_3$ at 25°C.

b In Nujol; br=broad

Table VII.4 ^{1}H nmr data for various rhodium-bis(ditertiaryphosphine) complexes.[a]

Complex	δ, coordinated diphosphine	
	aliphatic	phenyl
$Rh(dpm)_2CO^+BF_4^-$	4.2m, 4.7m[b,c]	7.5m[b,c]
$Rh(dpm)_2CO^+BF_4^-$	4.5m[c,d]	7.5m[c,d]
$Rh(dpp)_2CO^+BF_4^-$	1.9m, 2.45m[b,c]	7.4m[b,c]
$Rh(dpm)_2O_2^+BF_4^-$	3.8m, 4.5m	7.3m
$Rh(dpe)_2O_2^+BF_4^-$	2.2m	7.3m
$Rh(dpp)_2O_2^+BF_4^-$	1.7m, (2-3)m	7.4m
$Rh(dpp)_2H_2^+BF_4^-$	1.9m, 2.3m, 3.1m[c,e]	7.0m, 7.3m, 7.5m, 7.9m, 8.1m[c,e]
$Rh(diop)_2H_2^+BF_4^-$	1.2s, 2.3m, 2.9m, 3.3m[e]	7.5m[e]
$HRh(dpm)_2Cl^+Cl^-$	4.6m, 5.0m	7.3m
$HRh(dpe)_2Cl^+Cl^-$	2.3m, 2.8m	7.3m
$HRh(dpp)_2Cl^+Cl^-$	1.6m, 2.3m, 2.8m	7.4m
$HRh(dpm)_2Cl^+BF_4^-$	4.5m, 4.9m	7.3m
$HRh(dpe)_2Cl^+BF_4^-$	2.3m, 2.8m	7.3m
$HRh(dpp)_2Cl^+BF_4^-$	1.6m, 2.3m, 2.8m	7.4m

a Measured in ppm (downfield positive) from TMS in $CDCl_3$; s=singlet, m-multiplet.

b Under argon atmosphere

c In acetone-d_6

d Under CO atmosphere

e Under hydrogen atmosphere

Table VII.5 $^{31}P\{^{1}H\}$ nmr data for various rhodium-bis(ditertiaryphosphine) complexes.[a]

Complex	δ[b], ppm	J_{Rh-P}, Hz	J_{P-P}, Hz	T, °C
$Rh(dpm)_2CO^+BF_4^-$[c]	+22.27	102.4	-	25
" [c]	+19.38 +20.83	97.5 115	-	-50
$Rh(dpm)_2CO^+BF_4^-$[d]	+22.59	97.5	-	25
" [d]	+19.80	97.1	-	-50
$Rh(dpp)_2CO^+BF_4^-$[c]	- 6.80	133	-	25
$Rh(dpp)_2CO^+BF_4^-$ [d]	-15.13 +12.87	122.5 85.1	30	25
" [d]	- 5.14 + 9.94	91.6 114.7	46	-50
$Rh(dpm)_2O_2^+BF_4^-$	+14.39 +30.80	112.4 82	38	25
$Rh(dpe)_2O_2^+BF_4^-$	-57.6	132.7	-	25
$Rh(dpe)_2O_2^+C\ell^-$	-51.3 -44.3	126	7.7	-80[e]
$Rh(dpp)_2O_2^+BF_4^-$	-14.90 +12.68	122.5 84.9	30	25
$Rh(dpp)_2H_2^+BF_4^-$[f]	-19.96 - 9.12	99.6 82.2	30	-50
$Rh(diop)_2H_2^+BF_4^-$ [f]	-19.9 - 3.8	103 90	—[g]	25
" [f]	-21.40 - 6.4	103 90	19.7	-50
" [f]	-21.60 - 7.7	103.6 90	19.2	-85
$HRh(dpm)_2C\ell^+C\ell^-$	+16.70	84.3	-	25
"	+15.40	82.6	-	-60
$HRh(dpe)_2C\ell^+C\ell^-$	-51.80	93.8	-	25
"	-56.46	94.2	-	-60
$HRh(dpp)_2C\ell^+C\ell^-$	- 2.34	91	-	25
"	-14.3 + 5.4	-	-	-50[h]
"	-16.0 + 6.4	-	-	-85[i]
$HRh(dpm)_2C\ell^+BF_4^-$	+16.9	84.4	-	25
$HRh(dpe)_2C\ell^+BF_4^-$	-51.5	94.7	-	25
$HRh(dpp)_2C\ell^+BF_4^-$	- 2.56	91	-	25

contd.

a Measured in ppm (upfield positive) from 85% H_3PO_4. Shifts for the free ligands ($CDC\ell_3$ or $CH_2C\ell_2$) occur at +22.25 (dpm), +12.51 (dpe), +17.25 (dpp), +15.95 (dpb), and +22.50 (diop).

b In $CH_2C\ell_2$ - acetone-d_6 (2:1 V/V).

c Under Ar.

d Under CO

e Value from ref. 3.

f Under H_2.

g See text.

h A broadened doublet.

i A doublet of doublet of triplets was obtained although it was not well resolved.

under CO.

VII.2.1.2 - CO was bubbled through a yellow solution of $Rh(dpe)_2^+BF_4^-$ (0.20g, 0.20 mmol) in $CH_2C\ell_2$ (5 ml) for $\sim$½h. No change in colour was observed. Slow addition of diethyl ether yielded only yellow crystals of the starting complex.

VII.2.1.3 - Reaction of CO with $Rh(dpb)_2^+BF_4^-$ using procedure VII.2.1.1 yielded a yellow complex contaminated with a white powder. The infrared (Nujol mull) showed carbonyl bands at 1962 and 2003 cm^{-1}. Calc., for example, for $Rh(dpb)(dpb^*)(CO)_2^+BF_4^-$: C = 63.41%; H = 5.10%. Found: C = 57.92%; H = 4.91%. Attempts to synthesize $[Rh(dpb)_2CO]C\ell$ via an exchange reaction, by stirring trans - $RhC\ell(CO)(PPh_3)_2$ with 3 moles excess dpb in benzene, similar to the method used for preparing bis-(diphosphine)-iridium complexes[3], also gave a mixture of products, the infrared showing carbonyl bands at 1910 and 1941 cm^{-1}.

VII.2.1.4 - Using procedure VII.2.1.1, $Rh(diop)_2^+BF_4^-$ reacted with CO to give a yellow solid. The ir (Nujol mull) showed terminal CO bands at 1976 and 2015 cm^{-1} but a low elemental analysis (calc. for $Rh(diop)(diop^*)(CO)_2^+BF_4^-$) suggested that the solid isolated was a mixture of complexes.

Reaction of $Rh(diop)_2C\ell$ with CO in benzene followed by addition of diethyl ether yielded a yellow complex that showed two carbonyl bands (Nujol) at 1926 and 1974 cm^{-1}. The same bands have been reported for $[Rh(diop)(diop^*)(CO)_2]C\ell$ obtained by a different method.[12] However, an additional ir band at 308 cm^{-1} assigned to ν(Rh-Cℓ), not reported in literature[12], suggests that the complex is probably contaminated with some neutral rhodium species. Repetition of the literature preparation[12] also yielded a mixture of complexes.

VII.2.2 Dioxygen complexes

The literature method[6] with a slight modification was used to prepare the dioxygen complexes.

VII.2.2.1 $Rh(dpm)O_2^+BF_4^-$ - Oxygen was bubbled through an orange solution of $Rh(dpm)_2^+BF_4^-$ (0.22 g, 0.23 mmol) in methanol (20 ml). The solution became cloudy after a few minutes and a dark brown solid separated that was washed with methanol and dried under suction for a few hours.

VII.2.2.2 $Rh(\overset{\frown}{P}P)_2O_2^+BF_4^-$ ($\overset{\frown}{P}P$ = dpe, dpp) - Through a methanol solution of $Rh(\overset{\frown}{P}P)_2^+BF_4^-$ (0.30 g, 0.30 mmol) was bubbled O_2 gas. The resulting solution was concentrated to a 5 ml volume when a solid separated. The mixture was cooled to 0°C and the solid was filtered, washed with diethyl ether and dried under suction. The dpe complex was greenish brown while the dpp analogue was brown.

VII.2.2.3 - A deep red solution of $Rh(dpb)_2^+BF_4^-$ (0.25 g, 0.24 mmol) in methanol (20 ml) slowly changed to dark brown under oxygen over a period of one day. Addition of diethyl ether precipitated a brown solid that was a mixture of products; the ir showed bands at 851 and 1120 cm^{-1} possibly attributable to $\nu(O_2)$ and $\nu(P\text{-}O)$ respectively.[15] Calculated for $Rh(dpbO_2)_2O_2^+BF_4^-$: C = 59.07%; H = 4.92%;. Found: C = 52.68%; H = 4.98%.

VII.2.2.4 - No visible colour change was observed on stirring $Rh(diop)_2^+BF_4^-$ under an oxygen atmosphere even after four days in methanol. Addition of diethyl ether precipitated a yellow complex that mostly contained the starting material (via ir) and the system was not studied further.

VII.2.3 Dihydride complexes

VII.2.3.1 - Reaction of H_2 with the $Rh(\overset{\frown}{P}P)_2^+BF_4^-$ complexes ($\overset{\frown}{P}P$ = dpm, dpe) in CH_2Cl_2 yielded only the starting complex in both cases.

VII.2.3.2 $\underline{Rh(dpp)_2H_2^+BF_4^-}$ - H_2 was bubbled through a deep red solution of $Rh(dpp)_2^+BF_4^-$ (0.36 g, 0.35 mmol) in CH_2Cl_2 (10 ml). Within a few minutes the colour changed to light yellow. Diethyl ether was added to induce crystallization and the solution was cooled to 0°C. The white crystals so obtained were filtered, washed with ether, dried over H_2, and finally stored under H_2.

VII.2.3.3 $\underline{Rh(diop)_2H_2^+BF_4^-}$ - When a deep red solution of $Rh(diop)_2^+BF_4^-$ (0.41 g, 0.34 mmol) in CH_2Cl_2 (10 ml) was stirred under H_2, the colour slowly changed to light yellow in ~½h. The off-white crystals, obtained using procedure VII.2.3.2, were stored under H_2.

VII.2.3.4 - No change in colour was observed when $Rh(dpb)_2^+BF_4^-$ (0.22 g, 0.21 mmol) in CH_2Cl_2 (5 ml) was stirred under H_2. The solid isolated using procedure VII.2.3.2 was probably contaminated with the starting complex. Calc. for $Rh(dpb)_2H_2^+BF_4^-$: C = 64.39%; H = 5.56%.Found: C = 62.73%; H = 5.53%. The ir showed a sharp band at 2072 cm^{-1} assigned to ν(H-Rh), while the high field ^1H nmr in $CDCl_3$ at 25°C was a pair of multiplets centered around 20.3τ

VII.2.4 $\underline{HRh(\overset{\frown}{P}\,\overset{\frown}{P})_2Cl^+A^-}$ complexes

VII.2.4.1 $\underline{HRh(dpm)_2Cl^+Cl^-}$ - HCl(g) was bubbled through an orange solution of $Rh(dpm)_2Cl$ (0.30 g, 0.33 mmol) in methanol (15 ml). The solution turned colourless instantaneously and a white solid separated after a few minutes stirring. The solid was filtered, washed with methanol a few times, and dried in vacuo to give white microcrystals. The same product was isolated starting with $Rh(dpm)_2^+BF_4^-$.

VII.2.4.2 $\underline{HRh(\overset{\frown}{P}\,\overset{\frown}{P})_2Cl^+Cl^-}$ ($\overset{\frown}{P}\,\overset{\frown}{P}$ = dpe and dpp) - Through an ethanol solution (~15 ml) of $Rh(\overset{\frown}{P}\,\overset{\frown}{P})_2Cl$($\overset{\frown}{P}\,\overset{\frown}{P}$ = dpe or dpp (0.37 g, ~0.4 mmol))

was bubbled HCℓ(g). The solution turned light yellow instantaneously. After a few minutes stirring, excess HCℓ(g) was removed by a flow of argon; concentration to ∿5 ml followed by addition of 20 ml ether yielded light yellow crystals on cooling to 0°C. The complex was filtered, washed with diethyl ether, and dried in vacuo. The $HRh(dpe)_2C\ell^+C\ell^-$ complex has been prepared earlier via a different route.[7,8]

VII.2.4.3 Reaction of HCℓ(g) with $[Rh(\overset{\frown}{P}\overset{\frown}{P})_2]A$ ($\overset{\frown}{P}\overset{\frown}{P}$ = dpb and diop; A=Cℓ,BF_4)

Method I - HCℓ(g) was bubbled through a deep red solution of $Rh(dpb)_2C\ell$ (0.23 g, 0.23 mmol) in $CH_2C\ell_2$ (5 ml). The color instantaneously changed to light yellow. After removing excess HCℓ by bubbling argon, the solution was concentrated to ∿2 ml, and THF (5 ml) was added. Slow addition of diethyl ether precipitated a light yellow compound that was filtered, washed with ether a few times, and dried in vacuo; it appeared, however, to be a mixture of products.

Method II - The colour turned instantaneously to light yellow when HCℓ(g) was bubbled through a deep red solution of $Rh(dpb)_2C\ell$ in benzene. After a few minutes stirring, the light yellow solid that separated was filtered, washed with benzene and dried in vacuo; again, however, a mixture of products resulted. The ir (Nujol) showed bands at 2150 cm^{-1} (br), assigned to ν(H-Rh), and at 280 and 290(sh) cm^{-1} corresponding to ν(Rh-Cℓ). The high-field ^1H nmr in $CDC\ell_3$ at 25°C showed a broad multiplet centered around 26.5τ. Calc. for $HRh(dpb)_2C\ell^+C\ell^-$: C = 65.43%; H =5.45%. Found: C = 61.26%; H = 5.24%.

Reaction of HCℓ(g) with $Rh(diop)_2^+BF_4^-$ also gave a light yellow mixture of products by both methods. ir (Nujol): ν(H-Rh) = 2130 cm^{-1} (br); ν(Rh-Cℓ) = 278 and 290 cm^{-1}. In addition, broad bands at 3500-3600 cm^{-1}

and at ∿1600 cm^{-1} were also observed. The high-field ^1H nmr in $CDC\ell_3$ at 25°C showed an extremely broad multiplet centered around 22.0τ. Calc. for $HRh(diop)_2C\ell^+C\ell^-$: C = 63.54%; H = 5.55%. Found: 58.29%; H = 5.46%.

All the reactions described in section VII.2.4 gave the same products when HCℓ.DMA was used instead of HCℓ(g).

VII.2.4.4 $\underline{HRh(\widehat{P\ P})_2C\ell^+A^-}$ ($\widehat{P\ P}$ = dpm, dpe, and dpp; A = BF_4, PF_6, SbF_6)

The complexes were prepared in each case from the corresponding chloro complex. In a typical preparation, AgA (0.14 mmol) in acetone (5 ml) was added to a $CH_2C\ell_2$ (5 ml) solution of $HRh(\widehat{P\ P})_2C\ell^+C\ell^-$ (0.14 mmol). A white precipitate of AgCℓ formed instantaneously. The solution was filtered and concentrated to a 2 ml volume, followed by addition of THF (3 ml). Diethyl ether was added to precipitate the product that was filtered, washed with ether, and dried in vacuo.

Attempts were also made to prepare the $HRh(\widehat{P\ P})_2C\ell^+A^-$ complexes by a procedure used by Miller and Caulton[3] to prepare the corresponding iridium complexes. Thus in a typical preparation, a slight excess of aqueous HBF_4 or HPF_6 was added to an ethanol solution of $Rh(\widehat{P\ P})_2C\ell$ ($\widehat{P\ P}$ = dpm, dpe, and dpp). The yellow or orange complexes that precipitated were filtered, washed with ethanol and dried. The infrared spectra of all these complexes showed characteristic bands of the anion (BF_4 or PF_6) but no hydride band was observed. The complexes were not studied further.

When two moles of the AgA salt (A = BF_4, PF_6, SbF_6) per mole of rhodium were stirred overnight in the dark with the $HRh(\widehat{P\ P})_2C\ell^+C\ell^-$ complexes, the products were identified as the known $HRh(\widehat{P\ P})_2C\ell^+A^-$ species rather than expected dications of the type $[HRh(\widehat{P\ P})_2][A]_2$.

VII.3 Results and Discussion

Oxidative or just simple addition of XY molecules (XY=O_2, H_2, HCℓ, and CO) to square-planar rhodium(I)- and iridium(I)-bis(diphosphine) cationic complexes is fairly common[10-13] and a number of iridium(I) and iridium(III)-bis(diphosphine)(diphosphine = dpm, dpe, and dpp) complexes have been prepared using this method.[10,11] The product from the reaction always incorporates one mole of XY to give complexes of the type $Ir(\widehat{P\ P})_2XY^+$. We have used this method in an attempt to prepare several rhodium(I)- and rhodium(III)-bis(diphosphine) complexes (Table VII.1) starting with four- and five-coordinate rhodium(I) complexes of the type $Rh(\widehat{P\ P})_2A$ ($\widehat{P\ P}$ = dpm, dpe, dpp, dpb, and diop; A=Cℓ,BF_4)[16] via reaction [VII.1]:

$$[Rh(\widehat{P\ P})_2]A + \underline{n}XY \rightleftharpoons [Rh(\widehat{P\ P})_2(XY)_{\underline{n}}]A \qquad [VII.1]$$

The value of $\underline{n}$ and the extent of reaction [VII.1] varies with the particular diphosphine used (Table VII.2). Gas-uptake data indicate that the value of $\underline{n}$ is independent of the nature of solvent.

Tables VII.1-VII.5 list analytical, conductivity, gas-uptake, and spectroscopic data for the isolated complexes. For the sake of simplicity, the complexes have been classified as five- and six-coordinate, and will be discussed separately in sections VII.3.1 and VII.3.2 respectively.

VII.3.1 The five-coordinate carbonyl complexes of rhodium(I)

Analytically pure complexes are obtained via reaction [VII.1] for $\widehat{P\ P}$ = dpm or dpp with XY=CO, $\underline{n}$=1, and A=BF_4. The $Rh(dpe)_2^+BF_4^-$ complex, like the chloride analogue[12], does not add CO. The method seems simpler than one reported for the preparation of $[Rh(dpp)_2CO]Cℓ$ using $[RhCℓ(COD)]_2$ and a five-fold excess of dpp in benzene under CO which gives

a mixture of products.[12] The P⌒P = dpb and diop, and A=BF_4 complexes react with > 1 mole of CO per rhodium (Table VII.2) to give presumably, some dicarbonyl species (ir data), although a pure complex was not isolated. Any such dicarbonyl could maintain four or five coordination by dissociation of one or two ligating P atoms. Attempts to prepare $[Rh(dpb)_2CO]C\ell$ via an exchange reaction, used for the preparation of $[Ir(P⌒P)_2CO]C\ell$ (P⌒P = dpm, dpe, and dpp) complexes[3], again yielded a mixture of complexes that were not identified. An unsuccessful attempt has been made by Sanger[12] to prepare pure $[Rh(dpb)_2CO]C\ell$ via a different method. The ^{31}P nmr spectra of the carbonyl mixture of dpb and diop were too complicated to yield any useful information.

Reaction of CO with $Rh(diop)_2C\ell$ yields a yellow solid that shows ir bands at 1926 and 1974 cm^{-1} (ν(CO)) and 308 cm^{-1}(w) (ν(Rh-Cℓ)). A carbonyl complex prepared by Sanger[12] by a different procedure was reported to have the same ir CO bands but no ν(Rh-Cℓ) was reported, and the complex was thought to be $[Rh(diop)(diop^*)(CO)_2]C\ell$ with an ionic chloride. We repeated the literature preparation and isolated a solid with ir bands identical to those of the solid obtained by our method. The Rh-Cℓ band at 308 cm^{-1} (that of $Rh(diop)_2C\ell$ is at 284 cm^{-1}) and conductivity data in nitromethane at 25°C, Λ = 28 $mho.cm^2\ mol^{-1}$ (under argon) and 37 $mho.cm^2 mol^{-1}$ (under CO), suggest that the chloride is only partially ionized in solution; a mixture of complexes, one with the proposed[12] ionic structure (A), and

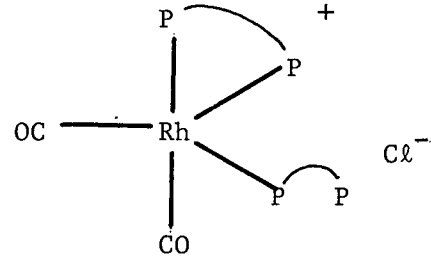

(A)

others such as RhCℓ(CO)(diop) or RhCℓ(CO)(diop)(diop*) could account for the data.

The structures of the isolated rhodium complexes were determined from the data in Tables VII.1-VII.5. The ir spectra of the dpm and dpp complexes show only one terminal CO band, in each case, at 1948 and 1961 cm^{-1}, respectively. Conductivity data in nitromethane under CO show that both complexes are 1:1 electrolytes (for 1:1 electrolytes, Λ=75-95 $mho.cm^2mol^{-1}$[17]). The complexes are fairly stable in the solid state but in solution the CO is readily lost, as evidenced from spectroscopic data. Thus under argon, methanol solutions of the dpm and dpp complexes show visible absorption maxima at 385 and 446 nm, and at 412 nm, respectively, characteristic of $Rh(dpm)_2^+BF_4^-$ and $Rh(dpp)_2^+BF_4^-$ (Table IV.2,chapter IV). Also, for example, the ^1H nmr spectrum of the dpm complex in acetone-d_6 under argon shows two multiplets for the methylene protons; under CO a single multiplet is observed, again showing the labile character of the CO ligand (Table VII.4).

Variable temperature ^{31}P nmr data in $CH_2C\ell_2$-acetone-d_6 for the carbonyl complexes are given in Table VII.5. The ^{31}P nmr spectrum of the dpm complex under argon is a broadened doublet at 25°C (Fig.VII.1a), but becomes a sharp pair of doublets at -50°C (Fig.VII.1b). Under CO, the spectrum is a sharp doublet both at 25°C and -50°C (e.g. Fig. VII.1c). On the other hand, the ^{31}P nmr of the dpp complex under argon is a sharp doublet at 25°C (Fig.VII.2a). Under CO at 25°C, the spectrum is a doublet of doublet of triplets slightly broadened at the base, (Fig.VII.2b) but this sharpens at -50°C (Fig.VII.2c).

For five-coordinate complexes, there are two possible structures (B) and (C). A sharp doublet in the ^{31}P nmr spectrum could indicate all 4P

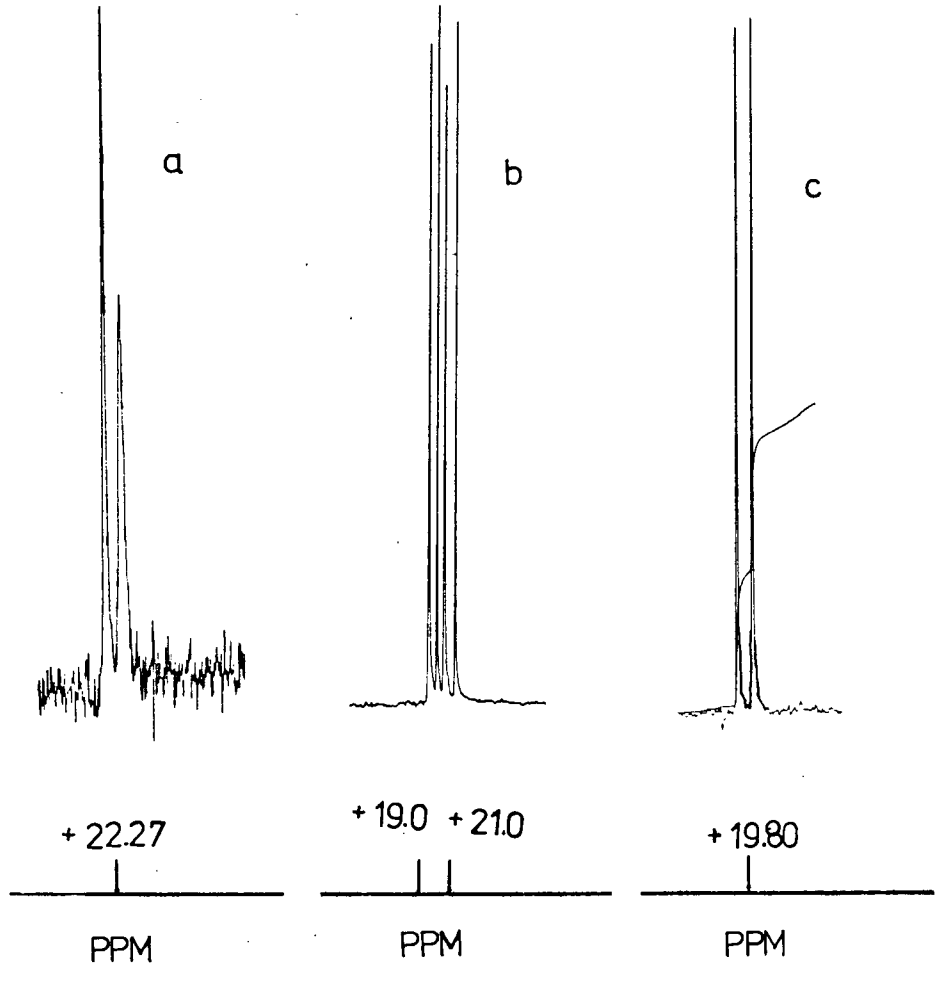

Figure VII.1 ^{31}P nmr spectra of $Rh(dpm)_2CO^+BF_4^-$ in $CH_2C\ell_2$-acetone-d_6 (2/1=V/V)

a. Under Ar at 25°C.

b. Under Ar at -50°C.

c. Under CO at -50°C.

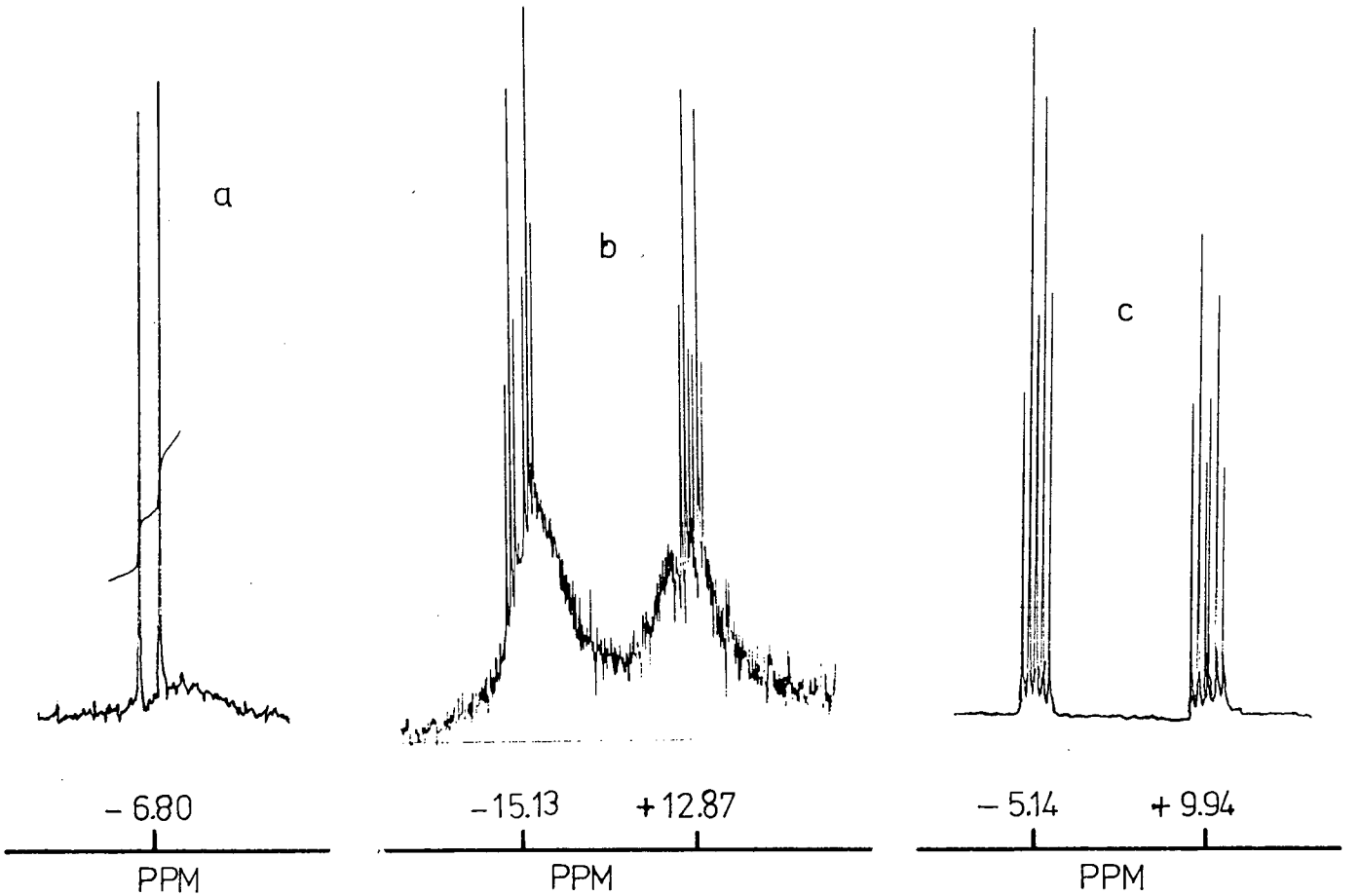

Figure VII.2 ^{31}P nmr spectra of $Rh(dpp)_2CO^+BF_4^-$ in CH_2Cl_2-acetone-d_6 (2/1=V/V)

a. Under Ar at 25°C.

b. Under CO at 25°C.

c. Under CO at -50°C.

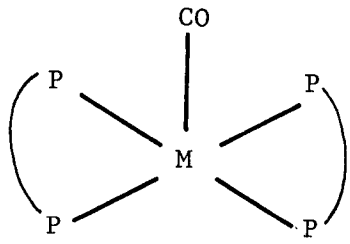

(B) Square pyramid (SP)

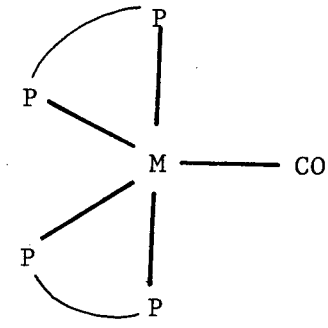

(C) Trigonal bipyramid (TBP)

atoms equivalent corresponding to a SP structure or a fluxional TBP structure, whereas a doublet of doublet of triplets must pertain to a TBP structure (M=Rh). Miller and Caulton[3] have done related ^{31}P nmr studies on analogous iridium complexes; a singlet, measured at -21°C for $[Ir(dpe)_2CO]C\ell$, changed at -93°C to a pattern characteristic of the TBP geometry, consistent with the solid state structure reported earlier[5]. Structure (C) has also been assigned[3] to the $[Ir(dpm)_2CO]C\ell$ complex, which exhibits a singlet in the ^{31}P nmr spectrum even at -92°C. Similarly, $Fe(\overset{\frown}{P}P)(CO)_3$ complexes are non-rigid to the lowest accessible temperatures when $\overset{\frown}{P}P$ = dpm[18] or dpe [19]. A decrease in rearrangement barrier between structures (B) and (C) in the order dpp>dpe>dpm has been suggested.[3]

The ^{31}P nmr spectra of our rhodium systems can readily be explained. The $Rh(dpp)_2CO^+BF_4^-$ complex loses CO readily under argon at 25°C, and the sharp ^{31}P nmr doublet corresponds to that of the $Rh(dpp)_2^+BF_4^-$ species (see Table IV.4). Under CO at 25°C, $Rh(dpp)_2CO^+$ is still fluxional but the ^{31}P nmr pattern at -50°C is consistent with a static TBP structure. With the dpm system under argon at 25°C, the broadened doublet is due to an equilibrium mixture of $Rh(dpm)_2^+$ and $Rh(dpm)_2CO^+$ complexes. At -50°C, the doublet at +20.83 ppm (J_{Rh-P}=115 Hz) is due to the $Rh(dpm)_2^+$ complex (see Table IV.4), and the second doublet can be assigned to the $Rh(dpm)_2CO^+$

complex. The spectrum under CO from 25°C to -50°C shows only the one doublet due to $Rh(dpm)_2CO^+$, variation of the chemical shift with temperature being well known.[20,21] The complex is considered to be fluxional, the TBP structure not being achieved even at -50°C.

VII.3.2 Six-coordinate complexes of rhodium(III)

Addition of O_2 to $Rh(\overset{\frown}{P}P)_2^+BF_4^-$ complexes ($\overset{\frown}{P}P$ = dpm, dpe, and dpp) precipitates analytically pure complexes of the formula $Rh(\overset{\frown}{P}P)_2O_2^+BF_4^-$ via reaction [VII.1]. $Rh(dpe)_2O_2^+$ has been obtained earlier[6] as a PF_6^- salt using a similar method. A solution of $Rh(dpb)_2^+BF_4^-$ slowly absorbs ∿3 moles of O_2 (Table VII.2) but the isolated product is a mixture that has not been separated. The bis(diop) cation reacts extremely slowly with O_2 (Table VII.2) and no product incorporating oxygen could be isolated.

The $Rh(\overset{\frown}{P}P)_2^+BF_4^-$ ($\overset{\frown}{P}P$ = dpm and dpe) complexes do not react with H_2. The nonreactivity of $Rh(dpe)_2^+$ towards H_2 has been reported earlier.[22,23] With $\overset{\frown}{P}P$ = dpp and (+)-diop, the corresponding dihydrides were readily isolated; the carbon analysis is somewhat low for the diop complex (Table VII.1) due to the presence of solvent (CH_2Cl_2) in the crystals. A dihydride complex is also formed with $\overset{\frown}{P}P$ = dpb, but it was not possible to isolate this complex in pure form, the impurity probably being the starting complex. A H_2:Rh stoichiometry of only ∿0.6 was observed in gas-uptake experiments.

Oxidative addition of HCl to $Rh(\overset{\frown}{P}P)_2Cl$ complexes ($\overset{\frown}{P}P$ = dpm, dpe, and dpp) results in the formation of corresponding $HRh(\overset{\frown}{P}P)_2Cl^+Cl^-$ species, but the carbon analyses for all these complexes are low (Table VII.1). The method is similar to the one used for the preparation of analogous iridium(III) complexes where again low carbon analyses were found, and

these were attributed to the presence of some chloride containing species.[10] The same explanation seems likely for the rhodium complexes; a chloride analysis of 8.1% found for $HRh(dpe)_2Cl^+Cl^-$ compares with the theoretical value of 7.30%. The complexes were not further purified even after three recrystallizations. With $\overset{\frown}{P}\,\overset{\frown}{P}$ = dpb and diop, the reaction with HCl appears to give more complex mixtures as judged from ir and other data. In the case of diop, a side reaction involving ligand cleavage by HCl seems likely as inferred from a broad ir band in the 3500-3600 cm^{-1} region ($\nu(H_2O)$ and $\nu(OH)$) and a band at ~1600 cm^{-1} ($\nu(H_2O)$). Such acetal cleavage by acids is well known[24] and has also been observed in some related ruthenium-dios complexes[25], where dios is a sulfoxide analogue of diop ($-PPh_2$ replaced by $-SOCH_3$).

The $HRh(\overset{\frown}{P}\,\overset{\frown}{P})_2Cl^+A^-$ complexes ($\overset{\frown}{P}\,\overset{\frown}{P}$ = dpm, dpe, and dpp; A=BF_4, PF_6, SbF_6) are obtained analytically pure by the treatment of $HRh(\overset{\frown}{P}\,\overset{\frown}{P})_2Cl^+Cl^-$ with AgA, followed by recrystallization from CH_2Cl_2-THF-ether. Details are given only for the BF_4 complexes. The low carbon analysis in the case of the dpp complex is due to the presence of solvent in the crystals (Table VII.1). An alternative method, similar to one developed by Miller and Caulton[3] for preparing $HIr(\overset{\frown}{P}\,\overset{\frown}{P})_2Cl^+A^-$ complexes,was also used, and involved treatment of $Rh(\overset{\frown}{P}\,\overset{\frown}{P})_2Cl$ with aqueous HA (A=BF_4,PF_6), but this gave unidentified complexes containing no hydride ligand.

Following the procedure in a recent report[4] on the preparation of $HIr(\overset{\frown}{P}\,\overset{\frown}{P})_2^{2+}$ ($\overset{\frown}{P}\,\overset{\frown}{P}$ = dpe and dpp) complexes, addition of 2 moles of $AgBF_4$ per mole of $HRh(\overset{\frown}{P}\,\overset{\frown}{P})_2Cl^+Cl^-$ gave only the known $HRh(\overset{\frown}{P}\,\overset{\frown}{P})_2Cl^+BF_4^-$ complexes, as judged from ir and nmr data. No $HRh(\overset{\frown}{P}\,\overset{\frown}{P})_2^{2+}(BF_4^-)_2$ complexes were detected.

Tables VII.1 and VII.3-VII.5 list data for the various rhodium(III)

complexes.

The molar conductivity data (Table VII.1) show that all isolated rhodium(III) complexes are 1:1 electrolytes in nitromethane at 25°C.

The spectroscopic data provide useful information about the structures of these complexes. The O_2 ligand in $Rh(\overset{\frown}{P}\ \overset{\frown}{P})_2O_2^+$ complexes is readily detected in the ir region as a peroxide[15] (Table VII.3), showing that O_2 binds to the metal in a side-on ($M\langle^{O}_{O}$) fashion to give formally six-coordinate rhodium(III) complexes; $Rh(dpe)_2O_2^+PF_6^-$ has been reported earlier[6] but the $\nu(O_2)$ band could not be seen due to PF_6^- bands in the same region. Visible spectra of the dpm and dpp complexes in $CH_2C\ell_2$ under argon at 25°C showed continua (increasing absorption on going from 450-350 nm), whereas the dpe complex showed an absorption maximum at 407 nm, the same as that of $Rh(dpe)_2^+$ (see Table IV.2),: this is consistent with other data (see below) showing that O_2 binding in the dpm and dpp cases is irreversible but is reversible in the dpe case. This reversible O_2 binding by the dpe complex has been observed before.[6] The ^{31}P nmr spectra of these dioxygen complexes (Fig.VII.3) are consistent with structure (D), which is established in the solid state for the $Rh(dpe)_2O_2^+PF_6^-$ complex.[6]

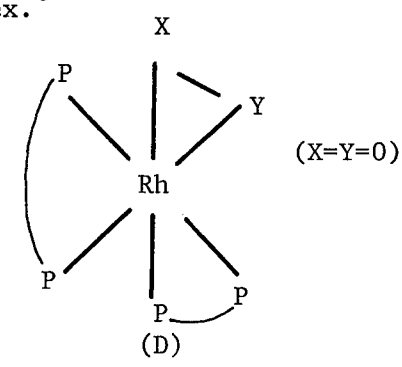

(D)

The dpm and dpp complexes are nonfluxional upto 25°C. The ^{31}P nmr spectrum of the dpe complex[3] is a doublet of doublet of triplets at

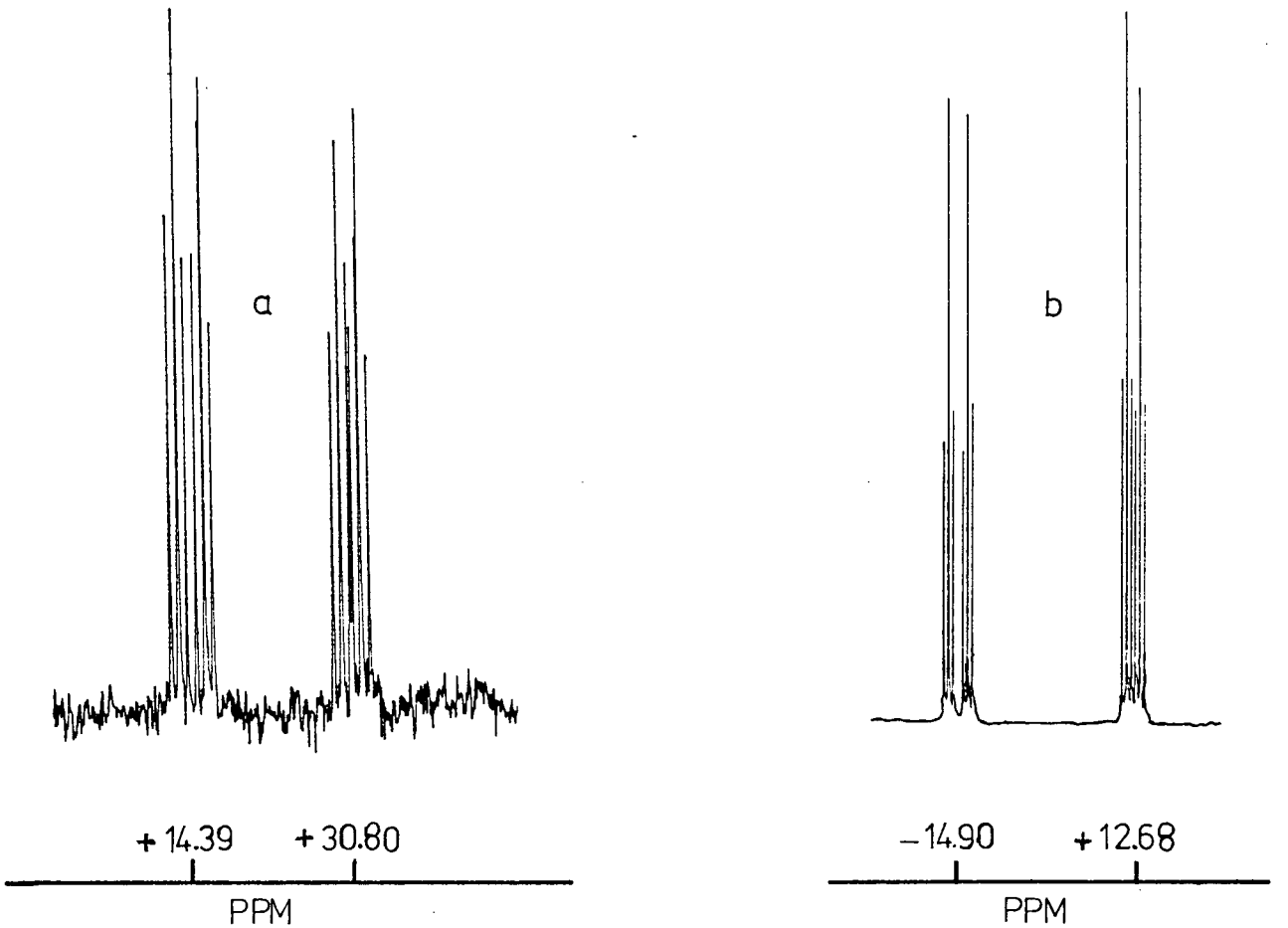

Figure VII.3 ^{31}P nmr spectra in CH_2Cl_2-acetone-d_6 (2/1=V/V) at 25°C of:

a. $Rh(dpm)_2O_2^+BF_4^-$.

b. $Rh(dpp)_2O_2^+BF_4^-$.

-80°C consistent with structure (D); the doublet at 25°C (Table VII.5) is due to $Rh(dpe)_2^+$. The reversible O_2 binding by the dpe complex will be discussed in more detail in section VII.5.

The high-field ^1H nmr at 25°C for the $Rh(\overset{\frown}{P}P)_2H_2^+BF_4^-$ ($\overset{\frown}{P}P$ = dpp, diop) complexes is a pair of multiplets (Fig.VII.4, Table VII.3), suggesting different environments for the two hydride ligands. The same nmr pattern has been reported for $Rh[P(CH_3)_3]_4H_2^+$ at 25°C and was attributed to a cis-dihydride.[26] Infrared data are consistent with the presence of terminal hydrides (Table VII.3). The $^{31}P\{^1H\}$ nmr spectra of these complexes show two resonances (Fig.VII.5) as expected for complexes with a cis configuration. The resonance at lower field is attributed to the 2P atoms trans to each other whereas the resonance at higher field is due to the P atoms trans to hydrides; these assignments are based on literature[26] data. A variable temperature study on the $Rh(diop)_2H_2^+$ complex suggests that the resonance at higher field is temperature dependent whereas the lower field resonance is independent of temperature (Fig.VII.5). The presence of two resonances at all temperatures rules out the possibility of cis-trans rearrangement that have been observed in complexes of the type ML_4H_2 (M=Fe,Ru:L=phosphine, phosphite etc.)[27,28]. Thus the temperature dependence of one set of resonances can be attributed to mutual exchange of the 2P atoms trans to hydrides. This is not unreasonable because a phosphorus ligand trans to a hydride ligand is not in a particularly stable environment, as judged by the inability of several rhodium(I)-mono(diphosphine) complexes to add H_2.[13,29]

The $Rh(dpp)_2H_2^+BF_4^-$ complex loses hydrogen immediately in solution as seen by changes in the visible spectrum. The reversible reaction of H_2 with $Rh(diop)_2^+$ has already been described in detail in chapter VI.

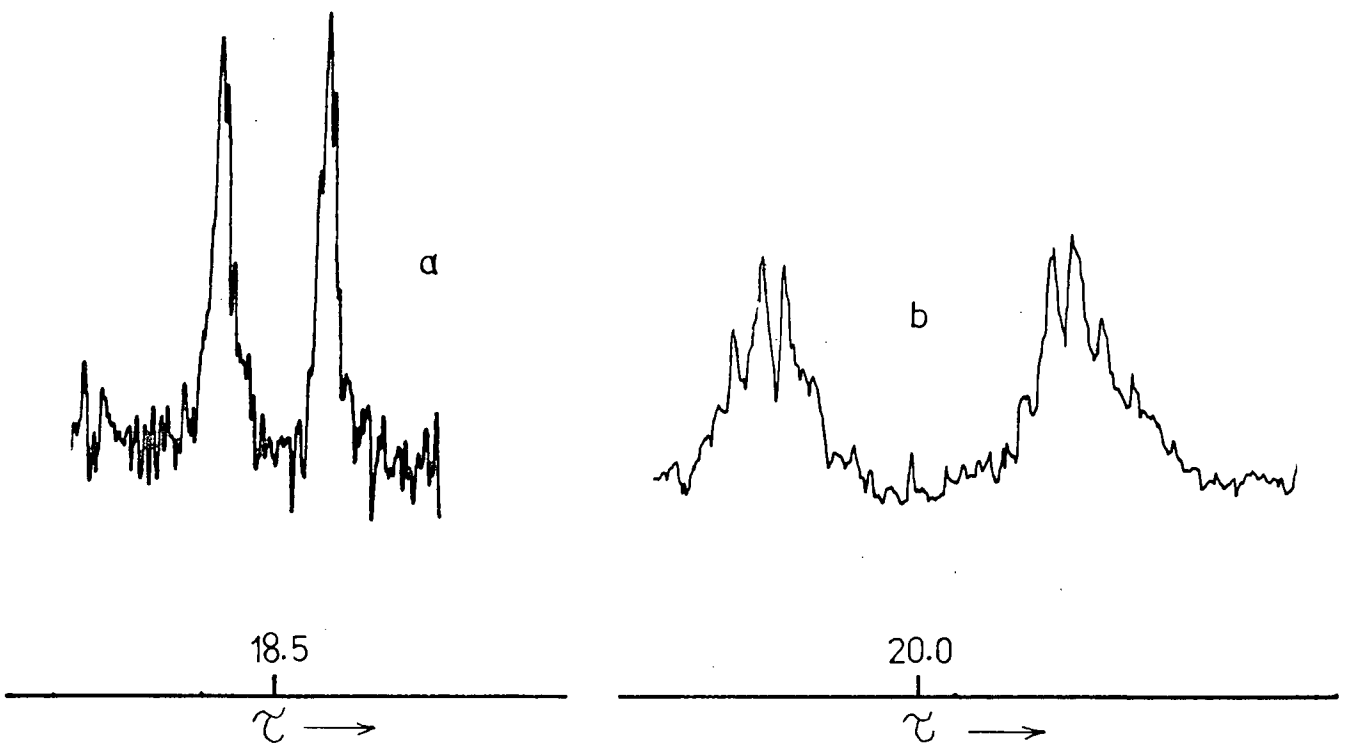

Figure VII.4 High-field ^{1}H nmr spectra at 25°C (under H_2) of: a. $Rh(dpp)_2H_2^+BF_4^-$ in acetone-d_6.
b. $Rh(diop)_2H_2^+BF_4^-$ in $CDC\ell_3$.

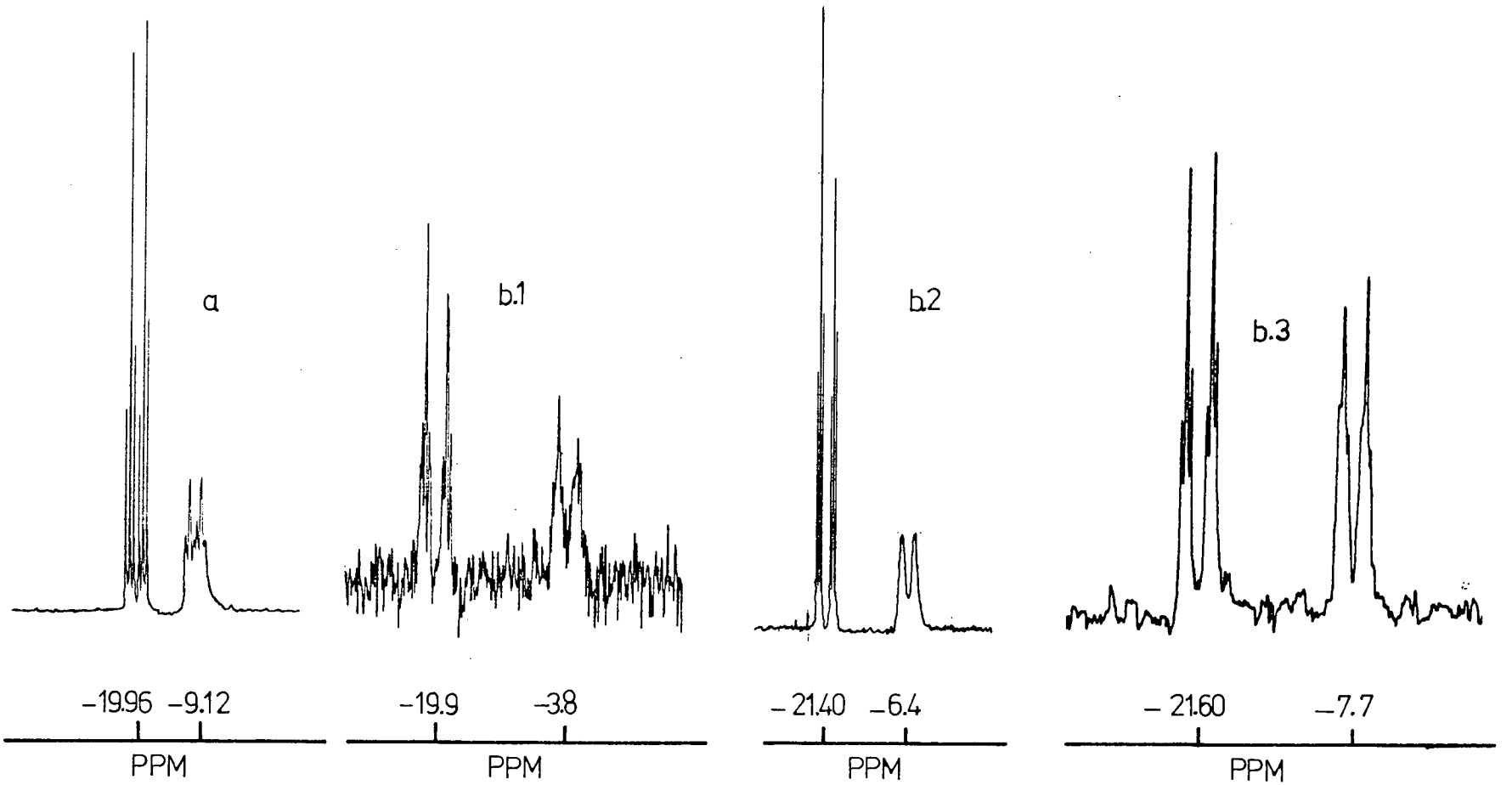

Figure VII.5 $^{31}P\{^{1}H\}$ nmr spectra in $CH_2C\ell_2$-acetone-d_6 (2/1=V/V) of:

(a) $Rh(dpp)_2H_2^+BF_4^-$ at -50°C.

(b) $Rh(diop)_2H_2^+BF_4^-$ at (1) 25°C, (2) -50°C, and (3) -85°C.

The hydride ligand in the $HRh(P\frown P)_2C\ell^+A^-$ (A=Cℓ,BF_4) complexes is readily detected by ir (Table VII.3), as well as by high-field ^1H nmr at 25°C (Figure VII.6, Table VII.3). The dpe and dpp complexes are stable in solution, but lose HCℓ in basic solvents (e.g. DMA) to give $Rh(dpe)_2^+$ and $Rh(dpp)_2^+$, respectively (readily identified from visible bands on comparison with the known values given in Table IV.2). The dpm complex is different and does not lose HCℓ even in DMA.

The $^{31}P\{^1H\}$ nmr spectra of the $HRh(P\frown P)_2C\ell^+$ complexes are sharp doublets at 25°C (Figs.VII.7 and VII.8). These doublets could be due to 4 equivalent P atoms coupling to rhodium in a trans structure (E).

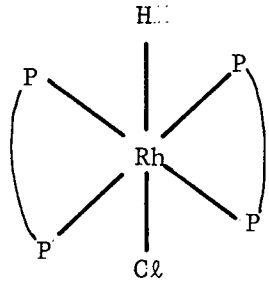

(E) trans

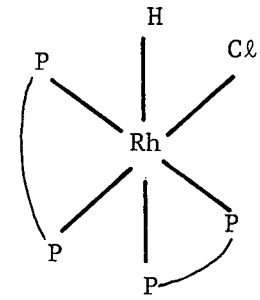

(F) cis

However, the $^{31}P\{^1H\}$ nmr spectrum of the dpp complex is temperature dependent (Table VII.5) and approximates to a doublet of doublet of triplets at -85°C (Fig. VII.8) characteristic of the cis geometry (this results from the H and Cℓ site exchange being too fast even at -85°C to be distinguishable[3]). The spectra of the dpm and dpe complexes do not show any temperature dependence (Figure VII.7), and this could be due to fluxional behaviour even at -60°C, as assumed for the corresponding iridium complexes.[3] Some interesting data have been obtained very recently on a related six-coordinate ruthenium(II) complex, $HRuC\ell(diop)_2$.[30,31] The $^{31}P\{^1H\}$ and ^1H nmr spectra of this complex were interpreted in terms of a cis geometry[30], but an x-ray crystal structure

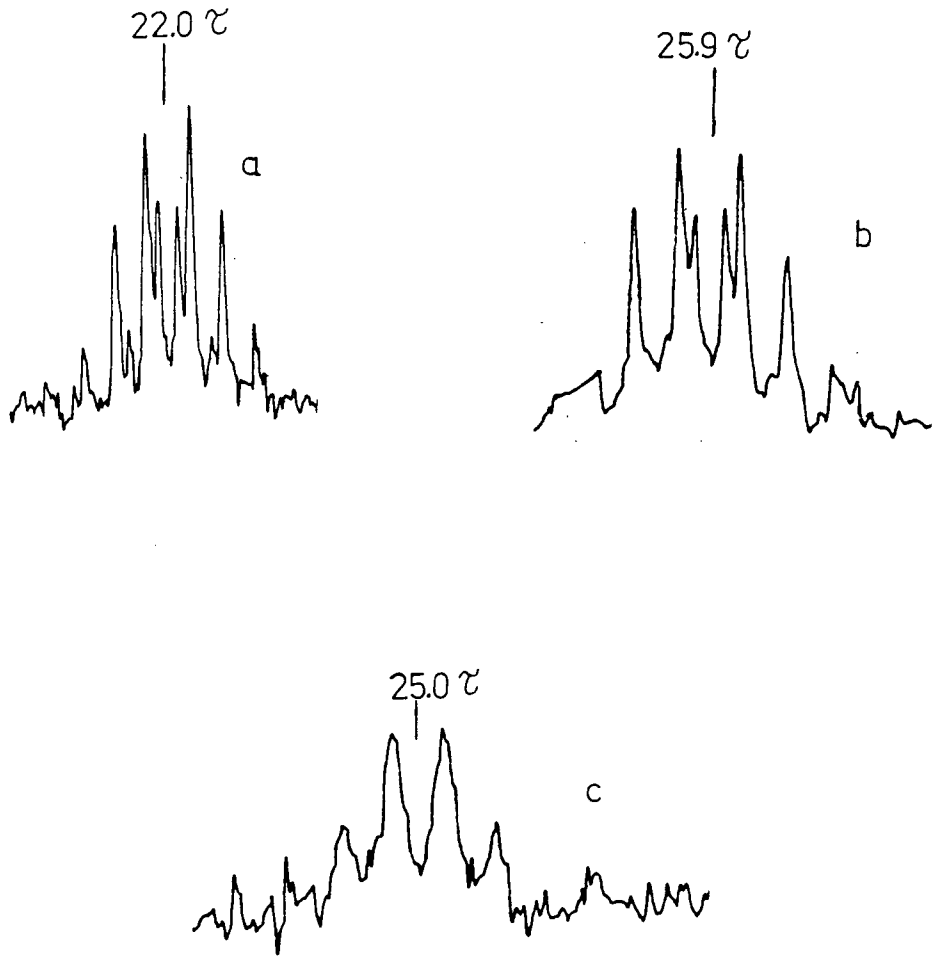

Figure VII.6 High-field ^{1}H nmr spectra of:

(a) $HRh(dpm)_2C\ell^+C\ell^-$,

(b) $HRh(dpe)_2C\ell^+C\ell^-$, and

(c) $HRh(dpp)_2C\ell^+C\ell^-$ in $CDC\ell_3$ at 25°C.

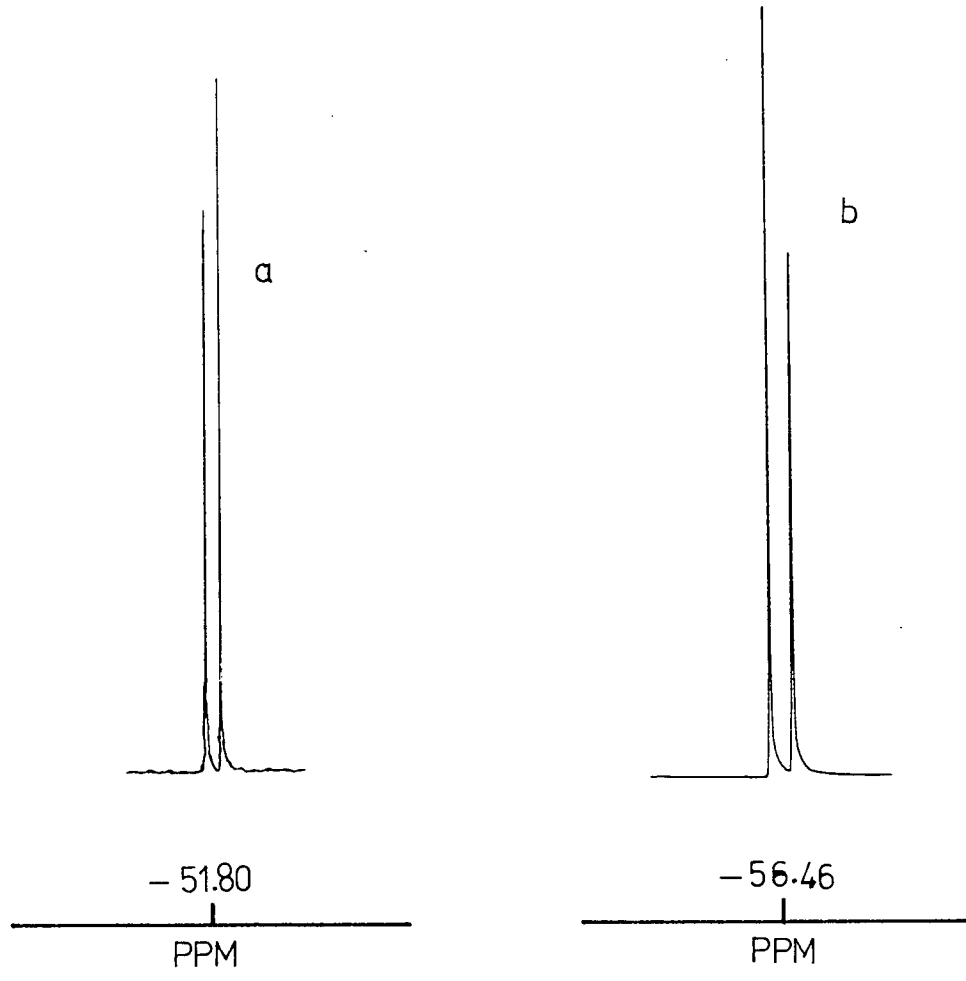

Figure VII.7 $^{31}P\{^{1}H\}$ nmr spectra of $HRh(dpe)_2Cl^+Cl^-$ in CH_2Cl_2-acetone-d_6 (2/1=V/V) at a. 25°C and b. -60°C.

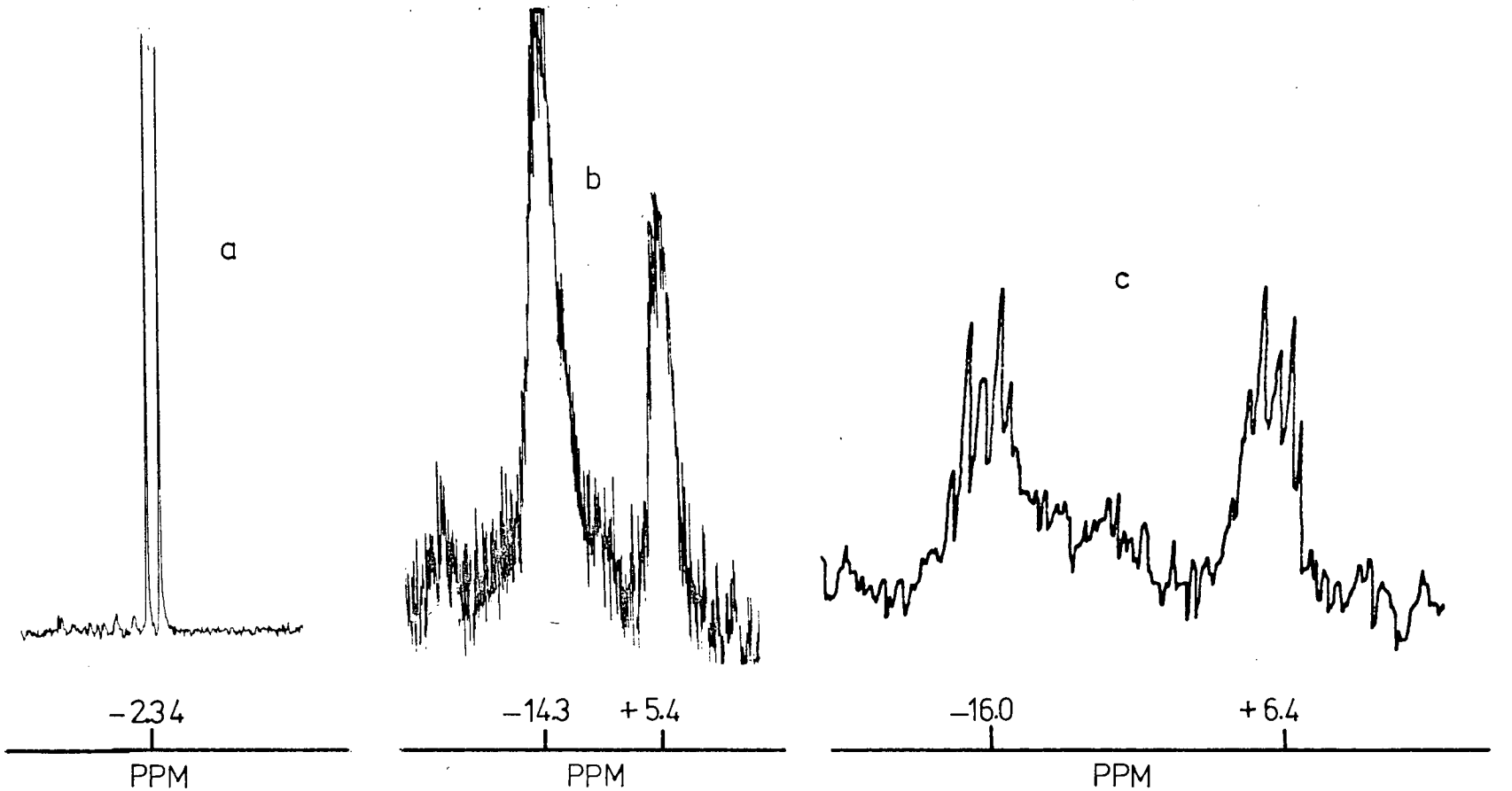

Figure VII.8 $^{31}P\{^{1}H\}$nmr spectra of $HRh(dpp)_2C\ell^+C\ell^-$ in $CH_2C\ell_2$-acetone-d_6 (2/1=V/V) at: a. 25°C, b. -50°C, and c. -85°C.

determination[31] shows this complex to have trans geometry. The inequivalence of the P atoms arises from a bending of 2P atoms toward the hydrogen, and the other two toward the chlorine: the dioxolane ring of the diop fixes the configuration of the seven-membered chelate ring and the geometry distorts to minimize phenyl-phenyl interactions. Without the dioxolane ring (i.e. in the corresponding dpb complex), the four carbon backbone can twist and can lead to pseudo C_{4v} symmetry, and the hydride did appear as a quintet.[31] Thus it is not possible to assign unequivocally structures to the rhodium dpm and dpe complexes solely on the basis of the ^{31}P nmr data.

VII.4 Attempted use of $HRh(\widehat{P\ P})_2C\ell^+A^-$ complexes in catalytic hydrogenation

An earlier claim that $HRh(dpe)_2C\ell^+C\ell^-$[7,8] is among the most active catalysts known for the hydrogenation of olefins prompted us to test the catalytic activity of the $HRh(\widehat{P\ P})_2C\ell^+A^-$ ($\widehat{P\ P}$ = dpm, dpe, dpp; A=Cℓ, BF_4) complexes reported in this chapter. Thus under conditions ([Rh]=2×10^{-3}M, [substrate]=0.1M, 30°C, 2-methoxyethanol=5 ml, P_{H_2}=1 atm) similar to those used in the literature reports[7,8], no hydrogenation of cyclohexene or itaconic acid was observed. The complexes were found to be inactive even at 60°C.

VII.5 Preliminary kinetic studies

From the limited stopped-flow data at 30°C on the addition of H_2, O_2, and CO to the $Rh(\widehat{P\ P})_2^+BF_4^-$ complexes (Table VII.6), no obvious correlation between the rate of addition and the size of the diphosphine is suggested. For the dpp complex, the ease of addition decreases in the order $CO>H_2>O_2$. The rates are independent of the nature of solvent.

Since the pseudo first-order rate constant for the reaction of O_2 with

Table VII.6 Pseudo first-order rate constant[a] k at 30°C for the reaction $Rh(P\frown P)_2^+BF_4^- + XY \xrightarrow{k} Rh(P\frown P)_2XY^+BF_4^-$

P⌒P	XY	k x 10^3, s^{-1}	Final[C][b] x 10^4, M
dpm	O_2	943	0.93
"	CO	—[c]	1.16
dpp	H_2	768	1.23
"	"	720[d,e]	1.23
"	O_2	3.9	1.22
"	"	3.7[d]	1.34
"	"	2.9[d,e]	1.34
"	CO	14690	1.22
"	"	14120[d]	1.16
dpb	H_2	13	2.45
diop	"	—[f]	1.05

a In CH_2Cl_2; P_t=1.0 atm.

b Final [C] = $\frac{\text{Initial[Rh]}}{2}$; final P_{H_2} = 280 mm.

c Too fast.

d In methanol; final P_{gas} = 320 mm.

e Final P_{gas} = 35 mm.

f Reaction complicated; see Chapter VI for details.

g For P⌒P=dpe and XY=O_2, see Table VII.7.

the dpp complex does not vary linearly with the gas pressure (Table VII.6), the mechanism of these addition reactions does not seem to be a simple one-step reaction [VII.2]. The fractional order dependence on O_2 can probably be explained by a scheme similar to that suggested for

$$Rh(\overset{\frown}{P}P)_2^+ + XY \longrightarrow Rh(\overset{\frown}{P}P)_2XY^+ \qquad [VII.2]$$

the reaction of H_2 with the $Rh(diop)_2^+$ cation (section VI.4.1). However, the k_3'' step for the O_2 reaction must now be rapid since only one overall pseudo first-order rate process is observed. More data are needed to substantiate such a mechanism.

The reversible reaction of O_2 with $Rh(dpe)_2^+BF_4^-$ was studied in more detail using visible spectroscopy. Thus the evolution of O_2 from $Rh(dpe)_2O_2^+BF_4^-$ in methanol at 30°C under argon gave spectral changes that showed an isosbestic point at 372 nm, and the final spectrum corresponded to that of the $Rh(dpe)_2^+$ species (Fig.VII.9(A)). The changes analyzed for a first-order reaction (Fig.VII.9(B)) to give k_{-1}(Table VII.7) which was found to be independent of the nature of solvent. Visible studies on the reaction of O_2 with $Rh(dpe)_2^+BF_4^-$ in methanol at 30°C,which does not go to completion,yield k_e,the sum of the pseudo first-order forward rate constant and the deoxygenation rate constant (Fig.VII.10 (A and B); Table VII.7). K_1 was calculated from the rate constant data to be $\sim$0.6±0.1 atm^{-1}. The value of k_e determined at 300 mm of O_2 is approximate due to the small spectral changes observed. (If the forward reaction were first-order in O_2, the k_e value at 300 mm should have been about 3.4 s^{-1}). K_1 was also estimated directly (e.g. from the spectral data in Fig.VII. 10.A) using equation [VII.3] to be $\sim$0.4 atm^{-1} both at 700 mm and 300 mm O_2

$$K_1 = \frac{[Rh(dpe)_2O_2^+]}{[Rh(dpe)_2^+][O_2]} \qquad [VII.3]$$

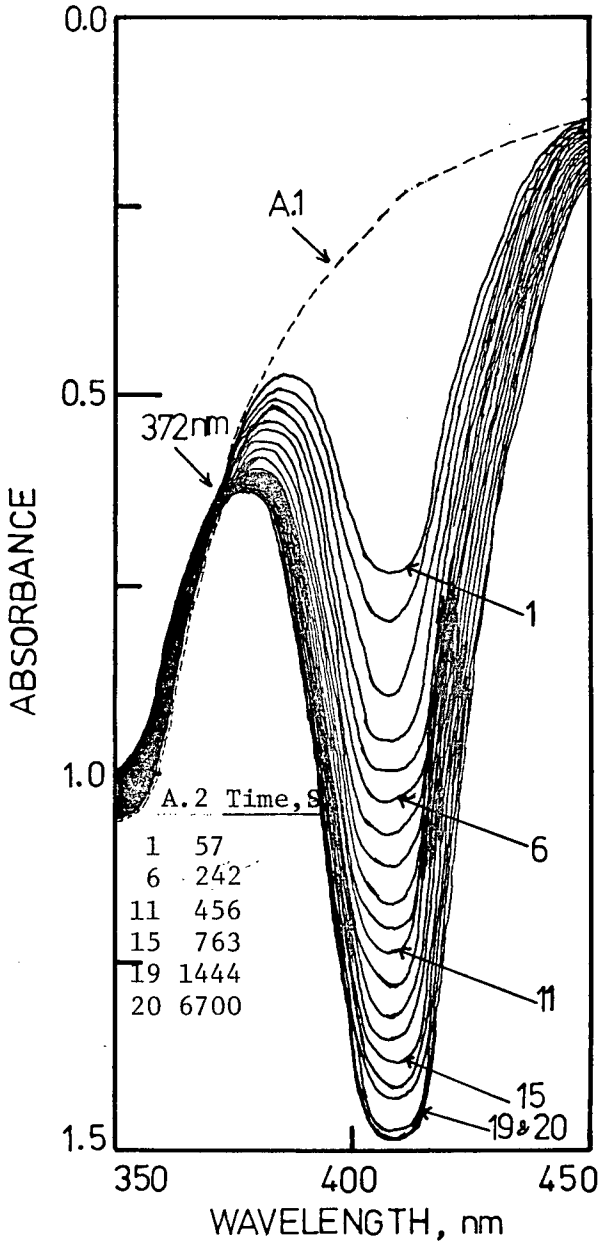

Figure VII.9(A) Spectral changes obtained for 0_2 loss from $Rh(dpe)_2O_2^+BF_4^-$ ($3.7x10^{-4}M$) in methanol at 30°C (solution under argon). A.1 represents the spectrum of the $Rh(dpe)_2O_2^+BF_4^-$ complex.

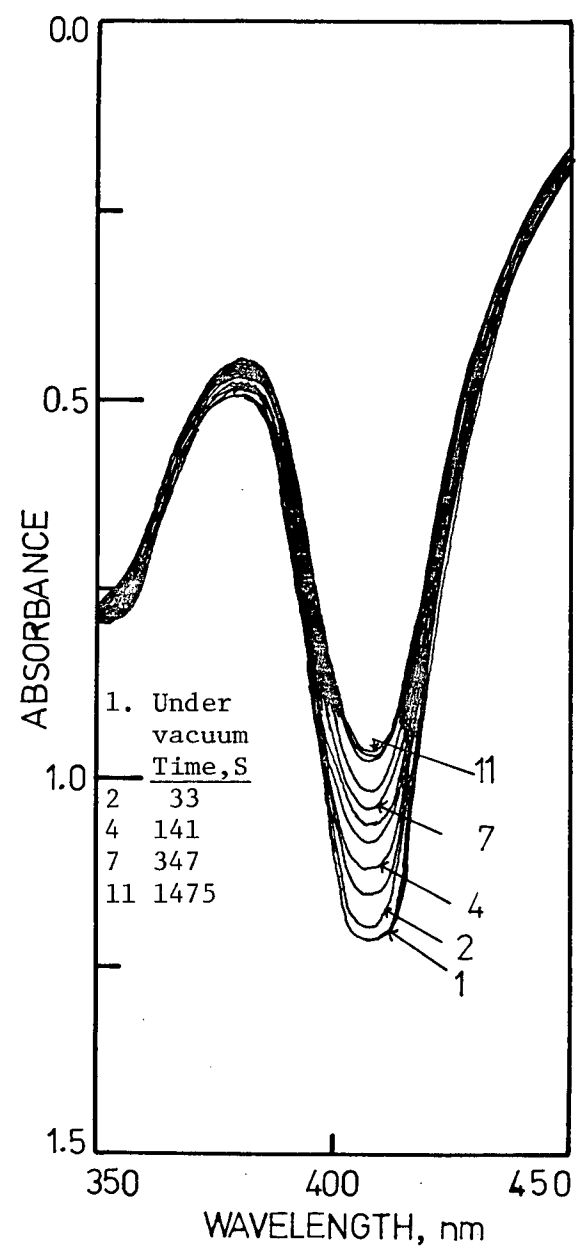

Figure VII.10(A) Spectral changes obtained at 30°C on adding 0_2 (1 atm) to solutions of $Rh(dpe)_2^+BF_4^-$ ($2.9x10^{-4}M$) in methanol.

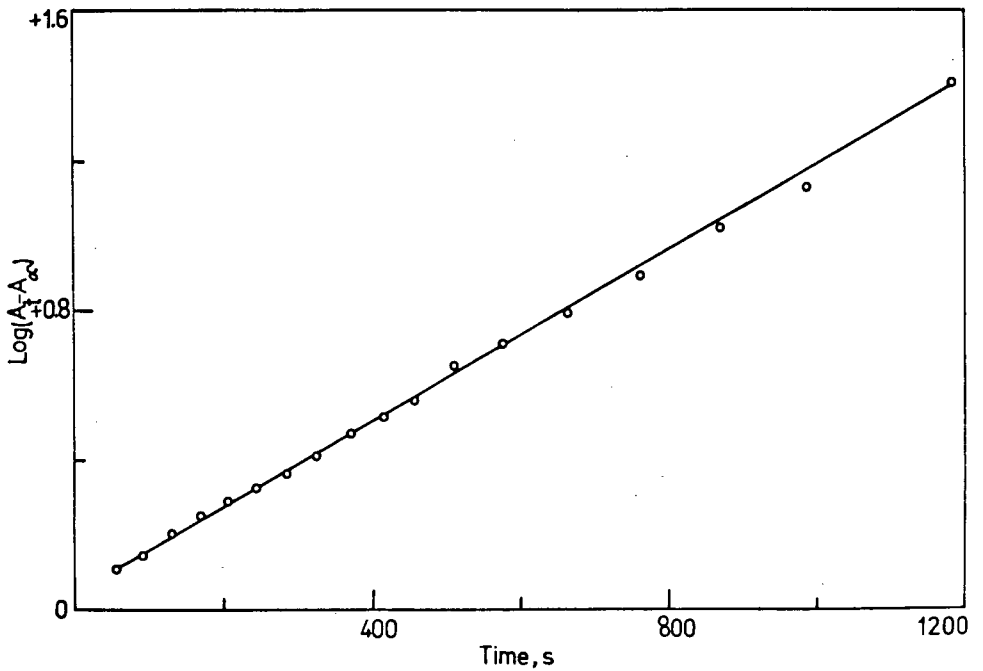

Figure VII. 9(B) Plot of $\log(A_t - A_\infty)$ vs time for spectral changes in Fig.VII.9(A).

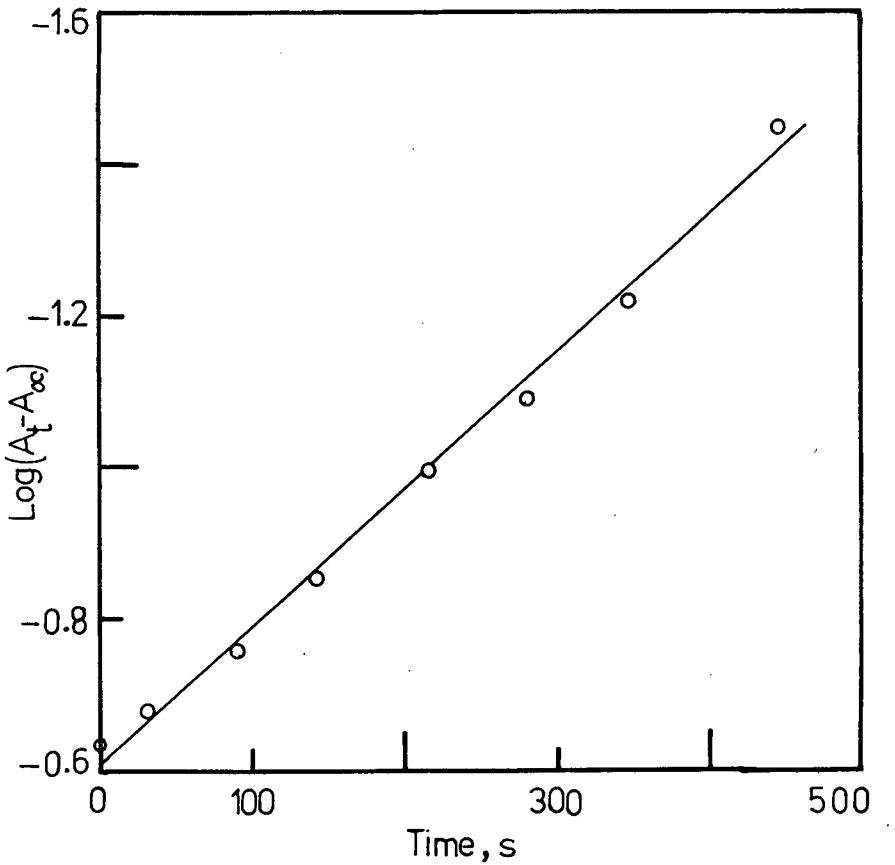

Figure VII.10(B) Plot of $\log(A_t - A_\infty)$ vs time for spectral changes in Fig. VII.10(A).

Table VII.7 Data at 30°C for the determination of equilibrium constant K_1 for the reaction

$$Rh(dpe)_2^+BF_4^- + O_2 \underset{}{\overset{K_1}{\rightleftharpoons}} Rh(dpe)_2O_2^+BF_4^-$$

$[C]\times10^4$, M	P_{O_2}, mm	Solvent	$k_{-1}\times10^3$, s^{-1}	k_e[a]$\times10^3$, s^{-1}	K_1, atm^{-1}
3.73	-	DMA	2.64	-	-
3.63	-	MeOH	2.65	-	-
2.90	700[b]	MeOH	-	4.2	∿0.6(±0.1)
3.04	300[b]	MeOH	-	2.7[c]	-

[a] $k_e = k_1' + k_{-1}$, $k_1' = k_1[O_2]$, $K_1 = k_1/k_{-1}$

[b] Error ±50 mm.

[c] Value in large error.

pressures. The two values are in reasonable agreement with the kinetically determined value of $\sim 0.6 \pm 0.1$ atm^{-1}. For the closely related reaction of $[Rh(2\text{=phos})_2]A$ (2=phos= cis-ϕ_2P-(CH=CH)-$P\phi_2$; A=BPh_4) with O_2 in chlorobenzene at 25°C, K_1 has been estimated previously[11] to be 350 M^{-1}. Using solubility data for O_2 in methanol ($\sim 5 \times 10^{-3}$ M atm^{-1} at 20°C[32]) yields $K_1 \gtrsim 100$ M^{-1} for the dpe system, quite comparable to the value for the 2=phos system.

CHAPTER VIII

GENERAL CONCLUSIONS, AND RECOMMENDATIONS FOR FUTURE WORK

The aim of the work described in this thesis was to study rhodium catalysts incorporating bis(ditertiaryphosphine) ligands, including chiral ones, and their potential as catalysts, particularly for hydrogenation. Several important findings are summarized below, together with some suggestions for further study.

Bis(ditertiaryphosphine)-rhodium(I) complexes have been synthesized by a simple method starting with the cyclooctene dimer $[RhCl(C_8H_{14})_2]_2$ and adding the appropriate ditertiaryphosphine:

$$[RhCl(C_8H_{14})_2]_2 + 4\ P\frown P \longrightarrow 2\ Rh(P\frown P)_2Cl + 2C_8H_{14} \qquad [VIII.1]$$

($P\frown P = \phi_2P(CH_2)_nP\phi_2$ (n=1-4) and (+)-diop)

Cationic complexes were then prepared by adding AgA(A=BF_4,PF_6,SbF_6) to the chloro complexes, while use of borohydride yielded some corresponding hydrido complexes. Spectroscopic studies revealed that the dpe and dpp $Rh(P\frown P)_2Cl$ complexes contained an ionic chloride, while the analogous dpm, dpb, and diop complexes were neutral in non-polar solvents but ionic in polar solvents. High molar conductivity values in nitromethane for the five-coordinate dpe and dpp hydrides (approaching that for 1:1 electrolyte) suggest a reaction with the nitroalkane solvent. There are only a few other complexes that catalyze the hydrogen reduction of nitroalkanes to amines (see ref. 30, chapter IV), and further investigation into this possibility seems worthwhile.

The solution structures of the chloro, hydrido, and cationic complexes were studied using variable ^{31}P nmr spectroscopy. ^{1}H nmr data showed a

solvent-dependent deshielding of the ortho protons (as compared to meta and para protons) of the phenyl group in some of the complexes. A 'virtual coupling' of the ligand CH_2 protons with the rhodium in the $Rh(dpm)_2^+$ complex was observed, the P atom of the ligand also showing an unusual highfield shift on coordination to rhodium.

Preliminary kinetic data for the catalytic hydrogenation of IA showed that the activity increased with increasing chain length of the diphosphine, and the cationic and hydrido complexes were generally more active than the corresponding chloro complexes.

Kinetic and spectroscopic studies on the $HRh(diop)_2$-catalyzed hydrogenation of IA‡ has revealed the importance of a species HRh(diop)(diop*), containing a monodentate diop ligand. The hydrogenation mechanism then follows the fairly common 'unsaturate' route via alkyl formation and subsequent reaction with H_2 (equations [VIII.2]-[VIII.4]). Some side reactions

$$HRh(diop)_2 \rightleftharpoons HRh(diop)(diop^*) \qquad [VIII.2]$$

$$HRh(diop)(diop^*) + olefin \rightleftharpoons Rh(diop)(diop^*)(alkyl) \qquad [VIII.3]$$

$$Rh(diop)(diop^*)(alkyl) + H_2 \longrightarrow HRh(diop)(diop^*) + S.P. \qquad [VIII.4]$$

in this system involving protonation of the catalyst by the acid substrate to give $Rh(diop)_2^+$ and H_2, and protonation of an intermediate alkyl by the alcohol solvent to give $Rh(diop)_2^+$ and saturated product, were also indicated. The non-acidic substrate styrene was hydrogenated using $HRh(diop)_2/H_2$ via the same unsaturate route, but as expected, acid decomposition of the catalyst was no longer observed.

‡ Study of this particular itaconic acid system constituted the bulk of my Master Thesis.

Several bis(diop) - rhodium complexes were used effectively for the asymmetric hydrogenation of some prochiral substrates, optical yields of >90% being obtained in the hydrogenation of N-acylaminoacrylic acids. In hydrogenation of IA, the optical yield of ∿50% is the highest yet reported. The results indicated that steric factors at the olefinic bond as well as coordination of the -NHCOR group to rhodium through the >C=O moiety were important, whereas the participation of the acid function of substrates did not seem important, at least in terms of hydrogenation rates. The rates were slower in the more strongly coordinating DMA, compared to n-butanol-toluene mixtures.

The solvent medium generally did not greatly affect the degree of asymmetric induction using the $HRh[(+)\text{-diop}]_2$ or $Rh[(+)\text{-diop}]_2^+$ complexes, but a reversal of configuration was noted when $Rh[(+)\text{-diop}]_2C\ell$ was used as a catalyst in DMA or in n-butanol-toluene mixtures. The solution chemistry associated with the chloride complex is complicated, and a more detailed study on this complex should be undertaken. An unusual increase in optical yield with increasing temperature for the hydrogenation of IA using $HRh[(+)\text{-diop}]_2$ or $Rh[(+)\text{-diop}]_2^+$ is possibly due to a different mechanism being operative at the different temperatures (see below).

Asymmetric hydrogenation of several substrates was effected using the $[RhC\ell(CO)(+)\text{-diop}]_2$ dimer but this complex is far less active than the bis(diop) systems, or the mono(diop)-rhodium complexes studied by other workers.

The $Rh(diop)_2^+$-catalyzed hydrogenation of IA was studied in detail. The kinetic data in n-butanol-toluene (2:1) at 15°C suggested that the hydrogenation proceeded mainly via the 'hydride' route outlined in equations [VIII.5]-[VIII.7]:

$$Rh(diop)_2^+ + H_2 \rightleftharpoons Rh(diop)_2H_2^+ \qquad [VIII.5]$$

$$Rh(diop)_2H_2^+ + IA \rightleftharpoons Rh(diop)(diop^*)(H)_2(IA)^+ \qquad [VIII.6]$$

$$Rh(diop)(diop^*)(H)_2(IA)^+ \longrightarrow Rh(diop)_2^+ + S.P. \qquad [VIII.7]$$

A complete inhibition of the catalytic hydrogenation in the presence of added diop (diop:Rh>0.2) is difficult to account for, but it has been tentatively attributed to formation of a polymeric species (equation [VIII.8]):

$$nRh(diop)_2H_2^+ + diop \longrightarrow [Rh(diop)(diop^*)H_2^+]_n \qquad [VIII.8]$$

Efforts should be made to substantiate this, and also in view of the unusual increase of asymmetric induction with increasing temperature for the IA system, the mechanism should be reinvestigated at the higher temperature.

The reaction of $Rh(diop)_2^+$ with H_2 alone (Reaction VIII.5) was studied in detail. Based on the stopped-flow kinetics, and other spectroscopic data, the series of consecutive reactions outlined in equation [VIII.9] were postulated:

$$Rh(diop)_2^+ + S \rightleftharpoons Rh(diop)(diop^*)S^+ \xrightarrow{H_2} Rh(diop)(diop^*)(H)_2S^+ \xrightarrow{-S} Rh(diop)_2H_2^+ \qquad [VIII.9]$$

The reverse dehydrogenation reaction showed a simple first-order kinetic dependence on the $Rh(diop)_2H_2^+$ species. The kinetics may however be deceptively simple in terms of the mechanism, if the reverse of equation [VIII.9] is followed. These reactions and the role of solvated species is critically important for a better understanding of asymmetric hydrogenation, and require much more detailed study using a wider range of concentrations, temperatures, solvents, and with the other chelating phosphines.

More generally, the reactions of $[Rh(\overset{\frown}{P}\,\overset{\frown}{P})_2]A$ complexes (A=Cℓ,BF_4) with CO, O_2, H_2, and HCℓ(g),have yielded isolable complexes of the type $[Rh(\overset{\frown}{P}\,\overset{\frown}{P})_2XY]A$ ($\overset{\frown}{P}\,\overset{\frown}{P}$ = dpm, dpp; XY=CO, $\overset{\frown}{P}\,\overset{\frown}{P}$ = dpm, dpe, dpp; XY=O_2, $\overset{\frown}{P}\,\overset{\frown}{P}$=dpp, (+)-diop; XY=$H_2$, and $\overset{\frown}{P}\,\overset{\frown}{P}$=dpm, dpe, dpp; XY=HCℓ). Variable temperature ^{31}P nmr data suggested cis geometries with two sets of equivalent P atoms for the formally d^6 six-coordinate dioxygen and dihydrido complexes. The HCℓ complexes were more fluxional and cis structures could be assigned only to the dpp system; the dpm and dpe complexes indicated equivalent P atoms (possibly trans structures) even at -60°C. A crystal structure of one of these dpm or dpe complexes would be extremely useful. For the five-coordinate CO complexes, a TBP structure was assigned to the dpp complex; the dpm complex was fluxional even at -60°C.

Preliminary stopped-flow data on the addition of CO, O_2, and H_2 to the $Rh(\overset{\frown}{P}\,\overset{\frown}{P})_2^+$ complexes have been obtained. In the dpp case, the rate increased in the order $CO>H_2>O_2$, but some of these reactions may involve multi-stage processes (cf. equation [VIII.9]) and these overall correlations have little value, unless some rate constants for the individual forward and/or reverse reaction steps can be elucidated. Such data are invaluable in terms of the catalytic potential of such "small gas molecule" systems (e.g. catalytic decarbonylation by the $Rh(dpe)_2Cℓ$ and $Rh(dpp)_2Cℓ$ complexes has very recently been reported (see ref. 9b, chapter IV)), and more detailed kinetic studies on these systems are already in progress in this laboratory.

REFERENCES

CHAPTER I

1. L. Pasteur, Ann. Chim. Phys. [3] 24, 442 (1848).
2. R. J. Block, Chem. Rev., 38, 501 (1946).
3. C. W. Huffman and W. G. Shelly, Chem. Rev., 63, 625 (1963); E. N. Safonova and V. M. Belikov, Russ. Chem. Rev., 36, 375 (1967).
4. W. R. Brode and R. W. Van Dolah, Ind. Eng. Chem., 39, 1157 (1947).
5. S. Akabori, S. Sakurai, Y. Izumi, and Y. Fujii, Nature, 178, 323 (1956).
6. S. Akabori, Y. Izumi, Y. Fujii, and S. Sakurai, J. Chem. Soc. Jap. Pure Chem. Sec. (Nippon Kagaku Zasshi), 77, 1374 (1956); S. Akabori, Y. Izumi, and Y. Fujii, ibid., 78, 886 (1957).
7. Y. Izumi, Angew. Chem. Int. Edit., 10, 871 (1971).
8. Y. Orito, S. Niwa, and S. Imai, Chem. Lett., 1131 (1977).
9. N. Izumiya, S. Lee, T. Kanmera, and H. Aoyagi, J. Am. Chem. Soc., 99, 8346 (1977).
10. J. F. Young, J. A. Osborn, F. H. Jardine, and G. Wilkinson, Chem. Comm., 131 (1965).
11. F. A. Jardine, J. A. Osborn, G. Wilkinson, and J. F. Young, Chem. Ind. (Lond.), 560 (1965).
12. B. R. James, 'Homogeneous Hydrogenation', John Wiley and Sons, New York, 1973.
13. B. Bogdanovic, Angew. Chem. Int. Edit., 12, 954 (1973).
14. L. Marko and B. Heil, Catal. Rev., 8, 269 (1973).
15. H. B. Kagan, Pure Appl. Chem., 43, 401 (1975).
16. J. D. Morrison, W. F. Masler, and M. K. Newberg, Adv. Catal., 25, 81 (1976); J. D. Morrison, W. F. Masler, and S. Hathaway, in

"Catalysis in Organic Syntheses 1976" (P. N. Rylander and H. Greenfield, eds.), Academic Press, New York, 1976, p.203.

17. B. R. James, Adv. Organomet. Chem., 17, 319(1979).

18. B. D. Vineyard, W. S. Knowles, M. J. Sabacky, G. L. Bachman, and D. J. Weinkauff, J. Am. Chem. Soc., 99, 5946 (1977) and references therein.

19. M. D. Fryzuk and B. Bosnich, J. Am. Chem. Soc., 99, 6262 (1977).

20. W. R. Cullen and E.-S. Yeh, J. Organomet. Chem., 139, C13 (1977).

21. T. P. Dang and H. B. Kagan, Chem. Comm., 481 (1971).

22. H. B. Kagan and T. P. Dang, J. Am. Chem. Soc., 94, 6429 (1972).

23. W. Dumont, J. C. Poulin, T. P. Dang, and H. B. Kagan, J. Am. Chem. Soc., 95, 8295 (1973).

24. H. B. Kagan, N. Langlois, and T. P. Dang, J. Organomet. Chem., 90, 353 (1975).

25. T. P. Dang, J. C. Poulin, and H. B. Kagan, J. Organomet. Chem., 91, 105 (1975).

26. D. Sinou and H. B. Kagan, J. Organomet. Chem., 114, 325 (1976).

27. G. Gelbard and H. B. Kagan, Tetrahedron, 32, 233 (1976).

28. Y. Chauvin, D. Commereuc, and R. Stern, J. Organomet. Chem., 146, 311 (1978).

29. W. R. Cullen, A. Fenster, and B. R. James, Inorg. Nucl. Chem. Lett., 10, 167 (1974).

30. Y. Chevailier, Docteur-Ingenieur Thesis, Paris, 1970; through reference 22.

31. D. Mahajan, M.Sc. Dissertation, U.B.C., Vancouver, B.C., 1976; B. R. James and D. Mahajan, Isr. J. Chem., 15, 214 (1977).

32. J. Vilim and J. Hetflejs, Collect. Czech. Chem. Comm., 43, 122 (1978).

33. J. M. Brown and P. A. Chaloner, J. Chem. Soc. Chem. Comm., 321 (1978).

34. F. Pruchnik, Inorg. Nucl. Chem. Lett., 9, 1229 (1973).

35. F. Pruchnik, Inorg. Nucl. Chem. Lett., 10, 661 (1974).

36. F. N. Tebbe, 2nd Joint CIC/ACS conference, 1977, Inorg. 087; J. M. Manriquez, D. R. McAlister, R. D. Sanner, and J. E. Bercaw, J. Am. Chem. Soc., 98, 6733 (1976).

37. J. Halpern and B. R. James, Can. J. Chem., 44, 671 (1966).

38. P. S. Hallman, B. R. McGarvey, and G. Wilkinson, J. Chem. Soc. (A), 3143 (1968).

39. R. Cramer, E. Jenner, R. Lindsay, and U. Stolberg, J. Am. Chem. Soc., 85, 1691 (1963).

40. J. Halpern and J. B. Milne, Proc. Int. Congr. Catal., 2nd, Paris, 445 (1960).

41. J. Halpern, J. Harrod, and B. R. James, J. Am. Chem. Soc., 88, 5150 (1966).

42. B. Hui, Ph.D. Dissertation, U.B.C., Vancouver, B.C., 1969.

43. J. Kwiatek, I. L. Mador, and J. K. Seyler, Adv. Chem. Ser., 37, 201 (1963).

44. M. G. Burnett, P. J. Connolly, and C. J. Kemball, J. Chem. Soc. (A), 800 (1967).

45. J. Halpern, Adv. Chem. Serv., 70, 1 (1968).

46. R. G. Banks and J. M. Pratt, J. Chem. Soc. (A), 854 (1968) and references therein.

47. J. Kwiatek and J. K. Seyler, Adv. Chem. Ser., 70, 207 (1968)

and references therein.

48. H. M. Feder and J. Halpern, J. Am. Chem. Soc., 97, 7186 (1975).

49. R. L. Sweany and J. Halpern, J. Am. Chem. Soc., 99, 8335 (1977).

50. L. Vaska and J. W. Diluzio, J. Am. Chem. Soc., 83, 2784 (1961).

51. P. B. Chock and J. Halpern, J. Am. Chem. Soc., 88, 3511 (1966).

52. L. Vaska, Acc. Chem. Res., 1, 335 (1968), and references therein.

53. B. R. James, A. D. Rattray, and D. K. W. Wang, J. Chem. Soc. Chem. Comm., 792 (1976).

54. V. V. Ipatieff, Jr. and V. G. Tronev, Compt. Rend. Acad. Sci., U.S.S.R. 1, 629 (1935).

55. M. Iguchi, J. Chem. Soc. Jap., 60, 1287 (1939).

56. J. Halpern, Quart. Rev., 10, 463 (1956).

57. J. Halpern, Adv. Catal., 9, 302 (1957).

58. J. Halpern, Adv. Catal., 11, 301 (1959).

59. J. Halpern, Collect. Pap. Symp. Coord. Chem., 351 (1964).

60. J. R. Shapley, R. R. Schrock, and J. A. Osborn, J. Am. Chem. Soc., 91, 2816 (1969).

61. R. R. Schrock and J. A. Osborn, J. Chem. Soc. Chem. Comm., 567 (1970).

62. R. R. Schrock and J. A. Osborn, J. Am. Chem. Soc., 93, 2397 (1971).

63. R. R. Schrock and J. A. Osborn, J. Am. Chem. Soc., 93, 3089 (1971).

64. R. R. Schrock and J. A. Osborn, J. Am. Chem. Soc., 98, 2134 (1976).

65. R. R. Schrock and J. A. Osborn, J. Am. Chem. Soc., 98, 2143 (1976).

66. R. R. Schrock and J. A. Osborn, J. Am. Chem. Soc., 98, 4450 (1976).

67. P. B. Hitchcock, M. PcPartlin, and R. Mason, Chem. Comm., 1366 (1969).

68. J. A. Osborn, F. H. Jardine, J. F. Young, and G. Wilkinson, J. Chem. Soc. (A), 1711 (1966).

69. M. A. Bennett and P. A. Longstaff, Chem. Ind. (Lond.), 846 (1965).

70. J. P. Candlin and A. R. Oldham, Discuss. Faraday Soc., 46, 60 (1968).

71. F. H. Jardine, J. A. Osborn, and G. Wilkinson, J. Chem. Soc. (A), 1574 (1967).

72. S. Montelatici, A. van der Ent, J. A. Osborn, and G. Wilkinson, J. Chem. Soc. (A), 1054 (1968).

73. F. H.Jardine and G. Wilkinson, J. Chem. Soc. (C), 270 (1967).

74. D. D. Lehman, D. F. Shriver, and I. Wharf, J. Chem. Soc. Chem. Comm., 1486 (1970).

75. C. A. Tolman, P. Z. Meakin, D. L. Linder, and J. P. Jesson, J. Am. Chem. Soc., 94, 2762 (1974).

76. B. R. James and G. L. Rempel, Discuss. Faraday Soc., 46, 48 (1968).

77. J. Hjortkjaer, Adv. Chem. Ser., 132, 133 (1974).

78. C. K. Brown and G. Wilkinson, J. Chem. Soc. (A), 2753 (1970) and references therein.

79. R. E. Hermon, S. K. Gupta and D. J. Brown, Chem. Rev., 1, 21 (1973).

80. G. Dolcetti and N. W. Hoffman, Inorg. Chim. Acta, 9, 269 (1974).

81. W. O. Haag and D. D. Whitehurst, Belg. Pat., 721, 686 (1969).

82. R. H. Grubbs, L. C. Kroll, J. Am. Chem. Soc., 93, 3062 (1971).

83. R. H. Grubbs, C. Gibbons, L. C. Kroll, W. C. Bonds, and C. H. Brubaker, J. Am. Chem. Soc., 95, 2373 (1973).

84. C. U. Pittman, Jr., and G. O. Evans, Chem. Tech., 560 (1973).

85. J. Manassen, D. D. Whitehurst, J. C. Bailar, Jr., S. Carra, M. Graziani, K. Mosbach, R. C. Pitkethly, E. K. Pye, and J. J. Rooney, in "Catalysis Progress in Research" (F. Basolo and R. L. Burwell, Jr., eds.), Plenum, New York and London, 1973, p.177.

86. J. C. Bailar, Jr., Catal. Rev., 10, 17 (1974).

87. Z. M. Michalska and D. E. Webster, Plat. Met. Rev., 18, 65 (1974).

88. D. Commereuc and G. Martino, Rev. Int. Fr. Pet., 30, 89 (1975).

89. A. L. Robinson, Science, 194, 1261 (1976).

90. Yu. I. Ermakov, Catal. Rev., 13, 77 (1976).

91. E. Bayer and V. Schurig, Chem. Tech., 212 (1976).

92. N. Takaishi, H. Imai, C. A. Bertelo, and J. K. Stille, J. Am. Chem. Soc., 98, 5400 (1976).

93. C. U. Pittman, Jr., and R. M. Hanes, J. Am. Chem. Soc., 98, 5402 (1976).

94. R. H. Grubbs, E. M. Sweet, and S. Phisanbut, in "Catalysis in Organic Syntheses 1976" (P. N. Rylander and H. Greenfield, eds.), Academic Press, New York, 1976, p.153.

95. C. U. Pittman, Jr., S. Jacobson, L. R. Smith, W. Clements, and H. Hiramoto, in "Catalysis in Organic Syntheses 1976" (P. N. Rylander and H. Greenfield, eds.), Academic Press, New York, 1976, p.161.

96. J. I. Crowley and H. Rapoport, Acc. Chem. Res., 9, 135 (1976).

97. F. R. Hartley and P. N. Vezey, Adv. Organomet. Chem., 15, 189 (1977).

98. M. S. Scurrell, Plat. Met. Rev., 21, 92 (1977).

99. C. U. Pittman, Jr., A. Hirao, C. Jones, R. M. Hanes, and Q. Ng, Ann. N. Y. Acad. Sci., 295, 15 (1977).

100. J. Falbe, "Carbon Monoxide in Organic Synthesis," Springer-Verlag, Berlin, 1970; R. Kummer, H. J. Nienburg, H. Hohenschutz, and M. Strohmeyer, Adv. Chem. Ser., 132, 19 (1974).

101. F. J. Smith, Plat. Met. Rev., 19, 93 (1975); Chem. & Eng. News, April 26, 1976, p.25.

102. F. E. Paulik, Catal. Rev., 6, 49 (1972).

103. M. Orchin and W. Pupiluis, Catal. Rev., 6, 85 (1972).

104. L. Marko, in "Aspects of Homogeneous Catalysis," Vol. 2, (R. Ugo, ed.), Reidel, Dordrecht, 1974, p.3.

105. M. Tanaka, Y. Watanabe, T. Mitsudo, and Y. Takegami, Bull. Chem. Soc. Jap. 47, 1698 (1974).

106. F. Piacenti, M. Bianchi, and P. Frediani, Adv. Chem. Ser., 132, 283 (1974).

107. P. Pino, G. Consiglio, C. Botteghi, and C. Salomon, Adv. Chem. Ser., 132, 295 (1974).

108. P. Pino, F. Piancenti, and M. Bianchi, in "Organic Synthesis via Metal Carbonyls" (I. Wender and P. Pino, eds.), Vol. 2, Wiley, New York, 1977, p.43.

109. R. L. Pruett, Adv. Organomet. Chem., 17, 1(1979).

110. T. Nishiguchi and K. Fukuzumi, J. Am. Chem. Soc., 96, 1893 (1974).

111. T. Nishiguchi, K. Tachi, and K. Fukuzumi, J. Org. Chem., 40, 237, 240 (1975).

112. C. Masters, A. A. Kiffen, and J. P. Visser, J. Am. Chem. Soc., 98, 1357 (1976).

113. H. Imai, T. Nishiguchi, and K. Fukuzumi, J. Org. Chem., 39, 1622 (1974).

114. Y. Sasson, P. Albin, and J. Blum, Tetrahedron Lett., 833 (1974).

115. Y. Sasson and J. Blum, J. Org. Chem., 40, 1887 (1975).

116. G. Descotes and D. Sinou, Tetrahedron Lett., 4083 (1976).

117. H. Imai, T. Nishiguchi, and K. Fukuzumi, Chem. Lett., 807 (1975).

118. H. Imai, T. Nishiguchi, M. Kobayashi, and K. Fukuzumi, Bull. Chem. Soc. Jap. 48, 1585 (1975).

119. H. Imai, T. Nishiguchi, and K. Fukuzumi, J. Org. Chem., 41, 665, 2688 (1976).

120. Y. M. Y. Haddad, H. B. Henbest, J. Husbands, T. R. B. Mitchell, and J. Trocha-Grimshaw, J. Chem. Soc. Perkin(I), 596 (1974).

121. B. R. James and R. H. Morris, J. Chem. Soc. Chem. Comm., 929(1978).

122. L. K. Freidlin, Y. A. Kopyttsev, N. M. Nazarova, B. L. Lebedev, and B. L. Khusid, Izv. Akad. Nauk. S.S.S.R. Ser. Khim., 1325 (1974).

123. G. Briegen and T. J. Nestrick, Chem. Rev., 74, 567 (1974).

124. I. S. Kolomnikov, V. P. Kukolev, and M. E. Volpin, Russ. Chem. Rev., 43, 399 (1974).

125. K. Ohkubo, T. Aoji, K. Hirata,and K. Yoshinaga, Inorg. Nucl. Chem. Lett., 12, 837 (1976).

126. K. Ohkubo, K. Hirati, K. Yoshinaga, and M. Okada, Chem. Lett., 183, 577 (1976).

127. K. Ohkubo, T. Shoji, I. Terada, and K. Yoshinaga, Inorg. Nucl. Chem. Lett., 13, 443 (1977).

128. K. Ohkubo, T. Ohgushi, T. Kusaga, and K. Yoshinaga, Inorg. Nucl. Chem. Lett., 13, 631 (1977).

129. K. Ohkubo, T. Ohgushi, and K. Yoshinaga, Chem. Lett., 775 (1976).

130. K. Ohkubo, K. Sugahara, I. Terada, and K. Yoshinaga, Inorg. Nucl. Chem. Lett., 14, 297 (1978).

131. L. Horner and D. Degner, Tetrahedron Lett., 5889 (1968).

132. L. Horner, H. Büthe, and H. Siegel, Tetrahedron Lett., 4023 (1968).

133. L. Horner, H. Siegel, and H. Büthe, Angew. Chem. Int. Edit., 7, 942 (1968).

134. W. S. Knowles and M. J. Sabacky, Chem. Comm., 1445 (1968).

135. I. Jardine and F. J. McQuillin, Chem. Comm., 477 (1969).

136. P. Abley and F. J. McQuillin, J. Chem. Soc. (C), 844 (1971).

137. J. D. Morrison, R. E. Burnett, A. M. Aguiar, C. J. Morrow, and C. Phillips, J. Am. Chem. Soc., 93, 1301 (1971).

138. W. S. Knowles, M. J. Sabacky, and B. D. Vineyard, J. Chem. Soc. Chem. Comm., 10 (1972); Chem.Tech., 590 (1972).

139. W. S. Knowles, M. J. Sabacky, B. D. Vineyard, and D. J. Weinkauff, J. Am. Chem. Soc., 97, 2567 (1975).

140. T. Hayashi, T. Mise, S. Mitachi, K. Yamamoto, and M. Kumada, Tetrahedron Lett., 1133 (1976).

141. W. Beck and H. Menzel, J. Organomet. Chem., 133, 307 (1977); A. M. Aguiar, C. J. Morrow, J. D. Morrison, R. E. Burnett, W. F. Masler, and N. S. Bhacca, J. Org. Chem., 41, 1545 (1976).

142. R. Glaser, J. Blumenfeld, and M. Twaik, Tetrahedron Lett., 4639 (1977); R. Glaser, S. Geresh, J. Blumenfeld, and M. Twaik, Tetrahedron, 34, 2405 (1978).

143. C. Fisher and H. S. Mosher, Tetrahedron Lett., 2487 (1977).

144. K. Achiwa, J. Am. Chem. Soc., 98, 8265 (1976).

145. R. H. Grubbs and R. A. Devries, Tetrahedron Lett., 1879 (1977).

146. T. Hayashi, M. Tanaka, and I. Ogata, Tetrahedron Lett., 295 (1977).

147. M. Tanaka and I. Ogata, J. Chem. Soc. Chem. Comm., 735 (1975).

148. M. Fiorini, G. M. Giongo, F. Marcati, and W. Marconi, J. Mol. Catal. 1, 451 (1976); G. Pracejus and H. Pracejus, Tetrahedron Lett., 3497 (1977).

149. W. R. Cullen and Y. Sugi, Tetrahedron Lett., 1635 (1978).

150. J. Halpern, D. P. Riley, A. S. C. Chan, and J. J. Pluth, J. Am. Chem. Soc., 99, 8055 (1977).

151. R. Glaser, Tetrahedron Lett., 2127 (1975).

152. R. Glaser and B. Vainas, J. Organomet. Chem., 121, 249 (1976).

153. R. Glaser and J. Blumenfeld, Tetrahedron Lett., 2525 (1977).

154. R. Glaser, S. Geresh, J. Blumenfeld, B. Vainas, and M. Twaik, Isr. J. Chem., 15, 17 (1977).

155. R. Glaser and S. Geresh, Tetrahedron Lett., 2527 (1977).

156. S. Brunie, J. Mazan, N. Langlois, and H. B. Kagan, J. Organomet. Chem., 114, 225 (1976).

157. J. K. Beattie, Acc. Chem. Res., 4, 253 (1971).

158. R. G. Ball and N. C. Payne, Inorg. Chem., 16, 1187 (1977).

159. K. E. Koenig and W. S. Knowles, J. Am. Chem. Soc., 100, 7561 (1978).

160. T. Hayashi, T. Mise, and M. Kumada, Tetrahedron Lett., 4351 (1976) and references therein.

161. I. Ojima, T. Kogure, M. Kumagai, and K. Achiwa, 26th Int. Congr. Pure Appl. Chem., Tokyo, 1977, Abstract 9F51.

162. I. Ojima, T. Kogure, and K. Achiwa, J. Chem. Soc. Chem. Comm., 428 (1977).

163. K. Achiwa, Tetrahedron Lett., 3735 (1977).

164. A. Levi, G. Modena, and G. Scorrano, J. Chem. Soc. Chem. Comm., 6 (1975) and references therein.

165. I. Ojima, T. Kogure, and M. Kumagai, J. Org. Chem., 42, 1671 (1977).

166. H. B. Kagan, N. Langlois, and T. P. Dang, Tetrahedron Lett., 4865 (1973).

167. H. Boucher and B. Bosnich, J. Am. Chem. Soc., 99, 6253 (1977).

168. J. Ashley-Smith, Z. Douek, B. F. G. Johnson, and J. Lewis, J. Chem. Soc. Dalton Trans., 128 (1974); 1776 (1972); C. E. Holloway, G. Hulley, B. F. G. Johnson, and J. Lewis, J. Chem. Soc. (A), 1653 (1970); 53 (1969).

CHAPTER II

1. D. F. Shriver, "Manipulation of Air Sensitive Compounds," McGraw Hill, N.Y., 1969.
2. R. Rigo, M. Bressan, and A. Turco, Inorg. Chem., 7, 1460 (1968).
3. G. R. Ames and W. Davey, J. Chem. Soc., 1794 (1958).

CHAPTER III

1. H. B. Kagan, Pure Appl. Chem., 43, 401 (1975).
2. J. D. Morrison, W. F. Masler, and M. K. Newberg, Adv. Catal., 25, 81 (1976); J. D. Morrison, W. F. Masler, and S. Hathaway in "Catalysis in Organic Syntheses" (P. N. Rylander and H. Greenfield, eds.), Academic Press, New York, 1976, p.203.
3. B. R. James, Adv. Organomet. Chem., 17, 319(1979).
4. B. Bosnich and M. D. Fryzuk, 172nd Am. Chem. Soc. Meeting, San Francisco, 1976, Abstract 108; M. D. Fryzuk and B. Bosnich, J. Am. Chem. Soc., 99, 6262 (1977).
5. T. P. Dang and H. B. Kagan, J. Am. Chem. Soc., 94, 6429 (1972).
6. W. Dumont, J. C. Poulin, T. P. Dang, and H. B. Kagan, J. Am. Chem. Soc., 95, 8295 (1973).

7. P. Bonvicini, A. Levi, G. Modena, and G. Scorrano, J. Chem. Soc. Chem. Comm., 1188 (1972).

8. W. S. Knowles, M. J. Sabacky, and B. D. Vineyard, Adv. Chem. Ser., 132, 274 (1974).

9. Y. Chauvin, D. Commereuc, and R. Stern, J. Organomet. Chem., 146, 311 (1978).

10. W. R. Cullen, A. Fenster, and B. R. James, Inorg. Nucl. Chem. Lett., 10, 167 (1974); A. Fenster, B. R. James, and W. R. Cullen, Inorg. Syn., 17, 81 (1977).

11. Y. Chevailier, Docteur-Ingenieur Thesis, Paris, 1970; through Ref.5.

12. D. Mahajan, M.Sc. Dissertation, U.B.C., Vancouver, B.C., 1976.

13. B. R. James and D. Mahajan, Isr. J. Chem., 15, 214 (1977).

14. R. R. Schrock and J. A. Osborn, J. Am. Chem. Soc., 93, 2397 (1971); ibid, 98, 2134 (1976).

15. D. K. W. Wang, Ph.D. Dissertation, U.B.C., Vancouver, B.C., 1978.

16. A. Sanger, J. Chem. Soc. Dalton Trans., 120 (1977).

CHAPTER IV

1. L. Vaska and D. L. Catone, J. Am. Chem. Soc., 88, 5324 (1966).

2. K. A. Taylor, Adv. Chem., 70, 195 (1968).

3. J. S. Miller and K. G. Caulton, J. Am. Chem. Soc., 97, 1067 (1975).

4. M. J. Hopkinson and J. F. Nixon, J. Organomet. Chem., 148, 201 (1978).

5. A. Sacco and R. Ugo, J. Chem. Soc., 3274 (1964).

6. J. A. McGinnety, N. C. Payne, and J. A. Ibers, J. Am. Chem. Soc., 91, 6301 (1969).

7. Y. Chevailier, Docteur-Ingenieur Thesis, Paris, 1970; through H. B. Kagan and T. P. Dang, J. Am. Chem. Soc., 94, 6429 (1972).

8. A. Sacco, M. Rossi, and C. F. Nobile, J. Chem. Soc. Chem. Comm., 589 (1966).

9a. M. C. Hall, B. T. Kilbourn, and K. A. Taylor, J. Chem. Soc. (A), 2539 (1970).

9b. D. H. Doughty and L. H. Pignolet, J. Am. Chem. Soc., 100, 7083 (1978).

10. W. R. Cullen, A. Fenster, and B. R. James, Inorg. Nucl. Chem. Lett., 10, 167 (1974).

11. B. R. James and D. Mahajan, Isr. J. Chem., 15, 214 (1977).

12. J.C. Poulin, T.P. Dang, and H. B. Kagan, J. Organomet. Chem., 84, 87 (1975).

13. B. R. James, Adv. Organomet. Chem., 17,319(1979).

14. D. Sinou and H. B. Kagan, J. Organomet. Chem., 114, 325 (1976).

15. D. A. Slack and M. C. Baird, J. Organomet. Chem., 142, C69 (1977).

16. R. Brady, W. V. Miller, and L. Vaska, J. Chem. Soc. Chem. Comm., 393 (1974).

17. G. L. Geoffroy, M. S. Wrighton, G. S. Hammond, and H. B. Gray, J. Am. Chem. Soc., 96, 3105 (1974).

18. A. Van der Ent. and A. L. Onderdelinden, Inorg. Syn., 14, 92 (1973).

19. A. Fenster, B. R. James, and W. R. Cullen, Inorg. Syn., 17, 81 (1977).

20. D. G. Holah, A. N. Hughes, and B. C. Hui, Can. J. Chem., 55, 4048 (1977).

21. B. R. James, R. H. Morris, and K. J. Reimer, Can. J. Chem., 55, 2353 (1977), and references therein.

22. J. D. Morrison, W. F. Masler, and M. K. Neuberg, Adv. Catal., 25, 81 (1976).

23. R. R. Schrock and J. A. Osborn, J. Am. Chem. Soc., 98, 2134, 2143 (1976).

24. W. S. Knowles, M. J. Sabacky, B. D. Vineyard, and D. J. Weinkauff, J. Am. Chem. Soc., 97, 2567 (1975).

25. Y. Chauvin, D. Commereuc, and R. Stern, J. Organomet. Chem., 146, 311 (1978).

26. J. Chatt and B. L. Shaw, J. Chem. Soc. (A), 1437 (1966).

27. N. Ahmad, S. D. Robinson, and M. F. Uttley, J. Chem. Soc. Dalton Trans., 843 (1972).

28. R. Brady, B. R. Flynn, G. L. Geoffroy, H. B. Gray, J. Peone, Jr., and L. Vaska, Inorg. Chem., 15, 1485 (1976).

29. W. J. Geary, Coord. Chem. Rev., 7, 81 (1971).

30. J. F. Knifton, J. Org. Chem., 40, 519 (1975); ibid., 41, 1200 (1976).

31. K. C. Dewhirst, W. Keim, and C. A. Reilly, Inorg. Chem., 7, 546 (1968).

32. J. P. Jesson, "Stereochemistry and stereochemical nonrigidity in transition metal hydrides," in E. L. Muetterties, ed. Transition metal hydrides. Marcel Dekker, New York, 1971, p.110.

33. B. A. Frenz and J. A. Ibers in "Molecular structures of transition metal hydride complexes," E. L. Muetterties, ed. Transition metal hydrides. Marcel Dekker, New York, 1971, p.47.

34. R. W. Baker and P. Pauling, J. Chem. Soc. Chem. Comm., 1495 (1969).

35. B-K. Teo, A. P. Ginsberg, and J. C. Calabrese, J. Am. Chem. Soc., 98, 3027 (1976).

36. B. A. Frenz and J. A. Ibers in "Transition Metal Hydrides", E. L. Muetterties, Ed., Marcel Dekker, New York, 1971, pp 41-44.

37. S. H. Strauss, S. E. Diamond, F. Mares, and D. F. Shriver, Inorg. Chem., 17, 3064 (1978).

38. J. F. Nixon and A. Pidcock, Ann. Rev. NMR Spect., 2, 345 (1969).

39. P. E. Garrou, Inorg. Chem., 14, 1435 (1975).

40. A. Sanger, J. Chem. Soc. Dalton Trans., 120 (1977).

41. J. Halpern, D. P. Riley, A.S.C. Chan, and J. J. Pluth, J. Am. Chem. Soc., 99, 8055 (1977).

42. R. R. Schrock and J. A. Osborn, J. Am. Chem. Soc., 93, 2397 (1971).

43. M. A. Bennett, R. Charles, and T. R. B. Mitchell, J. Am. Chem. Soc., 100, 2737 (1978).

44. A. P. Ginsberg and W. E. Lindsell, Inorg. Chem., 12, 1983 (1973).

45. S. Brunie, J. Mazan, N. Langlois, and H. B. Kagan, J. Organomet. Chem., 114, 225 (1976).

46. B. D. Vineyard, W. S. Knowles, M. J. Sabacky, G. L. Backman, and D. J. Weinkauff, J. Am. Chem. Soc., 99, 5946 (1977).

47. R. G. Ball and N. C. Payne, Inorg. Chem., 16, 1187 (1977).

48. M. D. Fryzuk and B. Bosnich, J. Am. Chem. Soc., 99, 6262 (1977).

49. B. R. James, Homogeneous Hydrogenation, Wiley, New York, 1973, p.269.

50. B. R. James, R. S. McMillan, R. H. Morris, and D. K. W. Wang, Adv. Chem. Ser., 167, 122 (1978).

CHAPTER V

1. T. P. Dang and H. B. Kagan, Chem. Comm., 481 (1971); H. B. Kagan and T. P. Dang, J. Am. Chem. Soc., 94, 6429 (1972).

2. Y. Chauvin, D. Commereuc, and R. Stern, J. Organomet. Chem., 146, 311 (1978) and references therein.

3. B. R. James, Adv. Organomet. Chem., 17, 319 (1979) and references therein.

4. D. Sinou and H. B. Kagan, J. Organomet. Chem., 114, 325 (1976).

5. H. B. Kagan, V. Langlois, and T. P. Dang, J. Organomet. Chem., 90, 353 (1975).

6. T. P. Dang, J. C. Poulin, and H. B. Kagan, J. Organomet. Chem., 91, 105 (1975).

7. G. Gelbard, H. B. Kagan, and R. Stern, Tetrahedron, 32, 233 (1976).

8. R. Glaser, S. Geresh, and J. Blumenfeld, J. Organomet. Chem., 112, 355 (1976).

9. R. Glaser, Tetrahedron Lett., 2127 (1975).

10. R. Glaser and B. Vainas, J. Organomet. Chem., 121, 249 (1976).

11. R. Glaser and J. Blumenfeld, Tetrahedron Lett., 2525 (1977).

12. R. Glaser, S. Geresh, J. Blumenfeld, B. Vainas, and M. Twaik, Isr. J. Chem., 15, 17 (1977).

13. R. Glaser and S. Geresh, Tetrahedron Lett., 2527 (1977).

14. W. R. Cullen, A. Fenster, and B. R. James, Inorg. Nucl. Chem. Lett., 10, 167 (1974).

15. D. Mahajan, M.Sc. Dissertation, U.B.C., Vancouver, B.C., 1976; B. R. James and D. Mahajan, Isr. J. Chem., 15, 214 (1977).

16. J. A. McCleverty and G. Wilkinson, Inorg. Syn., 8, 211 (1966).

17. A. Sanger, J. Chem.Soc. Dalton Trans., 120 (1977).

18. R. Rossi and P. Diversi, Gazz. Chim. Ital., 98, 1391 (1968).

19. S. M. Birbaum, L.Levintow, R. B. Kingsley, and J. P. Greenstein, J. Biol. Chem., 194, 455 (1952).

20. J. P. Bakhshi and E. E. Turner, J. Chem. Soc., 171 (1961).

21. W. S. Knowles, M. J. Sabacky, and B. D. Vineyard, Adv. Chem. Ser., 132, 274 (1974).

22. B. D. Vineyard, W. S. Knowles, M. J. Sabacky, G. L. Bachman, and D. J. Weinkauff, J. Am. Chem. Soc., 99, 5946 (1977).

23. J. M. Brown and P. A. Chaloner, J. Chem. Soc. Chem. Comm., 321 (1978).

24. J. Halpern, Symposium on "Rhodium in Homogeneous Catalysis", Veszprém, Hungary, 1978, p.30.

25. R. Glaser, J. Blumenfeld, and M. Twaik, Tetrahedron Lett., 4639 (1977).

26. R. Glaser, S. Geresh, J. Blumenfeld, and M. Twaik, Tetrahedron, 34, 2405 (1978).

27. A. Loser, Dissertation, Universitat Bochum, 1973, through reference: B. Bogdanović, Angew. Chem. Int. Edit., 12, 954 (1973).

28. J. Hjortkjaer, Adv. Chem. Ser., 132, 133 (1974) and references therein.

29. M. D. Fryzuk and B. Bosnich, J. Am. Chem. Soc., 99, 6262 (1977).

30. W. R. Cullen and E.-S. Yeh, J. Organomet. Chem., 139, C13 (1977).

31. W. S. Knowles, M. J. Sabacky, and B. D. Vineyard, J. Chem. Soc. Chem. Comm., 10 (1972).

CHAPTER VI

1. D. Mahajan, M.Sc. Dissertation, U.B.C., Vancouver, B.C., 1976; B. R. James and D. Mahajan, Isr. J. Chem., 15, 214 (1977).

2. D. Sinou and H. B. Kagan, J. Organomet. Chem., 114, 325 (1976).

3. R. R. Schrock and J. A. Osborn, J. Am. Chem. Soc., 93, 2397 (1971).

4. D. A. Slack and M. C. Baird, J. Organomet. Chem., 142, C69 (1977).

5. R. R. Schrock and J. A. Osborn, J. Am. Chem. Soc., 98, 2134, 2143 (1976).

6. A. R. Sanger, J. Chem. Soc. Dalton Trans., 120 (1977).

7. J. Halpern, D. P. Riley, A. S. C. Chan, and J. J. Pluth, J. Am. Chem. Soc., 99, 8055 (1977).

8. J. M. Brown, P. A. Chaloner, and P. N. Nicholson, J. Chem. Soc. Chem. Comm., 646 (1978).

9. J. Hjortkjaer, Adv. Chem. Ser., 132, 133 (1974).

CHAPTER VII

1. S. D. Ibekwe and K. A. Taylor, J. Chem. Soc. (A), 1(1970).
2. G. Rouschias and W. Bedford, J. Chem. Soc. Dalton Trans., 2531 (1974).
3. J. S. Miller and K. G. Caulton. J. Am. Chem. Soc., 97, 1067 (1975).
4. M. J. Hopkinson and J. F. Nixon, J. Organomet. Chem., 148, 201 (1978).
5. J. A. J. Jarvis, R. H. B. Mais, P. G. Owston, and K. A. Taylor, Chem. Comm., 906 (1966).
6. J. A. McGinnety, N. C. Payne, and J. A. Ibers, J. Am. Chem. Soc., 91, 6301 (1969).
7. F. Pruchnik, Inorg. Nucl. Chem. Lett., 9, 1229 (1973).
8. F. Pruchnik, Inorg. Nucl. Chem. Lett., 10, 661 (1974).
9. D. H. Doughty and L. H. Pignolet, J. Am. Chem. Soc., 100, 7083 (1978).
10. L. Vaska and D. L. Catone, J. Am. Chem. Soc., 88, 5324 (1966).
11. L. Vaska, L. S. Chen, and W. V. Miller, J. Am. Chem. Soc., 93, 6671 (1971).
12. A. R. Sanger, J. Chem. Soc. Dalton Trans., 120 (1977).
13. D. A. Slack and M. C. Baird, J. Organomet. Chem., 142, C69 (1977).
14. D. Sinuo and H. B. Kagan, J. Organomet. Chem., 114, 325 (1976).
15. R. L. Augustine, R. J. Pellet, J. F. Van Peppen, and J. P. Mayer, Adv. Chem. Ser., 132, 111 (1974) and references therein; J. Lyons, Aspects of Homogeneous Catalysis, Vol. 3, 1 (1977).
16. B. R. James and D. Mahajan, Can. J. Chem., 57, 180 (1979).
17. W. J. Geary, Coord. Chem. Rev., 7, 81 (1971).
18. F. A. Cotton, K.I. Hardcastle, and G. A. Rusholme, J. Coord. Chem., 2, 217 (1973).
19. M. Akhtar, P. D. Ellis, A. G. MacDiarmid, and J. D. Odom, Inorg. Chem., 11, 2917 (1972).

20. S. H. Strauss, S. E. Diamond, F. Mares, and D. F. Shriver, Inorg. Chem., 17, 3064 (1978).

21. J. P. Jesson and P. Meakin, J. Am. Chem. Soc., 96, 5760 (1974).

22. A. Sacco, M. Rossi, and C. F. Nobile, Chem. Comm., 589 (1966).

23. M. C. Hall, B. T. Kilbourn, and K. A. Taylor, J. Chem. Soc. (A), 2539 (1970).

24. R. T. Morrison and R. N. Boyd, "Organic Chemistry," Allyn and Bacon Inc., Boston, 1959, Ist Ed., p.635.

25. R. S. McMillan, Ph.D. Dissertation, U.B.C., Vancouver, B.C., 1976.

26. R. R. Schrock and J. A. Osborn, J. Am. Chem. Soc., 93, 2397 (1971).

27. F. N. Tebbe, P. Meakin, J. P. Jesson, and E. L. Muetterties, J. Am. Chem. Soc., 92, 1068 (1970).

28. P. Meakin, L. J. Guggenberger, J. P. Jesson, D. H. Gerlach, F. N. Tebbe, W. G. Peet, and E. L. Muetterties, J. Am. Chem. Soc., 92, 3482 (1970).

29. J. Halpern, D. P. Riley, A.S.C. Chan, and J. J. Pluth, J. Am. Chem. Soc., 99, 8055 (1977) and references therein.

30. D. K. W. Wang, Ph.D. dissertation, U.B.C., Vancouver, B.C., 1978.

31. R. C. Ball, B. R. James, J. Trotter, D. K. W. Wang, and K. R. Dixon, J. Chem. Soc. Chem. Comm., 000 (1979).

32. Internat. Critical Tables, Vol. III, 262 (1928).